

**Advancing Skin Sensitization Assessment:  
The Development of an Immunocompetent Skin Model  
as a Non-Animal Alternative for Testing Skin Sensitizers**

Inaugural-Dissertation

to obtain the academic degree

Doctor rerum naturalium (Dr. rer. nat.)

submitted to the Department of Biology, Chemistry, Pharmacy  
of Freie Universität Berlin

By

Tarada Tripetchr

Berlin

2024

This thesis and all associated experiments were prepared and performed from May 2019 to April 2023 under the supervision of **Prof. Dr. Burkhard Kleuser** at the Institute of Pharmacy, Pharmacology and Toxicology, Freie Universität Berlin, Germany.

**1<sup>st</sup> Reviewer: Prof. Dr. Burkhard Kleuser**

Institute of Pharmacy - Pharmacology and Toxicology  
Freie Universität Berlin  
Königin-Luise-Str. 2+4, 14195, Berlin, Germany

**2<sup>nd</sup> Reviewer: Prof. Dr. Sarah Hedtrich**

Center of Biological Design, Berlin Institute of Health in der Charité (BIH)  
Käthe-Beutler-Haus  
Lindenberger Weg 80, 13125 Berlin, Germany

Date of defense: 19.09.2024

## ACKNOWLEDGMENTS

I am deeply grateful to Prof. Dr. Burkhard Kleuser and Prof. Dr. Sarah Hedtrich for giving me the opportunity to participate in this project. As someone once said, one's talents and potential can only shine when given a chance. Both Prof. Burkhard Kleuser and Prof. Dr. Hedtrich have been supportive and helpful mentors throughout the process while also allowing me to pursue my research interests and ideas. I also appreciate Prof. Dr. Kleuser's trust and generosity in providing me with the necessary resources and materials for my research.

I would also like to acknowledge Dr. Anna Löwa, Dr. Anne Kirstin Eichhorst, and Dr. Guy Yelland, who have taught me invaluable lessons on how to be a good scientist and researcher. They have shared their expertise and insights with me and have challenged me to improve my skills and knowledge.

Furthermore, I am thankful to Marla Dubau, who started as my supervisee and became my best lab partner. She has been a great collaborator and partner, who has helped me with the experiments and the review of the thesis and publications. Most importantly, she has also kept me connected with the working group and offered me constant support and encouragement even after I left the lab.

I would also like to express my gratitude to Dr. Vivian Kral and Dr. Ahmed Hasan for reviewing the thesis and publications and providing me with constructive feedback and suggestions. Finally, I would like to thank all the working group members for their assistance and cooperation throughout the project.

## SUMMARY

In the skin sensitization assessment, the *in vivo* method, specifically the Local Lymph Node Assay (LLNA), is regarded as the gold standard. However, to adhere to the 3R principle (Reduction, Refinement, and Replacement), which advocates for the Reduction, Refinement, and Replacement of animal testing, and to enhance the ethical standards of risk assessment, a greater number of *in vitro* and *in silico* testing methods have been developed. While these *in vitro* and *in silico* methods offer a higher throughput and a more ethical approach to risk assessment, they each come with their own set of limitations. For instance, most *in vitro* tests can only be used for a single readout. On the other hand, *in silico* methods lack physiological and biological feedback. The adverse outcome pathway (AOP) for skin sensitization, as defined by the Organization for Economic Cooperation and Development (OECD) guidelines, involves four key events, which are protein binding (Key Event 1 – KE1), keratinocyte activation (Key Event 2 – KE 2), dendritic cell activation (Key Event 3 – KE 3), and T-lymphocyte activation (Key Event 4 – KE 4) (OECD, 2014). While animal-based assays are reasonably accurate, their skin is physiologically different than human skin. Therefore, this thesis aimed to develop the 'ImmuSkin-MT', a 3D-human skin model with immune cells, designed to address the limitations inherent in *in vitro* skin sensitization assays. The thesis began with 2D co-culture of keratinocytes and immune cells, which have shown to fall short in detecting a skin sensitizer. In parallel to the development of the 2D co-culture assay, the advantages of the autologous in comparison to the allogenic 2D co-culture were investigated. The results indicated that within the donor pool used, allogenic 2D co-culture did not lead to an alloreactive response in the cells. Therefore, whether autologous or allogenic cell pairings were used in the co-culture, they had no impact on the development of the assay. Later, the project progressed and the 'ImmuSkin-MT', created from human hair follicle-derived keratinocytes (HFDK), fibroblasts (HFDF), and immune cells were developed. monocyte-derived Langerhans cells (MoLC) and CD4<sup>+</sup> naïve T-lymphocytes were integrated into the reconstructed human skin models (RHS). ImmuSkin-MT were topically exposed to various substances, including non-sensitizers and contact sensitizers. Using the MoLC activation and the stimulation index (SI) of T-lymphocytes, results demonstrate the effectiveness of ImmuSkin-MT in replicating KE 3 and 4 of skin sensitization in response to the skin sensitizers. This model presents a promising alternative to animal testing for contact sensitizers, contributing to more ethical and precise skin sensitization assessment techniques. In conclusion, ImmuSkin-MT represents a significant advancement in skin sensitization assessment by capturing multiple key events simultaneously. The project's findings have the potential to optimize skin sensitization testing methods, providing more accurate, reliable, and ethical alternatives to traditional animal-based assays.

## ZUSAMMENFASSUNG

Für die Bewertung der Hautsensibilisierung gilt die *in vivo*-Methode, insbesondere der Local Lymph Node Assay (LLNA), als Goldstandard. Um jedoch dem 3R-Prinzip (Reduction, Refinement, und Replacement) gerecht zu werden und die ethischen Standards der Risikobewertung zu verbessern, wurde eine Vielzahl von *in vitro*- und *in silico*-Testmethoden entwickelt. Obwohl diese *in vitro*- und *in silico*-Methoden einen höheren Durchsatz und einen ethischeren Ansatz für die Risikobewertung bieten, haben sie jeweils ihre eigenen Grenzen. Beispielsweise können die meisten *In vitro* Tests nur für eine einzige Messung verwendet werden. Andererseits fehlt den *in silico*-Methoden das physiologische und biologische Feedback. Der adverse outcome pathway (AOP) für Hautsensibilisierung, wie er in den Leitlinien der Organisation für wirtschaftliche Zusammenarbeit und Entwicklung (OECD) definiert ist, umfasst vier Schlüsselereignisse: Proteinbindung (Key Event 1 - KE 1), Aktivierung von Keratinozyten (Key Event 2 - KE 2), Aktivierung von dendritischen Zellen (Key Event 3 - KE 3) und Aktivierung von T-Lymphozyten (Key Event 4 - KE 4) (OECD, 2014). Obwohl Tierversuche recht genau sind, unterscheidet sich ihre Haut physiologisch von der menschlichen Haut. Aus diesem Grund zielt diese Arbeit darauf ab, „ImmuSkin-MT“ zu entwickeln, ein 3D-Hautmodell mit Immunzellen, das entwickelt wurde, um die Einschränkungen von In-vitro-Hautsensibilisierungstests zu überwinden. Die Arbeit begann mit der 2D-Kokultur von Keratinozyten und Immunzellen, die sich als unzureichend für die Erkennung eines Hautsensibilisators erwies. Parallel zur Entwicklung des 2D-Kokultur-Assays wurden die Vorteile der autologen im Vergleich zur allogenen 2D-Kokultur untersucht. Die Ergebnisse zeigten, dass bei dem verwendeten Spenderpool die allogene 2D-Kokultur nicht zu einer alloreaktiven Reaktion der Zellen führte. Daher hatte die Verwendung von autologen oder allogenen Zellpaaren in der Kokultur keinen Einfluss auf die Entwicklung des Assays. Im weiteren Verlauf des Projekts wurde „ImmuSkin-MT“ entwickelt, das aus Keratinozyten-abgeleiteten Haarfollikeln (HFDK), Fibroblasten (HFDF) und Immunzellen besteht. Von Monozyten abgeleitete Langerhanszellen (MoLC) und CD4+ naive T-Lymphozyten wurden in rekonstruierte humane Hautmodelle (RHS) integriert. ImmuSkin-MT wurden topisch verschiedenen Substanzen ausgesetzt, darunter Nicht-Sensibilisatoren und Kontaktallergene. Unter Verwendung der MoLC-Aktivierung und des Stimulations-Index (SI) der T-Lymphozyten zeigen die Ergebnisse die Wirksamkeit von ImmuSkin-MT bei der Replikation von KE 3 und KE 4 der Hautsensibilisierung als Reaktion auf Hautsensibilisatoren.

Dieses Modell stellt eine vielversprechende Alternative zu Tierversuchen für Kontaktallergene dar und trägt zu ethischeren und genaueren Techniken zur Bewertung der Hautsensibilisierung bei. Zusammenfassend stellt ImmuSkin-MT einen bedeutenden Fortschritt in der Bewertung der Hautsensibilisierung durch die gleichzeitige Erfassung mehrerer Schlüsselereignisse dar. Die

Ergebnisse des Projekts haben das Potenzial, Hautsensibilisierungstests zu optimieren und genauere, zuverlässigere und ethisch vertretbarere Alternativen zu herkömmlichen Tierversuchen zu bieten.

## TABLE OF CONTENTS

CHAPTER 1 INTRODUCTION .....	1
1.1    Skin: The Biological Barrier of the Organism .....	1
1.2    The Skin as an Immune Organ .....	6
1.3    Immunology of Skin Sensitization .....	7
1.3.1    Sensitization Phase .....	7
1.3.2    Elicitation Phase.....	14
1.4    The Growing Importance of Skin Sensitization Assessment.....	15
1.5    Enhancing Skin Models: Toward Better Skin Sensitization Assays .....	20
1.6    From Hair Follicles to Skin Models .....	25
CHAPTER 2 AIM OF THE PROJECT .....	27
CHAPTER 3 RESEARCH DESIGNS, MATERIALS, AND METHODS.....	28
3.1    List of Devices, Reagents, and Plastic Wares .....	28
3.1.1    List of Devices .....	28
3.1.2    List of Reagents.....	29
3.1.3    List of Plastic Wares and Other Materials .....	32
3.2    Research Techniques.....	33
3.2.1    Flow Cytometry .....	33
3.2.2    Immunofluorescence (IF) Staining.....	33
3.2.3    Hematoxylin and Eosin Staining (H&E).....	34
3.2.4    3- (4,5-dimethylthiazol-2-yl)-2,5-diphenyltetrazolium bromide (MTT) Assay.....	35
3.2.5    Frozen Section Procedure.....	35
3.3    Preparation of Biological Samples.....	35
3.3.1    Juvenile Foreskin-derived Cells.....	35
3.3.2    Hair Follicle-derived Cells .....	36
3.3.3    Immune Cells .....	40
3.4    Experiment Designs.....	43
3.4.1    Characterization of Foreskin-derived and Hair Follicle-derived Cells.....	43
3.4.2    Cultivation Methods for HFDK.....	43
3.4.3    Culture Conditions of Naïve CD4+ T-lymphocytes.....	43
3.4.4    Co-Cultivation of HFDK with Naïve CD4+ T-lymphocytes .....	44
3.4.5    The Co-Culture of MoLC, T-Lymphocytes, and HFDK.....	46
3.4.6    Development of Immunocompetent Skin Model.....	48
CHAPTER 4 RESULTS .....	52
4.1    Hair Follicles as an Alternative Source for Keratinocytes and Fibroblasts .....	52
4.1.1    Comparative Analysis of Cell Properties from Hair Follicles and Foreskin .....	52
4.1.2    Efficacy of Different Hair Follicle Cell Culture Techniques.....	55
4.2    Dynamics of CD4+ T-Lymphocyte Cultivation.....	58
4.2.1    Time-Course of CD4+ Naïve T-Lymphocyte Cultivation.....	58

4.2.2	Impact of IL-2 on CD4+ T-Lymphocyte Activation.....	59
4.3	Interaction Dynamics in Keratinocyte and T-Lymphocyte Co-Cultures .....	63
4.3.1	Analysis of Medium Effects on Co-Cultivation .....	63
4.3.2	Comparative Study of Autologous versus Allogeneic Co-Cultures .....	68
4.3.3	The Impact of Different DNCB Dosage on HFDK and T-lymphocytes .....	71
4.3.4	Response Patterns of T-Lymphocytes in the Co-Culture to DNCB.....	73
4.4	Insights from Three-Cell Co-Culture Systems .....	76
4.4.1	Behavioral Dynamics of Immune Cells in Three-Cell Configurations.....	77
4.4.2	Comparative Immune Responses in Autologous vs. Allogenic Three-Cell Systems.....	79
4.4.3	Sensitivity to DNCB of The Three-Cell Culture .....	82
4.5	Advances in Immunocompetent Skin Models from Hair Follicle Cells .....	85
4.5.1	Character of The RHS from Hair Follicle-derived Cells.....	85
4.5.2	Optimal Culture Conditions for Skin Models .....	86
4.5.3	Characterization of The ImmuSkins .....	89
4.6	Application of Immunocompetent Skin Models in Sensitizers Detection .....	95
CHAPTER 5	DISCUSSION .....	104
5.1	Hair Follicles as an Alternative Source for Keratinocytes and Fibroblasts.....	104
5.2	Comparative Study of Autologous and Allogeneic Co-Cultures .....	107
5.3	Development of a Co-Culture-Based Skin Sensitization Assay .....	110
5.3.1	Response Patterns of T-Lymphocytes in the Co-Culture to DNCB.....	110
5.3.2	Sensitivity to DNCB of the Three-Cell Culture.....	111
5.4	Advances in Immunocompetent Skin Models .....	113
5.5	Application of Immunocompetent Skin Models in Sensitizer Detection .....	117
5.6	Outlook.....	120
CHAPTER 6	CONCLUSION .....	122
REFERENCES	.....	124
APPENDIX AND SUPPLEMENTALS	.....	I
APPENDIX 1	List of Figures .....	I
APPENDIX 2	List of Tables .....	III
LIST OF CONTRIBUTIONS	.....	IV
DECLARATION OF AUTHORSHIP	.....	V

## LIST OF ABBREVIATIONS AND ACRONYMS

Abbreviation and acronyms	Expansion
2D	Two-dimensional
2o3 DA	2 Out of 3 Defined Approach
3D	Three-dimensional
7-AAD	7-aminoactinomycin D
ADRA	Amino acid derivative reactivity assay
ADRA	Amino acid Derivative Reactivity Assay
AhR	Aryl hydrocarbon receptor
AMPK	AMP-activated protein kinase
AOP	Adverse outcome pathway
AP-1	Activator protein-1
APCs	Antigen-presenting cells
ARE	Antioxidant response element
ARE/EpRE	Antioxidant response element/electrophile response element
ARNT	Aryl hydrocarbon Receptor Nuclear Translocator
ATF3	Activating transcription factor 3
BMP	Bone morphogenetic proteins
BSA	Bovine serum albumin
cAMP	Cyclic adenosine monophosphate
CCL17	C-C motif chemokine ligand 17
CCL27	C-C motif chemokine ligand 27
CCR10	C-C chemokine receptor type 10
CCR4	C-C chemokine receptor type 4
CCR7	C-C chemokine receptor type 7
CD10	Cluster of differentiation 10
CD107	Cluster of differentiation 107, Langerin
CD1a	Cluster of differentiation 1a
CD25	Cluster of differentiation 25
CD29	Cluster of differentiation 29
CD4	Cluster of differentiation 4
CD44	Cluster of differentiation 44
CD45RA	Protein tyrosine phosphatase, receptor type, C
CD49f	Cluster of differentiation 49f
CD69	Cluster of differentiation 69
CD80	Cluster of differentiation 80
CD86	Cluster of differentiation 86
CD90	Cluster of differentiation 90
CER	Ceramide
CER[EOS]	Ceramide ester-linked omega-hydroxy fatty acid
CFSE	Carboxyfluorescein succinimidyl ester
CHOL	Cholesterol
CK1	Cytokeratin 1
CK10	Cytokeratin 10
CK14	Cytokeratin 14
CK5	Cytokeratin 5

<b>Abbreviation and acronyms</b>	<b>Expansion</b>
CLR	C-type lectin receptor
Csk	C-terminal Src kinase
CTLA-4	Cytotoxic T-lymphocyte-associated Protein 4
CXCL10	CXC-chemokine ligand 10
CXCL12	CXC-chemokine ligand 12
CXCR4	CXC-chemokine receptor 4
Cys	Cysteine
DCs	Dendritic cells
DC-SIGN	Dendritic cell-specific Intercellular adhesion molecule-3-grabbing non-integrin
DEJ	Dermal-epidermal junction
DMEM	Dulbecco's modified eagle medium
DMSO	Dimethylsulfoxide
DNA	Deoxyribonucleic acid
DNAJB4	DnaJ Heat Shock Protein Family Member B4
DNCB	2,4-dinitrochlorobenzene
DPBS	Dulbecco's phosphate-buffered saline
DPRA	Direct peptide reactivity assay
DPRA	Direct peptide reactivity assay
DRK	Deutsches rotes kreuz nord-ost
ECHA	European chemicals agency
ECM	Extra cellular matrix
EGF	Epidermal growth factor
EGFR	Epidermal growth factor receptor
eLCSA	Enhanced Loose Fit Co-culture Assay
ERK	Extracellular signal-regulated kinase
FACS	Fluorescent activated cell sorting
FBS	Fetal bovine serum
FBs	Fibroblasts
FGF	Fibroblast growth factor
FGM	Fibroblasts growth medium
GCLM	Glutamate-cysteine ligase modifier subunit
GHS	Globally Harmonized System of Classification and Labelling of Chemicals
Gly	Glycerol
GM-CSF	Granulocyte-macrophage colony-stimulating factors
GRHL3	Grainyhead-like transcription factor 3
H&E	Hematoxylin and Eosin
h-CLAT	Human cell line activation test
HEPES	Hydroxyethyl-piperazine ethane-sulfonic acid buffer
HFDF	Human hair follicle-derived fibroblasts
HFDK	Human hair follicle-derived keratinocytes
HFSC	Hair follicle stem cells
His	Histidine imidazole group
HLA	Human leukocyte antigen
HLA-DR	Human leukocyte antigen – DR isotype
HMOX1	Heme oxygenase 1 gene

<b>Abbreviation and acronyms</b>	<b>Expansion</b>
HTS-DCYA	High-Throughput Screening Method for the Detection of Reactive Electrophiles Assay
ICAM-1	Intercellular adhesion molecule 1
IF	Immunofluorescence
IFN- $\gamma$	Interferon $\gamma$
Ig	Immunoglobulin
IG	Isoeugenol
IGF	Insulin-like growth factor
IL-1	Interleukin 1
IL-1 $\beta$	Interleukin 1 $\beta$
IL-2	Interleukin 2
IL-4	Interleukin 4
IL-6	Interleukin 6
IL-8	Interleukin 8
IRS	Inner root sheath
ITSv1	Incorporating integrated testing strategy version 1
ITSv2	Incorporating integrated testing strategy version 2
KCs	Keratinocytes
KDM	Keratinocytes differentiation medium
kDPRA	Kinetic Direct Peptide Reactivity Assay
KE	Key Events
KE 1	Key Event 1
KE 2	Key Event 2
KE 3	Key Event 3
KE 4	Key Event 4
Keap-1	Kelch-like ECH-associated protein 1
KGF	Keratinocyte growth factor
KGM-2	Keratinocytes growth medium
KLF4	Kruppel-like factor 4
KTG	Keratinocyte transglutaminase
Lck	Lymphocyte-specific protein tyrosine kinase
LCs	Langerhans cells
LCSA	Loose Fit Co-culture Assay
LCSA-ly	Loose Fit Co-culture Assay-Lymphocytes
LLNA	Local lymph node assay
Lys	Lysine
MCP-1	Monocyte chemoattractant protein-1
M-CSF	Macrophage colony-stimulating factor
MFI	Median fluorescence intensity
MHC	Major histocompatibility complex
MMPs	Matrix metalloproteinases
MoDC	Monocyte-derived dendritic cells
MoLC	Monocyte-derived Langerhans cell
MRE	Metal response element
MTF	Metal-responsive transcription factor-1
MTT	3-(4,5-dimethylthiazol-2-yl)-2,5-diphenyltetrazolium bromide

<b>Abbreviation and acronyms</b>	<b>Expansion</b>
MUTZ-LC	MUTZ-3 derived Langerhans cells
NHDF	Normal human dermal fibroblasts
NHEK	Normal human epidermal keratinocytes
Nrf1	Nuclear respiratory factor 1
Nrf2	Nuclear factor erythroid 2-related factor 2
NT-4	Neurotrophin-4
OD	Optical density
OECD	Organization for Economic Cooperation and Development
ORM+	Outer root sheath medium
ORS	Outer root sheath
p63	Tumor protein p63
PBMCs	Peripheral blood mononuclear cells
PDGFB	Platelet-derived growth factor B
PGD2	Prostaglandin D2
PI3K/AKT	Phosphatidylinositol 3-kinase/protein kinase B
PPAR	Peroxisome proliferator-activated receptor
PPD	P-phenylenediamine
QSAR	Quantitative structure-activity relationship
RANTES	Regulated upon Activation, Normal T Cell Expressed and Presumably Secreted
REACH	Registration, Evaluation, Authorisation and Restriction of Chemicals
REST	Re1-silencing transcription
RHE	Reconstructed human epidermal models
RHS	Reconstructed human skin models
RHS-HFD	Hair follicle-derived RHS
RHS-FD	Fore skin-derived RHS
RKD1	The mix of 1:1 RPMI1640 basal and KDM
RN	Resorcinol
ROS	Reactive oxygen species
SI	Stimulation index
TARC	Thymus and Activation-Regulated Chemokine
TCR	T-lymphocyte receptor
TEMRA	Terminally differentiated T-cells re-expressing CD45RA
TGF- $\beta$	Transforming growth factor $\beta$
Th1	T-helper cells 1
Th17	T-helper cells 17
Th2	T-helper cells 2
TNBS	2,4,6-trinitrochlorobenzene
TNFR1	Type 1 TNF- $\alpha$ receptor
TNF- $\alpha$	Tumor necrosis factor- $\alpha$
Treg	Regulatory T-cells
TRP	Transient receptor potential
TRPA1	Transient receptor potential ankyrin 1
TRPM	Transient receptor potential melastatin
TRPV1	Transient receptor potential vallinoid 1
TRPV4	Transient receptor potential vallinoid 4
Trypsin-EDTA	Trypsin-Ethylenediaminetetraacetic acid

<b>Abbreviation and acronyms</b>	<b>Expansion</b>
UV	Ultraviolet
VEGF	Vascular endothelial growth factor
VEGFA	Vascular endothelial growth factor A
Wnt	Wingless/integrated
XRE	Xenobiotic response element
ZAP-70	Zeta-chain-associated protein kinase 70



# CHAPTER 1 INTRODUCTION

## 1.1 Skin: The Biological Barrier of the Organism

The skin comprises the epidermis and the dermis. The epidermis hosts diverse cell populations, including immune cells such as resident Langerhans cells (LC). However, its primary constituents are keratinocytes, found in varying states of differentiation. Within the epidermis, distinct layers of keratinocytes exist, spanning from the basal layer to the spinosum, granulosum, and stratum corneum (Moreci & Lechler, 2020) (**Figure 1**). In contrast, the dermis is primarily characterized by the presence of extracellular matrix (ECM) and fibroblasts. It also serves as a niche for immune cells, including dendritic cells (DC), mast cells, macrophages, and T-lymphocytes.

Moving deeper to the skin's foundation, the dermis, this layer lies beneath the epidermis and plays a crucial role in providing structural and nutritional support. The dermis consists of two sublayers, which are the papillary dermis and the reticular dermis, each differing in the density and arrangement of collagen fibers, blood vessels, and cellular components. The primary cell type in the dermis is the fibroblast, which assumes the responsibility of synthesizing and maintaining the ECM. The ECM, in turn, imparts strength, elasticity, and hydration to the skin.

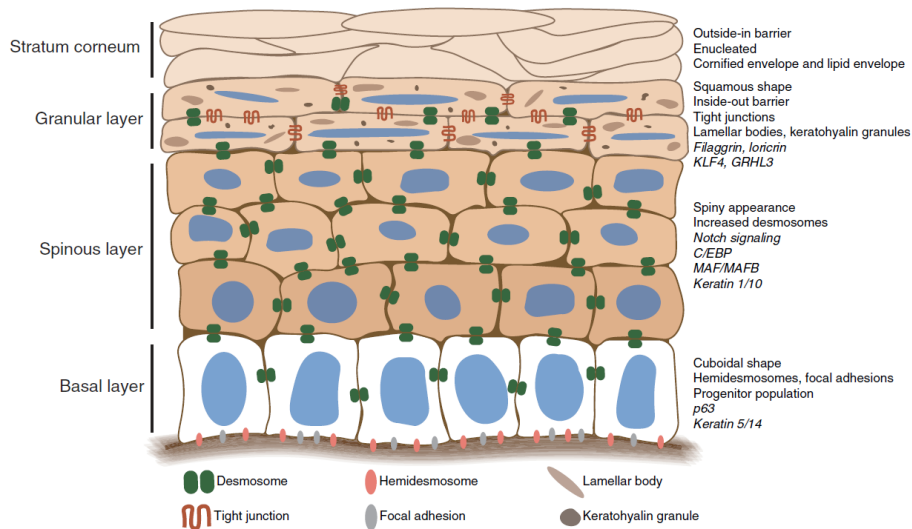


**Figure 1. The layers and components of the epidermis including the markers and proteins expressed in each layer.** The basal layer, spinous layer, granular layer, and stratum corneum were depicted in the illustration. Moreover, the desmosome, hemidesmosome, lamellar body, tight junction, focal adhesion, and keratohyalin granule, which are the tight junction proteins are indicated. The illustration is taken from Moreci & Lechler (Moreci & Lechler, 2020).

The ECM, a prominent component of the dermis, encompasses collagens, proteoglycans, glycosaminoglycans, elastin, laminins, fibronectins, and other vital proteins. Fibroblasts, as the primary cellular architects, are the major contributors to the production of these crucial proteins (Karamanos et al., 2021). Collagen, in particular, assumes a central role, with types I, II, III, and IV being the primary variants synthesized by fibroblasts, where types I and IV predominate in the skin (Matei et al., 2019; Prockop, 1982). Collagen type I, classified as fibril-forming collagen, lends mechanical strength to tissues, while collagen type IV adopts a unique role as a network-forming collagen (Kadler et al., 2007). The distinctive triple-helix structure of type I collagen contributes to tissue strength (Bella & Hulmes, 2017), whereas type IV collagen assembles into a two-dimensional reticular network, distinct from the typical fibrillar structure seen in other collagen types (**Figure 2**). This network provides critical structural support at the basement membrane, the boundary that demarcates the epidermis from the dermis (Onursal et al., 2021).

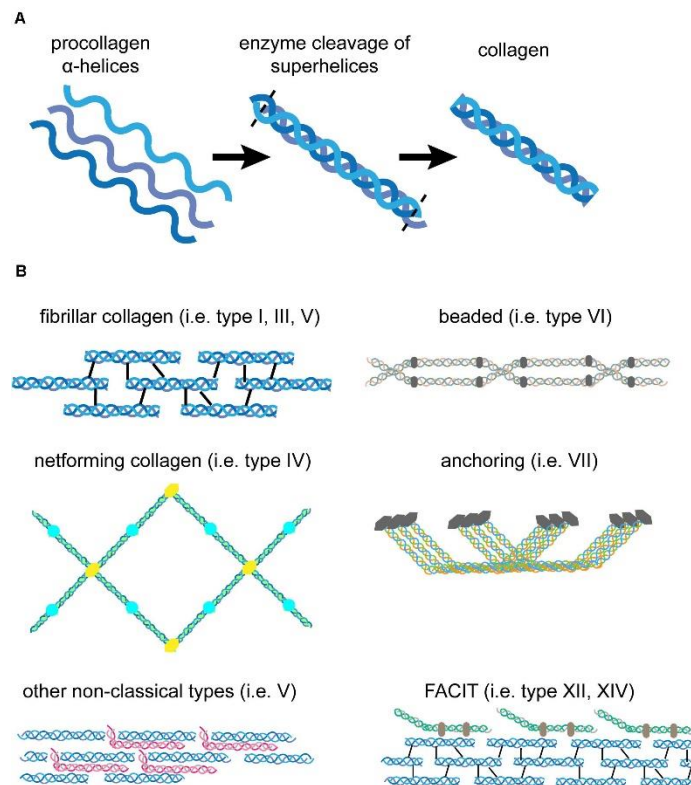


**Figure 2. Collagen structures and provides an example of collagen that exhibits this arrangement. A)** Indicate the forming of collagen from procollagen. **B)** The different structures of collagen; fibrillar collagen, beaded filament collagen, netforming collagen, anchoring fibril, and fibril associated collagens with interrupted triple helices (FACIT). The illustration is taken from Pfister et al. (Pfisterer et al., 2021).

The reticular dermis, located beneath the papillary dermis, is predominantly composed of dense irregular connective tissue characterized by the prevalence of type I collagen and a proportion of elastic fibers. This layer not only endows the skin with strength and elasticity but also accommodates various skin appendages, including hair follicles, sweat glands, sebaceous glands,

arrector pili muscles, and sensory receptors (**Figure 3**). The reticular dermis houses a deep vascular plexus branching into capillary loops within the papillary dermis. Additionally, it features free nerve endings extending from the reticular dermis to the epidermis, providing the skin with sensory function (**Figure 3**). Notably, reticular fibroblasts can differentiate into adipocytes, which are subsequently deposited into the subcutaneous layer of the skin (Driskell et al., 2013).

The papillary dermis, situated immediately beneath the epidermis, is characterized by loose connective tissue, which forms projections known as dermal papillae. These dermal papillae

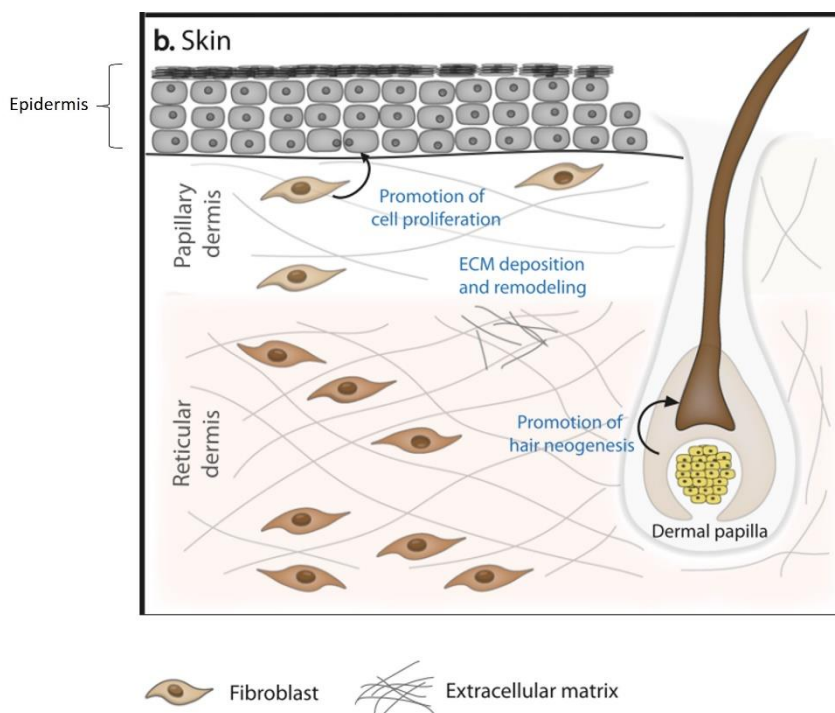


**Figure 3.** The reticular dermis and papillary dermis within the dermal layer and the rough indication of epidermis. The function of fibroblasts was included. The hair follicle, dermal papilla, and the extracellular matrix were depicted. The illustration was adapted from Gomes et al. (Gomes et al., 2021)

interlock with epidermal ridges. Type III collagen and elastic fibers are the primary constituents of papillary dermis, along with papillary fibroblasts, mast cells, macrophages, and other immune cells (**Figure 3**). Capillary loops within the papillary dermis supply blood to the epidermis and play a role in temperature regulation. Fibroblasts in this layer predominantly synthesize collagen type III, glycosaminoglycans, and proteoglycans (Smith & Melrose, 2015).

Although it remains unclear how different fibroblast subtypes contribute to supporting keratinocytes in the epidermis, fibroblasts, in general, are indispensable for maintaining skin homeostasis. Communication between these two cell types occurs through paracrine signaling mechanisms involving the secretion and reception of soluble mediators such as cytokines, growth factors, and matrix metalloproteinases (MMPs). These factors regulate crucial processes, including

cell proliferation, differentiation, migration, and the synthesis and degradation of the ECM. For instance, keratinocytes secrete interleukin 1 (IL-1), which induces fibroblasts to produce keratinocyte growth factor (KGF) and metalloproteinases. KGF, in turn, stimulates keratinocyte proliferation and migration. Metalloproteinases play a role in ECM degradation to facilitate wound closure (Russo et al., 2020).

Ascending through the skin layers, the dermal-epidermal junction (DEJ) marks the critical interface between the epidermis and the dermis beneath. The DEJ is pivotal for skin homeostasis, supporting epidermal stem cell niches, regulating the cellular microenvironment, and segregating fibroblasts from keratinocytes. Its structure features a basement membrane composed of the thinner lamina lucida, housing  $\alpha 6\beta 4$  integrins and bullous pemphigoid (BP) 180, and the denser lamina densa, containing collagen type IV, laminin, nidogen, and perlecan (Goletz et al., 2017).

In the stratum basale, keratinocyte stem cells maintain their pluripotency via the expression of p63 and active Notch and Wnt (Wingless/Integrated) signaling pathway (Nair & Krishnan, 2013; Okuyama et al., 2004; Pellegrini et al., 2001). P63 is key in regulating epidermal development by suppressing differentiation-promoting genes, while Wnt/ $\beta$ -catenin signaling is crucial for stem cell vitality and proliferation (Bonnet et al., 2021; Koster et al., 2004; Kouwenhoven et al., 2015). Additionally, the Notch pathway, triggered by interactions with neighboring cell ligands, aids in sustaining proliferation and inhibiting differentiation (Nguyen et al., 2006).

Keratinocyte differentiation is intricately regulated by various signaling pathways and molecular cues, with one significant factor being the downregulation of the E-cadherin signaling pathway. E-cadherin-mediated cell adhesion in the stratum basal helps to maintain the undifferentiated state of keratinocytes by promoting cell-cell adhesion and preventing migration (P. Young et al., 2003). The downregulation of E-cadherin signaling weakens cell-cell adhesion, allowing keratinocytes to detach from their neighbors and be pushed upwards as cells proliferate (Gutowska-Owsiak et al., 2020).

As keratinocytes ascend from the basal layer into the stratum spinosum, Wnt and Notch signaling decrease due to reduced ligand availability and p63 downregulation (N. Wu et al., 2012). This reduction permits activation of differentiation-associated transcription factors like Kruppel-like factor 4 (KLF4) and grainyhead-like transcription factor 3 (GRHL3). KLF4 competes with p63 for DNA binding sites, inhibiting p63 transcription (Cordani et al., 2010), while GRHL3 collaborates with RE1-Silencing Transcription (REST) to suppress migration inhibitors, promoting keratinocyte differentiation and migration (X. Chen et al., 2021; Klein et al., 2017). Additionally, calcium plays a crucial role in supporting these transcription factors and keratinocyte differentiation (Bikle et al.,

2012). In the basal layer, expressions of cytokeratin 5 (CK5), cytokeratin 14 (CK14), and p63 are typically observed, where CK14 and CK5 help maintain epidermal structure and regulate basal keratinocyte proliferation and differentiation (Alam et al., 2011; Feng & Coulombe, 2015; Jiang et al., 2020).

As keratinocytes progress to the stratum spinosum, changes in desmosomes from DSC2/3 and DSG2/3 to DSC1 and DSG1/4 occur, influenced by AP-1 in response to calcium and growth factors, enhancing tight junctions (L. Müller et al., 2021; Ng et al., 2000). AP-1 and Notch pathways also boost the expression of involucrin and filaggrin, crucial for forming a resilient cornified envelope and aggregating keratin for structural support (Adhikary et al., 2004; C. A. Young et al., 2017). Additionally, cytokeratin 1 (CK1) and cytokeratin 10 (CK10) predominate in the stratum spinosum, marking this layer (Maytin et al., 1999; Törmä, 2011).

The next layer is the stratum granulosum, which the differentiating keratinocytes from stratum spinosum was driven by the higher calcium level to become more differentiated and increase structural protein synthesis such as loricrin (Adams et al., 2015; Elias et al., 2002). During this phase, filaggrin, involucrin, and loricrin combine to form specialized organelles known as keratohyalin granules (Steinert & Marekov, 1995). The most common markers that can be used to characterize the stratum granulosum are filaggrin, loricrin, involucrin, and the presence of keratohyalin granules. Keratinocytes in this stage have started to become cornified, which can be described by the cells becoming more compact caused by numeral factors, including the cross-link of the proteins, the loss of organelles and nuclei, and the synthesis of lipids (Candi et al., 2005). These processes ensure the impermeability of the skin to potentially harmful substances.

Fully cornified keratinocytes in the stratum corneum have flattened out and stacked together to form the outermost layer of the skin. This layer comprises 15 to 20 layers of compressed corneocytes, notable for their lack of nuclei and cell organelles, which enhance their protective function. Instead, their cytoplasm is rich in filamentous keratin, which imparts mechanical strength (Matsui & Amagai, 2015).

The absence of nuclei in the stratum corneum results from the degradation of nuclear DNA during cornification, involving several pathways (Akinduro et al., 2016; Gdula et al., 2013; Yamamoto-Tanaka et al., 2014). A dense network of cross-linked proteins is formed by transglutaminases acting on structural proteins like involucrin and loricrin, catalyzing the formation of  $\epsilon$ -( $\gamma$ -glutamyl) lysine isopeptide bonds (Tharakan et al., 2010). The stratum corneum also consists of a lipid matrix located in the spaces between corneocytes. The major lipids in the stratum corneum are ceramides (CER), cholesterol (CHOL), and free fatty acids, which have different molecular structures and chain

lengths. One of the most unique and essential lipids is the  $\omega$ -acylceramide CER[EOS], which has a long fatty acid chain attached to the sphingosine base. CER[EOS] is thought to be essential for skin barrier properties by inducing the formation of a long-periodicity phase of 130 Å (LPP), which is a highly ordered lipid arrangement that minimizes water permeability (Kessner et al., 2008). The source of lipids found in the stratum corneum is mainly from the lamellar bodies, which are secretory vesicles produced by the keratinocytes in the granular layer just below the stratum corneum (Menon et al., 2012).

The lamellar bodies within the granular layer contain various lipids, enzymes, and antimicrobial peptides. Upon fusion with the plasma membrane of keratinocytes, these lipids undergo several modifications, including hydrolysis, desaturation, and acylation, to form the final lipid composition of the stratum corneum (Vietri Rudan & Watt, 2022). The arrangement of lipids in the stratum corneum is also influenced by cell signaling pathways, such as the peroxisome proliferator-activated receptor (PPAR) pathway, which regulates lipid synthesis and metabolism in the skin (Sertznig et al., 2012). Ultimately, the stratum corneum's remarkable attributes are the result of the coordinated efforts of keratinocytes, their intricate differentiation processes, and the reinforcement of barrier function by lipids and proteins produced in the stratum granulosum, creating a cohesive and protective layer on the skin's surface.

In the intricate tapestry of skin biology, the epidermis and dermis, each with distinct layers and cell populations, harmoniously collaborate to provide the body with the first line of defense and structural integrity.

## 1.2 The Skin as an Immune Organ

The skin serves not only as the body's primary barrier against environmental threats but also as a key player in the immune response. This largest organ of the body is equipped with a sophisticated network of immune cells that orchestrate innate and adaptive immune responses, crucial for maintaining overall skin health and integrity. Among these immune cells, LC, DC, and T-lymphocytes play pivotal roles in skin immunology, each contributing uniquely to immune surveillance and response.

LC are epidermal-resident antigen-presenting cells (APC) that form a network across the basal and suprabasal layers of the epidermis. As professional APCs, they are pivotal in the initiation and regulation of adaptive immune responses. They express high levels of major histocompatibility complex (MHC) class II molecules and co-stimulatory molecules, which are essential for T-lymphocyte activation. Upon antigen uptake and processing, LCs undergo maturation and migrate

to regional lymph nodes to present antigen peptides to naïve T-lymphocytes, thus priming the adaptive immune response. Their role is particularly critical in the context of contact hypersensitivity and pathogen entry through cutaneous routes (Nakajima et al., 2012).

Dendritic cells (DC) in the dermis are phenotypically diverse and functionally versatile. They patrol the dermal compartment and, like LC, are adept at antigen capture and presentation. Dermally-located DCs include subsets such as dermal interstitial DC, which are characterized by their expression of CD11c and MHC class II. These cells are crucial for the induction of immune tolerance under steady-state conditions and potentiate T-lymphocyte responses under inflammatory conditions. The migration of activated DCs to lymph nodes facilitates the polarization of T-lymphocyte responses, which can lead to different immunological outcomes based on the context and nature of the antigen (Merad et al., 2008).

T-lymphocytes in the skin include resident memory T-lymphocytes (TRM) and infiltrating effector T-lymphocytes, each playing distinct roles in immune surveillance and response. Upon activation by APCs, naïve T-lymphocytes differentiate into various effector subtypes, including Th1, Th2, Th17, and cytotoxic T-lymphocytes (CTLs), each orchestrating specific immune functions ranging from pathogen clearance to inflammation. Notably, TRMs persist in the skin and provide localized immune protection against previously encountered antigens, contributing to the skin's memory immune response. The interaction between skin-resident T-lymphocytes and other immune cells is mediated through cytokine and chemokine signaling, which is crucial for the recruitment and activation of immune cells during inflammatory responses (Clark, 2010).

Together, LC, DC, and T-lymphocytes constitute a dynamic and interdependent system within the skin's immune landscape. They ensure the skin can rapidly and effectively respond to infections, environmental insults, and other challenges, highlighting the complexity and importance of skin immunology.

## 1.3 Immunology of Skin Sensitization

### 1.3.1 Sensitization Phase

Skin sensitization is a term used to describe the skin's inflammatory response to chemicals. The chemical that could trigger such a response is identified as a skin sensitizer. Although skin sensitization can be mainly seen from the inflammatory signs on the skin, such as redness, the sensitization has already started before the inflammation occurs. There are two phases of skin sensitization, the first one is the sensitization phase, and the second one is the elicitation phase (**Figure 4**) (Rustemeyer et al., 2011).

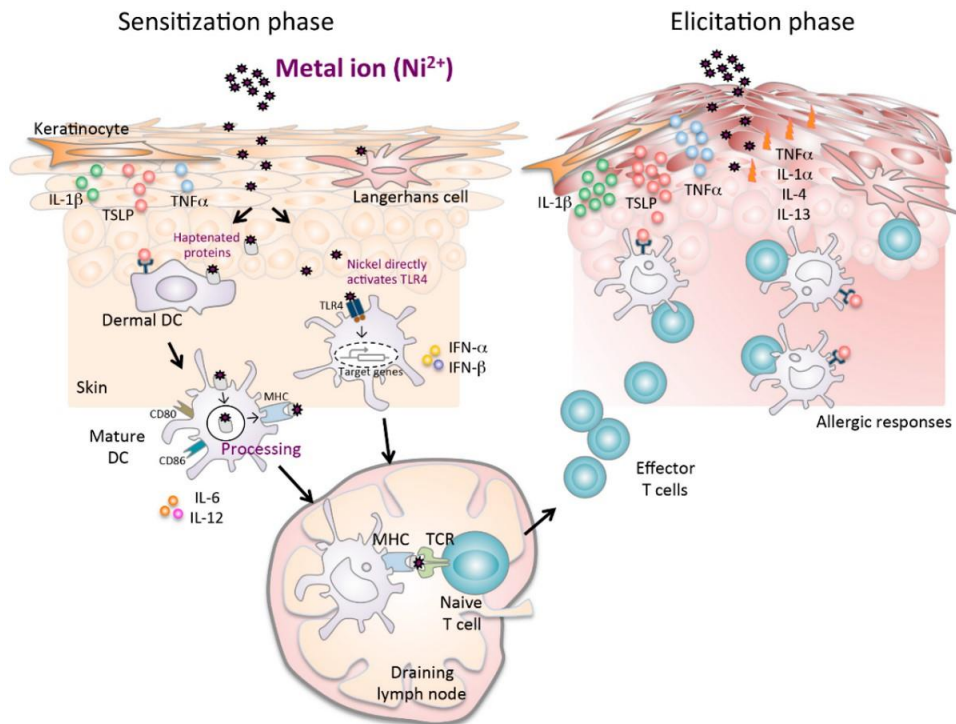


**Figure 4. The immune response to a metal ion in the context of skin sensitization, encompassing both the sensitization and elicitation phases.** It commences with the penetration of the hapten or ion through the skin, followed by the haptening process involving proteins and the subsequent responses of keratinocytes, Langerhans cells (LC), and dermal dendritic cells (DCs). The maturation of LC and DC is vividly depicted, highlighting their pivotal roles. Furthermore, the illustration elucidates the migration of antigen-presenting cells (APC) to the lymph nodes, where they present antigens to naïve T-lymphocytes. These naïve T-lymphocytes subsequently differentiate into effector T-lymphocytes, actively participating in the front-line response during the elicitation phase of skin sensitization. The source of illustration: (Lim et al., 2019).

It was first confirmed that, in the sensitization phase, it is required for the low molecular weight substance of less than 500kDa (hapten) to bind to the protein in the skin through a covalent bond (Aleksic et al., 2009; Seppälä & Mäkelä, 1998). The process of haptens binding to unspecific skin proteins, known as protein haptening, is a key step in developing inflammatory reactions (Erkes & Selvan, 2014; Mayer, 1956; Singleton et al., 2016). This process involves the formation of a covalent bond between the electrophilic components of the hapten and the nucleophilic side chains of amino acids in the target proteins within the skin such as lysine amino group (Lys), cysteine sulfhydryl group (Cys), and histidine imidazole group (His) (Divkovic et al., 2005; Lemus & Karol, 1985). Electrophilic components are parts of the hapten that are attracted to electrons and can accept an electron pair. On the other hand, nucleophilic side chains of amino acids are parts of the protein that can donate an electron pair (Aleksic et al., 2007; Kusharyoto et al., 2002). The interaction between these two components results in a covalent bond, which is a type of chemical bond that involves the sharing of electron pairs between atoms and forms a complex structure between hapten and proteins (Chipinda et al., 2011). This complex structure can be recognized by epidermal LC, keratinocytes, and dermal DC.

Not all chemicals can act as haptens, for example, if they are too big to penetrate the skin or if they are not reactive enough to form a covalent bond with proteins (Elahi et al., 2004; Wass & Belin, 1990). The chemicals that can act as a haptens can be categorized as a haptens, pre-haptens, and pro-haptens. As mentioned, haptens can form a complex with proteins directly, while pre-haptens substances require non-metabolic activation for the substances to bind to the protein, and the metabolic activation is necessary for pro-haptens to become immunogenic (Aptula et al., 2007; Karlberg et al., 2013). The activation of pre-haptens most often occurs via a radical pathway with the formation of highly sensitizing hydroperoxides as the primary oxidation products. Most of these hydroperoxides are unstable. Often, they cannot be detected and are only identified as a result of secondary oxidation products being formed. Pre-haptens are actuated abiotically outside the skin substantially by autoxidation (Casati et al., 2016). Autoxidation is a process that involves the response of a substance to oxygen in the air. This process can lead to the conformation of ROS, which can also result in the transformation of pre-haptens into haptens (Sköld et al., 2004). In addition to autoxidation, pre-haptens can also be actuated by exposure to ultraviolet (UV) light. UV light exposure can lead to chemical bonds in the pre-haptens to break, leading to the conformation of reactive species that can form a complex structure with proteins (Urbisch et al., 2016). Pro-haptens are substances that are initially non-reactive and non-allergenic. However, when they encounter the skin, they can undergo a biochemical transformation to become haptens, which are capable of triggering an immune response. This transformation process is typically facilitated by enzymes present in the skin, such as the Cytochrome P450 enzymes (Bergström et al., 2007; Gerberick et al., 2009; Hansson et al., 1995).

In the epidermis, the detection of haptens-protein complexes involves LC and keratinocytes. The epidermal layer primarily comprises keratinocytes, which account for approximately 90% of its composition (McGrath et al., 2008). However, the role of keratinocytes extends beyond providing structural integrity; they also play a pivotal role in the skin's immune responses (Mann et al., 2001; McCully et al., 2012; Tamoutounour et al., 2019).

Keratinocytes can react to skin sensitizers through a currently known pathway, which is the Kelch-like ECH-associated protein 1 (Keap1)- nuclear factor erythroid 2-related factor 2 (Nrf2)- antioxidant response element (ARE) pathway, and a less known pathway; transient receptor potential (TRP) channels. To combat these threats, keratinocytes employ a system involving the Keap1-Nrf2-ARE pathway. Keap1 serves as a sensor for cellular stress, including haptens exposure, and functions as a repressor of Nrf2 under normal conditions. When keratinocytes encounter haptens, a cascade of events is initiated. Haptens can covalently modify the Cys residues on Keap1 (Wakabayashi et al., 2004). In response to this modification, Nrf2 is released from Keap1

repression, allowing it to translocate into the nucleus of keratinocytes. In the nucleus, Nrf2 activates the ARE, which leads to the upregulation of several target genes, including the one transcribing IL-8, HMOX1, and reductases (El Ali et al., 2013).

TRP channels play a significant role in human keratinocytes. Keratinocytes express various sensory receptors present on sensory neurons, such as receptors of the TRP family. These include Transient Receptor Potential Vanilloid 1 (TRPV1), a primary transducer of painful heat and itch transduction, Transient Receptor Potential Vanilloid 4 (TRPV4), which is depicted as a heat sensor, while Transient Receptor Potential Melastatin (TRPM) and Transient Receptor Potential Ankyrin 1 (TRPA1) are both of ion channels (Talagas & Misery, 2019). Recent studies have demonstrated that the specific and selective activation of TRPV1 on keratinocytes is sufficient to induce pain (Talagas & Misery, 2019). Similarly, the targeted activation of keratinocyte-expressed TRPV4 elicits itch and the resulting scratching behavior, although TRPV4 is classically known as a heat sensor (Y. Chen et al., 2016; Darby et al., 2016). TRPV1 is a non-selective channel receptor widely expressed in skin tissues, including keratinocytes, peripheral sensory nerve fibers, and immune cells. It is activated by various exogenous or endogenous inflammatory mediators, triggering neuropeptide release and neurogenic inflammatory response (Xiao et al., 2023). In the epidermis, TRPM contributes to keratinocyte differentiation by regulating calcium influx. Calcium ions ( $Ca^{2+}$ ) released from intracellular stores as well as influx through the plasma membrane are essential to the skin function (M. Wang et al., 2021). TRPA1 is also one of the calcium ion channel and temperature sensors. However, it has also been found to be able to recognize electrophiles through the binding of it with key residues on the channel itself such as cinnamaldehyde, 2,4,6-trinitrochlorobenzene (TNBS), and 2,4-Dinitrochlorobenzene (DNCB) (Engel et al., 2011; Ishibashi et al., 2008; Sun & Chen, 2007; H. Wu et al., 2022). There could be potentially more pathways to be discovered. Keratinocytes play more of an enhancer role in sensing the haptens by secreting inflammatory cytokines, which then amplify the inflammatory response from both epidermal LC and dermal DC, as well as recruiting effectors  $CD4^+$  and  $CD8^+$  T-lymphocytes to the site (Jiang et al., 2020).

In parallel to the binding of electrophile substances or haptens to the keratinocytes, the hapten-protein complex will be recognized by the LC and dermal DC. These two are similar as they function as APCs, but LCs are located in the epidermis and are most prominent in the stratum spinosum, while DCs are situated in the dermis layer (BERMAN et al., 1983; Clayton et al., 2017). Both DCs and LCs extend their protrusions and create an immune network within each layer. Once the APCs encounter foreign substances, they engulf them through a process called phagocytosis (Blum et al., 2013). Within the APCs, these pathogens and foreign substances are broken down into smaller protein fragments in specialized compartments called lysosomes (Blander & Medzhitov, 2006).

These protein fragments, known as antigens, are then loaded onto a protein called MHC molecules. MHC molecules come in two classes, which are MHC-I for intracellular antigens and MHC-II for extracellular antigens. The loading of MHC-I molecules is facilitated by the proteasome, which degrades intracellular proteins into peptides, while MHC-II loading is aided by a protein complex called the invariant chain (Roche & Furuta, 2015). Once loaded, MHC molecules transport the antigenic peptides to the DC's surface, where they are presented to T-lymphocytes, initiating the adaptive immune response. In addition to MHC-II, LCs can be characterized by the expression of CD1a and CD207 (Langerin). CD1a is a monomorphic antigen-presenting molecule that binds the self and foreign cellular lipids for display to T-lymphocytes. CD207, also known as Langerin, is part of the C-type lectin receptor (CLR) family, which plays roles in binding pathogens (Mizumoto & Takashima, 2004). While DCs share the character of CD1a expression, they possess CD209 instead of CD207. CD209, also known as Dendritic Cell-Specific Intercellular adhesion molecule-3-Grabbing Non-integrin (DC-SIGN), is a type I transmembrane protein and a member of CLR that facilitates the recognition of pathogens (J. Li et al., 2022; Rahimi, 2020).

Once the APCs have processed antigen, they become mature, which can be characterized by the expression of CD83 and CD86. CD83 is a type I membrane protein that belongs to the immunoglobulin superfamily, which can be found on the surface of matured DC or soluble form secreted by matured APCs as well, the roles of CD83 are not limited to being a co-stimulatory molecules to bind with CD83 ligand on T-lymphocytes (Breloer & Fleischer, 2008), but also involve in regulating the expression of MHC-II and CD86 by effectively obstructing the interaction between MHC-II and the ubiquitin ligase known as MARCH1 which in turn prevent the degradation of MHC-II and CD86 (Tze et al., 2011). CD86 (B7-2) is a type I transmembrane glycoprotein from the superfamily of immunoglobulin. It is a co-stimulatory molecule that can often be found together with CD80 (B7-1), although their existence is independent of each other. The ligand of these molecules on T-lymphocytes is CD28, and cytotoxic T-lymphocyte-associated Protein 4 (CTLA-4), which are important for T-lymphocytes activation and survival (Maney et al., 2014; Y. Wang et al., 2011). Upon maturation, APCs will start presenting antigen to the recruited cells, but when the antigen is not recognized, they will start to migrate to the lymph node (Mbongue et al., 2014). The migration of LCs to the lymph node occurs after the initial encounter with inflammatory triggers such as haptens, TNF- $\alpha$ , IL-18 and IL-1 $\beta$  LCs move to the dermis through the play of CXC-chemokine receptor 4 (CXCR4) – CXC-chemokine ligand 12 (CXCL12), without depending on C-C motif chemokine receptor type 7 (CCR7) (Gallego et al., 2021; Villablanca & Mora, 2008). Following this, LCs and DCs situated in the dermis heighten their CCR7 expression, facilitating entry into the lymphatic system and onward journey toward the lymph node (Ohl et al., 2004).

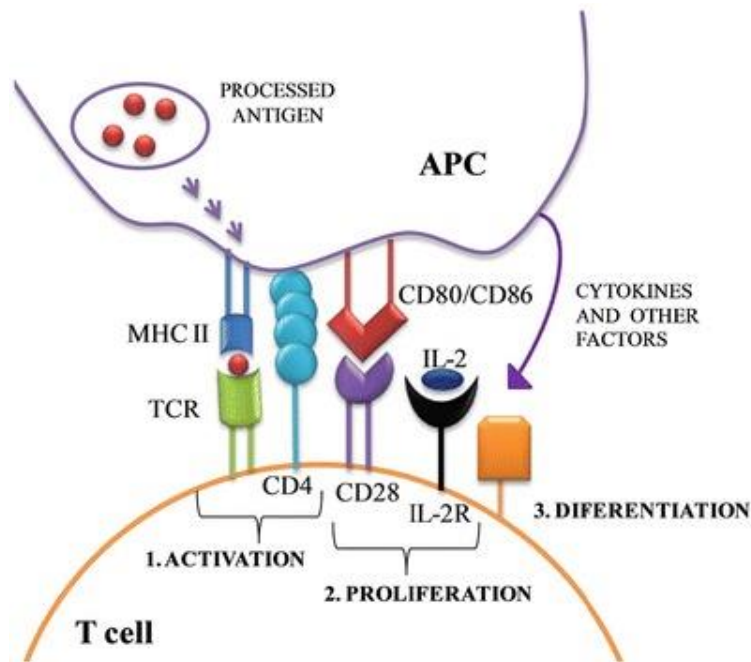


**Figure 5. The immune synapse between antigen-presenting cells (APC) and T-lymphocytes during the process of antigen presentation.** The figure outlines the three key steps of T-lymphocyte differentiation. Step 1 is the activation by major histocompatibility complex II (MHC-II) loaded with antigen binds with the T-cell receptor (TCR). Step 2 is the proliferation. During the second step, T-lymphocyte proliferation occurs as CD80/CD86 molecules from the APC match with CD28 on T-lymphocytes, and interleukin-2 (IL-2) binds to the IL-2 receptor on T-lymphocytes. Step 3 is the differentiation. In the final step involves the differentiation of T-lymphocytes into distinct character types, which is guided by cytokines and other factors. The figure is take from Lozano-Ojalvo et al. (Lozano-Ojalvo et al., 2015).

In the lymph node where the APCs encounter naïve CD4<sup>+</sup> T-lymphocytes, the antigen on MHC-II is presented to the T-lymphocytes for the T-lymphocytes to become activated. The activation of T-lymphocytes requires three signals. The first one is the binding of MHC-II with T-lymphocytes receptor (TCR) or CD3, and the second one is the binding of CD28 to CD80/CD86, the third signal is the binding of IL-2 to CD25 or IL-2 receptor (Joglekar & Li, 2021; Tai et al., 2018). Upon successful recognition and co-stimulation, intracellular signaling cascades are initiated within the T-lymphocyte. Key players in this phase include the protein kinase Lck, which phosphorylates the immunoreceptor tyrosine-based activation motifs (ITAMs) on the CD3 subunits of the TCR complex (Bozso et al., 2020). This leads to the recruitment and activation of Zeta-chain-associated protein kinase 70 (ZAP-70), which further phosphorylates downstream molecules, triggering multiple signaling pathways (Tewari et al., 2021). One of these pathways results in an increase in intracellular calcium levels, a critical factor in T-lymphocyte activation (Erdogmus et al., 2022). Elevated calcium activates the phosphatase calcineurin, which, in turn, is essential for the activation of the transcription factor NFAT (Nuclear Factor of Activated T-lymphocytes) (Wiese et al., 2017). Active NFAT translocates to the nucleus, cooperates with other transcription factors, and initiates the expression of IL-2 and other cytokines (J. U. Lee et al., 2018) (Figure 5).

IL-2 is a central cytokine in T-lymphocyte activation, as it stimulates the proliferation and differentiation of T-lymphocytes. Upon stimulation, CD4<sup>+</sup> upregulates CD69, which is a glycoprotein that is involved in T-lymphocyte migration and proliferation (Koyama-Nasu et al., 2022; López-Cabrera et al., 1993; Mita et al., 2018). Notably, CD4<sup>+</sup> T-lymphocytes can produce IL-2 themselves for their own IL-2 receptor (CD25), acting in an autocrine manner to fuel their own expansion (Ross & Cantrell, 2018). Moreover, naïve CD4<sup>+</sup> T-lymphocytes are known to express CD45RA and CCR7, but after the encounter with APCs, they change the pattern of characterization markers. CD45RA is a protein tyrosine phosphatase receptor associated with resting T-lymphocytes (Trowbridge & Thomas, 1994). The activation of T-lymphocytes leads to the loss of CD45RA expression, indicating a transition of naïve to effector or memory T-lymphocytes. CCR7 is known to guide naïve T-lymphocytes from the thymus into the lymph node (Britschgi et al., 2008; Bromley et al., 2005), which will be reduced upon activation to prevent T-lymphocytes to migrate back to lymphoid organs. The subset of T-lymphocytes can be considered as shown in the figure (Mahnke et al., 2013; R. Okada et al., 2008; Tian et al., 2017) (**Figure 6**).

As a result of activation, the activated CD4<sup>+</sup> T-lymphocytes undergo clonal expansion, yielding a substantial population of effector T-lymphocytes that can differentiate into various subsets, like T-helper cells 1 (Th1), T-helper cells 2 (Th2), T-helper cells 17 (Th17), or regulatory T-lymphocyte (Treg) cells, or memory T-lymphocytes depending on the specific signals and cytokines in their

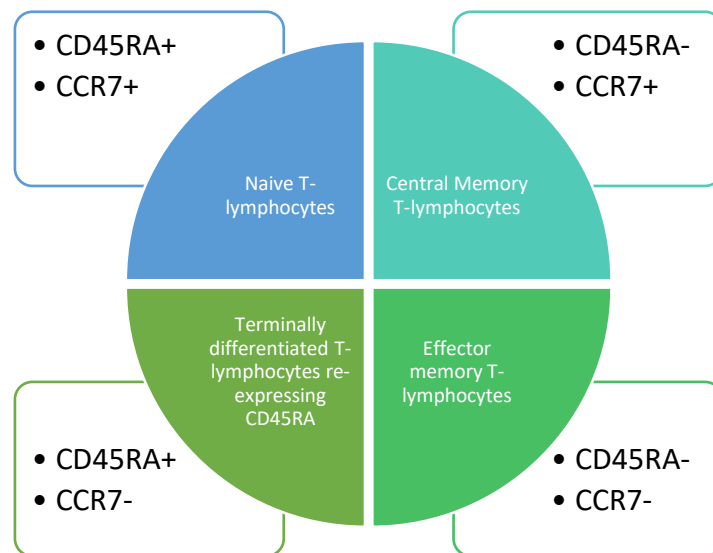


**Figure 6. T-lymphocyte subsets based on the expression of CD45RA and CCR7.** The upper left quadrant represents naïve T-lymphocytes, while the lower left quadrant depicts terminally differentiated re-expressing CD45RA (TEMRA) T-lymphocytes. Central memory T-lymphocytes are situated in the upper right quadrant, and effector memory T-lymphocytes reside in the lower right quadrant. Specifically, naïve T-lymphocytes are characterized by the presence of both CD45RA and CCR7. In contrast, TEMRA T-lymphocytes exclusively express CD45RA. Central memory T-lymphocytes express CCR7 only, and effector memory T-lymphocytes lack both CD45RA and CCR7 expression.

microenvironment (Sjaastad et al., 2021). Later on, the memory T-lymphocytes remain in the lymph node while the effector T-lymphocytes go back to the circulation or tissues depending on the type of effector T-lymphocytes itself and are ready to act once the antigen comes into contact with the skin for the second time (Ho & Kupper, 2019; Sallusto et al., 2004).

### 1.3.2 Elicitation Phase

The elicitation phase is the phase when the hapten comes into contact with the skin for the second time. The binding of the hapten to the protein in the skin occurs in similar steps as in the sensitization phase. APCs take up the hapten-protein complex and present it again with MHC-II. Activated LC and keratinocytes, the predominant cells in the epidermis, produce chemokines as a response to hapten exposure (Rustemeyer, 2022). For instance, C-C motif chemokine ligand 27 (CCL27-also known as cutaneous T-lymphocyte attracting chemokine, CTACK) is produced by keratinocytes, while C-C motif chemokine ligand 17 (CCL17) is produced by DC. The chemokines CCL27 and CCL17 act as chemoattractants specifically for T-lymphocytes, including CD4<sup>+</sup> T-lymphocytes, which are critical in the elicitation phase of skin sensitization (Goebeler et al., 2001). These chemokines bind to their respective receptors (CCR10 for CCL27 and CCR4 for CCL17) on the surface of T-lymphocytes. The lymphocytes are recruited to the site but not in an antigen-specific manner, which will be determined through the binding of APCs and the T-lymphocytes. Once the CD4<sup>+</sup> T-lymphocytes match with the antigen, they secrete inflammatory cytokines such as interferon-gamma (IFN- $\gamma$ ), IL-4, IL-17, and TNF- $\alpha$  (Kathamuthu et al., 2022; Martinez-Sanchez et al., 2018). This cytokine release, particularly in response to IFN- $\gamma$ , prompts keratinocytes to increase their expression of adhesion molecules and cytokines/chemokines (Chieosilapatham et al., 2021; Mestrallet et al., 2021). Consequently, this upregulation further stimulates the recruitment of additional immune cells, including T-lymphocytes, NK cells, macrophages, mast cells, and eosinophils, to the affected site (**Figure 4**).

In conclusion, skin sensitization is a complex immunological process that can lead to allergic contact dermatitis, a common occupational and environmental disease. The identification and characterization of skin sensitizers are essential for the prevention and management of this condition, as well as for the development of alternative methods to animal testing for testing the sensitization potential of substances. Several *in vitro* and *in silico* approaches have been proposed to assess the skin sensitization potential of chemicals, but none of them can fully capture the mechanistic diversity and variability of human responses. Therefore, a combination of multiple methods and integrated testing strategies is recommended to achieve a more accurate and reliable prediction of skin sensitization hazards.

## 1.4 The Growing Importance of Skin Sensitization Assessment

Skin sensitization is a growing health concern driven by chemicals that trigger allergic reactions upon skin contact. The increasing prevalence of allergic diseases, likely attributable to heightened chemical exposure since the industrial era, is a matter of serious concern. For instance, as reported by the European Chemicals Agency (ECHA), millions of Europeans now suffer from sensitivities to chemicals found in textiles and leather goods, with approximately 180,000 new cases emerging each year. These allergies manifest across a spectrum of reactions, ranging from mild skin irritations to severe symptoms, depending on the allergen's potency. Concerning overall skin sensitivity, data reveals that roughly 60-70% of women and 50-60% of men report experiencing some degree of sensitive skin (Farage, 2019).

This escalating trend in skin sensitivity constitutes a pressing health issue that warrants close attention. This has led to the imperative need to develop skin sensitization assays for assessing a substance's potential to induce allergic contact dermatitis, a form of skin inflammation resulting from repeated exposure to an allergen. To better understand and advance the testing of skin sensitizers, the OECD has put forward an AOP outlining four key events occurring during the skin sensitization process (OECD, 2014). Skin sensitization unfolds in two phases, with the initial phase being the induction or sensitization phase. The initial event is the conjugation of haptens from organic chemical substances with skin proteins (KE 1). Simultaneously, an inflammatory response in keratinocytes is provoked by the formation of hapten-protein complexes (KE 2). Subsequently, the protein-hapten complex induces the maturation and migration of epidermal LC and DC (KE 3), which present the antigen to CD4<sup>+</sup> T-lymphocytes, resulting in T-lymphocyte activation and proliferation (KE 4). It is crucial to acknowledge that the process of skin sensitization is remarkably complex, and the AOP provides a simplified representation of the intricate sequence of events (**Figure 7**).

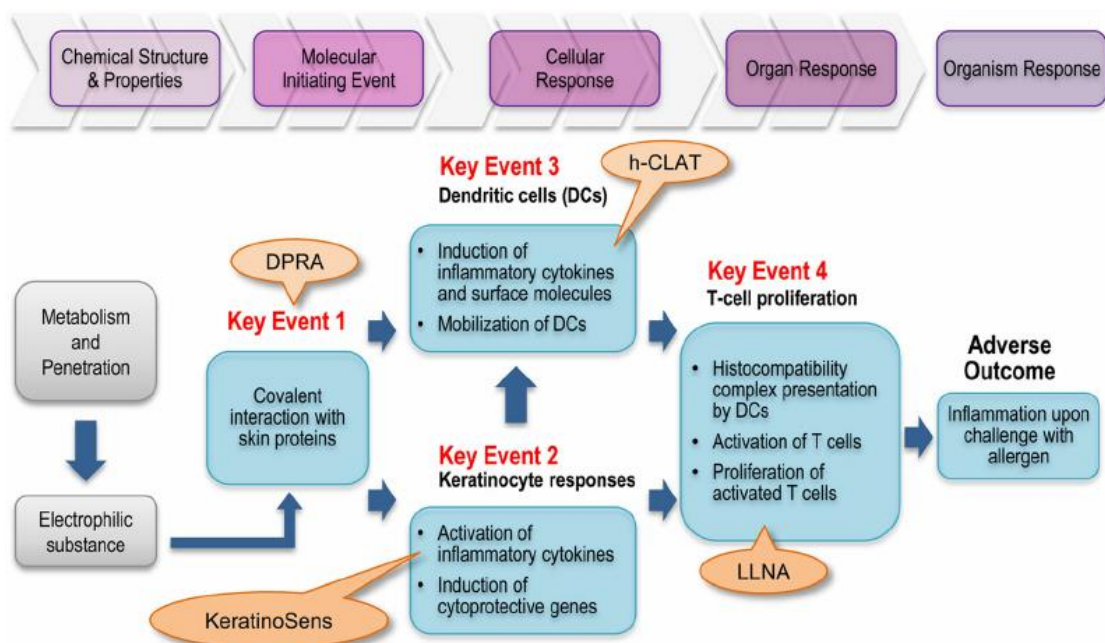


**Figure 7. The adverse outcome pathway (AOP) of skin sensitization, as defined by the OECD.** It presents the four key events, along with their corresponding molecular or cellular responses. Additionally, for each key event, an example of an OECD-approved skin sensitization assay is provided. The figure is taken from Stricklan et al. (Strickland et al., 2016). Acronym explanation: Direct Peptide Reactivity Assay (DPRA), the Human Cell Line Activation Test h-CLAT, and Local Lymph Node Assay (LLNA).

The AOP framework is a vital tool in toxicology, designed to elucidate the sequence of events that occur from a molecular initiating event to an adverse outcome. In the context of skin sensitization, the AOP aids in comprehending the molecular and cellular changes that lead to the development of allergic contact dermatitis. Each key event in the AOP can be explained in greater detail as follows.

KE 1: Conjugation of haptens - This event involves the binding of haptens, which are small electrophilic molecules, to proteins within the skin. It is a pivotal step, as it transforms an otherwise harmless chemical into a potential allergen. The formation of hapten-protein complexes can induce an immune response.

KE 2: Inflammatory response of keratinocytes - When haptens bind to skin proteins, it triggers an inflammatory response in keratinocytes, which are the predominant cell types in the epidermis. This inflammatory response can lead to the release of pro-inflammatory cytokines.

KE 3: Maturation and migration of LCs and DCs - The protein-hapten complexes formed in KE 1 can trigger the maturation and migration of LC in the epidermis and dermal DC. These cells are responsible for capturing antigens and presenting them to immune cells.

KE 4: T-Lymphocyte activation and proliferation - The presentation of antigens by LC and DC to CD4<sup>+</sup> T-lymphocytes initiates T-lymphocyte activation and proliferation. This step is pivotal, as it sets in motion the adaptive immune response characteristic of allergic contact dermatitis.

There are different types of skin sensitization assays *in chemico*, *in vivo*, *in vitro*, and *in silico*. Each type of assay plays a distinct role in assessing skin sensitization potential, offering valuable insights at different stages of the testing process. The variety of available assays ensures a comprehensive evaluation of the sensitization risk associated with various substances, ultimately contributing to better safety assessments. *In chemico* assays utilize chemical methods to evaluate a substance's reactivity with synthetic peptides that mimic skin proteins which is the KE1. For example, the Direct Peptide Reactivity Assay (DPRA) (Bauch et al., 2012; OECD, 2023b), Amino acid Derivative Reactivity Assay (ADRA) (Wanibuchi et al., 2019), and kinetic Direct Peptide Reactivity Assay (kDPRA) (OECD, 2023b) measures the depletion of cysteine or lysine residues in the peptides after incubating them with a test substance. The decrease of these residues signifies the haptentation, the first event of skin sensitization. DPRA is recognized for its ability to assess the skin sensitization potential of chemicals by simulating their interaction with skin proteins, particularly with regard to haptentation—a critical step in the sensitization process (Bauch et al., 2011; OECD, 2023b).

*In vivo* assays employ animals, such as mice or guinea pigs, to observe and evaluate skin responses following the application of a substance. For instance, the LLNA is a widely used *in vivo* assay done in mice that measures the proliferation of lymphocytes in the lymph nodes draining the site of application, which is KE4. LLNA has demonstrated good predictive accuracy and reliability and is considered a robust tool for evaluating the sensitization potential of chemicals (Kimber et al., 1986; OECD, 2010). *In vitro* assays rely on cultured cells or tissues to assess the activation of immune cells, or the expression of biomarkers associated with skin sensitization. For instance, the Human Cell Line Activation Test (h-CLAT) measures the upregulation of CD86 and CD54 molecules on the surface of monocytic cells following exposure to a test substance. h-CLAT is a valuable *in vitro* assay that reflects the molecular and cellular events involved in the early stages of skin sensitization (Ashikaga et al., 2006; OECD, 2023d; Sakaguchi et al., 2009a). *In silico* is the up-and-coming field where the collected experiment data are utilized to develop a program that could predict either just on key event or all key events. The *in silico* models are based on existing open-source databases such as SkinSensDB, Registration, Evaluation, Authorisation and Restriction of Chemicals (REACH), and National Toxicology Program as a source to make predictions (Johnson et al., 2020). This database could be derived either from the *in chemico* assays, *in vivo*, or *in vitro* assays. For example, Quantitative Structure-Activity Relationship (QSAR) models are employed to forecast the sensitization hazard of chemicals by analyzing their structural properties and activity. QSAR models have demonstrated good predictivity for skin sensitization hazard assessment (Yordanova et al., 2019).

Skin sensitization assays are important for assessing the safety of various products, such as cosmetics, drugs, or chemicals, which may encounter human skin. However, there are also some limitations and challenges associated with the existing skin sensitization assays.

*In chemico* assays offer several advantages, making them a valuable component of a weight-of-evidence approach for skin sensitization assessment. Their simplicity, speed, cost-effectiveness, and animal-free nature make them attractive options. These assays can aid in reducing the occurrence of false positive and false negative results. By assessing the reactivity of substances with synthetic peptides that mimic skin proteins, *in chemico* assays provide essential insights into the sensitization potential of chemicals, especially in the context of haptentation. While *in chemico* assays offer valuable data, it is crucial to recognize their limitations. These assays primarily address one aspect of the complex mechanism of skin sensitization, focusing on hapten-protein conjugation. They do not account for other critical factors, such as metabolism, bioavailability, immunogenicity, or individual variability. Therefore, *in chemico* assays cannot be used as standalone methods to predict skin sensitization hazard or risk and must be complemented by other assays that cover different key events in the AOP for skin sensitization.

*In vivo* assays offer unique advantages by providing information on the potency, dose-response relationship, and the potential to induce systemic or local allergic reactions in animals. These assays account for factors like skin metabolism, penetration, and immunological responses, which may not be fully captured by *in vitro* or *in chemico* methods. *In vivo* tests offer a comprehensive view of the sensitization potential of substances. *In vivo* assays have their limitations, including ethical concerns, animal welfare issues, high costs, variability, and limited applicability to certain substances or mixtures. There may also be differences between animal species and humans, affecting the accuracy of predictions. It is evident that the accuracy of the LLNA compared to the human data is approximately 72-78% (Tourneix et al., 2019; van Huygevoort, 2017). Additionally, regulatory restrictions, such as the EU ban on animal testing of cosmetic ingredients (Regulation (EC) No. 1223/2009) and a strong recommendation from the authorities to follow the 3R principle, have led to a shift towards non-animal testing methods. The 3R principle was developed with the aim to Reduce, Refine, and Replace animal testing. These factors underscore the need for the development and validation of alternative methods that can predict skin sensitization potential without animal testing, leading to the emergence of *in vitro* and *in silico* assays.

*In vitro* assays offer ethical, humane, and cost-effective alternatives to animal testing. They are characterized by reduced resource requirements, faster results, and the ability to provide information on the molecular and cellular events underlying skin sensitization. *In vitro* assays play

a crucial role in understanding the early stages of sensitization and are a preferred choice for animal welfare. While *in vitro* assays offer numerous benefits, they may not fully capture the complexity and variability of the skin's immune system. The interactions between the skin and other organs and systems may not be faithfully represented. Additionally, the limited applicability of *in vitro* assays to detect all types of skin sensitizers or account for the exposure conditions of chemicals is a potential drawback. The variance in performance characteristics and validation status across different *in vitro* assays may impact their reliability and acceptance by regulatory authorities. However, it is noteworthy that non-animal methods have shown good predictivity for skin sensitization hazard assessment with a "2 out of 3 Defined Approach" (2o3 DA) prediction model showing accuracies of 90% or 79% compared to human or LLNA data, respectively (Urbisch et al., 2015). The 2 out of 3 prediction model is the practical method to combine different *in vitro* tests targeting different key events together to cover more key events in an experiment.

*In silico* skin sensitization assays are computational methods that use data and models to predict the potential of a substance to cause skin sensitization. These methods have some advantages and disadvantages compared to traditional animal testing or *in vitro* assays. One advantage of *in silico* methods is that they are faster and cheaper than animal testing or *in vitro* assays, which require more time, resources, and ethical approval. *In silico* methods can also provide mechanistic insights into the molecular pathways involved in skin sensitization, which can help identify safer alternatives or design strategies to reduce the sensitizing potential of a substance. Moreover, it has been shown that the *in silico* tools such as QSAR, DEREK Nexus, and six others can predict the skin sensitizers with 70-80% accuracy in comparison to human data (Golden et al., 2021). Despite the advantages, *in silico* methods are constrained by the availability and quality of data and models, limiting their coverage of the various facets of skin sensitization, including individual variability, complex interactions, and long-term effects. These computational methods may have uncertainties and limitations related to their validation and applicability domains, making it essential to exercise caution and combine *in silico* methods with other information sources for robust decision-making.

The importance of research and development in skin sensitization assays is underscored by the need for improved testing methods that overcome current limitations. By striving for more accurate, reliable, and ethical results, researchers can enhance the safety assessment of products and chemicals that interact with human skin, ultimately benefiting public health.

## 1.5 Enhancing Skin Models: Toward Better Skin Sensitization Assays

The development of *in vitro* skin models has been a long-standing goal for researchers in dermatology and tissue engineering. *In vitro* skin models can provide valuable insights into the structure, function, and pathology of human skin, as well as enable drug development and testing. This is comprehensively reviewed elsewhere (Niehues et al., 2018; Rousi et al., 2022; Sarama et al., 2022; Vilela De Sousa et al., 2023). The history of *in vitro* skin models can be traced back to 1981, when the skin graft was created by casting fibroblasts into the collagen lattice, with keratinocytes seeded on top (Bell et al., 1981b). Since then, this method has been employed to create more realistic and complex skin representative assays, such as monolayer cultures, three-dimensional (3D) tissue reconstruction such as reconstructed human epidermis (RHE), and RHS, and skin-on-chip (**Figure 8**).

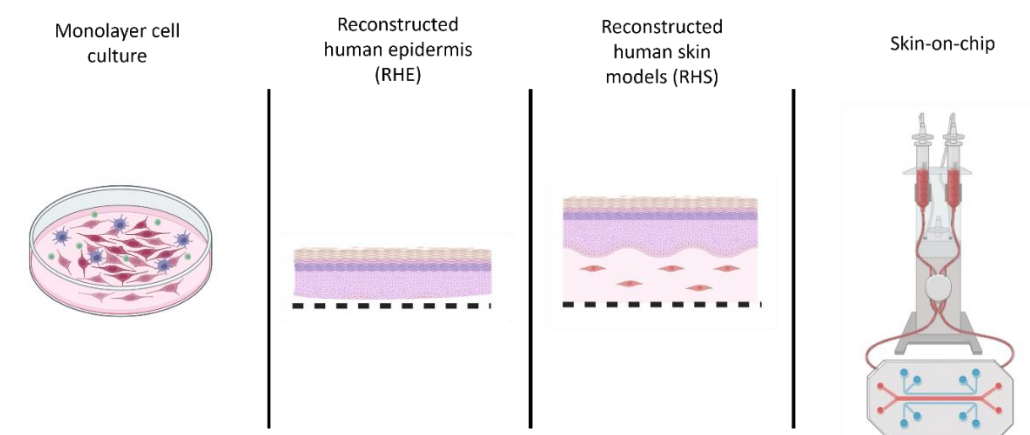


**Figure 8. The differences between each type of model.** From left to right; monolayer cell culture, a reconstructed human epidermis (RHE) containing only epidermis, a reconstructed human skin model (RHS) containing both epidermis and dermis (lower compartment), and skin-on-chip connecting to the perfusion system. Source of figure components: Biorender.com

Monolayer cultures are the simplest form of *in vitro* skin models, where keratinocytes or fibroblasts are grown on a flat surface. These models can be used to study basic cellular processes, such as proliferation, differentiation, and signaling. However, they lack the spatial organization and interactions of native skin. Three-dimensional tissue reconstruction involves the generation of multilayered skin equivalents that mimic the epidermis and/or dermis layers of human skin. These models can be derived from patient cells or genetically modified cells to create disease-specific or personalized skin models.

One of the most common types of 3D skin models is the RHE model, which consists of keratinocytes cultured on a porous membrane. The keratinocytes form a stratified epidermis with a functional stratum corneum, the outermost layer of the skin that provides a barrier against water

loss and external agents. RHE models can be used to test the irritancy, toxicity, and permeability of various substances on the skin (Agonia et al., 2022). However, RHE models do not fully represent the complexity of human skin, as they lack other cell types, such as fibroblasts, melanocytes, and immune cells, which are present in the epidermis, dermis, and hypodermis layers. Fibroblasts are responsible for producing collagen and elastin, the main structural proteins of the skin. Melanocytes produce melanin, the pigment that gives color to the skin and protects it from UV radiation. Immune cells, such as LCs and macrophages, play a role in defending the skin from infections and inflammation.

To overcome these limitations, RHS, which includes both epidermal and dermal components, has been developed. RHS is usually generated by seeding keratinocytes on top of a dermal equivalent, which is a scaffold containing fibroblasts made of collagen or other biomaterials that support the growth of fibroblasts (Bell et al., 1981a). RHS models, with their inclusion of both epidermal and dermal components, hold significant value in skin research. These models more accurately replicate the mechanical properties, vascularization, and innervation found in human skin compared to simpler RHE models. For example, RHS can effectively mimic the skin's vascular network, allowing for an in-depth examination of how substances interact with blood vessels and how skin may respond to injuries (Matei et al., 2019). This capacity for more realistic representation makes RHS models a powerful platform for a wide range of studies, from drug testing to understanding skin diseases and the wound healing process.

One of the main advantages of RHS is the higher physiological relevance without raising ethical concerns and regulatory barriers. However, apart from the structural inaccuracy, these models still lack some key immune cells. There are more than five different types of immune cells co-existing in native skin, for example, LC, DC, macrophages, resident T-lymphocytes, and mast cells. Due to the lack of these cells, the 3D skin models often cannot accurately portray immune cross-talk and the immunological responses to the external threats that would occur in the physiological skin. Researchers have been improving the skin model methods as well as the integration of the immune cells into the skin models to make them more biologically relevant, but only LCs or DCs were utilized using in skin sensitization assessment research, as stated in **Table 1**.

Immune cells	Model type	Incorporating/ integrating method	Application	Readout	References	
T-lymphocytes	Th1/Th7 or CCR6 <sup>+</sup> CLA <sup>+</sup> cells	3D RHS from primary cells	T-lymphocytes were cultured on the collagen gel, and then the matured RHS was placed onto the	To mimic psoriatic skin and to study the respond of the	T-lymphocyte infiltration into the RHS and the	(Shin et al., 2020)

Immune cells	Model type	Incorporating/ integrating method	Application	Readout	References
		T-lymphocyte-attached collagen gel	models to psoriasis drugs	expression of CD69 and CD25	
CD4+ T-lymphocytes or PBMCs	3D RHS from immortalized cells	T-lymphocytes were embedded in the collagen gel, and then the matured RHS was placed onto the T-lymphocyte layer	To study the cross-talk between CD4+ T-lymphocytes and fibroblasts in response to <i>c. albicans</i> infection	T-lymphocyte infiltration into the RHS, CXCL9, CXCL10, and CXCL11 secretion, and the inflammatory response of fibroblasts	(Kühbacher et al., 2017)
CD4+ T-lymphocytes	3D RHS from primary cells	T-lymphocytes were placed underneath the matured RHS	To investigate the trigger of T-lymphocyte infiltration into the filaggrin-deficient RHS	The infiltration of the T-lymphocytes in the RHS and the shift of T-lymphocyte profile according to cytokines secretion and gene expression	(Wallmeyer et al., 2017)
Th1 or Th2	3D self-assembled RHS from primary cells	Th1 or Th2 cells were mixed with various cytokines and topically added to the matured RHS	To investigate the method to induce psoriasis- and atopic dermatitis in 3D RHS	The inflammatory profile of the epidermis according to the marker expression and atopic dermatitis and psoriasis-related gene expression	(Morgner et al., 2023)
CD45RO+ T-lymphocytes	3D RHS from primary fibroblasts and HaCaT	The T-lymphocytes were embedded in the collagen layer, and the matured RHS was placed on top of it	To develop the RHS with eczematous dermatitis condition	The hallmark markers of the condition are keratinocyte apoptosis, change in E-cadherin, iCAM-1, NT-4	(Engelhart et al., 2005)

Immune cells	Model type	Incorporating/ integrating method	Application	Readout	References
				expression, and the secretion of IL-1 $\alpha$ , IL-6, IL-8, IP-10, TARC, MCP-1, RANTES, and eotaxin	
Th1 and Th17	3D RHS from seeding NHEK on de-cellularized dermis	T-lymphocytes were placed underneath the matured RHS	To study the cross-talk between keratinocytes and T-lymphocytes in psoriatic- and atopic RHS	Psoriasis-related gene expression, pro-inflammatory cytokines, and chemokines secretion	(Van Den Bogaard et al., 2014)
<b>Langerhans cells or dendritic cells</b>	MoDC 3D RHS from primary cells	MoDC were embedded into the agarose-fibronectin gel and placed between the dermal and epidermal layer	To study the respond of the models to skin sensitizers (DNCB)	MoDC migration, CD86 expression, and the secretion of IL-1 $\alpha$ , IL-6, and IL-8	(Chau et al., 2013)
	MUTZ-LC 3D RHS from primary cells	MUTZ-LC was resuspended with NHEK and seeded on the dermal layer	To study the response of the models to skin sensitizers (NiSO <sub>4</sub> and Resorcinol)	MUTZ-LC migration to the dermis, CD83 expression, and IL-1 $\beta$ expression	(Ouweland et al., 2011)
	MoLC and MoDC 3D RHS from primary cells	MoLC and MoDC were resuspended with NHEK and seeded on top of the dermal layer	To study the inflammatory response of the model to UV radiation	The secretion of pro-inflammatory cytokines	(Bechetoille et al., 2007)
	MUTZ-LC and MoLC 3D RHS from primary cells	MUTZ-LC or MoLC were resuspended with NHEK and seeded on top of the dermal layer	To study the response of the model to skin sensitizers (DNCB, isoeugenol, and sodium dodecyl sulfate)	The immune cell migration, the CD83, PD-L1, CXCR4 gene expression, and the IL-6	(Bock et al., 2018)

Immune cells	Model type	Incorporating/ integrating method	Application	Readout	References
				and IL-8 secretion	
MUTZ-LC	3D RHS from primary cells	MUTZ-LC were resuspended with NHEK and seeded on top of the dermal layer	Method development	-	(Laubach et al., 2011)

*Abbreviations and acronyms arranged alphabetically: DNCB; 2,4-dinitrochlorobenzene, ICAM-1; Intercellular Adhesion Molecule 1, MCP-1; Monocyte Chemoattractant Protein-1, MoDC; Monocyte-derived dendritic cells, MoLC; Monocyte-derived Langerhans cell, MUTZ-LC; MUTZ-3 derived Langerhans cells, NHEK; Normal human epidermal keratinocytes, NT-4; Neurotrophin-4, PBMC; peripheral blood mononuclear cells, RANTES; Regulated upon Activation, Normal T-Cell Expressed and Presumably Secreted, TARC; Thymus and activation-regulated chemokine, Th1; T-helper cell 1, Th17; T-helper cell 17, Th2; T-helper cell 2.*

**Table 1. The summary of the main types of immunocompetent skin models that involve Langerhans cells, and their relevance for skin sensitization research.**

To move closer to the physiological system where the skin is not a single static piece of organs but consists of an instant exchange of gases and nutrients as well as the traffic of immune cells via blood vessels, the skin-on-chip has been developed (J. J. Kim et al., 2019; Sung & Kim, 2023; Wufuer et al., 2016). It is a microfluidic device that integrates living cells and tissues into a miniaturized system that simulates the physiological and pathological conditions of a specific organ or tissue. There are different types of skin-on-chip, from putting the static skin models on a chip with a microfluidic system (Sriram et al., 2018; Tavares et al., 2020) to seeding the cells within the chip's chamber (Mori et al., 2017; Ramadan & Ting, 2016). This has been comprehensively reviewed elsewhere (Zoio & Oliva, 2022). One of the biggest advantages of on-chip technology is that it provides dynamic movement where it can mimic the flow of blood in the physiological skin and the small number of cell counts, which would make high-throughput screening adaptation possible. It has also been shown that the skin models cultured with a microfluid system can heal wounds faster than the static skin models (Rimal et al., 2021). It is important to note that, to properly set up the skin-on-chip, as it is rather a new tool, the cultivation setting often requires validation.

In conclusion, the development of two-dimensional (2D) cell culture, RHS, and skin-on-chip technologies represents a significant advancement in dermatological research. Each method has its advantages and disadvantages, and the choice of method requires careful consideration of physiological relevance and reproducibility. These innovative approaches offer more accurate and ethical alternatives to traditional animal testing, providing deeper insights into human skin physiology and pathology. As we continue to refine these models, they hold great promise for

accelerating the development of effective risk assessment platforms and treatments for skin inflammatory diseases.

## 1.6 From Hair Follicles to Skin Models

Hair follicles are complex mini-organs of the skin that extend from the epidermis through the dermis to the underlying adipose tissue. Their structure not only supports hair production but also houses an array of cell types pivotal for skin biology and regenerative medicine. The follicle can be anatomically divided into the root, containing the growth centers, and the shaft, which is visible above the skin surface and consists of the cuticle, cortex, and medulla (**Figure 9**). Each layer plays a specific role in hair protection and structure, making them critical to the overall function of the follicle (Martel et al., 2023).

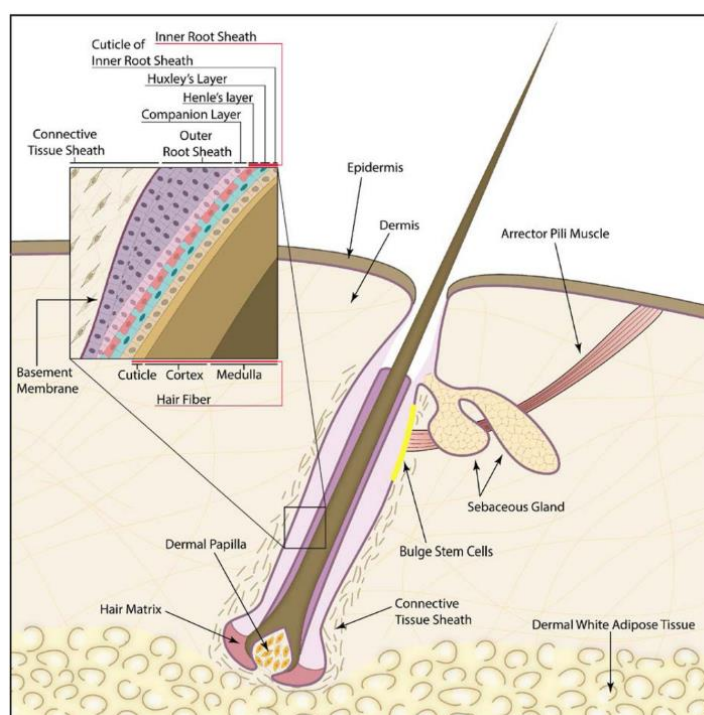


**Figure 9. The microanatomy of hair follicles.** Deeply situated within the dermis, hair follicles are depicted. Surrounding components, including the sebaceous gland, bulge stem cells, and the arrector pili muscle, are indicated. Additionally, the figure details the sublayers of the outer root sheath and inner root sheath enveloping the hair shaft as well as the layer within the hair shaft. The illustration is taken from Kiani et al. (Kiani et al., 2018).

The hair root is intricately associated with several important structures, including the arrector pili muscle and sebaceous glands, which are essential for the hair's response to environmental and physiological stimuli. Deep within the hair root, the inner root sheath (IRS) and outer root sheath (ORS) envelop the hair shaft, serving pivotal roles in the hair growth cycle. The IRS, which helps anchor the hair shaft, consists of specialized cells that contribute to the keratinization process, a

key mechanism where cells infuse with keratin to form a tough protective barrier hair (Joshi, 2011).

The ORS extends from the epidermal basal layer and is fundamental in maintaining the structural integrity of the hair follicle. It is composed of epithelial cells that provide not only physical support but also participate in molecular signaling pathways that dictate hair growth and cycling. This sheath is a critical source of keratinocytes, which are integral to skin barrier functions and pathologies (Martino et al., 2021).

Furthermore, the ORS houses a unique population of stem cells known as hair follicle stem cells (HFSC). Located predominantly in the bulge region, these HFSC possess remarkable regenerative capabilities, essential for the cyclic renewal of the hair follicle during the hair growth cycle. HFSC can differentiate into various cell types, including those found in the IRS and the hair matrix, thus playing a crucial role in hair regeneration and skin repair (Joulai Veijouye et al., 2017).

Adjacent to these structures, the dermal papilla, located at the base of the hair follicle, contains mesenchymal cells that interact with HFSC through paracrine signaling. This interaction involves the secretion of growth factors such as fibroblast growth factors (FGF) and transforming growth factors (TGF- $\beta$ ), which are critical for promoting cell proliferation and differentiation within the follicle (Kageyama et al., 2023; le Riche et al., 2019; Taghiabadi et al., 2020). These cells are a primary source of fibroblasts, which are essential for producing the extracellular matrix and collagen, fundamental for skin tissue engineering and wound healing processes (Kiesewetter et al., 1993; Limat et al., 1991; Limat & Hunziker, 1996).

Due to their easy access and non-invasive harvesting, along with their multipotent properties, hair follicles have emerged as an outstanding source for keratinocytes and fibroblasts. Furthermore, utilizing hair follicles as a cellular resource paves the way for the autologous approach to create RHS or RHE. Furthermore, the limitations associated with the use of cells solely from male donors or immortalized female cells such as HaCaT can be overcome. This broadens the applicability and relevance of skin models in research and therapeutic applications.

## CHAPTER 2 AIM OF THE PROJECT

The primary objective of this research project was to enhance the accuracy and versatility of skin sensitization testing by developing a novel immunocompetent skin model, designated as “ImmuSkin-MT.” This model aimed to reflect the complexities of human skin immune responses than existing methodologies, addressing the scientific, ethical, and economic challenges associated more effectively with chemical hazard assessment.

The project sought to overcome the limitations inherent in traditional skin sensitization assays, which predominantly relied on animal testing. Such methods, historically valuable, were increasingly viewed as inadequate due to ethical concerns and the evolving precision of *in vitro* techniques. The introduction of ImmuSkin-MT was intended to bridge this gap by enabling a more precise differentiation between skin sensitizers and non-sensitizers through a robust and efficient testing platform.

Key innovations of the ImmuSkin-MT included the integration of MoLC and T-lymphocytes, making it a more comprehensive model that simulated the immunological intricacies of native human skin. By incorporating more than one immune response, the model sought to reflect key events in skin sensitization more accurately than existing *in vitro* models, which often depicted isolated immunological events.

In addressing the urgent need for improved skin sensitization testing, the project also aligned with the 3R principle (Replace, Reduce, Refine), promoting methods that reduced reliance on animal testing while ensuring scientific rigor. The ultimate goal of the research was to provide a validated method that could be adopted in regulatory settings, offering a significant advancement in the field of dermatotoxicology safety assessment.

## CHAPTER 3 RESEARCH DESIGNS, MATERIALS, AND METHODS

### 3.1 List of Devices, Reagents, and Plastic Wares

#### 3.1.1 List of Devices

<b>Device</b>	<b>Model</b>	<b>Manufacturer</b>
Analytical Balance	XS205	Mettler Toledo, Columbus, USA
Analytical Balance	AW4202	Sartorius, Göttingen, Germany
Autoclave	V95	Systec GmbH, Linden, Germany
Cell counter	CASY 1 TT	Schärfe System GmbH, Reutlingen, Germany
Cell counter	NeucleoCounter NC-202™	Chemometec, Allerød, Denmark
Cell counter cassette	Via2 Cassette™	Chemometec, Allerød, Denmark
Cell incubator	HERA cell	Thermo Fisher Scientific, Waltham, USA
Cell incubator	HERA cell 240	Thermo Fisher Scientific, Waltham, USA
Centrifuge	Biofuge fresco	Heraeus, Hanau, Germany
Centrifuge	Jouan CR3i	Thermo Fisher Scientific, Waltham, USA
Centrifuge	Multifuge X3R	Heraeus, Hanau, Germany
Centrifuge	Rotilabo® Minizentrifuge	Carl Roth GmbH & Co. KG, Karlsruhe, Germany
Centrifuge	Megafuge 1.0 R	Heraeus, Hanau, Germany
Centrifuge	5415C	Eppendorf, Hamburg, Germany
CO <sub>2</sub> free incubator	WTB	Binder, Tuttlingen, Germany
CO <sub>2</sub> free incubator	Heraeus	Heraeus, Hanau, Germany
CO <sub>2</sub> free incubator	Incubator Hood TH10	Edmun Bühler, Bodelshausen, Germany
Cryo freezing container	Mr. Frosty™	Thermo Fisher Scientific, Waltham, USA
Cryostats	Leica CM 1510s	Leica Biosystems GmbH, Wetzlar, Germany
Flow Cytometer	BD FACS Canto™ II	BD Bioscience, Heidelberg, Germany
Flow Cytometer	CytoFLEX	Beckman Coulter, Krefeld, USA
Fluorescence phase contrast microscope	BZ-9000	Keyence GmbH, Neu-Isenburg, Germany
Fluorescence phase contrast microscope	BZ-8000	Keyence GmbH, Neu-Isenburg, Germany
Fluorescence phase contrast microscope	BZ-X800	Keyence GmbH, Neu-Isenburg, Germany
Forceps	anatomisch/chirurgisch	Carl Roth GmbH & Co. KG, Karlsruhe, Germany
Laminar flow hood	HERA safe	Heraeus, Hanau, Germany
Magnetic cell separation	MACS MultiStand	Miltenyi Biotec GmbH, Bergisch Gladbach, Germany
Magnetic cell separation	MidiMACS™ Separator	Miltenyi Biotec GmbH, Bergisch Gladbach, Germany
Magnetic cell separation	LS Column	Miltenyi Biotec GmbH, Bergisch Gladbach, Germany

<b>Device</b>	<b>Model</b>	<b>Manufacturer</b>
Magnetic stirrer	RCT basic IKAMAG™ Safety Control Magnetic Stirrer	IKA®-Werke GmbH & Co. KG, Staufen, Germany
Microcentrifuge		Eppendorf, Hamburg, Germany
Microplate reader	infinite M200 pro	Tecan Group Ltd., Männedorf, Switzerland
Microplate reader	Infinite M Plex	Tecan Group Ltd., Männedorf, Switzerland
Microplate shaker	Thermomixer comfort	Eppendorf, Hamburg, Germany
Microplate shaker	Titramax 100	Heidolph Instruments, Schwabach
Microplate shaker	MATRIX Orbital	IKA®-Werke GmbH & Co. KG, Staufen, Germany
Minicentrifuge	Color Sprout Plus Mini Centrifuge	Biozyme, Hessisch Oldendorf, Germany
Minicentrifuge	Mini centrifuge ROTILABO®	Carl Roth GmbH & Co. KG, Karlsruhe, Germany
Multipipettes	Eppendorf Multipipette E3	Eppendorf AG, Hamburg, Germany
Phase contrast microscope	Eclipse TS100	Nikon Instruments, Düsseldorf, Germany
Phase contrast microscope	Axiovert 400	Carl Zeiss NTS Ltd., Jena, Germany
Pipette helper	Eppendorf EasyPet	Eppendorf AG, Hamburg, Germany
Pipette helper	Pipetus®	Hirschmann Laborgeräte, Eberstadt, Germany
Pipettes	Eppendorf Research	Eppendorf AG, Hamburg, Germany
Precision balance	AW 4202	Sartorius, Göttingen, Germany
Precision balance	BL610	Sartorius, Göttingen, Germany
Ultra-Low Temperature Freezer (-20 °C)	FN 6192	Gorenje, Velenje, Slovenia
Ultra-Low Temperature Freezer (-20 °C)	FN 6192 CW	Gorenje, Velenje, Slovenia
Ultra-Low Temperature Freezer (-80 °C)	MDF-U500VX-PE	Panasonic, Osaka, Japan
Ultra-Low Temperature Freezer (-80 °C)	HERA Freeze 400 HFU TV Series	Thermo Fisher Scientific, Asheville, USA
Ultra-Low Temperature Freezer (-80 °C)	HERA Freeze TSX40086V	Thermo Fisher Scientific, Asheville, USA
Vortex	Vortex-Genie 2	Scientific Industries, Inc., Bohemia, USA
Water bath	GFL 1092	GFL mbH, Burgwedel, Germany

### 3.1.2 List of Reagents

<b>Reagent</b>	<b>Catalog number</b>	<b>Manufacturer</b>
1M hydroxyethyl-piperazineethane-sulfonic acid buffer pH 7.2 (HEPES)	15630080	Gibco, Waltham, Massachusetts, USA
7-AAD	75001	Stemcell Technologies, Vancouver, Canada
Accutase® solution	A6964-500ML	Sigma Aldrich, USA Aldrich, USA
Adenine	A2786	Sigma Aldrich, USA
Amphotericin B	PHR1662-500MG	Sigma Aldrich, USA

<b>Reagent</b>	<b>Catalog number</b>	<b>Manufacturer</b>
Anti-Hu CD1a	14-0019-82	Invitrogen, Carlsbad, USA
Anti-Hu CD4	317402	Biolegend, San Diego, USA
Anti-Hu CD86	374202	Biolegend, San Diego, USA
APC anti-human CD207 (Langerin) Antibody	352206	Biolegend, San Diego, USA
APC anti-human CD45RA	304112	Biolegend, San Diego, USA
APC anti-human CD69 Antibody	310910	Biolegend, San Diego, USA
APC/Cyanine7 anti-human CD4 Antibody	357416	Biolegend, San Diego, USA
Brilliant Violet 421™ anti-human CD69 Antibody	310930	Biolegend, San Diego, USA
Brilliant Violet 605™ anti-human CD86 Antibody	374214	Biolegend, San Diego, USA
Bovine serum albumin	A8806-5G	Sigma Aldrich, USA
anti-CD10-APC	312210	Biolegend, San Diego, USA
anti-CD1a Microbeads, human	130-051-001	Miltenyi Biotech, Bergisch Gladbach, Germany
CD207 (Langerin) Monoclonal Antibody (eBioL31), eBioscience™	14-2075-82	Invitrogen, Carlsbad, USA
anti-CD29-FITC	130-123-692	Miltenyi Biotech, Bergisch Gladbach, Germany
anti-CD44-eFluor450	48-0441-82	Invitrogen, Oregon, USA
anti-CD49f-PE	130-119-767	Miltenyi Biotech, Bergisch Gladbach, Germany
anti-CD90 percp cy5.5	328118	Biolegend, San Diego, USA
Cells staining buffer	420201	Biolegend, San Diego, USA
CellTrace™ CFSE Cell Proliferation Kit for flow cytometry	C34570	Invitrogen, Oregon, USA
Cholera Toxin	C8052-5MG	Sigma Aldrich, USA
CK10-PE	ab194231	Abcam, Cambridge, UK
CK14-FITC	130-119-728	Miltenyi Biotech, Bergisch Gladbach, Germany
CK5	ab224984	Abcam, Cambridge, UK
Claudin 1 Monoclonal antibody	37-4900	Invitrogen, Carlsbad, USA
Collagen I-PE	130-127-026	Miltenyi Biotech, Bergisch Gladbach, Germany
Collagen IV-PE	130-122-866	Miltenyi Biotech, Bergisch Gladbach, Germany
CytoFLEX Daily QC Fluorospheres	B53230	Beckman Coulter, Krefeld, Germany
DC generation medium	C-28053	Promocell, Germany
DermaCult™ Keratinocyte Expansion Medium	100-0500	Stemcells Technology, Vancouver, Canada
DMEM	D6546	Sigma Aldrich, USA
DMEM High Glucose	11960-044	Gibco, Waltham, Massachusetts, USA
Dimethyl sulfoxide (DMSO)	4720.1	Carl Roth, Karlsruhe, Germany
2,4-dinitrochlorobenzene	237329-10G	Sigma Aldrich, USA
Dulbecco's Phosphate-Buffered Saline (DPBS)	D8537	Sigma Aldrich, USA
Ethylenediaminetetraacetic acid (EDTA)	E6511-500g	Sigma Aldrich, Spain
Eosin G-Lösung 0.5% wasserig	X883.2	Roth, Karlsruhe, Germany
Epidermal Growth Factor	E9644	Sigma Aldrich, USA
F-12 Ham Nut Mix+GlutaMax™	31765-027	Gibco, Waltham, Massachusetts, USA
Fetal Bovine Serum, superior	S0615	Sigma Aldrich, USA
FITC anti-human CD197 (CCR7) Antibody	353216	Biolegend, San Diego, USA
FITC anti-human CD1a Antibody	300104	Biolegend, San Diego, USA

<b>Reagent</b>	<b>Catalog number</b>	<b>Manufacturer</b>
FSC 22 Frozen Section Compound	3801480	Leica Biosystem, Richmond, Illinois, USA
Glycerol	3783.1	Sigma Aldrich, USA
Goat anti-Mouse IgG (H+L), Alexa Fluor™ 555	A28180	Thermofischer, USA
Goat Anti-Mouse IgG H&L Alexa Fluor® 488	ab150113	Abcam, Cambridge, UK
Goat Anti-Mouse IgG H&L Alexa Fluor® 647	ab150115	Abcam, Cambridge, UK
Hemalum solution, according to Mayer	T865.2	Roth, Karlsruhe, Germany
Human GM-CSF, premium grade	130-093-866	Miltenyi Biotech, Bergisch Gladbach, Germany
Human IL-1 $\beta$ , premium grade	130-093-563	Miltenyi Biotech, Bergisch Gladbach, Germany
Human IL-4, premium grade	130-093-921	Miltenyi Biotech, Bergisch Gladbach, Germany
Human TGF- $\beta$ 1, premium grade	130-095-066	Miltenyi Biotech, Bergisch Gladbach, Germany
Human TNF- $\alpha$ , premium grade	130-094-023	Miltenyi Biotech, Bergisch Gladbach, Germany
Hydrocortisone	H0888	Sigma Aldrich, USA
ImmunoCult™	1000023381	Stemcells Technology, Vancouver, Canada
Insulin	11376497001	Roche, Basel, Switzerland
Isoeugenol	1909602	Sigma Aldrich, USA
KGM-2	C20211	Promocell, Germany
L-Glutamine	G7513	Sigma Aldrich, USA
Liothyronine	T2877	Sigma Aldrich, USA
Loricrin	ab198994	Abcam, Cambridge, UK
Lymphoprep	1114545	Stemcells Technology, Oslo, Norway
MACS® BSA Stock Solution	130-091-376	Miltenyi Biotech, Bergisch Gladbach, Germany
Naïve CD4 T-cells isolation kit, Human II	130-094-131	Miltenyi Biotech, Bergisch Gladbach, Germany
Normal Goat Serum	31873	Invitrogen, Oregon, USA
PE anti-human CD25 Antibody	356104	Biologend, San Diego, USA
Penicillin/Streptomycin	P4333	Sigma Aldrich, USA
Poly-D-Lysine hydrobromide	P6407-5MG	Sigma Aldrich, USA
P-phenyldiamine	P601-50g	Sigma Aldrich, China
ProLong™ Gold mounting medium with DAPI	P36931	Invitrogen, Oregon, USA
PureCol EZ Gel	5074	Merck, Burlington, MA, USA
Recombinant APC Anti-Involucrin antibody	ab305923	Abcam, Cambridge, UK
Resorcinol	398047-100G	Sigma Aldrich, India
Roti-Histol Fix 4%	P087.3	Roth, Karlsruhe, Germany
Roti Histokitt	6638.2	Carls Roth, Karlsruhe, Germany
Roti® Histol	6640.2	Roth, Karlsruhe, Germany
RPMI1640 +GlutaMax™	61870-010	Gibco, Waltham, Massachusetts, USA
Triton™ X-100	X100-500mL	Sigma Aldrich, USA
TrypLE	12563-029	Life Technologies Corporation, NY, USA
Trypsin-EDTA	T3924	Sigma Aldrich, USA
Tween®-20	655205-250ML	Merck, Burlington, MA, USA
UltraComp beads	01-2222-42	Invitrogen, Carlsbad, USA

Reagent	Catalog number	Manufacturer
Vimentin-FITC	130-116-508	Milteyi Biotech, Bergisch Gladbach, Germany

### 3.1.3 List of Plastic Wares and Other Materials

Plasticware and material	Catalog number	Manufacturer
0.4 $\mu$ M cell culture insert	353180	Corning Corporate, Durham, USA
1000 $\mu$ L Filter Tips	70.762.211	Sarstedt, Nümbrecht, Germany
100 $\mu$ L Filter Tips	70.760.212	Sarstedt, Nümbrecht, Germany
10mL Falcon tube	62.547.254	Sarstedt, Nümbrecht, Germany
12-well plate TC treated	3526	Costar, Durham, USA
20uL Filter Tips	70.1116.210	Sarstedt, Nümbrecht, Germany
24-well plate TC treated	3526	Costar, Durham, USA
300uL Filter Tips	70.765.210	Sarstedt, Nümbrecht, Germany
50mL Falcon tube	62.554.502	Sarstedt, Nümbrecht, Germany
50mL Leucosep	200.35	Greiner BioOne, Germany
8 $\mu$ M cell culture insert	353182	Corning Corporate, Durham, USA
96-well plate		Costar, Durham, USA
AESCULAP® SAFETY SCALPELS	BA818SU	Aesculap AG, Tuttlingen, Germany
Cover Slips L22x W50mm	1001142	Paul Marienfeld GmbH & Co.KG, Lauda-Königshofen, Germany
Cryomold onetime used	E62352-15	Electron Microscopy Sciences, Hatfield, PA, USA
Cryovials	10-500-26	Fisher Scientific, Hennigsdorf, Germany
Falcon 12 well plate	353503	Corning Corporate, Durham, USA
Falcon® 5 mL Round Bottom Polystyrene Test Tube, with Cell Strainer Snap Cap, 25/Pack, 500/Case	352235	Corning Science, Tamaulipas, Mexico
Low-Profile Disposable Blades 819	14035838925	Leica Biosystemm, Nußloch, germany
Nunc™ Lab-Tek™ Chamber Slide System	177380	Thermofischer Scientific, Waltham, USA
Polysine™ Adhesion Microscope Slides	J2800AMNZ	Epredia, Portsmouth, NH
Mr. Frosty Freezing container	5100-0001	Thermofisher Scientific, Waltham, USA
T150 Cells culture flask	90150	Sarstedt, Nümbrecht, Germany
T25 Cells culture flask	90026	Sarstedt, Nümbrecht, Germany
T75 Cells culture flask	83.3911.002	Sarstedt, Nümbrecht, Germany

## 3.2 Research Techniques

### 3.2.1 Flow Cytometry

At least  $1 \times 10^5$  cells were collected into a round bottom tube and subjected to centrifugation at specified speeds (350xg for 3 min for fibroblasts, 200xg for 5 min for keratinocytes, and 300xg for 10 min for immune cells). The resulting cell pellet was resuspended in 2 mL of cell staining buffer and underwent another centrifugation step. Post-centrifugation, the supernatant was promptly discarded to minimize loss. The cell pellet was then resuspended in a staining cocktail or cell staining buffer. For compensation, a drop of UltraComp Bead was added to separate round bottom tubes, followed by the addition of a single antibody as per the manufacturer's recommendation. Only one antibody per tube was used in the compensation bead tube. Unstained cells served as controls for cellular autofluorescence, with only 200  $\mu$ L of staining buffer added to the unstained cell tube. The staining cocktail or antibody, with a final volume of 200  $\mu$ L per tube and a final antibody concentration of 2.5 mg/mL, was employed for cell staining. Cells were incubated with the staining cocktail, antibody, or cell staining buffer for 30 minutes on ice in the absence of light. Following incubation, 1 mL of cell staining buffer was added to the tubes, and the cells underwent centrifugation to remove excess antibodies. The supernatant was discarded, and the cells were resuspended in 300  $\mu$ L of cell staining buffer. Median fluorescence intensity (MFI) and cell frequency were measured with FACS Canto™ II or CytoFLEX and analyzed utilizing FlowJo version 10.8.01 software. The compensation was calculated based on the compensation beads. Cells not expressing any marker (signal-negative cells) were gated based on the unstained cells.

### 3.2.2 Immunofluorescence (IF) Staining

The cells or tissue sections on a glass slide were fixed with 4% Roti-Histol Fix at room temperature for 10 minutes and washed once with phosphate-buffered saline (PBS) for 5 minutes. Subsequently, permeabilization was achieved with 0.5% Triton X-100 for 15 minutes, followed by a 5-minute PBS wash and a 10-minute PBS/BSA/Tween wash. PBS/BSA/Tween was prepared by adding 10% bovine serum albumin (BSA) and 10% Tween20 into PBS. The slide was treated with 5% goat serum for 30 minutes to reduce nonspecific protein binding. 100% goat serum was prepared by dissolving normal goat serum in 2 mL ddH<sub>2</sub>O. It was then incubated with the primary antibody overnight at 4°C in darkness, following the manufacturer's recommended dilution. After primary antibody incubation, the slide underwent three 10-minute washes with PBS/BSA/Tween. If a secondary antibody was needed, it was prepared with PBS/BSA/Tween per the manufacturer's instructions. The slide was then incubated with the secondary antibody in the dark at room temperature for 1 hour, followed by repeated PBS/BSA/Tween washing steps. The slide was

washed twice with PBS for 5 minutes each and briefly rinsed with ddH<sub>2</sub>O for about 30 seconds to remove any BSA residue. The chamber was detached, and the slide was air-dried in darkness. Two drops of ProLong™ Gold mounting medium with 4',6-diamidino-2-phenylindole (DAPI) were added to each slide, covered with a glass coverslip, and left to allow the mounting medium to harden for microscopy analysis. For long-term storage, slides can be kept at 4°C in darkness. Image observation and capture were performed using the BZx800 fluorescence microscope.

### 3.2.3 Hematoxylin and Eosin Staining (H&E)

The Polysine™ adhesion microscope slide with cells or tissue sections was fixed in 4% Roti-Histofix for 5 minutes at room temperature. Coplin jars were prepared following **Figure 10**. The slide was then placed in a staining rack and immersed in ddH<sub>2</sub>O for 30 seconds. Subsequently, the slide rack was placed in an acidic Hemalum solution according to Mayer for 5 minutes with gentle agitation. After this step, the slide rack was rinsed under running tap water for 5 minutes. The slide rack was transferred to a Coplin jar containing Eosin working solution for 30 seconds with agitation. The Eosin working solution was prepared by adding one drop of glacial acid to 100 mL of the Eosin Y solution 0.5% in water. Dehydration was achieved by immersing the slide in 96% Ethanol for 2 minutes, repeated twice, and then in 100% Ethanol for 2 minutes, also repeated twice. Finally, the slide rack was placed in a clearing agent, Roti®-Histol, for 2 minutes, which was repeated twice. After removal from the slide rack, the slide was air-dried before mounting with Roti®-Histokitt mounting medium and covered with a glass coverslip. For long-term storage, slides can be stored at 4°C. Image observation and capture were performed using the BZx800 fluorescence microscope.



**Figure 10.** The list of Coplin jars required for the hematoxylin and eosin staining.

### 3.2.4 3-(4,5-dimethylthiazol-2-yl)-2,5-diphenyltetrazolium bromide (MTT) Assay

The MTT stock solution, consisting of 5 mg of MTT in Dulbecco's phosphate-buffered saline (DPBS) was prepared and stored at -20°C. The stock solution was thawed at room temperature prior to the experiment. The stock solution was then diluted with cell culture medium at 1:10 (MTT stock solution to medium) and warmed to 37°C. Cells had their culture medium aspirated and were washed thrice with suitable DPBS volume for the cell culture vessel. The MTT-medium mixture, equivalent in volume to regular cell culture medium, was added to the cells. A background control, consisting of the MTT-medium mixture without cells, was also prepared. The cells were incubated with the MTT-medium mixture for 3 hours at 37°C in a 5% CO<sub>2</sub> incubator. Following incubation, the MTT-medium mixture was aspirated, and 250 µL of dimethyl sulfoxide (DMSO) was added to each well. Covered with aluminium foil, the cell culture vessel was shaken at 600 rpm for 5 minutes using a plate shaker. A plate reader measured absorption at wavelengths of 630 nm and 570 nm. Results were obtained by subtracting the optical density (OD) at 570 nm from the OD at 630 nm, with the background control value subtracted as well. A background control is the cell culture medium without cells. A higher value indicates greater metabolic activity in the cells.

### 3.2.5 Frozen Section Procedure

RHS were cut out together with the insert membrane and embedded in a cryomold containing a frozen section compound. Afterward, the cryomold was floated over liquid nitrogen to freeze the RHS from either hair follicle-derived cells (RHS-HFD) or foreskin-derived cells (RHS-FD). The frozen cryomold was wrapped in aluminium foil and stored at -80°C. To start the cryosectioning, the frozen tissue was placed in the -20°C cryostat for at least 30 minutes. Then cryostat was set up by placing the frozen tissue on a stand in the cryostat. The tissue was sectioned at 7 µm thickness. The sectioned tissue was transferred onto a Polysine™ adhesion microscope slide, and the slide was stored at -20°C to prevent the denaturation of the tissue.

## 3.3 Preparation of Biological Samples

### 3.3.1 Juvenile Foreskin-derived Cells

#### 3.3.1.1 *Normal Human Epidermal Keratinocyte (NHEK)*

All cell culture procedures were performed under sterile conditions using a laminar airflow sterile bench. A seeding density of 0.5-1x10<sup>6</sup> viable cells per T75 flask, using 12mL of keratinocyte growth medium (KGM-2), resulting in a cell density of 0.7-1.3 x 10<sup>4</sup> cells/cm<sup>2</sup>, was utilized. The medium was replaced after allowing the cells to adhere for at least 6 hours. The medium replacement was accomplished by first completely aspirating the old medium and non-adherent cells. Subsequently,

the flask was washed thrice with 10 mL of DPBS to remove any remaining residues thoroughly. Fresh medium was then added to the flask. This medium replacement procedure should be repeated every other day. The cell proliferation rate was calculated using the following formula:

$$\text{Cell proliferation rate} = \frac{\text{Harvested cells} - \text{Seeded cells}}{\text{cultivation days}}$$

The population doubling rate (hours) was calculated using the following formulas:

$$\text{Growth rate per day} = \frac{\ln\left(\frac{\text{harvested cells}}{\text{seeded cells}}\right)}{\text{cultivation time}} * 24\text{h}$$

$$\text{Population Doubling time} = \frac{\ln(2)}{\text{growth rate per day}} * 24$$

### 3.3.1.2 Normal Human Dermal Fibroblast (NHDF)

A population of 0.5-1x10<sup>6</sup> viable cells was resuspended in a fibroblast growth medium (FGM) and introduced into a T75 flask. FGM consisted of Dulbecco's Modified Eagle Medium - high glucose (DMEM), 10% Fetal Bovine Serum, Superior (FBS), and 1% L-glutamine. After an initial adherence period of at least 6 hours, the supernatant was removed entirely. The flask was washed three times with 10 mL of DPBS, discarding the supernatant each time. Subsequently, 12 mL of fresh FGM was added to the flask. The medium replacement was carried out every other day to support cell growth and maintenance.

## 3.3.2 Hair Follicle-derived Cells

Hair follicles were collected from anonymous, genetically male, and genetically female donors. All the donors are between 25 and 35 years old at the time of hair follicle collection. The method used to collect the hair follicles and outgrowth of the hair follicles was done according to A. Löwa (Limat & Hunziker, 1996; Löwa et al., 2018).

### 3.3.2.1 Preparation of the Feeder Cells and Transwell® Plate

The feeder cells were prepared by treating 3T3-J2 cells with 4 µg/ml of mitomycin C in the FGM. The cells were incubated for four hours in a 37°C with 5% CO<sub>2</sub> cell incubator. The medium was aspirated, and the cells were washed five times with DPBS. The cells were trypsinized and transferred into a cryovial and stored in liquid nitrogen. A Transwell® 6-well plate with 0.4 µM polyester membrane inserts was prepped by coating it with 200 µL of a 0.1 mg/mL Poly-D-Lysine

hydrobromide solution followed by a 30-minute incubation at room temperature. The solution was then aspirated from the Transwell® inserts, and the wells received a rinse with sterile tissue culture-grade water. Subsequently, the Transwell® plate was left to air-dry for at least two hours. Once the Transwell® plate was completely dry, the inserts were removed and placed upside down in a sterile container. Feeder cells were thawed, resuspended in 3T3 Medium, and seeded onto the inverted inserts at a  $1.5 \times 10^5$  cells/mL density. 3T3 medium was prepared with DMEM, 10% FBS, 10,000 IE/mL Penicillin/Streptomycin, and 4 mM L-Glutamine. These inserts containing feeder cells were then incubated in a 37°C 5% CO<sub>2</sub> incubator for a minimum of 3 hours, allowing ample time for the feeder cells to adhere. Following the adherence period, the liquid in the inserts was carefully aspirated. The inserts were placed back into the Transwell® plate, and 2mL of 3T3 medium was added to each well. The entire Transwell® plate was then subjected to an overnight incubation in a 37°C 5% CO<sub>2</sub> incubator. After the overnight incubation, the liquid within the wells and the inserts were aspirated. The inserts and wells subsequently underwent a thorough rinse with 2mL of DPBS. Finally, the wells were filled with ORS medium (ORM+). ORM+ medium contained DMEM, 21.5% Ham's F12 Nut mix + GlutaMax™, 10% FBS, 10,000 IE/mL penicillin/streptomycin, 0.4 µg/mL hydrocortisone,  $10^{-10}$  M Cholera toxin, 10 ng/mL epidermal growth factor (EGF), 5µg/mL insulin, 0.18 mM adenine, 4mM L-glutamine, and 2nM liothyronine.

### 3.3.2.2 *Cultivation of Hair Follicles*

Ten hair follicles, plucked from the back of the head of a donor using sterile forceps, were carefully transferred into one 2mL vial containing transport medium. The transport medium consisted of DMEM, 10,000 IE/mL penicillin/streptomycin, and 250µg/mL amphotericin. It is important to note that collectible hair follicles should exhibit an observable dermal sheath, initially appearing as a white sheath encasing the base of the hair strand. Eight 5cm<sup>2</sup> Petri dishes were prepared for subsequent steps. Four to five ml of rinsing medium were added to six Petri dishes, and another Petri dish was filled with 5 mL of DPBS, while an additional one received 5 mL of ORM+ Medium. The rinsing medium consisted of DMEM, 10,000 IE penicillin/streptomycin, 250µg/mL amphotericin, and 1M hydroxyethyl-piperazine ethane-sulfonic acid buffer pH 7.2 (HEPES). The hair follicles were then transferred into one of the Petri dishes filled with rinsing medium. Excess hair shafts were meticulously trimmed from each follicle, leaving only the portion enveloped by the white dermal sheath. A sequence of rinses was performed for each hair follicle by transferring them from one Petri dish to the other, including six rinses with rinsing medium followed by a single rinse with DPBS. Finally, the hair follicles were collected in the Petri dish containing ORM+. 1.8mL of ORM+ was added into the well. Subsequently, the hair follicles were carefully transferred onto the inserts. It is recommended to place ten hair follicles per insert to ensure proper

experimentation conditions. To prevent the hair follicles from drying out, a 10  $\mu$ L drop of ORM+ was applied to the dermal sheath of each hair follicle.

### 3.3.2.3 *The Outgrowth of Hair Follicle-derived cells*

Twenty-four hours after the hair follicles were placed onto the inserts, the 200  $\mu$ L ORM+ Medium was added on to each insert carefully. The hair follicles that do not comply with the insert membrane will not yield any HFDF or HFDK. The first medium replacement was performed one week after this step. Then, the medium replacement was performed every 3 days. The cells were harvested after 2-3 weeks of letting the HFDF and HFDK outgrow the hair follicles.

### 3.3.2.4 *Harvesting and Cultivation of Cells from Hair Follicles*

#### 3.3.2.4.1 *Hair Follicle-derived Fibroblast*

The medium within the inserts and wells was discarded. Subsequently, the inserts underwent a rinse with 1mL of PBS, and the wells were rinsed with 2 mL of DPBS twice. The rinsed inserts were then transferred to a Petri dish, where 1mL of Trypsin-EDTA or TrypLE was added to each insert. These inserts were incubated in a 37°C 5% CO<sub>2</sub> incubator for a 5-minute duration. During this incubation period, fibroblasts and several keratinocytes were expected to detach. A 50 mL tube containing 5-10 mL of FGM was prepared. Following the 5-minute incubation period, the supernatant from the inserts was collected into the tube filled with FGM. To ensure comprehensive cell collection, 1 mL of DPBS was added to the inserts, and efforts were made to flush the cells 2-3 times, with each rinse's supernatant collected into the same tube. Once again, 1mL of Trypsin-EDTA or TrypLE was added to the same inserts to collect any remaining cells. The collected cells underwent centrifugation at 470xg for 3 minutes at room temperature. Subsequently, the supernatant was aspirated, and the cell pellets were resuspended in 10 mL of DPBS. Another centrifugation step at 470xg for 3 minutes followed, with the supernatant again being aspirated. The cells were resuspended in 5mL of FGM and seeded into a T25 cell culture flask. The first medium replacement was conducted at least 6 hours after the seeding step, and subsequent medium replacements were performed every 2-3 days. For long-term storage, the cells were frozen and stored in a liquid nitrogen tank (see below for a detailed freezing method).

Before experiments, the cells were thawed and expanded in FGM on collagen-coated flasks up to passage 5. To prepare the collagen solution, refer to the provided table. The collagen used to coat flasks was PureCol EZ Gel. The collagen-coated flasks were left at room temperature overnight for the collagen to solidify before being stored at 4°C for up to 1 week. The lids were securely sealed and wrapped with parafilm to maintain flask sterility.

<i>Cell culture vessel</i>	<b>Cell growth area (cm<sup>2</sup>)</b>	<b>Collagen solution (mL)</b>	<b>Sterile filtered ddH<sub>2</sub>O (mL)</b>	<b>PureCol EZ Gel* (μL)</b>
<i>T25</i>	25	2	1.998	20
<i>T75</i>	75	6	5.94	60
<i>T150</i>	150	12	11.88	120

\* Concentration of the stock solution is 5 mg/mL

**Table 2. The amount of sterile filtered ddH<sub>2</sub>O and PureCol EZ Gel required to prepare collagen solution.** The volume of the collagen solution corresponds to 80 μL of the collagen solution for cell culture flask coating per 1 cm<sup>2</sup> of cell culture area.

#### 3.3.2.4.2 Hair Follicle-derived Keratinocyte

Once the fibroblasts were collected and 1mL of Trypsin-EDTA or TrypLE was added to the inserts, they were incubated in a 37°C 5% CO<sub>2</sub> incubator for another 10 minutes. Meanwhile, a 50 mL tube containing 10 mL of FGM was prepared for cell collection. To ensure thorough cell retrieval, 1 mL of PBS was added to the inserts to flush out any remaining cells. In cases where cells persisted, another 1 mL of Trypsin-EDTA or TrypLE was introduced into the inserts. Following this step, the inserts were incubated in a 37°C 5% CO<sub>2</sub> incubator for an additional 5-10 minutes. Subsequently, the cells from one donor were collected into the same tube. 2mL of serum-containing medium was added to stop the reaction, and the cell suspension was collected into the same tube. A further rinse with 1mL of PBS was performed on the inserts to ensure comprehensive cell retrieval, and the cell suspension was again collected into the same tube. The cell suspension underwent centrifugation at 250xg for 5 minutes at rt. Afterward, the supernatant was discarded, and the cells were resuspended in 10 mL of DPBS. Cell counting was conducted, followed by another centrifugation at 250xg for 5 minutes. The supernatant was discarded, and the cells were resuspended in 10 mL of KGM-2 before being seeded into a T75 cell culture flask. The first medium replacement was performed after at least 6 hours of the seeding step, and subsequent medium replacements occurred every 2-3 days until confluency reached 60-70%. The cells were then harvested and frozen in liquid nitrogen after approximately one week of cultivation (see below for a detailed freezing method). Subsequently, the cells were thawed and expanded in DermaCult™ keratinocyte expansion medium on collagen-coated flasks for up to 8 passages, following the previously mentioned method for preparing collagen-coated flasks. The cell proliferation rate was calculated using the formula presented above.

### 3.3.2.5 *The Freezing of Hair Follicle-derived Cells for Long-term Storage*

#### 3.3.2.5.3 Hair Follicle-derived Fibroblast

The supernatant was aspirated from the cells' culture flask, and the cells were washed with 10 mL DPBS 3 times. 1mL Trypsin-EDTA or TrypLE was added into the flask, and the cells were then incubated in the incubator with the lid screw closed tightly. After 5 minutes, light tapping against the flask helped to detach the cells. 3.6 mL FGM were added to stop the activity. The cells were resuspended and transferred to a 50 mL tube. The cells were centrifuged at 470xg for 3 minutes at room temperature. The supernatant was aspirated without disturbing the cell pellet. Then, the cells were resuspended in DPBS and centrifuged at 470xg for 3 minutes at room temperature. HFDF freezing medium was prepared and kept cold and away from the light. The HFDF freezing medium is composed of 80% FGM, 10% FBS, and 10% DMSO. After centrifugation, the supernatant was aspirated, and the cells were resuspended in an HFDF freezing medium. 1mL of  $0.5-2 \times 10^6$  cells/mL cell suspension in the freezing medium was added into a cryovial. The cryovials were placed in the prechilled Mr. Frosty freezing container before putting the whole container into a  $-80^{\circ}\text{C}$  freezer overnight. The vials were stored in liquid nitrogen for long-term storage.

#### 3.3.2.5.4 Hair Follicle-derived Keratinocyte

Accutase<sup>®</sup> solution was thawed at room temperature before use. The medium was aspirated from the cells' culture flask, and the cells were washed with 10 mL PBS 3 times. 5-10 mL Accutase<sup>®</sup> solution (depending on cell confluence) or TrypLE was added into the flask and the cells incubated for 30 minutes at room temperature. Afterward, light tapping against the flask helped to detach the cells. Cell suspension was collected into 50 mL tubes. The 10 mL DPBS was added into the flasks, and the cell suspension was collected in the same tube. Afterward, the cell suspension was centrifuged at 250xg for 5 minutes at room temperature. The supernatant was aspirated, and the cells were resuspended in 10 mL DPBS and counted. The HFDFK freezing medium was prepared and kept away from light on ice. The HFDFK freezing medium is made up of 90% KGM-2 and 10% DMSO. The cells were then resuspended in the freezing medium and transferred into the cryovial. 1mL of  $0.5-2 \times 10^6$  cells/mL cell suspension in the freezing medium was added into a cryovial. The cryovials were placed in the prechilled freezing container before putting the whole container into a  $-80^{\circ}\text{C}$  Freezer overnight. The vial was stored in liquid nitrogen for long-term storage.

### 3.3.3 Immune Cells

Immune cells were prepared either from the whole blood hair follicles donor or from the buffy coat obtained from Deutsches Rotes Kreuz Nord-Ost (DRK). The age and sex of buffy coat donors

are unknown. The immune cells are prepared according to a standard operating procedure established in the working group (see below).

### 3.3.3.1 *MoLC*

The buffy coat, sourced from DRK, or whole blood from hair follicle donors, underwent a 1:2 dilution with PBS-EDTA. PBS-EDTA was prepared by adding 516.4 mg/L of ethylenediaminetetraacetic acid into 500 mL DPBS. Subsequently, 30 mL of the diluted buffy coat was gently layered onto 15 mL of Lymphoprep™ in 50 mL tubes and centrifuged at 400xg for 45 minutes at 20°C with a break-off period. Post-centrifugation, the distinct layers of plasma, peripheral blood mononuclear cells (PBMC), additional plasma, platelets, and erythrocytes, were observed. The upper 15 mL of the plasma layer was aspirated, and PBMCs were collected into a new tube containing 10 mL of PBS-EDTA. The PBMC tube was filled with PBS-EDTA up to 50 mL and centrifuged at 300xg for 10 minutes at room temperature. The supernatant was then aspirated. PBMC pellets were resuspended in 50 mL of cold PBS-EDTA and centrifuged at 200xg for 15 minutes at 4°C. Cell counting utilized CASY cell counter or NucleoCounter® NC-202™. Approximately 150–200 x10<sup>6</sup> PBMCs were resuspended in a DC generation medium and plated in a T75 flask for 90 minutes. Non-adherent cells were either discarded or retained for naïve CD4+ T-lymphocyte isolation. The medium in the T75 flask was replaced with a DC generation medium supplemented with 20 ng/mL TGF-β1, 20 ng/mL IL-4, and 100 ng/mL GM-CSF. IL-4 was added only on day 0. Half of the medium was replaced every three days during the six-day culture. The fresh supplemented medium was prepared shortly before the medium changed. Post-culture CD1a microbeads and human cells facilitated the selective isolation of CD1a+ MoLC from the general MoLC population. CD1a+ cell isolation followed the standard protocol by Miltenyi Biotech. Briefly, cells were washed thrice with PBS-EDTA, pooled, and centrifuged at 300xg for 10 minutes at 4°C. Cell counting was performed using NucleoCounter™. Magnetic activated cell sorting (MACS) buffer, comprising 0.5% MACS BSA stock solution in PBS-EDTA, was prepared. The supernatant was discarded, and the cell pellet was resuspended in MACS Buffer at a concentration of 80 μL per 10<sup>7</sup> total cells. Then, 20 μL of CD1a Microbeads per 10<sup>7</sup> cells were added, and the cell suspension was incubated with the magnetic beads for 15 minutes in a refrigerator. After incubation, the cells were resuspended in 1-2 mL of MACS Buffer per 10<sup>7</sup> cells and centrifuged at 300xg for 10 minutes. The resulting cell pellet was resuspended in 500 μL of MACS Buffer per 10<sup>8</sup> cells and added to an LS magnetic column. Only CD1a+ cells passed through, while other cells were discarded. The LS column was washed thrice with 3 mL of MACS Buffer. The cells that passed through were also discarded. Subsequently, 5 mL of MACS Buffer was added to the column, and CD1a+ cells were released from the LS column using a provided plunger. The cells were then centrifuged at 300xg

for 10 minutes at 4°C, and the supernatant was completely aspirated. The MoLC were then ready for the experiment.

### 3.3.3.2 *Naïve CD4<sup>+</sup> T-lymphocytes*

PBMCs were isolated as previously described. A total of 100 – 200 x10<sup>6</sup> PBMCs were utilized to isolate naïve CD4<sup>+</sup> T-lymphocytes using the Naïve CD4<sup>+</sup> T-cells Isolation Kit Human II. The isolation procedure adhered to the guidelines outlined in the manufacturer manual. In summary, 10<sup>7</sup> cells were resuspended in 40 µL of MACS Buffer after determining the cell count. Subsequently, 10 µL of Naïve CD4<sup>+</sup> T-cell Biotin-Antibody Cocktail II per 10<sup>7</sup> cells were introduced into the cell suspension. This mixture was incubated at 4°C in darkness for 5 minutes. Following this, 30 µL of MACS Buffer per 10<sup>7</sup> cells was added, and the cell suspension was labeled with 20 µL of Naïve CD4<sup>+</sup> T-cell MicroBead Cocktail II per 10<sup>7</sup> cells, selectively targeting cells other than CD45RA<sup>+</sup>CCR7<sup>+</sup> cells. The cell suspension was again incubated in darkness for 10 minutes at 4°C. The labeled cell suspension was introduced into an LS magnetic column, where only CD45RA<sup>+</sup>CCR7<sup>+</sup> cells passed through, while other cells were retained within the magnetic column. Subsequently, freshly isolated CD4<sup>+</sup> Naïve T-lymphocytes were washed once with PBS-EDTA. These cells were then utilized in ongoing experiments.

### 3.3.3.3 *Immune Cell Characterization Using Flow Cytometry*

A minimum of 10<sup>5</sup> CD4<sup>+</sup> naïve T-cells or MoLC were collected into a round bottom tube. Subsequently, the cells underwent washing and staining procedures as outlined in the research technique section. For each type of cell, a distinct marker cocktail was prepared, tailored to the specific requirements of the experiment. The results were measured utilizing either FACS Canto™ II or CytoFLEX, and subsequent analysis involved the utilization of FlowJo v10 software. Initially, immune cells were gated based on the dot plot of forward scatter (FSC) vs. side scatter (SSC) to eliminate debris from consideration. Following this, immune cells were further gated using their characterization markers, which included CD4-APC-Cy7 for T-lymphocytes and CD1a-FITC for MoLC. To ensure the exclusion of non-viable cells, gating was performed exclusively for cells that were not positive for 7-AAD. Subsequently, the expression of phenotype markers and activation markers was assessed. This comprehensive approach allowed for the precise characterization and analysis of immune cell populations.

## 3.4 Experiment Designs

### 3.4.1 Characterization of Foreskin-derived and Hair Follicle-derived Cells

#### 3.4.1.1 *Immunofluorescence staining*

HFDK, HFDF, NHEK, and NHDF were isolated and cultivated as previously described.  $10^4$  HFDK, HFDF, NHEK, or NHDF were seeded onto a chamber slide for 24 hours. Afterward, the medium was aspirated completely, and the slide was washed with 1mL DPBS thrice. Then, the staining procedure was done as previously described in the [research technique section](#). The primary antibody was diluted according to the manufacturer's suggestion. Keratinocytes were incubated with CK10-PE and CK14-FITC. Fibroblasts were incubated with Vimentin-FITC and Collagen I-PE, or Collagen-VI-PE. The corrected total cell fluorescence (CTCF) was calculated using the following formular. The integrated density of the background and the cells were measured using ImageJ.

$CTCF =$

*Integrated Density of the cells - (Area of selected cell X Mean Integrated Density of background)*

#### 3.4.1.2 *Flow Cytometry*

$1 \times 10^6$  HFDK, HFDF, NHEK, or NHDF were collected into a round bottom tube. Then, the cells were washed and prepared as previously mentioned. Keratinocytes were stained with a cocktail of anti-cytokeratin 5 (CK5)-PE, anti-CD29-FITC, and anti-CD49f-PE. Fibroblasts were stained with a cocktail of anti-CD10-APC, anti-CD44-eFluor450, and anti-CD90-PerCP-Cyanine 5.5. The results were measured with CytoFLEX and analyzed with FlowJo V10.

### 3.4.2 Cultivation Methods for HFDK

HFDK or NHEK at passage 2 were cultivated in either DermaCult™ or KGM-2 after seven days of cultivation. The microscopic pictures of the cells were taken at x100 magnification. The cells were subcultured every five days up until passage 5. The cell number and the cell viability were accessed by the NeuCleoCounter 202™.

### 3.4.3 Culture Conditions of Naïve CD4+ T-lymphocytes

#### 3.4.3.1 *Time-Course Experiment*

A total of  $1 \times 10^6$  CD4+ naïve T-lymphocytes were isolated and subsequently cultured in 6-well plates using 2mL of RPMI1640 complete medium per well. The RPMI1640 complete medium composed of RPMI 1640+GlutaMax™ supplemented with 10% heat-inactivated FBS superior (hiFBS), 200

UI/mL of IL-2. Heat-inactivated FBS was prepared by warming the FBS to 60°C for 30 minutes. The cell medium was refreshed every three days throughout the culture period, which spanned six days. The medium replacement process involved centrifuging the cell suspension at 300xg for 10 minutes at 4°C. Half of the supernatant was discarded following centrifugation, and fresh medium was added. Flow cytometry analysis was conducted on day 0, day 3, and day 6 of the culture period. For this analysis, a panel of antibodies was employed, including APC/Cyanine7 anti-human CD4 antibody, APC anti-human CD45RA antibody, and FITC anti-human CD197 (CCR7) antibody, along with 7-aminoactinomycin D (7-AAD) for viability/mortality assessment. To perform the 7-AAD staining, the cells were appropriately stained with other antibodies and washed before the 7-AAD was added into the tube. The cells were then incubated with 7-AAD for at least 5 minutes before the measurement with FACS Canto™ II. The results were analyzed using FlowJo V10.

#### *3.4.3.2 The Effect of IL-2 Experiment*

Naïve CD4<sup>+</sup> T-lymphocytes were isolated using established methods. Subsequently, 1x10<sup>6</sup> cells were cultured in individual wells of a 6-well plate, employing 2 mL RPMI1640 complete medium per well. These cultures were divided into two groups, one with the addition of 200 UI/mL IL-2 and the other without IL-2 supplementation. The cultivation period spanned six days with medium replacement executed as previously described. On day 5, 25 µL/mL of ImmunoCult™ anti-CD3/CD28 (T-cell activator) was introduced into both the group with IL-2 and the non-supplemented cultures. This step stimulated the cells for 24 hours before concluding the experiment, and this group is referred to as D6+. The cells were collected for analysis on D0, D3, D6. Subsequently, the cells were prepared for analysis through staining with a panel of antibodies, including anti-CD4-APC/Cy7, anti-CD45RA-APC, anti-CCR7-FITC, and anti-CD69-Brilliant Violet 421™. Cell mortality was assessed by adding 5 µL of 7-AAD to the tube, followed by a 5-minute incubation on ice, in preparation for subsequent analytical procedures.

### 3.4.4 Co-Cultivation of HFDK with Naïve CD4<sup>+</sup> T-lymphocytes

#### *3.4.4.1 Co-Cultivation Medium*

The HFDK were thawed, washed twice with 10 mL PBS, and resuspended in 12 mL KGM-2. These HFDK were then seeded into 24-well plates at a density ranging from 1x10<sup>4</sup> to 2x10<sup>4</sup> HFDK per cm<sup>2</sup>. Following the seeding process, the cells were cultured for an initial 24-hour period before the first medium replacement. To facilitate adaptation of the HFDK to the co-culture conditions, the original KGM-2 medium was substituted with a 1:1 mixture of KGM-2 and co-culture medium such as KGM-2 without hydrocortisone (KGM-2 wo HC) or Mix2. After the initial 24 hours of seeding.

The cells continued to be cultured in this adaptation medium for an additional 24 hours. Following this adaptation phase,  $8 \times 10^4$  to  $10 \times 10^4$  naïve T-lymphocytes were introduced into the co-culture. The HFDK and naïve CD4+ T-lymphocytes were co-cultured in RPMI1640 basal, KGM-2, KGM-2 wo HC or Mix2 for three days. RPMI1640 basal and KGM-2 served as control. Afterward, T-lymphocytes were harvested for flow cytometry analysis. These T-lymphocytes were characterized using specific markers, including anti-CD4-APC/Cy7, anti-CD45RA-APC, anti-CCR7-FITC, and anti-CD69-Brialliant Violet 421™. 7-AAD was used to determine the mortality/viability of the cells. An MTT assay was also performed on the keratinocytes to evaluate their viability under the established co-culture conditions.

#### *3.4.4.2 Autologous and Allogeneic Co-Cultures*

HFDK from two donors were thawed, washed twice with 10 mL PBS, and resuspended in KGM-2. The cells were seeded at  $1 \times 10^4$  –  $2 \times 10^4$  HFDK/cm<sup>2</sup> in 24-well plates with 500 µL KGM-2 and cultured for 24 hours before the first medium change. To adapt the HFDK to the co-culture medium, KGM-2 was replaced with a 1:1 mix of KGM-2 and co-culture medium (KGM-2 wo HC or Mix2) after 24 hours of seeding. The cells were cultured in the adaptation medium for another 24 hours before adding  $8 \times 10^4$  –  $10 \times 10^4$  naïve T-lymphocytes isolated from one of the hair follicle donors' blood in the 500 µL co-culture medium only (KGM-2 wo HC or Mix2). The co-culture of the T-lymphocytes and HFDK from the same donor (autologous) or different donor (allogenic) was maintained for three days in the co-culture media, and then T-lymphocytes were harvested for flow cytometry analysis using anti-CD4-APC/Cy7, anti-CD45RA-APC, anti-CCR7-FITC, anti-CD69-Brialliant Violet 421™. 7-AAD was used to determine the mortality/viability of the cells. The results were measured by FACS Canto™ II and analyzed by FlowJo V10. MTT assay was performed on keratinocytes to assess their viability.

#### *3.4.4.3 DNCB Dose Finding Experiment*

A seeding density of  $2 \times 10^4$  HFDK per cm<sup>2</sup> was employed, and these cells were placed in a single well of a 24-well plate, initially using KGM-2. Subsequently, to facilitate adaptation to the experimental conditions, the medium was switched to the mix of Mix2 and KGM-2 and then finally to the 1mL Mix2 medium.  $1 \times 10^5$  naïve CD4+ T-lymphocytes were seeded into a well in a 24-well plate with 1 mL Mix2 medium. To prepare the desired concentrations of 0.1 mM, 1 mM, and 10 mM DNCB, a serial dilution of DNCB stock solution was carried out. An untreated control (UT) was included. Following the dilution process, 1 µL of either 0.1 mM, 1 mM, or 10 mM DNCB solutions was introduced into the well with HFDK or T-lymphocytes, which yielded final concentrations of 0.1 µM, 1 µM, or 10 µM DNCB, each concentration contained maximum 0.1% DMSO as a vehicle.

Cells were incubated with the substance for 24 hours. An MTT assay was performed to assess the viability of the HFDK. T-lymphocytes were stained with anti-CD4-APC/Cy7, anti-CD45RA-APC, anti-CCR7-FITC, anti-CD69-Brialliant Violet 421™, and 7-AAD to assess the impact of DNCB on the functionality and mortality of the cells. The results were measured by FACS Canto™ II and analyzed using FlowJo V10.

#### 3.4.4.4 *The Challenging of The Co-culture with DNCB*

HFDK were thawed, and  $2 \times 10^4$  HFDK/cm<sup>2</sup> were seeded on a 24-well plate with the KGM-2 before adapting into the 500  $\mu$ L Mix2 medium as previously described. Simultaneously,  $0.1 \times 10^6$  naïve T-lymphocytes were suspended in 500  $\mu$ L of Mix2 medium. This suspension was then introduced into the HFDK culture, resulting in a total volume of 1mL. After an incubation period of 24 hours to facilitate cell interactions, 1  $\mu$ L of 0.1 mM DNCB was added to each well. This addition yielded a final concentration of 0.1  $\mu$ M DNCB in the medium, with a 0.1% DMSO content. The cells were left to incubate with the substance for 24 or 48 hours. 25  $\mu$ L of the T-cell activator was used as a positive control and UT was included. Following exposure to DNCB, the T-lymphocytes were subjected to staining with CD4-APCcy7, and CD69-Brilliant Violet 450™. 7-AAD was used to determine the mortality/viability of the cells. The results were measured with FACS Canto™ II and analyzed with FlowJo V10. An MTT assay was performed to assess the viability of the HFDK.

#### 3.4.5 The Co-Culture of MoLC, T-Lymphocytes, and HFDK

##### 3.4.5.1 *Co-cultivation of T-Lymphocytes and MoLC*

HFDK were thawed, and  $1 \times 10^4$  –  $2 \times 10^4$  HFDK/cm<sup>2</sup> were seeded on a 24-well plate with the KGM-2 before adapting into the 500  $\mu$ L Mix2 medium. In parallel, MoLC were differentiated as previously described in the immune cell preparation section. On day six, after the MoLC were fully differentiated in DC generation medium,  $0.2 \times 10^6$  MoLC were resuspended in 400  $\mu$ L Mix2 medium and added into a well in a 24-well plate.  $0.1 \times 10^6$  T-lymphocytes were resuspended in 100  $\mu$ L Mix2 medium and added into well. The final volume of the medium in the well is 1mL. The well with only T-lymphocytes, or T-lymphocytes and MoLC were included in the experiment. The cells were co-cultured together for three days before the cell suspension containing MoLC and T-lymphocytes were collected for flow cytometry. The cells suspension was stained against CD4-APCcy7, CD69-Brilliant Violet 450™, CD1a-FITC, and CD86-Brilliant Violet 605™. 7-AAD was used to determine the mortality/viability of the cells.

#### 3.4.5.2 *Autologous and Allogeneic Co-Culture of Immune cells*

Monocytes were isolated from a donor and differentiated into MoLC as previously described. At the completion of MoLC differentiation, naïve CD4<sup>+</sup> T-lymphocytes were isolated from the same donor as monocytes using Naïve CD4<sup>+</sup> T-cell MicroBead Cocktail II.  $0.2 \times 10^6$  MoLC cells were resuspended in 500  $\mu$ L of Mix2 medium.  $0.1 \times 10^5$  naïve CD4<sup>+</sup> T-lymphocytes were resuspended in another 500  $\mu$ L of Mix2 medium. The two cell suspensions were combined to the final volume of 1mL and co-cultured together in a well in a 24-well plate for three days. Afterward, the cells were collected for flow cytometry. The cells were stained with CD4-APC/Cy7, anti-CD45RA-APC, anti-CCR7-FITC, anti-CD69-Brilliant Violet 421™, anti-CD1a-FITC, and anti-CD86 Brilliant Violet 605™. 7-AAD was used to determine the mortality/viability of the cells. The results were measured with CytoFLEX and analyzed by FlowJo V10.

#### 3.4.5.3 *Autologous and Allogeneic Co-Culture of The Three Cell Types*

The HFDK from two different donors were thawed and seeded into a 24-well plate at the concentration of  $2 \times 10^4$  cells/cm<sup>2</sup>. These cells were cultured in the adaptation protocol as previously described to adapt the cells cultured in KGM-2 into Mix2. In parallel, MoLC were differentiated following previously established protocols from the same donor or different donor as HFDK. On the fifth day of the experiment, naïve CD4<sup>+</sup> T-lymphocytes were isolated from the same donor whose MoLC were differentiated from and HFDK were isolated from or from entirely different donor. In the autologous co-culture, each cell types were from the same donor, and in allogeneic co-culture, each cell types were from different donors. T-lymphocytes, at a concentration of  $0.1 \times 10^6$  per well, were suspended in 500  $\mu$ L of Mix2 medium. Simultaneously,  $0.2 \times 10^6$  MoLC were suspended in 500  $\mu$ L of Mix2. The suspensions of both MoLC and T-lymphocytes were then combined to reach a final volume of 1 mL. Concurrently, the culture medium was removed from the HFDK, and the cells were subjected to three washes with DPBS. Following this preparation, the immune cell suspension, comprising both MoLC and T-lymphocytes, was introduced into the well-containing HFDK. The co-culture took place for three days. The T-lymphocytes and MoLC were subsequently harvested and subjected to flow cytometry staining using a panel of antibodies including anti-CD4-APC/Cy7, anti-CD45RA-APC, anti-CCR7-FITC, anti-CD69-Brilliant Violet 421™, anti-CD1a-FITC, and anti-CD86 Brilliant Violet 605™. 7-AAD was used to determine the mortality/viability of the cells. The results were measured with CytoFLEX and analyzed by FlowJo V10.

#### 3.4.5.4 *The Treatment of The Three Cells Co-Culture System with DNCB*

HFDC were cultured with MoLC, and T-lymphocytes as previously described. After a 24-hour facilitation period, two different concentrations of DNCB were added to the wells to allow the cells to acclimate to each other. Specifically, 1  $\mu\text{L}$  of a 0.1mM DNCB solution and 1  $\mu\text{L}$  of a 5mM DNCB solution were introduced into the culture medium. This resulted in final concentrations of 0.1  $\mu\text{M}$  DNCB and 5  $\mu\text{M}$  DNCB, both of which contained 0.1% DMSO. Following the exposure to DNCB, 7-AAD was used to determine the mortality/viability of the cells. The T-lymphocytes and MoLC, present in the co-culture were specifically stained using a panel of antibodies that included anti-CD4-APC/Cy7, anti-CD45RA-APC, anti-CCR7-FITC, anti-CD69-Brilliant Violet 421™, anti-CD1a-FITC, and anti-CD86 Brilliant Violet 605™. The results were measured with CytoFLEX and analyzed by FlowJo V10.8.01. This flow cytometry analysis enabled the evaluation of cell phenotypes and viability in response to DNCB exposure.

#### 3.4.6 Development of Immunocompetent Skin Model

##### 3.4.6.1 *RHS from Hair Follicle-derived Cells*

In this study, RHS-HFD or RHS-FD was created following a previously described method (Löwa et al., 2018). Briefly,  $0.5 \times 10^6$  HFDF or NHDF were suspended in PureCol EZ Gel and solidified at 37°C without CO<sub>2</sub> in an insert of a 12-well plate. Subsequently,  $0.9 \times 10^6$  HFDC or NHEK were seeded on top of the solidified dermis layer and incubated for 24 hours at 37°C with 5% CO<sub>2</sub>. The RHS-HFD or RHS-FD was then cultured in an air-liquid interface using keratinocyte differentiation medium (KDM) for 12 days. KDM contained DMEM (Gibco), 21.5% Ham's F12, 10% FBS, 0.4 $\mu\text{g}/\text{mL}$  hydrocortisone,  $10^{-10}\text{M}$  cholera toxin, 10ng/mL EGF, 5 $\mu\text{g}/\text{mL}$  insulin, 4mM L-glutamine, and 0.18mM adenine. On day 12, the RHS-HFD or RHS-FD was frozen as previously described. The RHS-HFD or RHS-FD was stained with H&E staining and IF staining as previously described. For the IF staining, the RHS-HDF or RHS-FD were stained against cytokeratin 14-FITC (CK14), cytokeratin 10-PE (CK10), loricrin, and claudin. The AlexaFluor®647 was used as a secondary antibody for loricrin. The AlexaFluor®647 was used as a secondary antibody for claudin. The epidermal thickness was measured using ImageJ.

##### 3.4.6.2 *Media Finding Experiment*

HFDC were thawed and seeded into a 24-well plate at the concentration of  $2 \times 10^4$  cells/cm<sup>2</sup>. HFDC were cultivated in KGM-2 for 2 days before changing to the mix of 50% KGM-2 and 50% test media. The test media were KDM, Mix2, RKD1 (50% RPMI1640 basal + 50% KDM), and DC generation medium. MoLC were differentiated from anonymous buffy coats. Naïve CD4+ T-lymphocytes were

freshly isolated. On the fifth day,  $0.5 \times 10^6$  CD4<sup>+</sup> naïve T-lymphocytes and  $0.5 \times 10^6$  MoLC were resuspended in the appropriate test medium. The test medium was KDM, Mix2, RKD1, or DC generation medium. RKD1 is the mix of 50% RPMI1640 basal + 50% KDM. Subsequently, the medium in the well-containing HFDK was aspirated, and the cells were washed three times with DPBS). Following the washing steps, the suspension of immune cells, which included MoLC and CD4<sup>+</sup> naïve T-lymphocytes, was added to the well. These cells were co-cultivated with HFDK for a 24-hour incubation period. After the co-culture, the immune cells were collected for flow cytometry analysis. CD4<sup>+</sup> naïve T-lymphocytes were specifically stained with antibodies against CD4-APC/Cy7, CD69-Brilliant Violet 421™, and CD25-PE. Meanwhile, MoLC were stained with antibodies targeting CD1a-FITC, CD207-APC (Langerin) Antibody, and CD86-Brilliant Violet™ 605. 7-AAD was used to determine the mortality/viability of the cells. The results were measured with CytoFLEX and analyzed by FlowJo V10.8.01.

#### 3.4.6.3 *Immunocompetent Skin Models*

The immunocompetent skin models (ImmuSkins) consisted of three-layer construct on the cell culture insert with or without T-lymphocytes in the lower chamber of the transwell. The three-layer construct refers to the epidermis, dermis, and subdermal layer. To immunocompetent skin models with MoLC alone (ImmuSkin-M),  $0.5-1 \times 10^6$  MoLC were resuspended in 100  $\mu$ L PureCol EZ Gel and solidified for 2 hours on 8  $\mu$ M cell culture inserts at 37°C without CO<sub>2</sub> to create the subdermal layer. The matured RHS, which consisted of the epidermis and the dermis, prepared as previously described, was cut out from the insert using a sterile scalpel and placed it on top of the solidified subdermal layer using sterile forceps. For the immunocompetent skin model with only naïve CD4<sup>+</sup> T-lymphocytes (ImmuSkin-T), an RHS was on top of a solidified acellular PureCol EZ Gel layer (subdermal layer).  $0.5-1 \times 10^6$  CD4<sup>+</sup> T-lymphocytes were labeled with CellTrace™ carboxyfluorescein succinimidyl ester (CFSE) Cell Proliferation Kits using the protocol provided by the company and placed in the lower chamber of the transwell containing DC generation medium (see below for detailed instruction of CFSE labeling). To create the immunocompetent skin model containing both MoLC and CD4<sup>+</sup> T-lymphocytes (ImmuSkin-MT), the subdermal layer was built similarly to ImmuSkin-M, followed by the addition of CFSE-labeled naïve CD4<sup>+</sup> T-lymphocytes into the lower chamber similar to ImmuSkin-T (**Figure 12**). On day 12, the three-layer construct from the ImmuSkins were frozen as previously described. The three-layer construct was stained with H&E staining and IF staining as previously described. For the IF staining, the RHS-HDF or RHS-FD were stained against cytokeratin 14-FITC (CK14), cytokeratin 10-PE (CK10), loricrin and claudin. The AlexaFluor®647 was used as secondary antibody for loricrin. The AlexaFluor®488 was used as secondary antibody for CD1a. To observe for T-lymphocytes within the three-layer construct, the

green fluorescent protein (GFP) channel was used to detect the signal from CFSE. The epidermal thickness was measured using ImageJ. The cells in the lower chamber of the transwell were collected for flow cytometry analysis staining against CD1a-FITC, CD4-APC-Cy7, CD86-Brilliant Violet 605™. 7-AAD was used to determine the mortality/viability of the cells. The results were measured with CytoFLEX and analyzed by FlowJo V10.8.01.

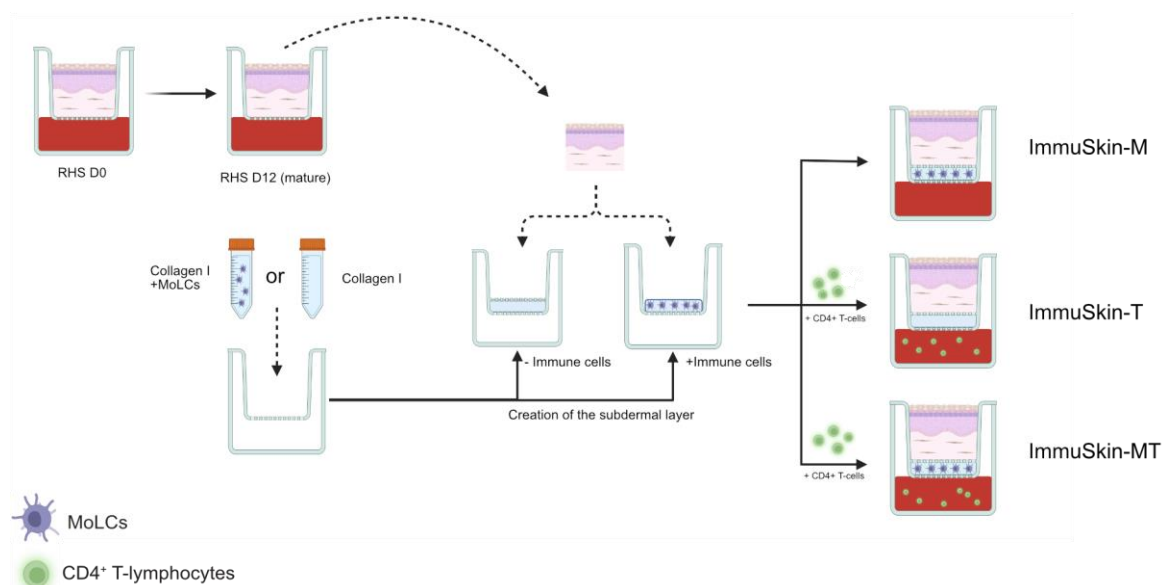


**Figure 11.** The illustration outlines the sequential creation of the immunocompetent skin models (ImmuSkin). It highlights the distinct phases of maturation in reconstructed human skin models (RHS) and the preparation of the subdermal layer. This layer either incorporates monocyte-derived Langerhans cells (MoLC) denoted as '+Immune cells,' as seen in ImmuSkin-M and ImmuSkin-MT, or remains acellular, indicated as '-Immune cells,' as observed in ImmuSkin-T. Furthermore, the illustration demonstrates the introduction of CD4<sup>+</sup> naïve T-lymphocytes into the well of the ImmuSkin-MT and ImmuSkin-T variants, while the absence of CD4<sup>+</sup> naïve T-lymphocytes is indicated in ImmuSkin-M.

#### 3.4.6.4 Skin Sensitization Assay

ImmuSkins were topically treated with 10 µL of different compounds: 0.1% DMSO, 500 µM Glycerol (Gly) prepared from 37 µL 99% glycerol with 963µL DMSO, 250 µM Resorcinol (RN) prepared from 27.5 mg RN and 1 mL DMSO, 300 µM Isoeugenol (IG) prepared from 45.8 µL IG and 954.2 µL DMSO, 5 µM DNCB, or 10 µM p-phenyldiamine (PPD) prepared from 500 µL 20 mM PPD with 500 µL DMSO. The 20 mM PPD was prepared by dissolving 2.16 mg PPD 1 mL DMSO. An inflammatory cytokine cocktail containing 50ng/mL TNF-α and 50ng/mL IL-1β was also used as a positive control for ImmuSkin-M. Additionally, a T-cell activator was included into the inflammatory cytokine cocktail as a positive control for ImmuSkin-T and ImmuSkin-MT by adding 25 µL into the well to ensure the T-cells activation. The stock solution of each skin sensitizer was prepared using DMSO as a solvent and diluted to 1:1000 in the DC generation medium, resulting in a treatment DMSO content of 0.1%. Unexposed ImmuSkin was included as an untreated control. The concentration of each skin sensitizer was carefully curated from different previous studies (Ahmed

et al., 2015; Basketter et al., 2005; Ouwehand et al., 2011; Rees et al., 2011). After 24 hours, the three-layer construct from the ImmuSkin-MT was frozen as previously described. The three-layer construct was stained with H&E staining and IF staining as previously described. For the IF staining, the three-layer construct was stained against cytokeratin 14-FITC (CK14), cytokeratin 10-PE (CK10), loricrin and claudin. The AlexaFluor®647 was used as secondary antibody for loricrin. The AlexaFluor®488 was used as secondary antibody for CD1a. To observe for T-lymphocytes within the three-layer construct, the GFP channel was used to observe the signal from CFSE. The cells in the lower chamber of the transwell were collected for flow cytometry analysis staining against CD1a-FITC, CD4-APC-Cy7, CD86-Brilliant Violet 605™. 7-AAD was used to determine the mortality/viability of the cells. The results were measured with CytoFLEX and analyzed by FlowJo V10.8.01. The epidermal thickness was measured using ImageJ.

#### *3.4.6.5 MoLC Migration and Maturation*

Cells obtained from the lower chamber of the transwell, specifically derived from ImmuSkin-M or ImmuSkin-MT, underwent staining with a combination of extracellular markers. This staining procedure involved using anti-CD1a-FITC, and anti-CD86-Brilliant Violet 605™. 7-AAD was used as viability/mortality marker. The marker expression levels were quantified using a CytoFLEX. MFI and cell frequency were analyzed utilizing FlowJo version 10.8.01 software. The migration of MoLC was determined by gating live CD1a<sup>+</sup> cells within the population and normalizing the migration rate to 10,000 events. Concurrently, the maturation of MoLC was assessed based on the MFI of CD86 within the live CD1a<sup>+</sup> cell population.

#### *3.4.6.6 CFSE Labeling to Assess T-lymphocyte Proliferation*

CD4<sup>+</sup> naïve T-lymphocytes were subjected to staining using the CellTrace™ CFSE Cell Proliferation kit, following the manufacturer's instructions. A 5 mM CFSE solution was initially prepared by combining substance B from the kit with substance A. This resulted in the formation of a 5mM CFSE solution. Subsequently, 1 µL of the prepared 5mM CFSE solution was added to a suspension containing 1x10<sup>6</sup> CD4<sup>+</sup> T-lymphocytes in 1mL of DPBS. The proliferation of these cells was assessed using flow cytometry. To perform the analysis, live CD4<sup>+</sup> T-lymphocytes were identified and isolated within the cell population. The proliferation rate was then quantified based on CFSE intensity, utilizing the proliferation algorithm integrated into FlowJo version 10.8.01. This detailed procedure allowed for an accurate evaluation of CD4<sup>+</sup> T-lymphocyte proliferation.

## CHAPTER 4 RESULTS

### 4.1 Hair Follicles as an Alternative Source for Keratinocytes and Fibroblasts

#### 4.1.1 Comparative Analysis of Cell Properties from Hair Follicles and Foreskin

The keratinocytes and fibroblasts isolated from human hair follicles are characterized in comparison to keratinocytes and fibroblasts isolated from juvenile foreskin. The method of hair follicle-derived cell isolation involved plucking hair follicles and carefully examining them to identify the presence of the ORS, which acts as the primary source of keratinocytes and fibroblasts of these cells. Subsequently, the hair follicles were cultured on an insert membrane of a Transwell® until the outgrowth covered approximately 80% of the insert membrane area (**Figure 12**). After this point, HFDK and HFDF were isolated from the outgrowth of these hair follicles and cultivated in their respective medium, which is keratinocyte growth medium (KGM-2) for HFDK, and FGM for HFDF. The NHEK and NHDF isolated from juvenile foreskin were thawed and cultivated in a similar method. A combination of flow cytometry and immunofluorescence (IF) staining techniques were used to characterize the cells.

The IF analysis and the corrected total cell fluorescence revealed exciting findings. The NHEK and HFDK exhibited similar levels of cytokeratin 14 (CK14), but HFDK had significantly higher levels of cytokeratin 10 (CK10) (**Figure 13A&B**). Additionally, it was observed that HFDF had significantly lower levels of collagen type I compared to NHDF, while collagen IV and vimentin levels remained consistent between the two cell types (**Figure 13C&D**).

It is noticeable that HFDs proliferate slower than foreskin-derived cells (FDs). For instance, the proliferation rate of HFDK at passage two requires 40.6 hours to double the population, while NHEK at passage two require only 24 hours on average (**Figure 14A**). The HFDF at passage two are found to double up the population after 63.3 hours, while the population of NHDF significantly requires twice as little time as the HFDF for population doubling. (**Figure 14B**).

The results from flow cytometry provided further insights into the similarity between NHEK and HFDK. While NHEK showed slightly lower expression of cytokeratin 5 (CK5) and CD29 compared to HFDK, these differences were not statistically significant (**Figure 14C**). On the other hand, CD49f expression was comparable between both cell types. Notably, CD10 was highly expressed in NHDF, while CD90 showed high expression in HFDF. CD44 expression levels were similar in both cell types (**Figure 14D**).

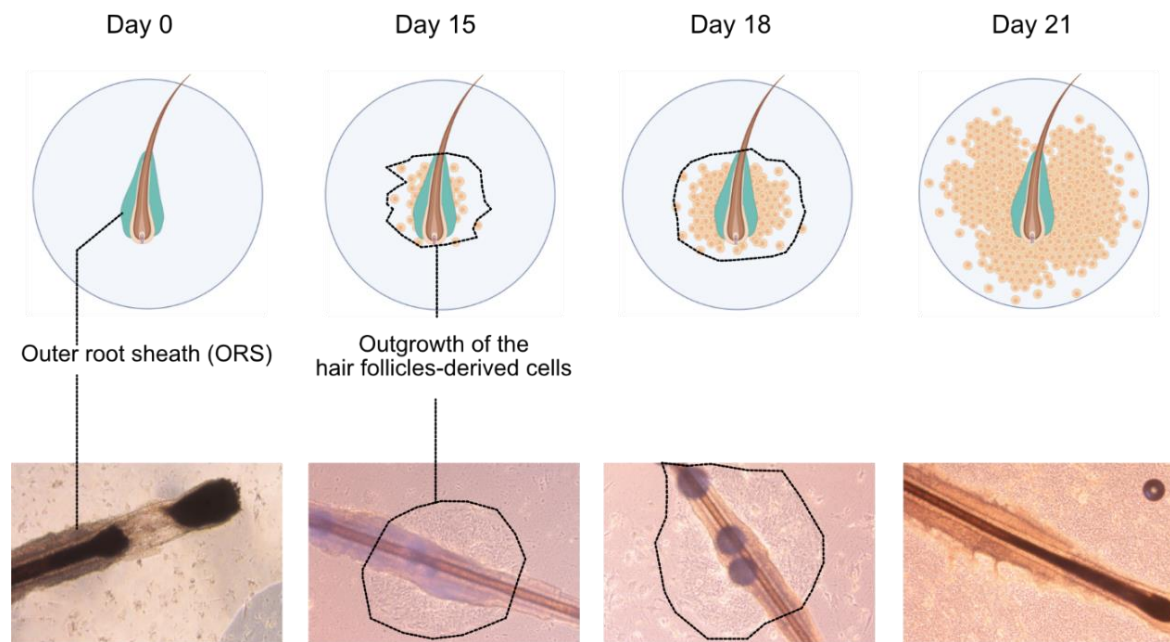


**Figure 12. Representative microscopic images and illustrations showing the outgrowth of hair follicles over 21 days.** Hair follicles were obtained from anonymous donors and cultured in a Transwell plate with feeder cells. After two weeks, outgrowth can be observed originating from the outer root sheath region of the hair follicles (the outgrowth is circled in black). Images were captured at a magnification of x200. n= 9. The illustration was generated with Biorender.com.

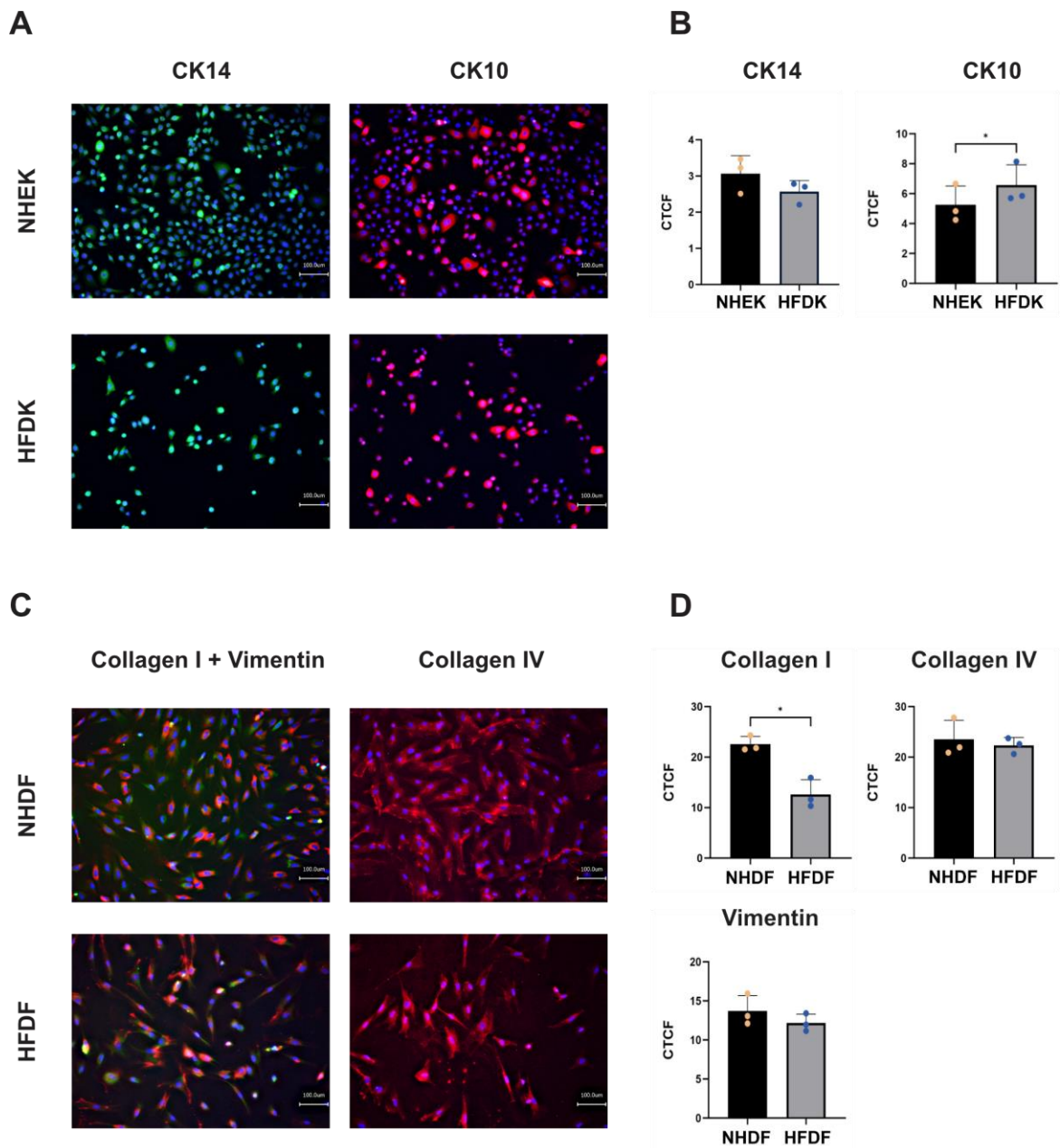


**Figure 13. Characterization of hair follicle-derived cells versus foreskin-derived cells by Immunofluorescence (IF) staining.** **A**) Results from IF staining of normal human epidermal keratinocytes (NHEK) and hair follicle-derived keratinocytes (HFDK) against cytokeratin 10 (CK10)-PE (red) and cytokeratin 14 (CK14)-FITC (green). **B**) The corrected total cell fluorescence (CTCF) of CK14-FITC and CK10-PE in HFDK and NHEK. **C**) IF staining of normal human dermal fibroblasts (NHDF) and hair follicle-derived fibroblasts (HFDF) against collagen I-PE (red), collagen IV (red), and vimentin-FITC (green). **D**) The CTCF of collagen I-PE, collagen IV-PE and vimentin-FITC in HFDF and NHDF. Nuclei were counterstained with 4',6-diamidino-2-phenylindole (DAPI, blue). Scale bar = 100  $\mu$ m. Data are presented as mean  $\pm$  SD. The paired t-test was used as statistical analysis. The p-values <0.05 (\*), <0.01 (\*\*), and <0.001 (\*\*\*) are indicated. n=3.

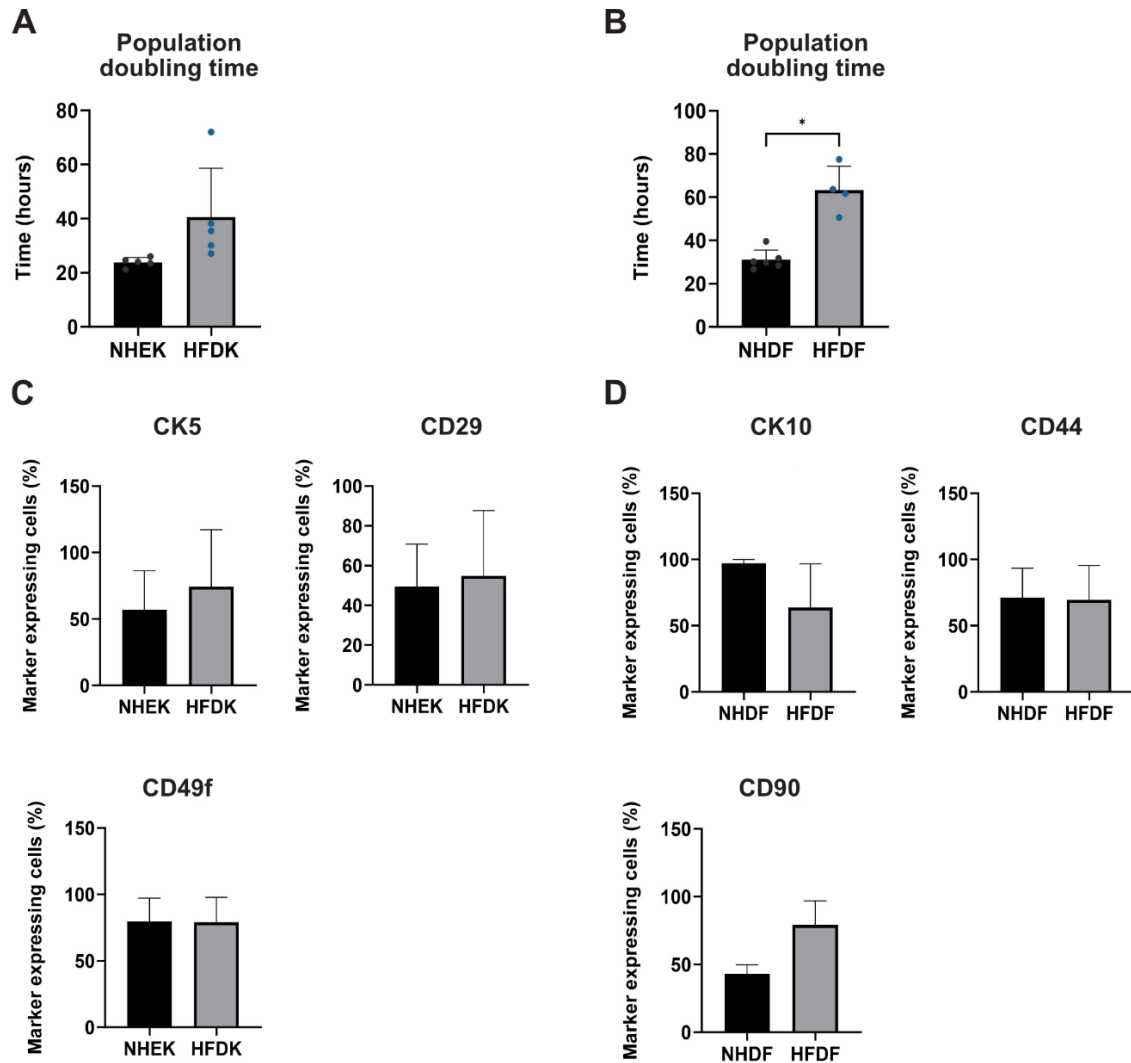


**Figure 14. Characterization of hair follicle-derived cells versus foreskin-derived cells by flow cytometry.** A) Population doubling time of keratinocytes from each source. B) Population-doubling time of fibroblasts from each source. C) Normal human epidermal keratinocytes (NHEK) and hair follicle-derived keratinocytes (HFDK) were stained for CD29-FITC, CD49f-PE, and CK5-PE which are well-known characterization markers for keratinocytes. D) Normal human dermal fibroblasts (NHDF) and HFDF were stained for CD10-APC, CD44-eFluor450, and CD90-PerCP-Cyanin5.5. Scale bar = 100  $\mu$ m. Data are presented as mean  $\pm$  SD. The paired t-test was used as a statistical analysis method. The p-values <0.05 (\*), <0.01 (\*\*), and <0.001 (\*\*\*) are indicated. n=3-6.

#### 4.1.2 Efficacy of Different Hair Follicle Cell Culture Techniques

The slower proliferation of HFDK compared to NHEK prompted the optimization of cultivation methods. Initially, KGM-2 was the chosen medium for HFDK, but the newly introduced medium, DermaCult™, piqued the interest. Thus, the experiment was conducted to compare the proliferation rate and viability of HFDK in both media. The viability was determined using the NeucleoCounter NC-202™.

At passage two, HFDK exhibited cobblestone morphology and formed colonies as expected in both media. Intriguingly, at passage five, HFDK cultured in DermaCult™ retained their proliferation

capacity, whereas those in KGM-2 lost this ability (**Figure 15A**). Cell division rate assessments at passage two revealed significantly faster proliferation in DermaCult™, with HFDK yielding  $2 \times 10^6$  new cells per day, as opposed to KGM-2, which only produced  $0.65 \times 10^5$  new cells per day (**Figure 15B**). Cell viability remained above 80% in both media (**Figure 15C**).

Additionally, the division rate of cells at each passage when cultured in DermaCult™ was assessed. This revealed that proliferating capacity increased in the third and fourth passages before declining in the fifth passage. Conversely, cells cultured in KGM-2 exhibited regression in proliferation with each subculture. The statistical analysis highlighted significantly higher proliferation rates at passages three, four, and five for cells cultivated in DermaCult™ compared to those in KGM-2 (**Figure 15D**).

In conclusion, the DermaCult™ provides the necessary nutrition required by keratinocytes and prolongs the ability to proliferate the cells up to at least passage five without affecting the cell viability. Therefore, the new medium is more suitable for the HFDK' cultivation than the KGM-2.

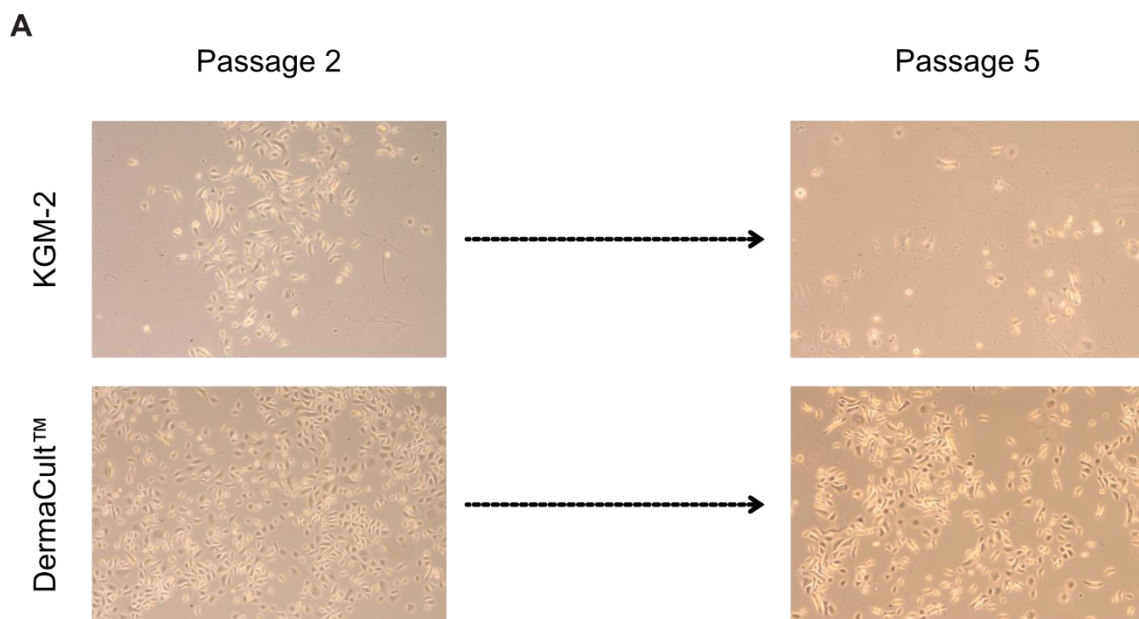


**Figure 15. Assessing the viability and proliferation of hair follicle-derived keratinocyte (HFDK) in various culture media.**

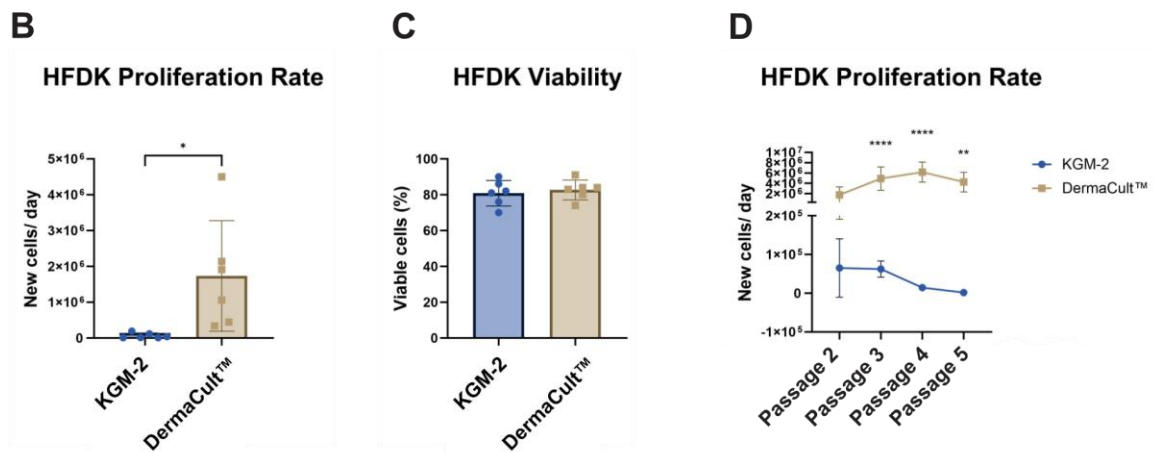


**Figure 15.** (Continued from previous page). **Assessing the viability and proliferation of hair follicle-derived keratinocyte (HFDK) in various culture media.** HFDK were cultured in two distinct media, namely KGM-2 and DermaCult™, from passages two to five. **A)** Representative microscopic images of HFDK at passage two and passage five in both KGM-2 and DermaCult™ media. The images were taken at a magnification of x100. **B)** The proliferation rate of HFDK at passage two, cultured in either KGM-2 or DermaCult™. **C)** Viability assessment of HFDK at passage two, cultured in either KGM-2 or DermaCult™ by NucleoCounter™. **D)** The division rate of HFDK was measured over passage two to five, indicating their growth and expansion dynamics. Data are presented as the mean ± SD. Statistical comparisons between two groups were performed using paired t-tests, while comparisons between multiple parameters were analyzed using one-way ANOVA with Sidak's multiple comparison correction. The p-values were represented as follows: \*  $p < 0.05$ , \*\*  $p < 0.01$ , \*\*\*  $p < 0.001$ , and \*\*\*\*  $p < 0.0001$ .  $n=3-6$

In summary, the results highlight the potential interchangeability of cells derived from hair follicles with those obtained through more conventional methods like skin biopsies or surgeries. While there are subtle differences in marker expression, particularly with CK10 and collagen type I, these cells exhibit overall similarities, suggesting that they can be used interchangeably in various scientific and clinical contexts. This exchangeability offers the possibility of obtaining the cells sourced from a donor multiple times and opens doors for innovative applications in cell-based research and therapies. The limitation of time required for cell division being longer in HFDs than in FDs is remarkable, but this limitation has been overcome by optimizing the cultivation method.

## 4.2 Dynamics of CD4<sup>+</sup> T-Lymphocyte Cultivation

### 4.2.1 Time-Course of CD4<sup>+</sup> Naïve T-Lymphocyte Cultivation

The naïve status of T-lymphocytes was determined from the co-expression of CD45RA and CCR7 on the T-lymphocytes. The central memory T-lymphocyte (CM) character is indicated by the absence of CD45RA (CD45RA<sup>-</sup>CCR7<sup>+</sup>). When the naïve T-lymphocytes become effector T-lymphocytes (TEM), they lose the expression of both CD45RA and CCR7 (CD45RA<sup>-</sup>CCR7<sup>-</sup>). Lastly, the TEM can re-express CD45RA again, which is also known as terminally differentiated T-cells (TEMRA; CD45RA<sup>+</sup>CCR7<sup>+</sup>) (Larbi & Fulop, 2014; Sallusto et al., 1999). Due to this reason, it is necessary to investigate how long the T-lymphocytes can maintain the naïve status in the *in vitro* culture in the presence and absence of IL-2, a well-known cytokine necessary for T-lymphocytes survival and function.

In this study, naïve CD4<sup>+</sup> lymphocytes were isolated from anonymous buffy coats and were cultured in RPMI1640 complete medium supplemented with IL-2 for different periods, which were 24 hours, three days, and six days. Subsequently, the marker presentation of T-lymphocytes was analyzed using flow cytometry.

A decrease in the percentage of T-lymphocytes expressing CD45RA and CCR7 (naïve CD4<sup>+</sup> T-lymphocytes) out of total cultivated naïve T-lymphocytes over time was revealed by the results, with a significant drop being observed on day six. Initially, at day zero (D0), day one (D1), and day three (D3), the frequencies of CD4<sup>+</sup> naïve T-lymphocytes were found to be comparable, with over 90% of the cell population still expressing both CD45RA and CCR7. However, by day 6 (D6), the frequency of naïve CD4<sup>+</sup> T-lymphocytes had significantly decreased to less than 50% (**Figure 16A&B**).

Conversely, a notable increase in the proportion of TEMRA (CD45RA<sup>+</sup>CCR7<sup>+</sup>) was observed with time. This population went from below 10% to exceeding 50% on day six, suggesting the loss of CCR7 expression over time (**Figure 16C**).

Cell mortality was assessed by measuring the MFI of 7-AAD, where a high MFI indicates high mortality. Although a general trend of increasing cell mortality over time was observed, no significant difference in cell mortality was noted between D0, D1, D3, and D6, and there is no correlation between time and mortality (**Figure 16D**).

In conclusion, it was found that CD4<sup>+</sup> naïve T-lymphocytes retained their original characteristics when cultured in RPMI1640 complete + IL-2 for up to 6 days before becoming TEMRA. These

findings contribute to a better understanding of T-lymphocyte behavior in culture and provide relevant information for research involving naïve T-lymphocyte maintenance and differentiation.

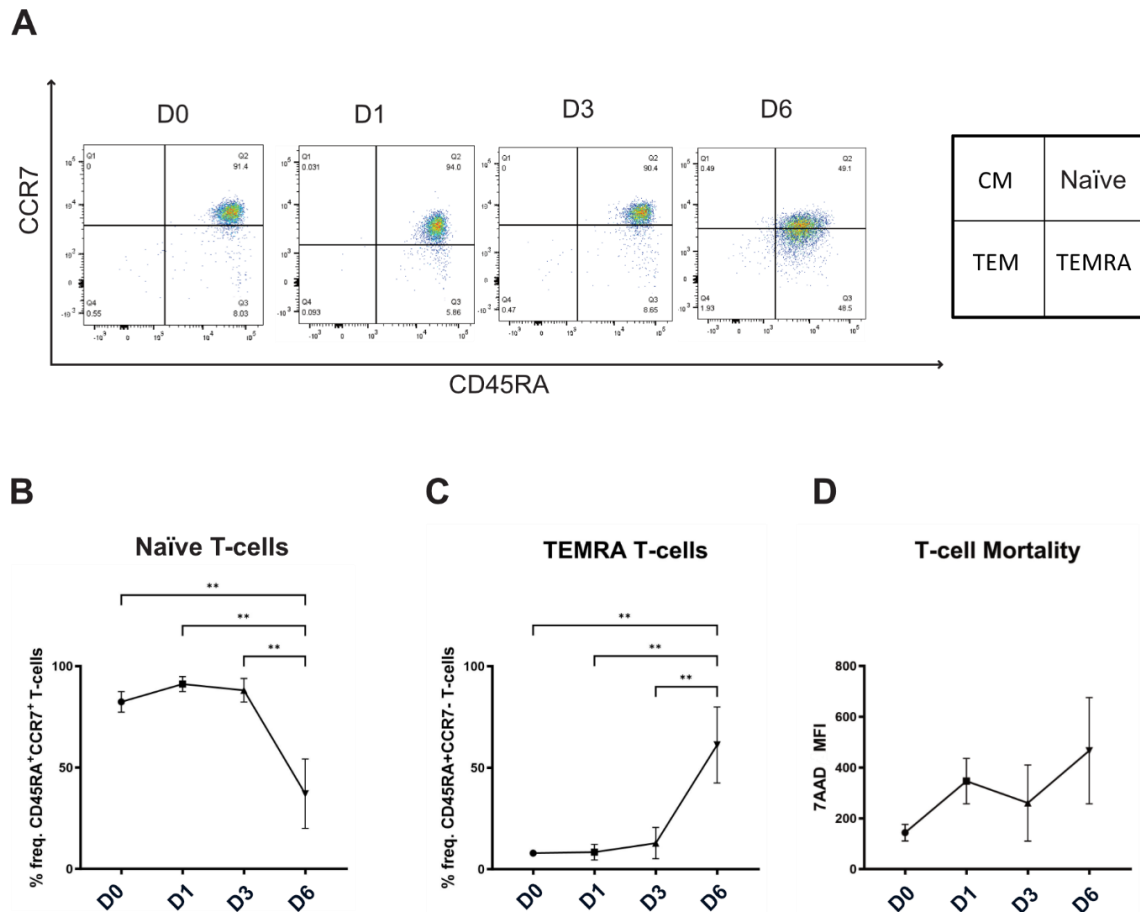


**Figure 16. Changes in T-lymphocyte phenotype and mortality over time.** D0 refers to freshly isolated T-lymphocytes, while D1, D3, and D6 refer to one, three, and six days of cultivation. At each time point, T-lymphocytes were stained for CD45RA-APC and CCR7-FITC to observe their naïve status, where both markers are expressed by the cells and analyzed using flow cytometry. Cell mortality was determined using 7-AAD. **A)** Representative dot plots of CD45RA vs CCR7 for each time point. **B)** Frequencies of CD4<sup>+</sup> cells expressing CD45RA and CCR7 (naïve T-lymphocytes). **C)** Frequencies of CD4<sup>+</sup> cells expressing CD45RA but not CCR7 (terminally differentiated T-lymphocyte or TEMRA). **D)** The mortality of T-lymphocytes was determined from the median fluorescence intensity (MFI) of 7-AAD. The higher the 7-AAD MFI, the higher the mortality. Results were statistically analyzed using ordinary one-way ANOVA with Tukey multiple comparison test. The p-values <0.05 (\*), <0.01 (\*\*), and <0.001 (\*\*\*) are indicated. n = 3.

#### 4.2.2 Impact of IL-2 on CD4<sup>+</sup> T-Lymphocyte Activation

IL-2, a well-known constituent of T-lymphocyte culture media, is recognized for its pivotal role in autoregulation, particularly in activated CD4<sup>+</sup> T-lymphocytes. However, one of the primary objectives of this project is to compare *in vitro* skin sensitization assays, both autologous and allogeneic. Consequently, the need arises to reduce external components, including IL-2, in the

developing assay or to seek alternative substitutes. In this context, an investigation was undertaken into the requirement of IL-2 for naïve CD4<sup>+</sup> T-lymphocyte culture and its impact on the ability of T-lymphocytes to be stimulated.

The results revealed changes in the distribution of T-lymphocyte phenotypes over time. By day six, a greater number of T-lymphocytes had their CCR7 expression diminished. To observe if the naïve T-lymphocyte without IL-2 can be activated, the cells were incubated with T-cell activator for 24 hours. The results show a significant reduction in the CD45RA<sup>+</sup>CCR7<sup>+</sup> population was observed only following incubation with the T-cell activator (**Figure 17A&B**). Notably, the analysis of CD69 expression indicated a substantial upregulation of the MFI of CD69 in CD4<sup>+</sup> T-lymphocytes after exposure to T-cell activator (**Figure 17C**). T-lymphocyte mortality, as assessed by 7-AAD, remained consistent throughout the six-day cultivation period (**Figure 17D**).

Furthermore, a comparison was made between the frequencies of naïve T-lymphocytes, CD69 MFI, and T-lymphocyte mortality in cultures with and without IL-2 at each time point. Interestingly, on day 6, fewer naïve T-lymphocytes were found in the well containing IL-2. However, when T-cell activator, the T-lymphocyte activator, was introduced into the well, both conditions appeared to have a comparable percentage of naïve T-lymphocytes (**Figure 18A**). Moreover, the activation marker upregulation and mortality analysis indicated no significant differences between T-lymphocytes cultured with or without IL-2 (**Figure 18B&C**).

In conclusion, the findings suggest that IL-2 is not indispensable for T-lymphocyte cultivation over up to six days. Furthermore, supplementing T-lymphocyte cultivation with IL-2 does not augment T-lymphocyte activation nor reduce T-lymphocyte mortality. Consequently, excluding IL-2 from the culture medium is feasible, provided that the culture period does not exceed six days. These results contribute to developing an alternative and simplified culture protocol for the *in vitro* skin sensitization assay.

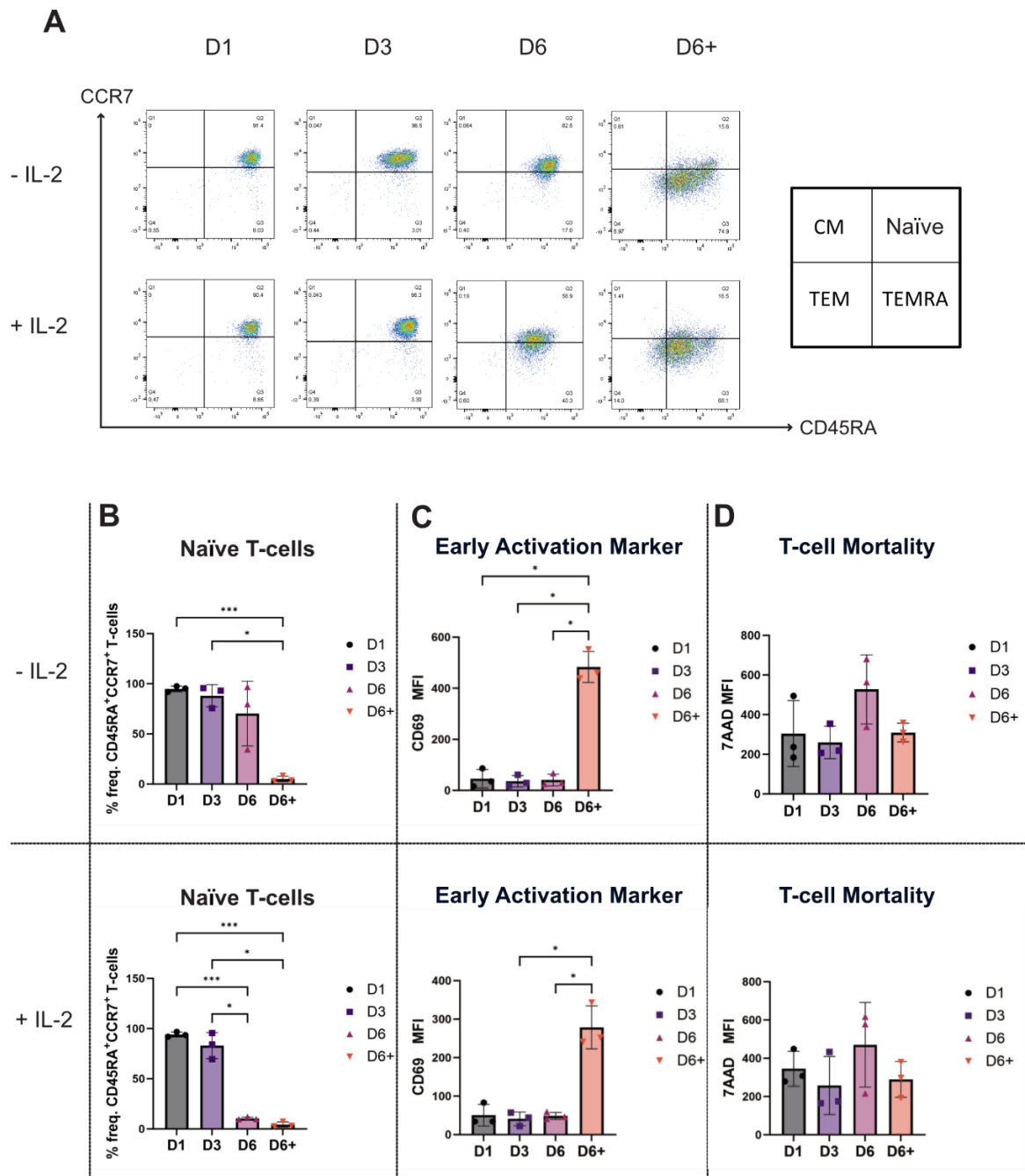


**Figure 17. Changes in T-lymphocyte phenotype and mortality over time in the presence of IL-2 or without IL-2.** T-lymphocytes were cultured with or without IL-2 for six days. D1, D3, and D6 refer to one, three, and six days of cultivation, respectively, while D6+ refers to five days of cultivation with additional 24 hours of stimulation using T-cell activator. At each time point, T-lymphocytes were stained for the naïve T-lymphocyte markers CD45RA and CCR7, as well as the early activation marker CD69. Results were analyzed using flow cytometry and cell mortality was determined using 7-AAD. A) Representative dot plots of CD45RA vs. CCR7 for each time point and culture condition. B) Frequencies of CD4<sup>+</sup> cells expressing CD45RA and CCR7. C) The median fluorescence intensity (MFI) of CD69 in CD4<sup>+</sup> cells reflecting activation of the cells. D) T-lymphocyte mortality based on MFI of 7-AAD. Results were statistically analyzed using ordinary two-way ANOVA with multiple comparisons and Tukey correction. The *p*-values <0.05 (\*), <0.01 (\*\*), and <0.001 (\*\*\*) are indicated. *n* = 3.

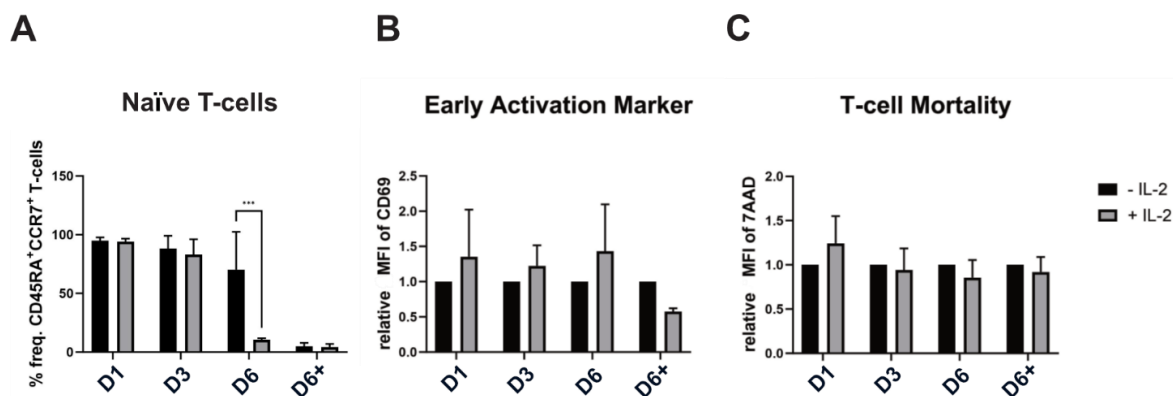


**Figure 18. The direct comparison of IL-2 effects on frequency T-lymphocytes over the course of six days.** The frequency of naïve T-lymphocytes, the activation, and the mortality from the whole T-lymphocyte population were investigated. D1, D3, and D6 refer to one, three, and six days of cultivation, and D6\* refers to five days of cultivation with additional 24 hours of stimulation using T-cell activator respectively. At each time point, T-lymphocytes were stained for the naïve T-lymphocyte markers CD45RA and CCR7 and the early activation marker CD69. Results were analyzed using flow cytometry and cell mortality was determined using 7-AAD. **A)** Frequencies of CD4<sup>+</sup> cells expressing CD45RA and CCR7. **B)** Relative median fluorescence intensity (MFI) of CD69 in CD4<sup>+</sup> cells. **C)** Relative MFI of 7-AAD. Results were statistically analyzed using two-way ANOVA with multiple comparisons and Sidak correction. The p-values <0.05 (\*), <0.01 (\*\*), and <0.001 (\*\*\*) are indicated. n = 3.

Establishing a standardized T-lymphocyte cultivation protocol is essential for laboratory research. Such protocols need a thorough evaluation to ensure their suitability for future experiments. Thus, this study investigated the T-lymphocyte culture conditions from a time-course perspective.

In summary, significant insights into T-lymphocyte behavior in culture, particularly in the context of IL-2 usage, have been uncovered in the investigation. The native characteristics of naïve CD4<sup>+</sup> T-lymphocytes were retained for up to 6 days when cultured in RPMI1640 + IL-2, and it was observed that IL-2 is not essential for sustaining T-lymphocyte survival and characteristics within this timeframe. These findings are crucial for developing a simplified and alternative culture protocol for *in vitro* skin sensitization assays, ultimately contributing to the improved comparability of various test conditions.

### 4.3 Interaction Dynamics in Keratinocyte and T-Lymphocyte Co-Cultures

The immune response in the skin relies also on the interplay between keratinocytes and T-lymphocytes. Traditionally, their communication was believed to occur through secreted molecules, but recent findings show that keratinocytes can express antigen-presenting molecules, suggesting a potential direct interaction (Black et al., 2007; Tamoutounour et al., 2019).

The question arose if *the co-cultivation of HFDK and naïve CD4+ T-lymphocytes lead to T-lymphocyte activation.*

#### 4.3.1 Analysis of Medium Effects on Co-Cultivation

This study explored the co-culture of T-lymphocytes and HFDK to identify optimal culture media for both cell types and assess their impact on cell mortality and activation. The Mix2 and keratinocytes growth medium without hydrocortisone (KGM-2 wo HC), based on previous research by Geisendörfer (Geisendörfer, 2022), were found to be favorable to harmonize the interaction between the HFDK and the immune cells like MoLC. The Mix2 medium is the mix of 1:1 RPMI1640 basal and KGM-2 wo HC. Therefore, this experiment used Mix2 and KGM-2 wo HC as test cultivation media. The RPMI1640 complete (standard immune cell medium presented in figures as RPMI1640) and KGM-2 (standard keratinocyte medium) acted as control media.

Flow cytometry analysis revealed consistent CD45RA expression in CD4+ T-lymphocytes across all media. Cells cultivated in RPMI1640 complete showed the highest CCR7 expression, while the CD69 expression significantly increased in T-lymphocytes cultured in KGM-2. The mortality of T-lymphocyte was determined from the MFI of 7-AAD. The higher the 7-AAD, the higher the mortality of the cells. Although it is not statistically significant, the 7-AAD MFI of the cells cultivated in KGM-2, KGM-2 wo HC, and the Mix2 was slightly elevated in comparison to the cell cultivated in RPMI1640 complete, indicating slightly increased mortality (**Figure 19A**).

Co-culturing T-lymphocytes with HFDK in different media resulted in significantly lower CD45RA levels compared to the RPMI 1640 complete. CCR7 expression decreased in T-lymphocytes cultured in other media, while CD69 expression was highest in T-lymphocytes cultured in KGM-2. Notably, 7-AAD MFI level was significantly higher in T-lymphocytes cultured in any other media than RPMI1640 complete, reflecting the increased mortality of the cells in those alternative media (**Figure 19B**).

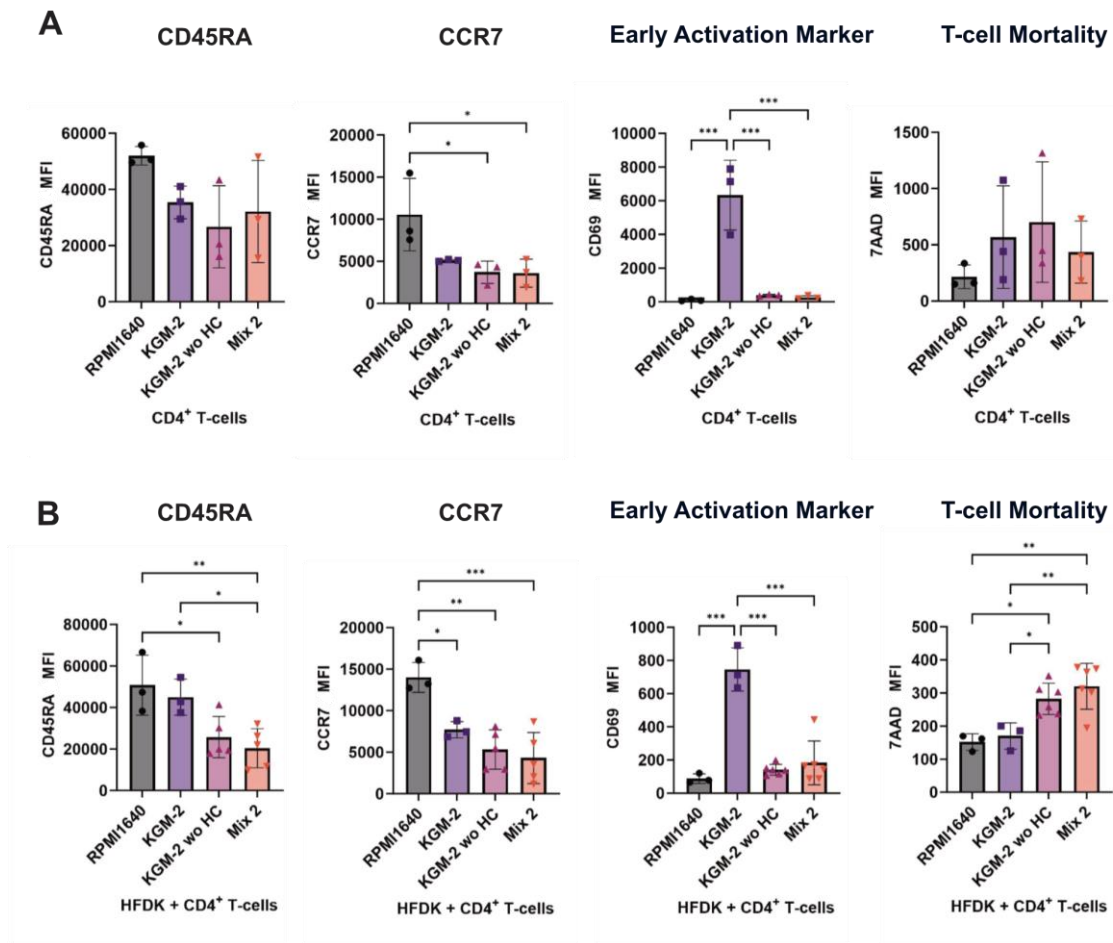
MTT assay results showed that HFDK exhibited the highest metabolic rate in Mix2, followed by KGM-2, KGM-2 wo HC, and RPMI1640 complete, respectively. Although no significant differences

were observed, microscopic images revealed that the HFDK morphology appeared more distorted in other media compared to KGM-2 (**Figure 20**). While T-lymphocyte functionality and mortality deteriorate when exposed to culture media other than RPMI 1640 complete, it is essential to acknowledge the altered morphology of HFDK in immune cell-appropriate media like RPMI 1640 complete. Furthermore, T-lymphocytes cultured in Mix2 and KGM-2 wo HC do not exhibit any signs of auto-activation, which make these two media an ideal alternative to the RPMI1640 complete and KGM-2.

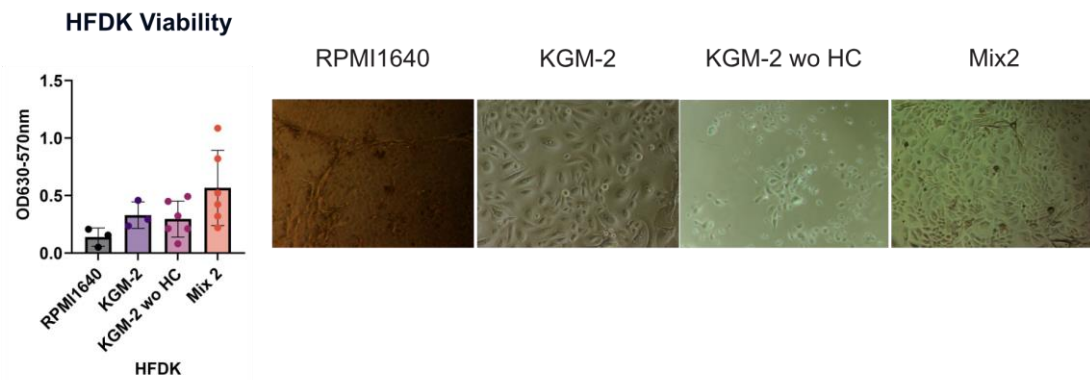
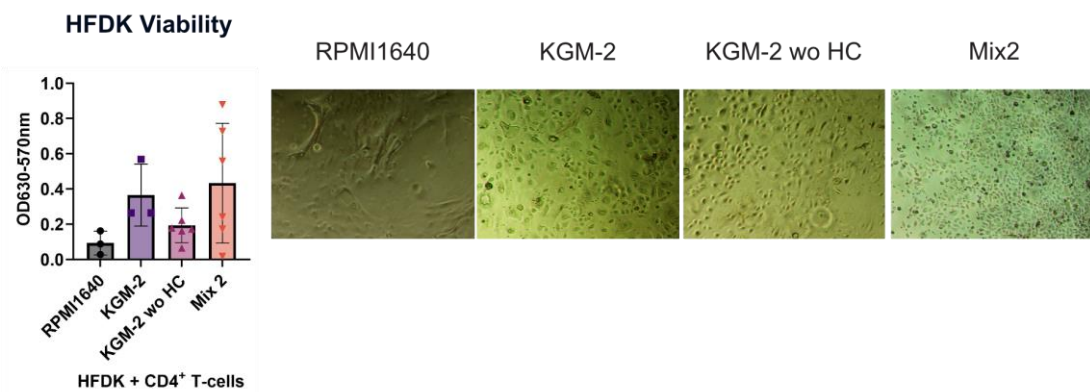
After establishing the suitability of KGM-2 wo HC and Mix2 for co-culture over standard media like RPMI1640 complete or KGM-2, characterization and comparison of cells between single-cell cultures and co-cultures were conducted. In KGM-2 wo HC medium, CD45RA and CCR7 expressions showed no significant differences between the culture conditions. However, co-cultured T-lymphocytes displayed an elevated CCR7 expression trend. Co-cultivation of T-lymphocytes with HFDK led to a lower basal CD69 level, which persisted even when the co-culture was exposed to a T-lymphocyte activator. Importantly, co-culture did not affect the viability of either T-lymphocytes or HFDK (**Figure 21**). Furthermore, the T-lymphocyte activator did not significantly alter HFDK viability.

Similarly, in the Mix2 medium, CD45RA, CCR7, and CD69 levels were comparable in both single-cell and co-culture conditions. However, co-cultured T-lymphocytes exhibited significant CD69 upregulation upon T-lymphocyte activator exposure. The viability comparisons between single-cell and co-culture conditions showed no notable differences either in HFDK or T-lymphocytes. Successful T-lymphocyte activation did not compromise HFDK viability (**Figure 22**).

In summary, flow cytometry and MTT assay results show that KGM-2 influences T-lymphocyte functionality without increasing mortality. Both Mix2 and KGM-2 wo HC are suitable for T-lymphocyte and HFDK co-cultivation, but Mix2 stands out as more efficient. Co-culturing cells in KGM-2 resulted in a subdued T-lymphocyte response, while Mix2 facilitated a robust response, making it a preferable option due to its lack of immunosuppressive effects from HFDK.



**Figure 19. Effects of co-culture media and hair follicle-derived keratinocytes (HFDK) on CD4<sup>+</sup> T-lymphocyte activation and differentiation.** Naïve CD4<sup>+</sup> T-lymphocytes were isolated from human peripheral blood and cultured for three days in the presence or absence of HFDK in RPMI1640 complete (RPMI1640), KGM-2 complete (KGM-2), KGM-2 without hydrocortisone (KGM-2 wo HC), or Mix2. The cells were then stained with antibodies against CD45RA, CCR7, CD69, and 7-AAD and analyzed by flow cytometry. **A)** Expression of CD45RA, CCR7, CD69, and mortality of T-lymphocytes cultured alone in each medium. **B)** Expression of CD45RA, CCR7, CD69, and mortality of T-lymphocytes co-cultured with HFDK in each medium. The higher the 7-AAD MFI reflecting the higher the mortality. Data are presented as mean  $\pm$  SD. Statistical analysis was performed using one-way ANOVA with Tukey's multiple comparisons test. The  $p$ -values  $<0.05$  (\*),  $<0.01$  (\*\*), and  $<0.001$  (\*\*\*) are indicated.  $n=3-6$ .

**A****B**

**Figure 20. Viability and morphology of hair follicle-derived keratinocytes (HFDK) in co-culture media with or without CD4<sup>+</sup> T-lymphocytes.** HFDK were isolated from human hair follicles and cultured for three days in the presence or absence of naïve CD4<sup>+</sup> T-lymphocytes in RPMI1640 complete, KGM-2 complete, KGM-2 without hydrocortisone (KGM-2 wo HC), or Mix2. HFDK viability was assessed using the absorbance value from MTT assay. The absorbance value was calculated by subtracting the optical density (OD) at 570 nm from OD at 630 nm (OD630-570nm). The higher the OD630-570nm, the higher the cell viability. **A)** The viability of HFDK and representative microscopic images of cells in different media. **B)** The viability of HFDK co-cultured with T-lymphocytes and representative microscopic images of cells in different media. Images were captured at a magnification of x100. Data are presented as mean ± SD. Statistical analysis was performed using one-way ANOVA with Tukey's multiple comparisons test. The p-values <0.05 (\*), <0.01 (\*\*), and <0.001 (\*\*\*) are indicated. n=3-6.

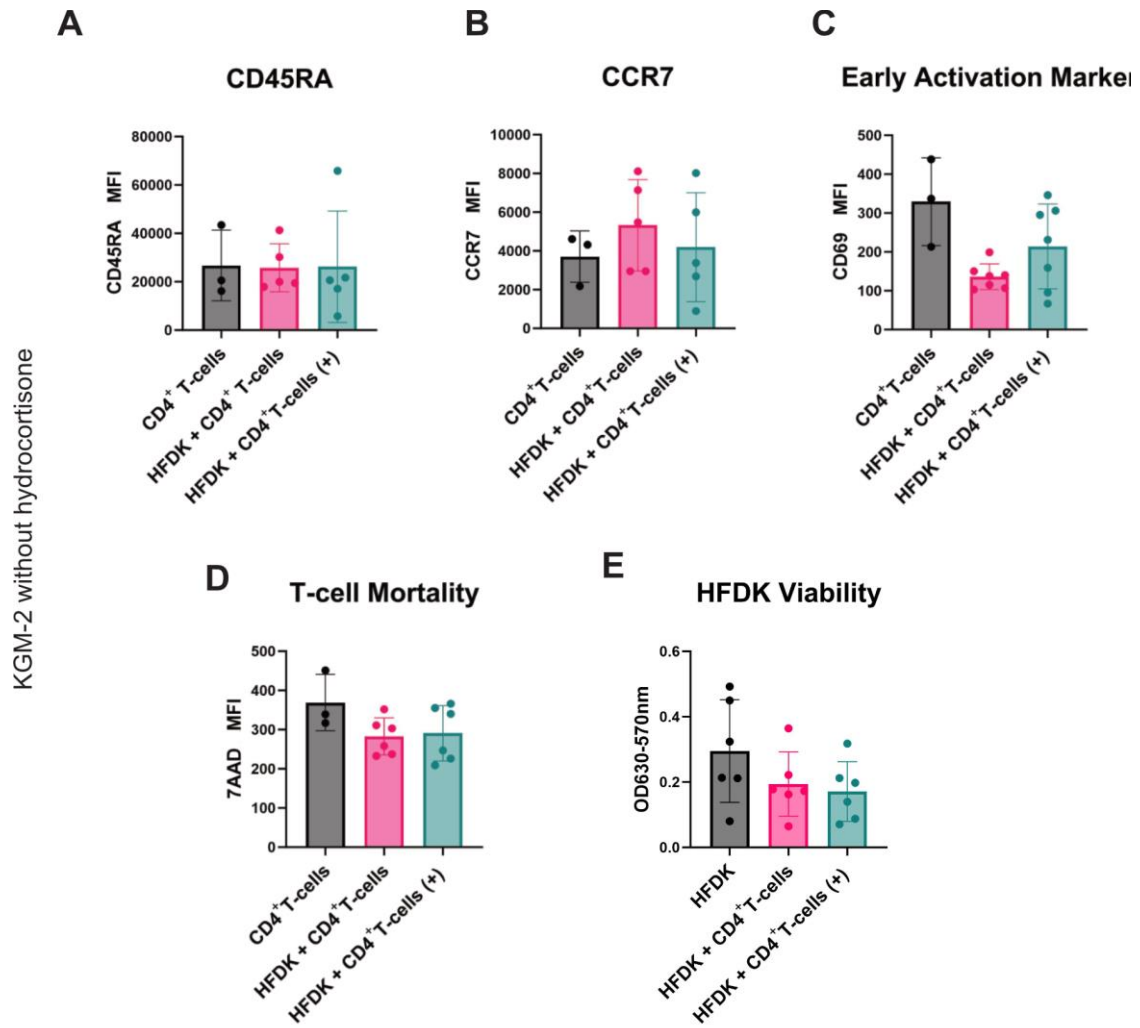


**Figure 21.** Comparison of single culture and co-culture of naïve CD4<sup>+</sup> T-lymphocytes and hair follicle-derived keratinocytes (HFDK) in KGM-2 without hydrocortisone (KGM-2 wo HC) either alone or with HFDK, for three days. T-lymphocytes were then collected for flow cytometry analysis and HFDK viability was assessed using the absorbance value from MTT assay. The absorbance value was calculated by subtracting the optical density (OD) at 570 nm from OD at 630 nm (OD<sub>630-570nm</sub>). The higher the OD<sub>630-570nm</sub>, the higher the cell viability. Co-culture incubated with anti-CD3/CD28 for 24 hours before flow cytometry analysis is indicated as “HFDK + CD4<sup>+</sup> T-lymphocytes (+)”. Cells were stained with antibodies against CD45RA, CCR7, and CD69, and 7-AAD was used as a mortality marker for T-lymphocytes. **A&B)** Character of T-lymphocytes **C)** The activation level of T-lymphocytes, **D)** Mortality of T-lymphocytes. **E)** The viability of HFDK. For T-lymphocytes, the high 7-AAD MFI reflects high mortality. Data are presented as mean ± SD. Statistical analysis was performed using one-way ANOVA with Tukey’s multiple comparisons test. The p-values <0.05 (\*), <0.01 (\*\*), and <0.001 (\*\*\*) are indicated. n=3-6.

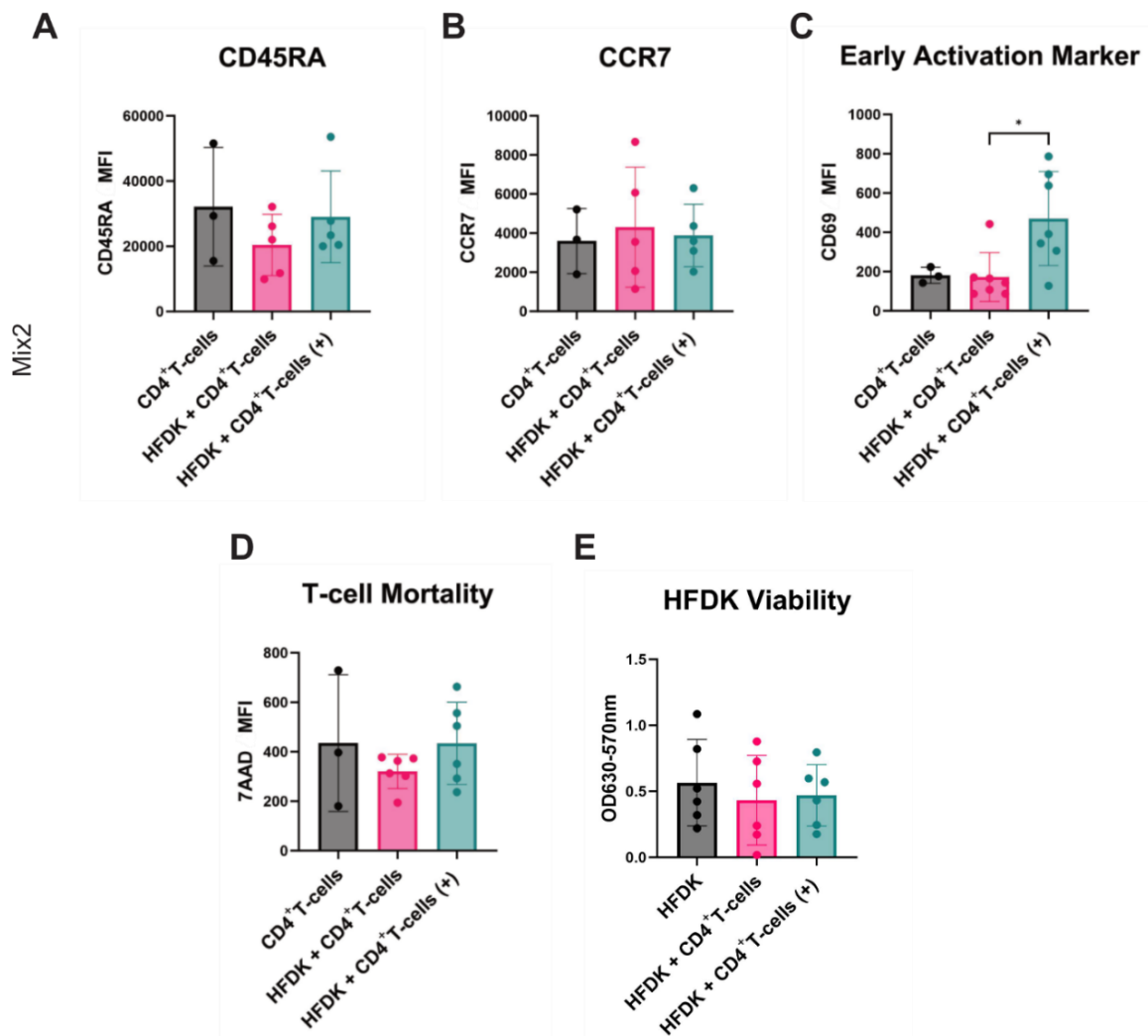


**Figure 22. Comparison of single culture and co-culture of naïve CD4<sup>+</sup> T-lymphocytes and hair follicle-derived keratinocytes (HFDK).** Naïve T-lymphocytes were cultured in Mix 2, either alone or with HFDK, for three days. T-lymphocytes were then collected for flow cytometry analysis and HFDK viability was assessed using the absorbance value from MTT assay. The absorbance value was calculated by subtracting the optical density (OD) at 570 nm from OD at 630 nm (OD630-570nm). The higher the OD630-570nm, the higher the cell viability. Co-culture incubated with T-cell activator for 24 hours before flow cytometry analysis is indicated as “HFDK + CD4<sup>+</sup> T-lymphocytes (+)”. Cells were stained with antibodies against CD45RA, CCR7, and CD69, and 7-AAD was used as a mortality marker for T-lymphocytes. **A&B)** Character of T-lymphocytes **C)** The activation level of T-lymphocytes, **D)** Mortality of T-lymphocytes. **E)** The viability of HFDK. For T-lymphocytes, the high 7-AAD MFI reflects high mortality. Data are presented as mean  $\pm$  SD. Statistical analysis was performed using one-way ANOVA with Tukey’s multiple comparisons test. The p-values <0.05 (\*), <0.01 (\*\*), and <0.001 (\*\*\*) are indicated. n=3-6.

#### 4.3.2 Comparative Study of Autologous versus Allogeneic Co-Cultures

Given that T-lymphocytes are recognized as the primary effectors in host vs. graft disease, a key aspect of this project involves the utilization of T-lymphocytes and HFDK. It is of interest to explore the feasibility of developing an autologous assay and to assess whether the autologous assay exhibits greater potential than the allogeneic counterpart.

To accomplish the aim, co-culture experiments were conducted using T-lymphocytes and HFDK from the same individual (autologous) and different individuals (allogeneic). These experiments were performed in KGM-2 wo HC or Mix2. The phenotype and the mortality of the co-cultured T-lymphocytes were assessed using flow cytometry. The viability of HFDK was analyzed through MTT assays.

The results indicate that T-lymphocytes co-cultured with autologous HFDK exhibited similar levels of CD45RA, CCR7, CD69, and mortality as those co-cultured with allogeneic HFDK in KGM-2 wo HC medium (**Figure 23**). This suggests that the origin of HFDK did not significantly impact T-lymphocyte activation or survival in this medium. However, MTT analysis revealed a trend toward higher HFDK viability when co-cultured with autologous T-lymphocytes compared to allogeneic T-lymphocytes in both KGM-2 wo HC and Mix2 media. This implies that autologous T-lymphocytes exhibited less cytotoxicity towards HFDK in both media.

Interestingly, it can be observed that T-lymphocytes co-cultured with autologous HFDK tended to have lower CD69 levels than those co-cultured with allogeneic HFDK in the Mix2 medium (**Figure 24**). CD69 is an early activation marker for T-lymphocytes, suggesting that autologous HFDK might dampen T-lymphocyte activation in this medium. These findings highlight subtle differences between autologous and allogeneic co-cultures of HFDK and T-lymphocytes.

Briefly, the study demonstrates that T-lymphocytes exhibit similar behavior when co-cultured with autologous HFDK (same donor) and allogenic HFDK (different donor). Different culture media do not lead to a different interaction between the cells. However, the HFDK co-cultured with autologous T-lymphocytes appear to show a trend of lower mortality. Notably, allogenic HFDK may have an autoactivation effect on T-lymphocytes in the Mix2 medium. These findings suggest that the choice of cell source and culture conditions can influence the interaction between T-lymphocytes and HFDK, which has potential implications for assay development strategies.

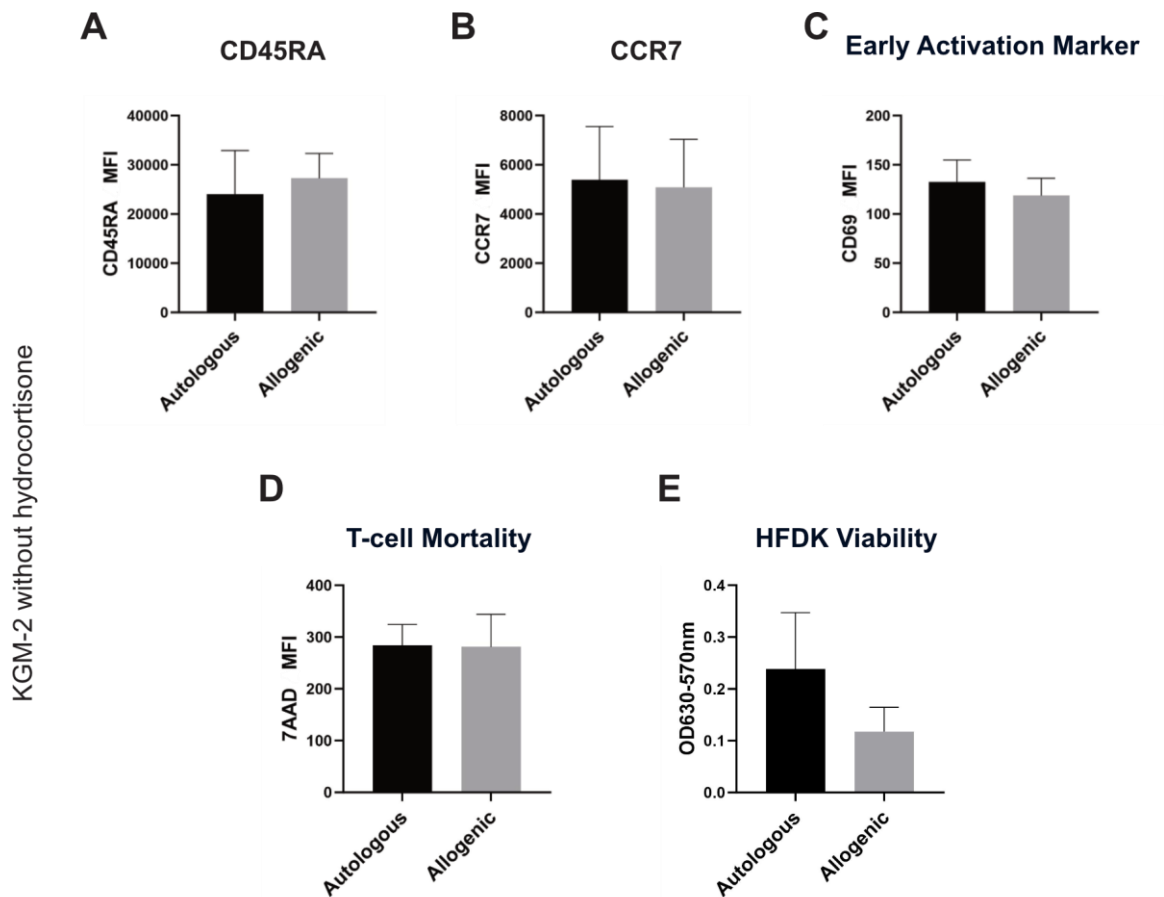


**Figure 23. Comparison of T-lymphocyte phenotype and hair follicle-derived keratinocytes (HFDK) viability between autologous and allogeneic co-cultures.** T-lymphocytes and HFDK were co-cultured for three days in KGM-2 without hydrocortisone before T-lymphocytes were collected for flow cytometry analysis. HFDK viability was assessed using the absorbance value from the MTT assay. The absorbance value was calculated by subtracting the optical density (OD) at 570 nm from OD at 630 nm ( $OD_{630-570nm}$ ). The higher the  $OD_{630-570nm}$ , the higher the cell viability. T-lymphocytes were stained with antibodies against CD45RA, CCR7, CD69, and 7-AAD. The higher the 7-AAD level, the higher cell mortality. **A&B)** Character of T-lymphocytes **C)** The activation level of T-lymphocytes, **D)** Mortality of T-lymphocytes. **E)** The viability of HFDK. Data are presented as mean  $\pm$  SD. Statistical analysis was performed with the paired t-test. The p-values  $<0.05$  (\*),  $<0.01$  (\*\*), and  $<0.001$  (\*\*\*) are indicated.  $n=3-6$ .

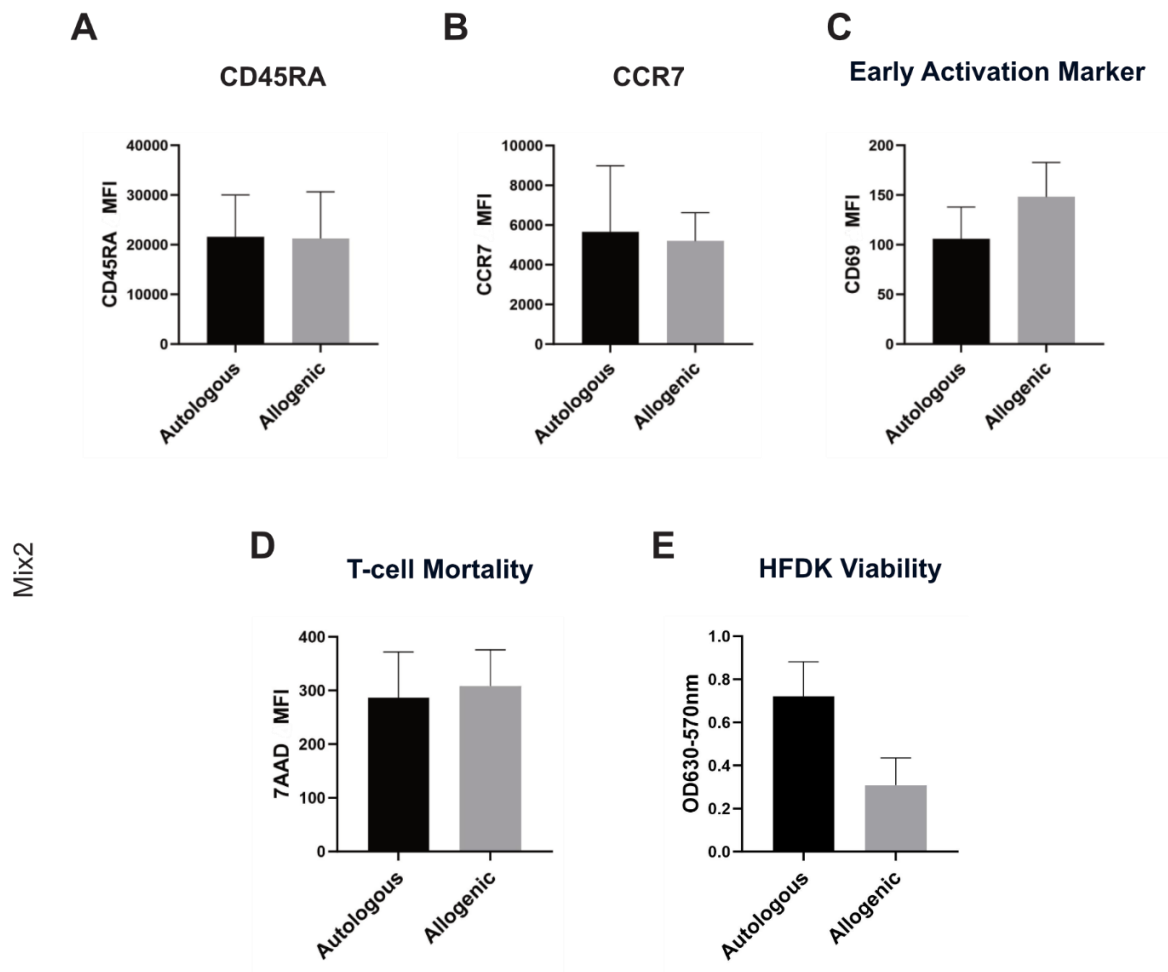


**Figure 24. Comparison of T-lymphocyte phenotype and hair follicle-derived keratinocytes (HFDK) viability between autologous and allogeneic co-cultures.** T-lymphocytes and HFDK were co-cultured for three days in Mix2 medium before T-lymphocytes were collected for flow cytometry analysis. HFDK viability was assessed using the absorbance value from the MTT assay. The absorbance value was calculated by subtracting the optical density (OD) at 570 nm from OD at 630 nm (OD630-570nm). The higher the OD630-570nm, the higher the cell viability. T-lymphocytes were stained with antibodies against CD45RA, CCR7, CD69, and 7-AAD. The higher the 7-AAD level, the higher cell mortality. **A&B)** Character of T-lymphocytes **C)** The activation level of T-lymphocytes, **D)** Mortality of T-lymphocytes. **E)** The viability of HFDK. Data are presented as mean  $\pm$  SD. Statistical analysis was performed with the paired t-test. The p-values <0.05 (\*), <0.01 (\*\*), and <0.001 (\*\*\*) are indicated. n=3-6.

#### 4.3.3 The Impact of Different DNCB Dosage on HFDK and T-lymphocytes

Various concentrations of DNCB, a well-established potent skin sensitizer, were administered to isolated T-lymphocytes to evaluate their impact on both cell mortality and function. Separately, the HFDK were treated with the same range of DNCB concentrations, and the viability of the cells was assessed. The cells were incubated with the substance for 24 hours.

Flow cytometry analysis was employed to examine the effects of these concentrations. The results revealed that treating T-lymphocytes with a concentration of 10  $\mu$ M DNCB led to a noteworthy

reduction in CD45RA expression while having no discernible effect on CCR7 expression (**Figure 25A&B**). Conversely, when T-lymphocytes were directly exposed to 1  $\mu$ M and 10  $\mu$ M DNCB, there was a significant increase in 7-AAD MFI, which indicates increased cell mortality (**Figure 25C**).

In parallel, HFDK were subjected to the same range of DNCB concentrations. The assessment of the viability of HFDK revealed a significant decline, commencing with the exposure to 0.1  $\mu$ M DNCB. More notably, a more pronounced reduction in the viability of the HFDK was observed when HFDK were treated with 1  $\mu$ M and 10  $\mu$ M DNCB (**Figure 25D**).

These findings collectively suggest that a concentration of 0.1  $\mu$ M DNCB is the most suitable for maintaining T-lymphocyte function without leading to the upregulation of 7-AAD expression, which is an indication of higher cell death in the context of 2D co-culture. Moreover, even though the 0.1  $\mu$ M DNCB resulted in reduced HFDK viability, it is still acceptable when compared to the viability of HFDK after the 1  $\mu$ M and 10  $\mu$ M DNCB treatment.

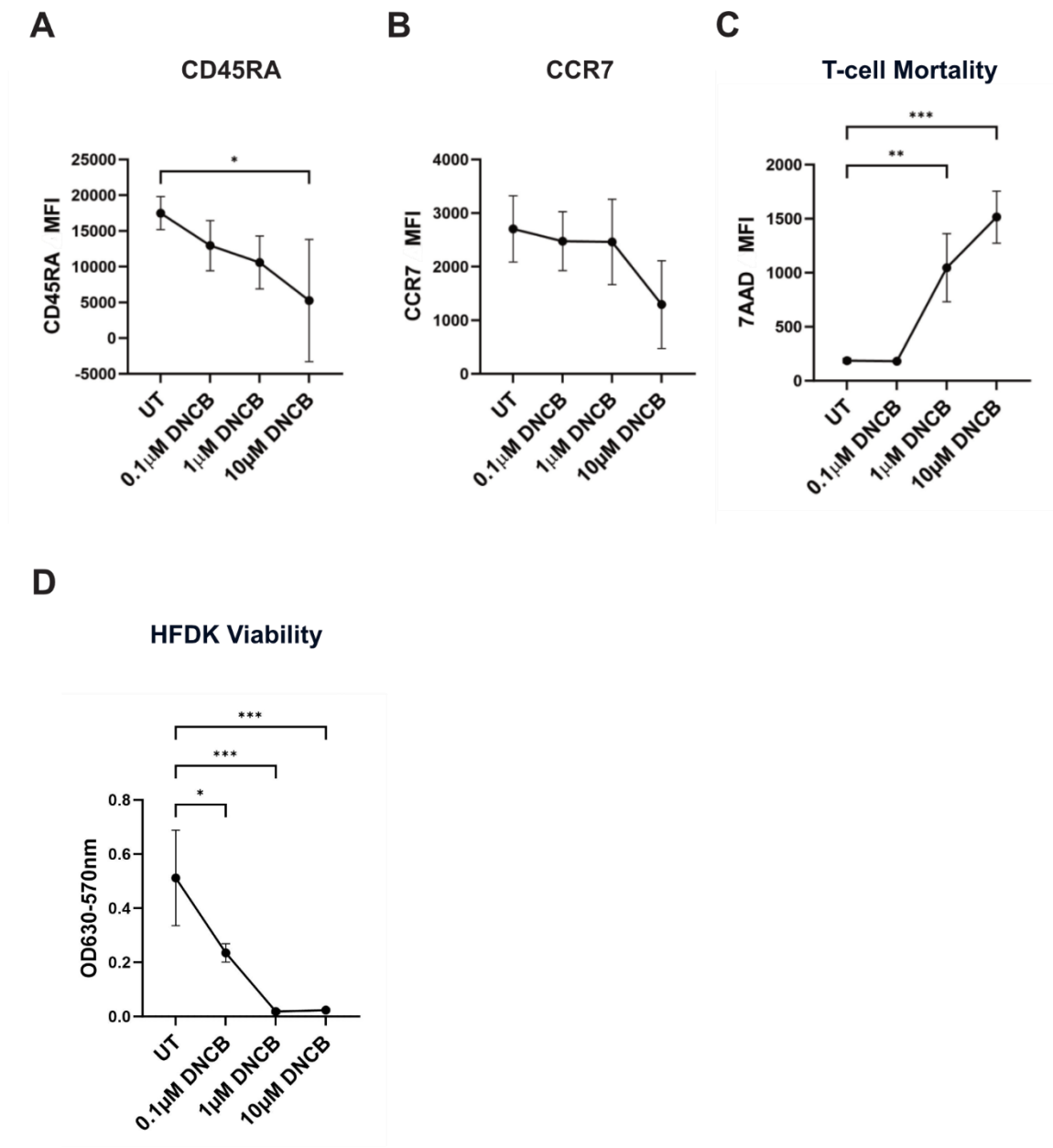


**Figure 25. The effect of 2,4-Dinitrochlorobenzene (DNCB) concentration on the character, mortality, and viability of the cells.** T-lymphocytes or hair follicle-derived keratinocytes (HFDK) were incubated in 0.1 μM, 1 μM, and 10 μM of DNCB for 24 hours then the cells were collected for flow cytometry analysis. **A)** Effect of DNCB concentration on CD45RA expression, **B)** CCR7 expression, and **C)** T-lymphocyte mortality. The higher the 7-AAD MFI the higher mortality of the cell. **D)** The viability of HFDK. HFDK viability was assessed using the absorbance value from the MTT assay. The absorbance value was calculated by subtracting optical density (OD) at 570 nm from OD at 630 nm (OD630-570nm). The higher the OD630-570nm, the higher the cell viability. Data are presented as mean ± SD. Statistical analysis was performed using one-way ANOVA with Dunnett's multiple comparisons test. The p-values <0.05 (\*), <0.001 (\*\*), and <0.001 (\*\*\*) are indicated. n=3.

#### 4.3.4 Response Patterns of T-Lymphocytes in the Co-Culture to DNCB

Following the determination of the appropriate concentration, the subsequent step involves assessing the sensitizing capability within the co-culture environment. DNCB, a well-known

strong skin sensitizer, is the ideal starting point for evaluating the response of the 2D co-culture system comprising HFDK and T-lymphocytes to the DNCB.

The cells were co-cultured and treated with a concentration of 0.1  $\mu\text{M}$  DNCB. The T-cell activator serves as positive control. The treatment duration was either 24 or 48 hours. Subsequently, T-lymphocytes were harvested for flow cytometry analysis, and HFDK underwent an MTT assay.

Flow cytometry results following 24 hours of treatment revealed that the co-culture treated with 0.1  $\mu\text{M}$  DNCB did not exhibit an induced expression of CD69 when compared to the untreated control. Importantly, significant upregulation of CD69 was observed in the positive control group (**Figure 26A**). The evaluation of cell viability, both for T-lymphocytes and HFDK, indicated similar outcomes across all experimental groups (**Figure 26B&C**). These findings collectively suggest that the 2D co-culture system did not exhibit a response to the treatment during the initial 24 hours.

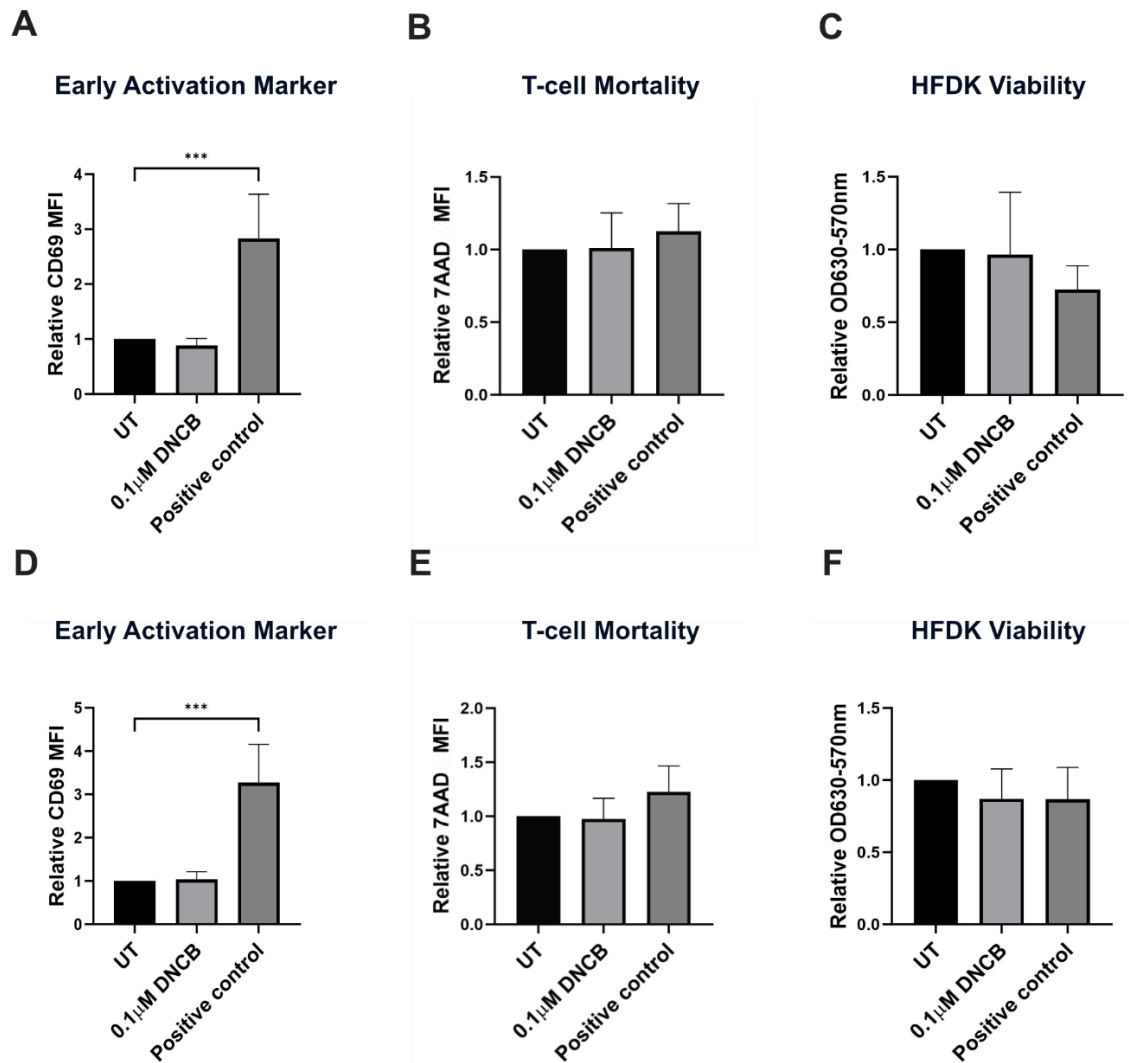


**Figure 26.** The effect of treating a 2D co-culture of hair follicle-derived keratinocytes (HFDK) and T-lymphocytes with 0.1 μM DNCB. The co-culture was incubated with 0.1 μM 2,4-Dinitrochlorobenzene (DNCB) or anti-CD3/CD28 for 24 hours before T-lymphocytes were collected for flow cytometry analysis. Anti-CD3/CD28 serves as a positive control. The untreated control (UT) was included. MTT assay was performed on HFDK to assess cell viability. Anti-CD3/CD28 was used as a positive control. T-lymphocytes were stained with anti-CD69. The 7-AAD was used to investigate T-lymphocyte mortality. The results are presented as relative to the untreated control. **A&D)** T-lymphocyte activation in comparison to the UT. **B&E)** T-lymphocyte mortality in comparison to the UT. In T-lymphocytes, the high 7-AAD indicates high mortality. **C&F)** Viability of HFDK based on the absorbance calculated from optical density (OD) 630-570nm in comparison to the UT. In HFDK, the higher the OD630-570nm value, the higher the cell viability. Results are presented as mean ± SD. Statistical analysis was performed using one-way ANOVA with Dunnett's multiple comparisons test. The p-values <0.05 (\*), <0.01 (\*\*), and <0.001 (\*\*\*) are indicated. n=3-6.

Similarly, the 48-hour treatment yielded results consistent with the 24-hour response. The cells displayed a notable increase in CD69 levels in response to the positive control (**Figure 26D**). Furthermore, the treatment did not have an adverse effect on cell viability (**Figure 26E&F**). Furthermore, a statistical analysis comparing the 24-hour and 48-hour treatments revealed no significant difference between the two time periods, indicating that extending the treatment to 48 hours did not result in a more robust or enhanced response (**Figure 27**).

In summary, this investigation meticulously refined co-culture parameters for T-lymphocytes and HFDK, discerning KGM-2 wo HC and Mix2 as optimal media choices. These media demonstrated the preservation of cellular functionality while upholding viability, with Mix2 particularly enhancing T-lymphocyte responsivity. Analysis of autologous and allogeneic co-cultures revealed negligible impacts of HFDK origin on T-lymphocyte activation or survival. Dose-response profiling identified 0.1  $\mu$ M DNCB as the most suitable concentration for both cell types. Furthermore, 2D co-culture experiments involving HFDK and T-lymphocytes, treated with 0.1  $\mu$ M DNCB, evinced an absence of substantial reactivity. Viability assessments across varied time points affirmed the persistence of cellular integrity. These outcomes decisively negate the proposition that HFDK, in isolation, can effectively function as APCs. The results underscore the indispensability of classical APCs, such as LC and DC.

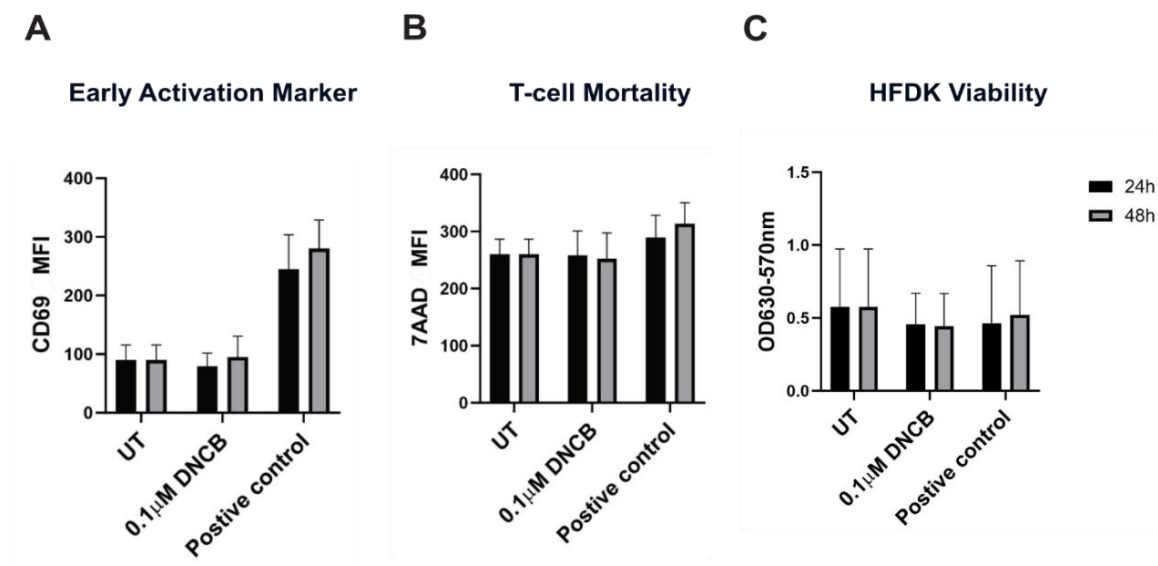


**Figure 27.** The direct comparison between the effect of 24-hour and 48-hour treatment with 2,4-Dinitrochlorobenzene (DNCB) on a co-culture of hair follicle-derived keratinocytes (HFDK) and T-lymphocytes. The co-culture was incubated with DNCB for either 24 or 48 hours before T-lymphocytes were collected for flow cytometry analysis. MTT assay was performed on HFDK to assess cell viability. Anti-CD3/CD28 was used as a positive control. T-lymphocytes were stained with anti-CD69 and 7-AAD was used to investigate T-lymphocyte viability. **A)** Absolute CD69 MFI of T-lymphocytes. **B)** The viability of T-lymphocytes. In T-lymphocytes, the higher 7-AAD indicates lower cell viability. **C)** The viability of HFDK based on the absorbance. In HFDK, the absorbance was calculated by subtracting OD at 570 nm from OD at 630 nm (OD630-570nm) to assess HFDK viability. The higher the OD630-570nm, the higher the cell viability. Results are presented as mean  $\pm$  SD. Statistical analysis was performed using two-way ANOVA with Sidak multiple comparisons test. The *p*-values <0.05 (\*), <0.01 (\*\*), and <0.001 (\*\*\*) are indicated. *n*=6.

#### 4.4 Insights from Three-Cell Co-Culture Systems

The initial skin sensitization phase involves a complex interaction among keratinocytes, APCs, and CD4+ T-lymphocytes. Keratinocytes play a crucial role in activating LC and DC, which capture and present the skin sensitizer to CD4+ T-lymphocytes. T-lymphocytes respond to the presented

sensitizer, transforming into effector T-lymphocytes that migrate back to the skin, marking the initiation of the elicitation phase.

Intriguingly, the earlier research findings in this thesis have underscored that T-lymphocytes, whether in isolation or co-culture with HFDK, do not exhibit any response to DNCB treatment, a potent skin sensitizer. Consequently, it becomes imperative to incorporate LCs into the co-culture system, given their pivotal role as mediators facilitating communication between T-lymphocytes and keratinocytes.

#### 4.4.1 Behavioral Dynamics of Immune Cells in Three-Cell Configurations

In this experimental setup, T-lymphocytes, MoLC, and HFDK have been co-cultured together within a medium known as Mix2. Leveraging the collective insights gleaned from the previous research in this thesis and the work from Geisendörfer (Geisendörfer, 2022), Mix2 emerges as a promising medium for the co-cultivation of MoLC, T-lymphocytes, and HFDK.

From the T-lymphocytes aspect, T-lymphocyte characterization reveals a noteworthy upregulation of CD45RA in co-cultivation with HFDK and MoLC (**Figure 28A**). Although a trend of decreased CCR7 expression is observable in the co-culture of three cells, it fails to attain statistical significance (**Figure 28B**). There is a distinct trend toward upregulation of CD69 in T-lymphocytes when co-cultured in the presence of HFDK and MoLC (**Figure 28C**). Furthermore, the 7-AAD level is at its lowest when T-lymphocytes are cultured solely with MoLC, reflecting the lowest cell mortality, yet this difference does not reach statistical significance, allowing it to be considered comparable across all culture conditions (**Figure 28D**). These findings collectively suggest that MoLC and HFDK do not influence T-lymphocyte mortality and do not significantly trigger T-lymphocyte responses.

From the MoLC side, the results have shown that MoLC and MoLC co-cultured with T-lymphocytes appear to have similar levels of CD86 expression. CD86 is a maturation marker of the MoLC, which signifies the activation of the cells. Interestingly, when the HFDK are included in the co-culture mix, MoLC have significantly upregulated the CD86 expression (**Figure 28E**). The co-culture, however, does not influence the mortality of the MoLC (**Figure 28F**).

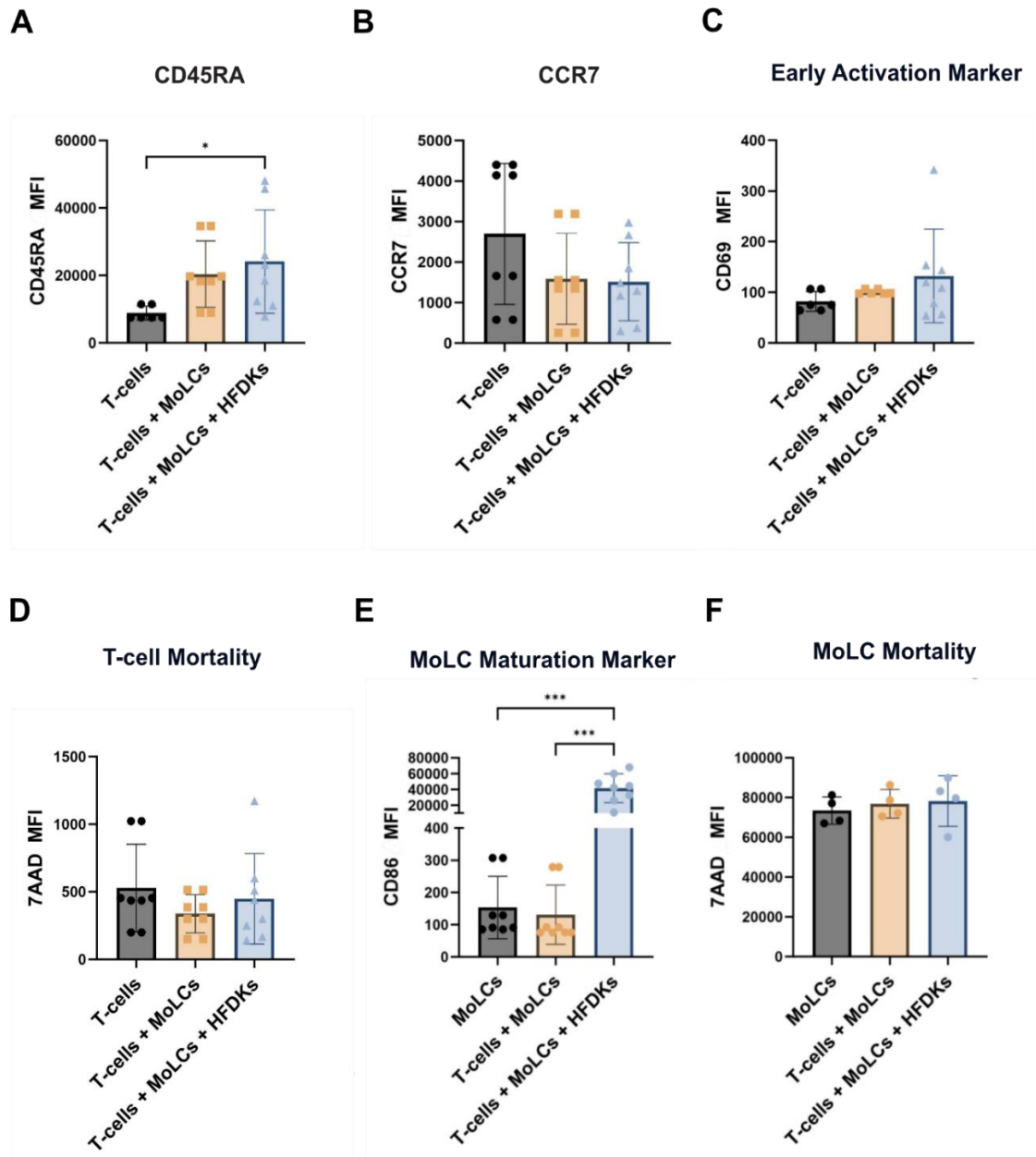


**Figure 28. Characterization of T-lymphocytes and monocyte-derived Langerhans cells (MoLC) from a co-culture of hair follicle-derived keratinocytes (HFDK), MoLC, and CD4+ naïve T-lymphocytes.** The co-culture was performed in Mix2 medium for three days, after which immune cells were harvested for flow cytometry analysis T-lymphocytes were labeled with (A) anti-CD45RA, (B) anti-CCR7, and (C) anti-CD69 antibodies. CD45RA and CCR7 are naïve T-lymphocyte characterization markers. CD69 is an early activation marker of T-lymphocytes. D&F) Cell mortality was determined using 7-AAD. The high 7-AAD MFI reflects high cell mortality. E) MoLC maturation was measured from the expression of CD86. Data are presented as mean  $\pm$  SD. Statistical analysis was performed using two-way ANOVA with the Tukey multiple comparisons test. The p-values <0.05 (\*), <0.01 (\*\*), and <0.001 (\*\*\*) are indicated. N=4-8

## 4.4.2 Comparative Immune Responses in Autologous vs. Allogenic Three-Cell Systems

The distinction between autologous and allogenic co-culture of these cells is one of the central themes in this project. Consequently, this aspect was also explored within the context of co-culturing the three cell types. Autologous cells are anticipated to facilitate coexistence among different cell types without inducing immune responses, while allogenic cells are expected to yield contrary outcomes.

### 4.4.2.1 *Interaction Dynamics between T-lymphocytes and MoLC*

The autologous and allogenic co-cultures of T-lymphocytes and MoLC were investigated to explore alloreactivity, primarily mediated through the interaction of immune cells.

The result shows that T-lymphocytes cultured with the MoLC from the same donor (autologous) have significantly higher CD45RA expression than T-lymphocytes cultured with the MoLC from different donors (allogenic) (**Figure 29A**). The levels of CCR7, CD69 (Early activation markers), and T-lymphocyte mortality are similar between the autologous and allogenic co-culture (**Figure 29B-D**). On the MoLC side, a trend suggests higher maturation marker expression in the autologous co-culture setting, but this trend is not statistically significant (**Figure 29E**). Additionally, the co-culture has no increase in cell mortality (**Figure 29F**).

In brief, the immune cells from the donor pools do not elicit a reaction when paired with each other, indicating the potential for combining these donors in experimental settings.

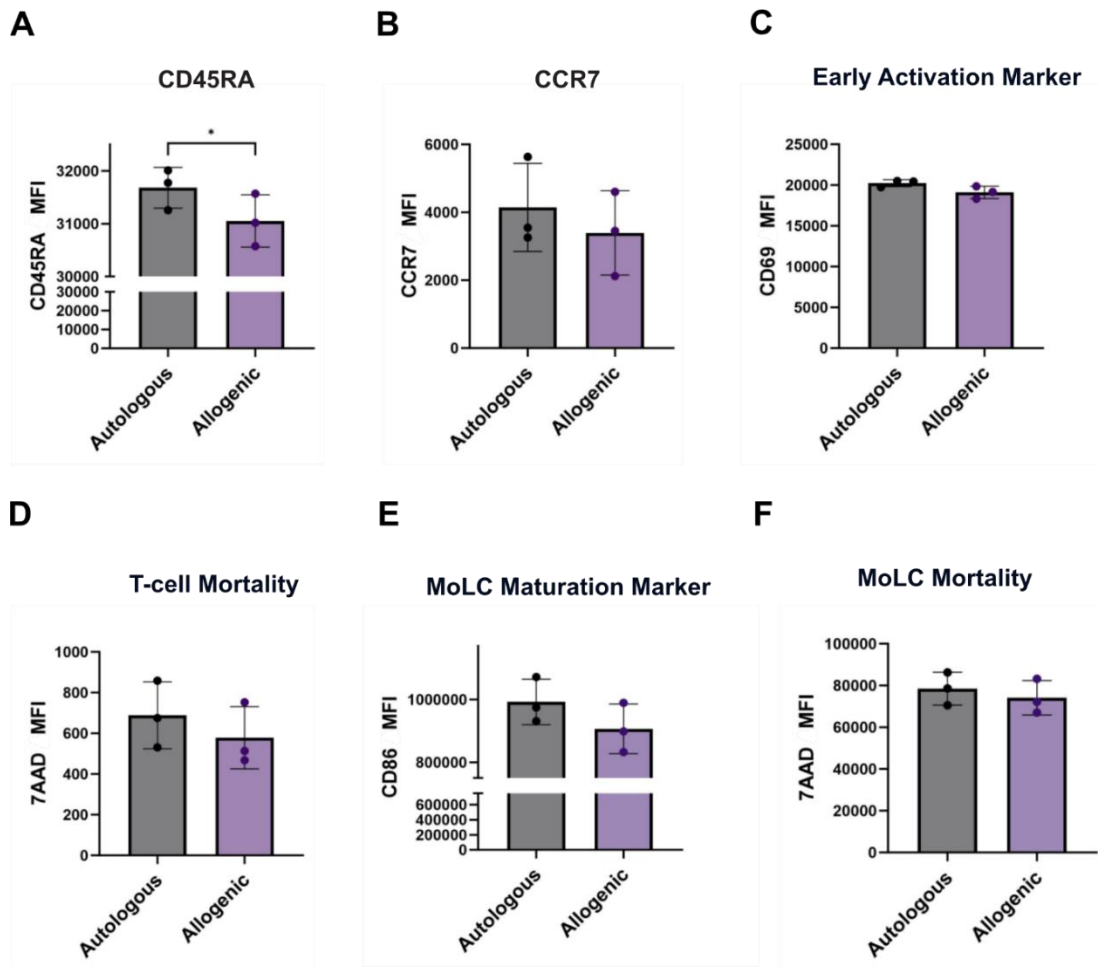


**Figure 29. The characterization of T-lymphocytes and monocyte-derived Langerhans cells (MoLC) from the autologous versus allogenic co-culture.** MoLC and CD4+ naïve T-lymphocytes from the same donor (autologous) or different donor (allogenic) were co-cultured in Mix2 medium for three days. Afterward, the immune cells were harvested for the flow cytometry analysis. T-lymphocytes were labeled with (A) anti-CD45RA, (B) anti-CCR7, and (C) anti-CD69 antibodies. CD45RA and CCR7 are naïve T-lymphocyte characterization markers. CD69 is an early activation marker of T-lymphocytes. D&F) Cell mortality was determined using 7-AAD. The high 7-AAD MFI reflects high cell mortality. E) MoLC maturation was measured from the expression of CD86. Data are presented as mean ± SD. Statistical analysis was performed using a paired T-test. The p-values <0.05 (\*), <0.01 (\*\*), and <0.001 (\*\*\*) are indicated. n=3

#### 4.4.2.2 Interaction Dynamics among T-lymphocytes, MoLC, and HFDK

Following the investigation of autologous and allogenic co-cultures of immune cells, the influence of HFDK in the co-culture setup was examined. All cells originate from the same donor in autologous co-culture, whereas in allogenic co-culture, each cell comes from a different donor.

From the T-lymphocytes aspect, the results demonstrate that the levels of CD45RA are comparable between the two culture conditions (Figure 30A). Interestingly, a noteworthy trend indicates upregulation of CCR7 in allogenic co-culture, as well as upregulation of CD69 MFI and 7AAD MFI in autologous co-culture (Figure 30B-D). However, these findings lack statistical evidence to highlight the differences. Furthermore, the cultivation of MoLC with autologous HFDK and T-lymphocytes does not seem to promote the expression of CD86 compared to MoLC cultivated in

an allogenic setting (**Figure 30E**). Additionally, the autologous cultivation setting does not result in reduced or increased mortality of the cells (**Figure 30F**).

Autologous cultivation does not appear to have an advantage over allogenic co-culture regarding the auto-activation level or the cell characterization marker expression.

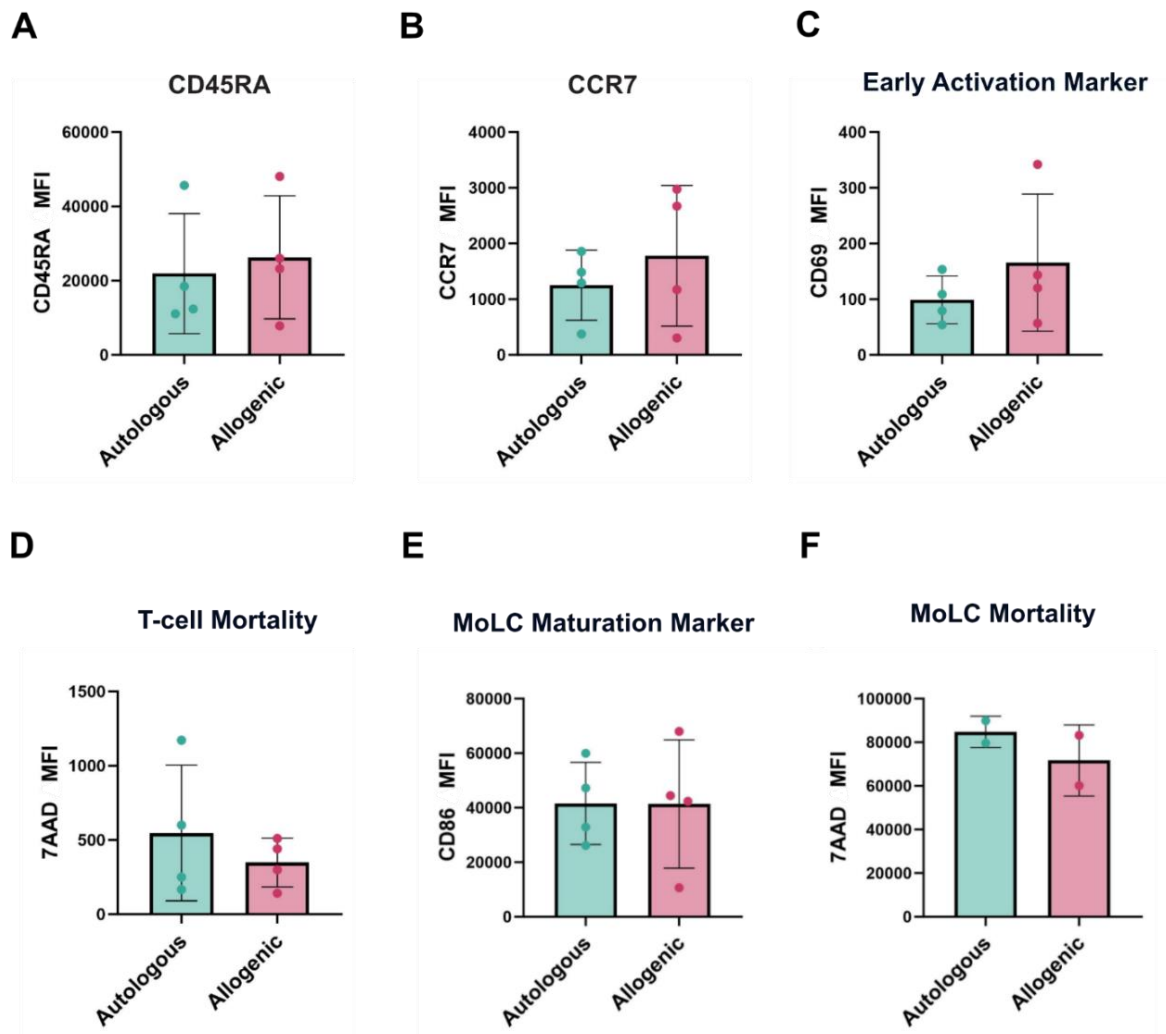


**Figure 30. The characterization of T-lymphocytes and monocyte-derived Langerhans cell (MoLC) from the autologous versus allogenic co-culture of three cell types.** MoLC and CD4+ naïve T-lymphocytes from the same donor or different donor were co-cultured with matching hair follicle-derived keratinocytes (HFDK-autologous) or non-matching HFDK (allogenic) in Mix2 medium for three days. Afterward, the immune cells were harvested for the flow cytometry analysis. T-lymphocytes were labeled with (A) anti-CD45RA, (B) anti-CCR7, and (C) anti-CD69 antibodies. CD45RA and CCR7 are naïve T-lymphocyte characterization markers. CD69 is an early activation marker of T-lymphocytes. **D&F**) Cell mortality was determined using 7-AAD. The high 7-AAD MFI reflects high cell mortality. **E**) MoLC maturation was measured from the expression of CD86. Data are presented as mean  $\pm$  SD. Statistical analysis was performed using a paired T-test. The p-values <0.05 (\*), <0.01 (\*\*), and <0.001 (\*\*\*) are indicated. n=2-4

#### 4.4.3 Sensitivity to DNCB of The Three-Cell Culture

Building upon the established experimental conditions, the co-culture of the three cell types in Mix2 medium for three days provides an appropriate and stable environment for the investigation. Importantly, this co-culture setup has consistently failed to induce T-lymphocyte activation, which aligns with the prior observations. The current research objective is to evaluate the responsiveness system to skin sensitizers, with DNCB, a widely acknowledged extreme sensitizer, selected as the test agent.

Flow cytometric analysis after DNCB exposure has elucidated persistent CD45RA and CCR7 expression levels across treated and untreated cohorts, regardless of tested DNCB concentration (**Figure 31A&B**). Notably, while there is a trend towards CD69 upregulation, it fails to attain statistical significance (**Figure 31C**). The exclusive significant response presents in the positive control group, thereby validating the integrity of the experimental design. DNCB treatment exerts no significant effect that leads to changes in the mortality of the cells, as reflected by unaltered 7AAD levels (**Figure 31D**). In the co-culture setting, DNCB concentration did not increase T-lymphocyte mortality. However, when T-lymphocytes are cultured alone, DNCB shows cytotoxic effects at concentrations as low as 1  $\mu$ M (**see Chapter 4.3.3 Figure 25**).

Furthermore, the MoLC did not exhibit upregulation of the maturation marker (CD86) after treatment with either DNCB or the positive control (**Figure 31E**). In terms of cell mortality, the treatment demonstrated a progressive trend of 7-AAD corresponding to the increase in DNCB concentration and the positive control indicating the increase in cell mortality. It is important to note that the treatment's effect on cell mortality did not reach statistical significance (**Figure 31F**).

In summary, the three cell co-culture system, currently under scrutiny regarding its reactivity towards DNCB, surprisingly resulted in unresponsiveness to this extreme sensitizer. This outcome poses substantive questions concerning the utility of this assay for skin sensitizer assessment, thereby necessitating further refinement and exploration of the experimental framework.

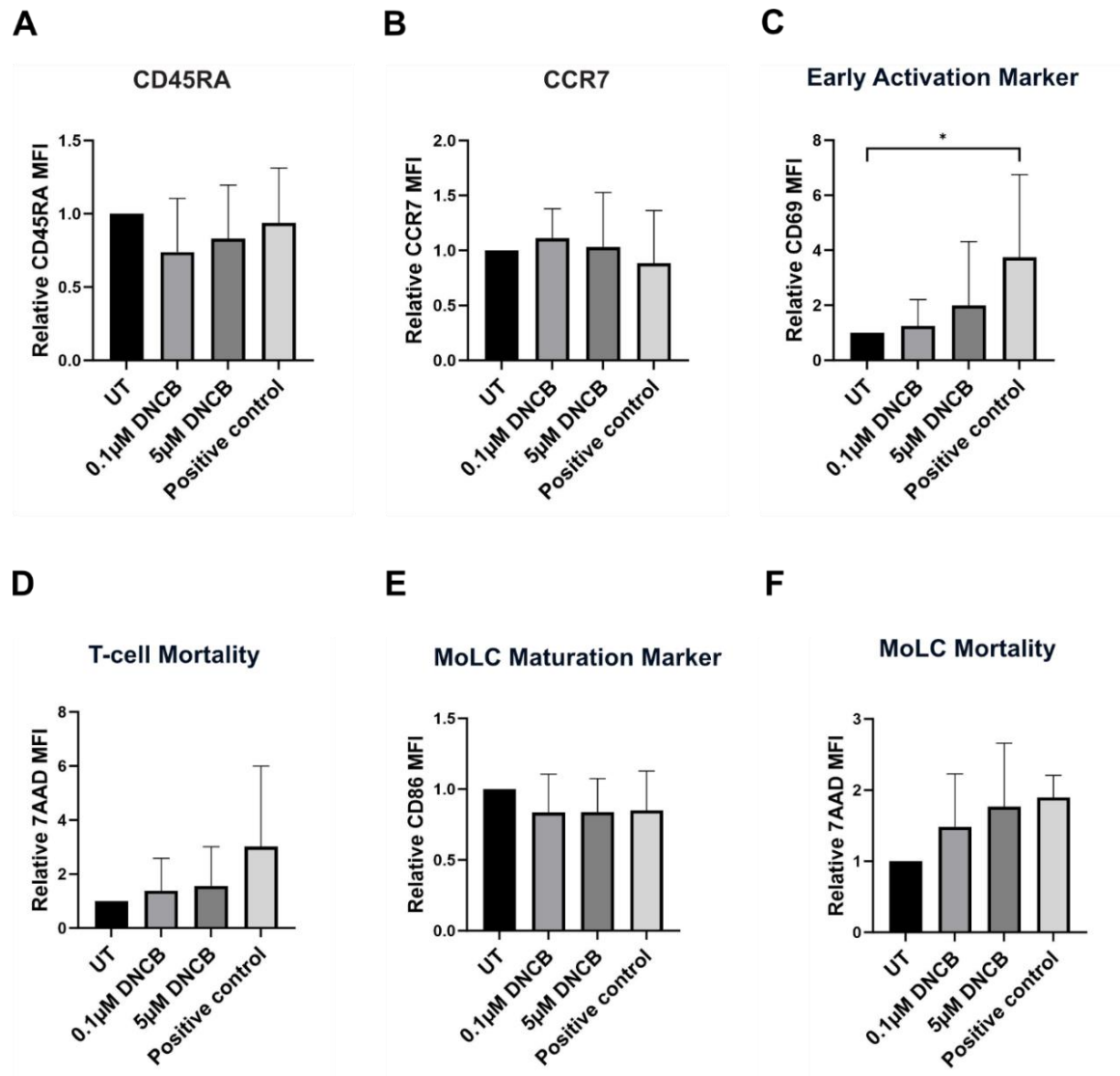


**Figure 31.** The effect of 2,4-Dinitrochlorobenzene (DNCB) on T-lymphocyte and monocyte-derived Langerhans cells (MoLC) from the three cells co-culture. T-lymphocytes were co-cultured with hair follicle-derived keratinocytes (HFDK), and MoLC in Mix 2 medium. The co-culture was treated with 0.1 or 5 μM DNCB. The co-culture was incubated with the DNCB for three days. Afterward, T-lymphocytes were labeled with (A) anti-CD45RA, (B) anti-CCR7, and (C) anti-CD69 antibodies. CD45RA and CCR7 are naïve T-lymphocyte characterization markers. CD69 is an early activation marker of T-lymphocytes. (D&F) Cell mortality was determined using 7-AAD. The high 7-AAD MFI reflects high cell mortality. (E) MoLC maturation was measured from the expression of CD86. The results are presented as mean ± SD. The data was statistically analyzed using one-way ANOVA with Dunnett correction for multiple comparisons. The p-values <0.05 (\*), <0.01 (\*\*), and <0.001 (\*\*\*) are indicated. n=3-8

The research has revealed intriguing aspects of how MoLC, T-lymphocytes, and HFDK interact in skin sensitization studies. According to the expression of CD86, the results demonstrate MoLC maturation in the presence of HFDK. The autologous and allogeneic co-culture findings suggest that donors do not play a role in this maturation, underlining the interaction between the MoLC and the HFDK.

Moreover, these findings focus on how co-culturing MoLC with T-lymphocytes or T-lymphocytes and HFDK did not trigger T-lymphocyte activation. This fact could be advantageous for other

experiments involving the co-cultivation of these two cells. Subsequent experiments revealed a self-activation tendency in MoLC in the presence of HFDK within the co-culture setup. This self-activation did not result in the effective processing and presentation of new antigens to T-lymphocytes. Consequently, the initially chosen method was deemed unsuitable for testing skin sensitizers.

In conclusion, the research highlights the complexities of understanding skin sensitization mechanisms and how these cell types interact. Although the initial expectations were not met, these unexpected findings emphasize the need for ongoing investigation and improvement of the experimental approach.

## 4.5 Advances in Immunocompetent Skin Models from Hair Follicle Cells

According to previous results, the simple two-dimensional (2D) co-culture in the well has not led to the expected outcomes. Therefore, the method was re-evaluated. It is unclear if the over-activation of MoLC led to the unresponsiveness of the whole system to the stimulants, or it could be that it is simply unsuitable for culturing the cells in a 2D environment. It is evident that the 3-dimensional (3D) environment is closer to the physiological environment and can promote cell differentiation reflecting the phenotype found in physiological skin (Huang et al., 2022). RHS are often matured in a transwell plate to achieve the air-liquid interface culture. Additionally, Gibbs et al. also used transwell cultivation for the LC migration to test skin sensitizers (Gibbs et al., 2013). Due to this fact, the immunocompetent skin models (ImmuSkin) were developed by combining the idea of both skin models and transwell migration assay with the addition of T-lymphocytes to increase the resemblance to the physiological skin.

### 4.5.1 Character of The RHS from Hair Follicle-derived Cells

The RHS-HFD were compared to the RHS-FD. Both were built using the same method, and these skin models were subjected to cryosectioning and subsequent staining with H&E staining as well as IF staining techniques targeting CK10, CK14, loricrin, and claudin.

Subsequent analysis of H&E and IF staining revealed loricrin, CK10, CK14, and claudin localization patterns in both RHS-FD and RHS-HFD. H&E staining showed similar patterns in both RHS-FD and RHS-HFD, with the dermis appearing pink and the epidermis pale pink/purple, while the stratum corneum exhibited a darker pink/purple color. Nuclei in all layers were stained dark purple. In the epidermis, keratinocytes displayed larger, round nuclei, particularly in the lower epidermal layers, with nuclei becoming flatter as cells migrated upward. The dermal layer comprised elongated cells with smaller nuclei, characteristic of fibroblasts. Both RHS-FD and RHS-HFD exhibited fully stratified epidermis (**Figure 32A&B**).

In the IF staining, CK14 was expressed from the stratum basale to the stratum granulosum in RHS-FD and RHS-HFD. CK10 was expressed in the stratum spinosum and stratum granulosum, while loricrin was found in the stratum granulosum and stratum corneum. Claudin, a marker for tight junction, appears to be within the stratum granulosum layer in both types of RHS (**Figure 32A&B**).

The epidermal thickness of RHS-FD measured 193  $\mu\text{m}$ , while RHS-HFD measured 137  $\mu\text{m}$ . The difference in these measurements was not statistically significant (**Figure 32C**), suggesting that RHS-HFD and RHS-FD have similar effects overall. This finding is consistent with the hypothesis and supports the potential of RHS-HFD as an alternative to RHS-FD.

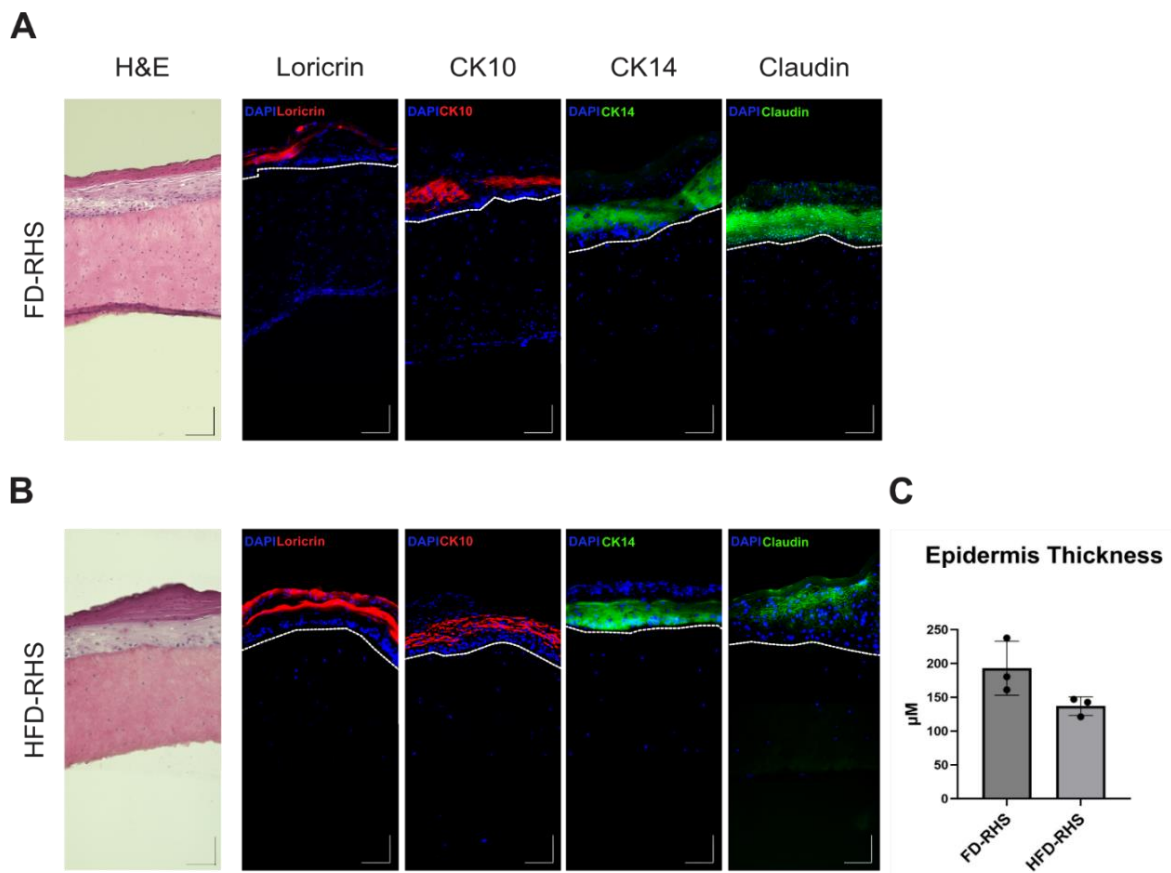


**Figure 32. The comparison of reconstructed human skin models from foreskin-derived cells (RHS-FD) and hair follicle-derived cells (RHS-HFD).** Reconstructed human skin models (RHS) were sectioned and stained with Hematoxylin and Eosin (H&E) staining and immunofluorescence (IF) staining to assess marker expression and morphology. Both types of RHS were stained for cytokeratin 14 (CK14)-green, cytokeratin 10 (CK10)-red, loricrin-red, and claudin-green. CK14 signified stratum basale. CK10 is the marker for stratum spinosum and granulosum. Stratum corneum is characterized by loricrin. The tight junction of the cells is presented by Claudin. Scale bar = 100 µm. Epidermal thickness was measured using the measuring function in ImageJ based on the scale bar. **A)** the representative microscopic pictures of RHS-FD. **B)** the representative microscopic picture of RHS-HFD. **C)** Epidermal thickness of RHS-FD and RHS-HFD. 4',6-diamidino-2-phenylindole (DAPI-blue) was used as nuclei marker. White dotted lines in the result of IF staining indicate the border of the epidermal and dermis layers, the epidermal layer being the upper layer and the dermis being the lower layer. Data are presented as mean ± SD. The paired T-test was used to analyze the data statistically. The p-values <0.05 (\*), <0.01 (\*\*), and <0.001 (\*\*\*) are indicated. n=3.

#### 4.5.2 Optimal Culture Conditions for Skin Models

Before introducing the immune cells into the RHS-HFD, it is necessary to determine the medium that can harmonize all aspects of this model. The three types of cells were cultivated together in the 2D environment in standard RHS medium (KDM), the Mix2 medium (50% RPMI1640 + 50% KGM-2 wo HC), which was preferred in the previous experiments with 2D co-culture, the mix of 50% RPMI1640 basal and 50% KDM (RKD1), or the DC generation medium. The cells were cultivated together for three days and characterized using flow cytometry.

The result shows that the level of CD1a, which is known to be the characterization marker of pan DC, appeared to be lower when the cells were cultured in KDM and RKD1 than in Mix2 and in the DC generation medium. In contrast, the level of CD207, an LC characterization marker, appeared to be significantly higher in the cells from KDM and RKD1 than in Mix2. The cells cultured in the DC generation medium have a comparable level of CD207 as the cells cultured in the Mix2. From the characterization marker alone, KDM or RKD1 seems favorable for the co-culture. However, the cells cultivated in these media appear to have significantly higher maturation marker levels than those cultivated in Mix2. The cells from the DC generation medium have comparable levels of maturation marker as the cells in Mix2. Lastly, the cells cultivated in KDM and RKD1 demonstrated significantly higher 7AAD levels than those from Mix2, while the cells from Mix2 had higher 7-AAD levels than those cultivated in the DC generation medium (**Figure 33**). The low 7-AAD level of the cells cultured in the DC generation medium indicates that the cells are the most viable in the medium compared to other tested media.

From the T-lymphocyte side, the result points to the trend of a slightly higher early activation marker in KDM and the lowest early activation marker in the DC generation medium without being statistically significant. The level of the late activation marker and 7-AAD are comparable in all tested media. The result indicates that the T-lymphocytes are not activated by the different components in the medium alone, and the medium does not increase the mortality of the cells either (**Figure 34**).

In conclusion, the DC generation medium appears to be the most beneficial medium for harmonizing immune cells with skin models. The significant differences between cells from each medium are in the level of CD207, CD86, and 7AAD, where KDM and RKD1 not only promote the CD207 expression but also induce a higher level of CD86 expression and lead to more cell death than the other two media. In comparing Mix2 and the DC generation medium, the DC generation medium has significantly resulted in lower cell mortality than Mix2. Apart from these results, Mix2 is the combination of RPMI1640 with KGM-2 wo HC, which the KGM-2 or KGM-2 wo HC are not suitable for the skin model as it prevents the keratinocytes from differentiating and forming the stratum corneum. Moreover, different media do not appear to influence T-lymphocytes based on the investigation of CD45RA, CCR7, CD69 marker presentation, and T-lymphocyte mortality. Considering this, the DC generation medium is the most suitable medium for immunocompetent skin models (ImmuSkins).

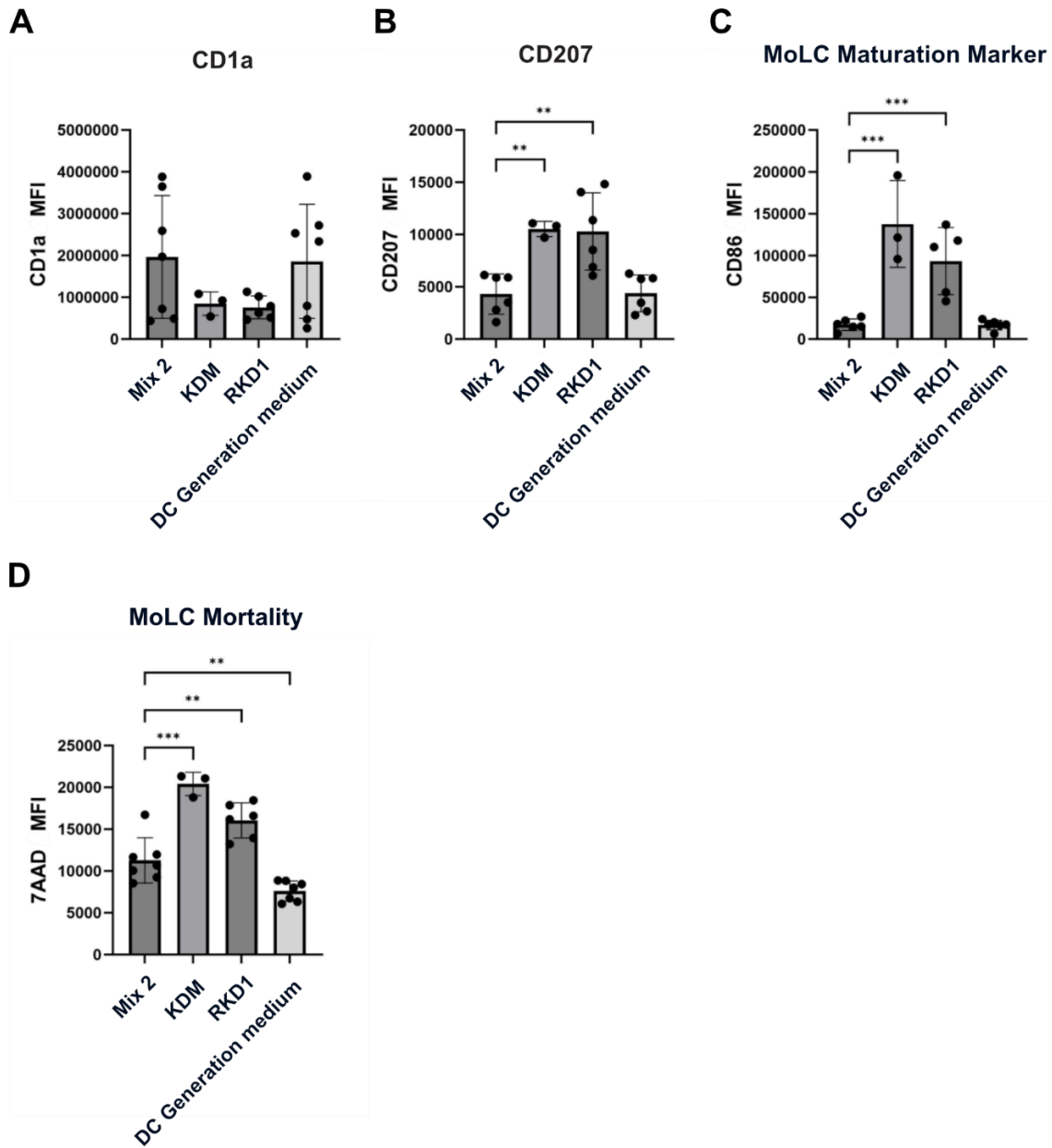


**Figure 33. Characterization of monocyte-derived Langerhans cells (MoLC) from co-culture in different media.** MoLC were co-cultured with T-lymphocytes and hair follicle-derived keratinocytes (HFDK) in a well for three days in one of the following media, 1:1 RPMI 1640 basal: KGM-2 without hydrocortisone (Mix2), Keratinocyte differentiation medium (KDM), 1:1 RPMI1640 basal: KDM (RKD1), or DC Generation Medium. Cells were collected for flow cytometry and stained with anti-CD1a-FITC (pan dendritic cells characterization marker), anti-CD207-APC (Langerhans cells characterization marker), and anti-CD86-BV605 (Langerhans cell maturation marker). Cell mortality was determined by 7-AAD staining. The higher 7-AAD level indicates the higher cell mortality. Data are presented as mean  $\pm$  SD. Ordinary one-way ANOVA with Dunnett's correction for multiple comparisons was used to analyze the data. The p-values  $<0.05$  (\*),  $<0.01$  (\*\*), and  $<0.001$  (\*\*\*) are indicated.  $n=3-6$ .

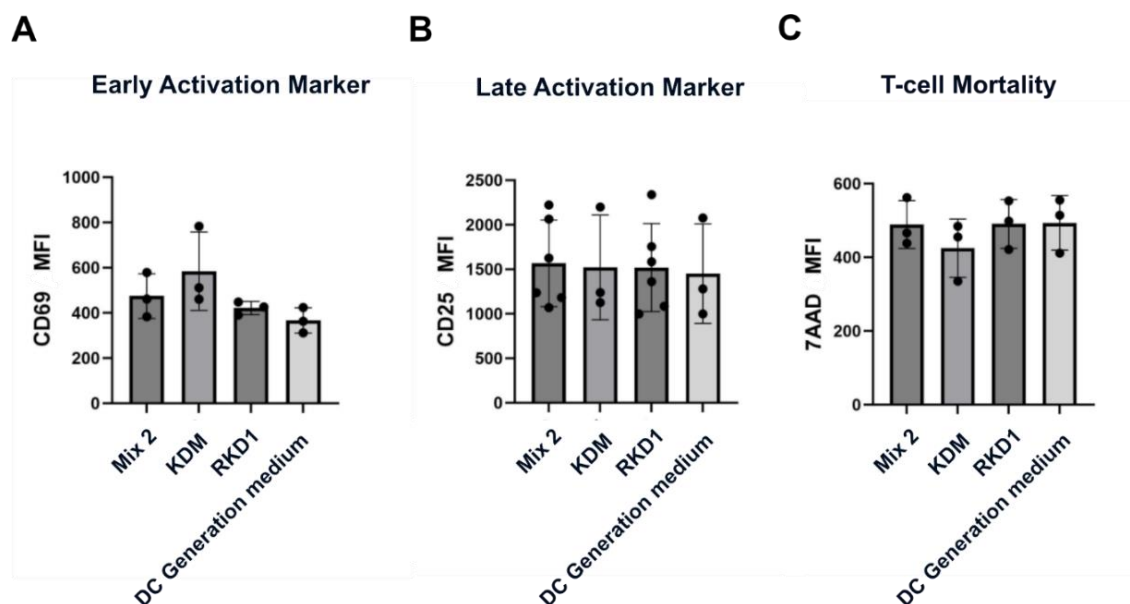


**Figure 34. The characterization of T-lymphocytes from the co-culture in different media.** T-lymphocytes were co-cultured with monocyte-derived Langerhans cells (MoLC) and hair follicle-derived keratinocytes (HFDC) in a well for three days in 1:1 RPMI 1640 basal: KGM-2 without hydrocortisone (Mix2), Keratinocytes differentiation medium (KDM), 1:1 RPMI1640 basal: KDM (RKD1), or DC Generation medium. The cells were collected for flow cytometry. The cells were stained with anti-CD69-BV421 (T-lymphocytes early activation marker), and anti-CD25-PE (T-lymphocytes late activation marker). Cell mortality was determined by 7-AAD staining. The higher 7-AAD level indicates the higher cell mortality. Data are presented as mean  $\pm$  SD. Ordinary one-way ANOVA with Dunnett's correction for multiple comparisons was used to analyze the data. The  $p$ -values  $<0.05$  (\*),  $<0.01$  (\*\*), and  $<0.001$  (\*\*\*) are indicated.  $n=3-6$ .

#### 4.5.3 Characterization of The ImmuSkins

To confirm that immune cells do not adversely affect the structural integrity of the immunocompetent skin models (ImmuSkins), an evaluation was conducted on three distinct variations, which are ImmuSkin integrating both MoLC and T-lymphocytes (ImmuSkin-MT), ImmuSkin containing solely MoLC (ImmuSkin-M), and ImmuSkin featuring only T-lymphocytes (ImmuSkin-T). The ImmuSkins comprised a three-layer construct placed on the cell culture insert, with the option of including or excluding T-lymphocytes in the lower chamber of the transwell.

ImmuSkin-M was constructed by creating a MoLC-incorporated collagen matrix and placing the mature RHS on top of it, resulting in a three-layer construct composed of the epidermis, the dermis, and the immune cell-containing subdermal layer. These three layers were positioned on an insert of a transwell plate. The lower chamber of the transwell of ImmuSkin-M contains only DC generation medium. In contrast, ImmuSkin-T was constructed with an acellular collagen matrix instead of a collagen matrix containing MoLC and the addition of T-lymphocytes in the lower chamber of the transwell, simulating the lymph node area (**Figure 36**). Lastly, the ImmuSkin-MT had a similar three-layer structure as the ImmuSkin-M, with T-lymphocytes in the lower chamber of the transwell. The three-layer construct was frozen and cryosectioned while the cells in the lower chamber were taken for flow cytometry analysis.

Results obtained from H&E staining demonstrate that all ImmuSkins exhibit a consistent three-layer structure, comprising a stratified epidermis, dermis, and a subdermal layer, as expected. The subdermal layer differs, with an immune cell-containing subdermal layer in ImmuSkin-M and ImmuSkin-MT or an acellular subdermal layer in ImmuSkin-T. In the immune cell-containing subdermal layer, visible dark purple dots indicate cell nuclei, while such nuclei are absent in the acellular subdermal layer (**Figure 35A**).

Furthermore, the thickness of the epidermal layer was assessed in each ImmuSkin variant. The analysis yielded comparable results, reaffirming that the presence or absence of immune cells does not significantly influence keratinocyte differentiation (**Figure 35B**).

The results of the IF staining indicate consistent expression patterns across all ImmuSkins. Loricrin is present in the stratum corneum. CK14 is the marker for the stratum basal, and CK10 indicates the stratum spinosum and granulosum of the epidermis because CK14 is related to the basal state of the keratinocytes, while CK10 represents the differentiated keratinocytes. CK14 was found expressed in the stratum basal and CK10 was found in the layer of stratum spinosum and stratum granulosum of both RHS-FD and RHS-HFD as expected. Loricrin is a known marker for the cornified layer in epidermis or stratum corneum, which can also be found in the stratum corneum of both types of RHS.

Moreover, the claudin expression is found in a similar location of RHS-FD and RHS-HFD. In both RHS, claudin was found to be expressed in the stratum granulosum. Claudin is the marker for tight junction and is more commonly associated with the stratum granulosum, which is a higher layer in the epidermis.

CD1a<sup>+</sup> cells are exclusively found in the subdermal layer of ImmuSkin-M and ImmuSkin-MT. No DAPI signal was observed in subdermal layer of ImmuSkin-T, confirming the absence of cells in that layer.

As expected, T-lymphocytes tagged with CFSE are not detected in the three-layer construct of either ImmuSkin-M, ImmuSkin-T, or ImmuSkin-MT, indicating that they do not migrate from the lower chamber of the transwell into the three-layer construct. The appearance and epidermal hallmark markers in ImmuSkin-M and ImmuSkin-T are similar to ImmuSkin-MT (**Figure 36**), validating the structural integrity of the models.

The flow cytometry analysis of cells from the lower chamber of the transwell demonstrates that the ImmuSkin-M exhibits only CD1a<sup>+</sup> cells (MoLC) and ImmuSkin-T exhibits only CD4<sup>+</sup> cells (T-lymphocytes). The ImmuSkin-MT contains both CD1a<sup>+</sup> and CD4<sup>+</sup>, indicating that both MoLC and T-lymphocytes are present in the lower chamber of the transwell (**Figure 37A**). The baseline comparison of MoLC migration and the MFI of CD86 between ImmuSkin-M and ImmuSkin-MT is

comparable, indicating that the presence of T-lymphocytes does not hinder MoLC maturation and migration, as expected (**Figure 37B&C**). Furthermore, a comparison of T-lymphocyte proliferation between ImmuSkin-T and ImmuSkin-MT reveals a significant increase in proliferation in the presence of MoLC (**Figure 37D**), underscoring the critical role of MoLC in promoting T-lymphocyte activation and proliferation.

These results indicate that the ImmuSkin-MT shows success of integrating MoLC and including T-lymphocytes in the lower chamber of the transwell without compromising the structural integrity of the three-layer construct. The results also show that MoLC can migrate and mature in both ImmuSkin-MT and ImmuSkin-M, while T-lymphocytes can only proliferate in ImmuSkin-MT, where MoLC are present. These results confirm that the ImmuSkin-MT can reproduce the essential features of the skin immune system, such as the cross-talk between MoLC and T-lymphocytes.

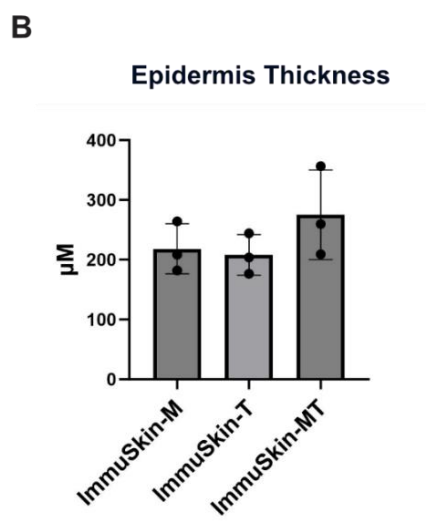
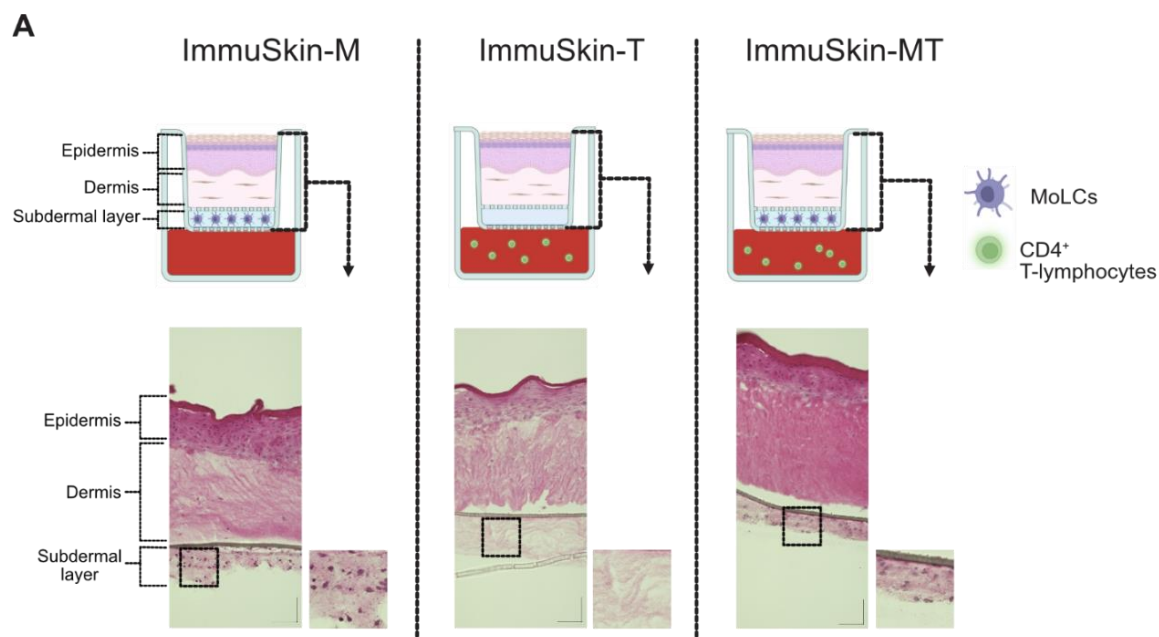


**Figure 35. The characterization of the three-layer constructs from ImmuSkin-MT, ImmuSkin-M, and ImmuSkin-T using Hematoxylin and Eosin (H&E) staining.** Each ImmuSkin type is illustrated to show its respective cell composition, followed by (A) representative microscopic images from H&E staining. The scale bar is 100  $\mu\text{m}$ . The three-layer construct which contains epidermis, dermis, and subdermal layer of each ImmuSkin variant are shown. (B) Epidermal thickness of each ImmuSkin type. Data are presented as mean  $\pm$  SD. Ordinary one-way ANOVA with Tukey's correction for multiple comparisons was used to analyze the data. Scale bar = 100  $\mu\text{m}$ . The p-values <0.05 (\*), <0.01 (\*\*), and <0.001 (\*\*\*) are indicated.  $n=3$ .

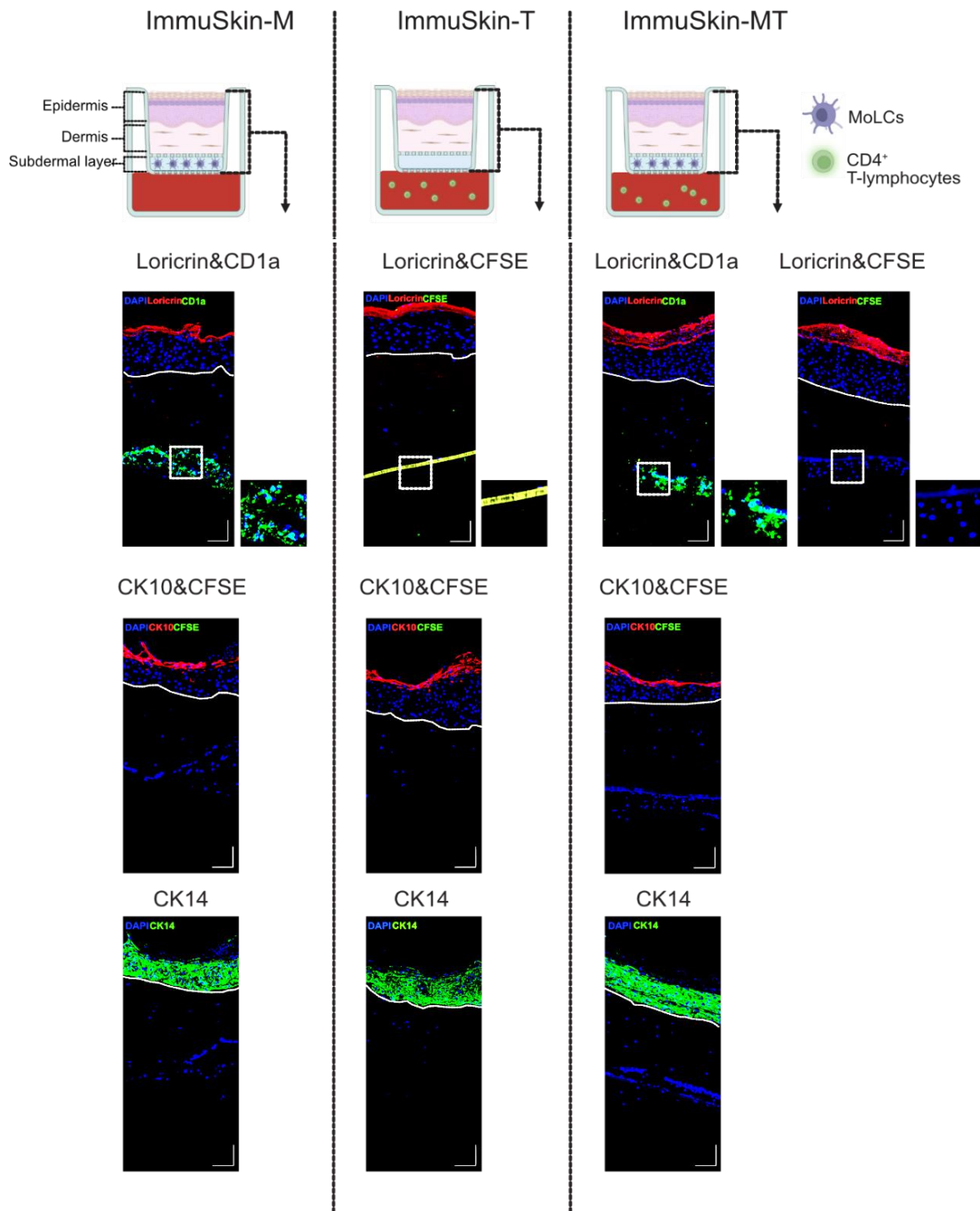


**Figure 36. The characterization of the three-layer constructs from ImmuSkin-MT, ImmuSkin-M, and ImmuSkin-T using immunofluorescence (IF) staining.** Each ImmuSkin type was illustrated to depict its three-layer construct which is composed of the epidermis, dermis, and subdermal layer and followed by representative microscopic images from IF staining. The ImmuSkins were stained against loricrin-red, cytokeratin 14 (CK14)-green, cytokeratin 10 (CK10)-red, and dendritic cell characterization marker which is CD1a-green. 4',6-diamidino-2-phenylindole (DAPI-blue) was used as a nucleus counter-staining. CK14 signified stratum basale. CK10 is the marker for stratum spinosum and granulosum. Stratum corneum is indicated by loricrin. The carboxyfluorescein succinimidyl ester (CFSE-green) is an indicator of T-lymphocytes, which are absent from the epidermis, dermis, and subdermal layer. A magnified view is highlighted within a small square box, focusing on the subdermal region to showcase the detailed distribution of CD1a+ cells in the subdermal layer. The epidermis and (continued from the previous page) dermis are separated by a white dotted line. In some pictures, a membrane of the transwell insert is presented in a bright yellow-green strip. Scale bar = 100  $\mu$ m. n=3.

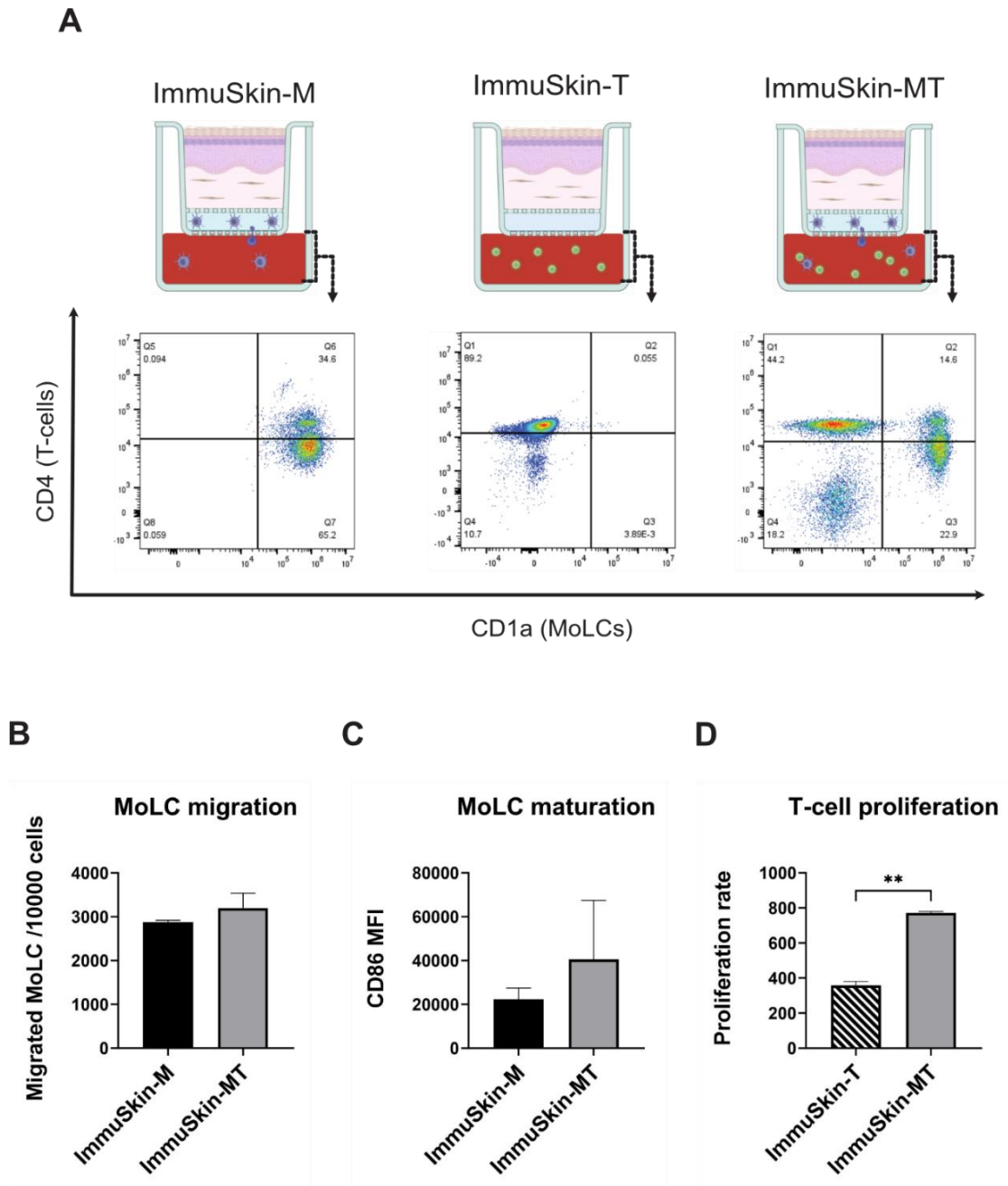


**Figure 37. The comparison of cells obtained from the lower chamber of transwell of Immuskin-MT, Immuskin-M, and Immuskin-T.** Cells collected from the lower chamber of each Immuskin variant were subjected to flow cytometry analysis and stained with CD1a-FIT-C (pan dendritic cell marker), CD86-BV605 (Langerhans cell maturation marker), and anti-CD4-APC-cyanine-7 (CD4+ T-lymphocyte marker). **A)** Each Immuskin type was illustrated to depict its respective cell composition. Representative dot plots indicate T-lymphocyte populations and monocyte-derived Langerhans cells (MoLC) from each Immuskin type. The upper left of the quadrant represents T-lymphocytes, while MoLC are represented by the lower right of the quadrant. **B)** MoLC migration rate, **C)** MoLC maturation, and **D)** T-lymphocyte proliferation. The black bar represents immune cells from Immuskin-M, the striped bar represents immune cells from Immuskin-T, and the gray bar represents (continued from the previous page) immune cells from Immuskin-MT. The data is presented as mean  $\pm$  SD, and statistical significance is indicated as  $p$ -values  $<0.05$  (\*),  $<0.01$  (\*\*), and  $<0.001$  (\*\*\*). The paired  $t$ -test was employed for statistical analysis.  $n=3$ .

This study highlights the significance of selecting an appropriate medium for cultivating immune cells within skin models. The DC generation medium emerges as the most favorable choice,

demonstrating superior characteristics in terms of CD207, CD86 expression, and lower cell mortality. Notably, KDM and RKD1 show promising results in certain aspects but are accompanied by higher cell death rates. In contrast, Mix2 exhibits limitations due to its impact on keratinocyte differentiation.

Furthermore, integrating immune cells into skin models proves successful, with no adverse effects on the epidermal layer's thickness or keratinocyte differentiation. The structural integrity of the models remains intact, and the essential features of the skin immune system, such as dendritic cell layers and MoLC-T-lymphocyte cross-talk, are successfully replicated in the ImmuSkin-MT model.

In conclusion, this novel immunocompetent skin model provides a more biologically relevant platform for studying skin sensitization processes. Key immune cells offer valuable insights into the interplay between different immune components and potentially contribute to the development of improved skin sensitization assays.

#### 4.6 Application of Immunocompetent Skin Models in Sensitizers Detection

Having successfully developed immunocompetent skin models containing both MoLC and T-lymphocytes, the next step requires evaluating their performance. *In vitro* models, although straightforward, can be tailored to detect specific pivotal events within the AOP. Based on such knowledge, *in vitro* models covering KE 1, 2 or 3 have been proposed and implemented into the OECD guidelines (OECD, 2022, 2023d, 2023c). Although current OECD-approved *in vitro* models can address these key events, they fall short of covering KE 4 and combining different key events in one assay. Thus, the OECD suggests a combination of *in vitro* skin sensitization assays with other tests to evaluate the response (OECD, 2023a). The ImmuSkin-MT, offering the possibility to detect multiple key events in a single assay, introduces a higher level of complexity to *in vitro* skin sensitization models, bridging some of the gaps between their simplicity and the intricacy of *in vivo* models.

Each ImmuSkin was topically treated with a skin sensitizer from each potency class. The potency class of the skin sensitizers is considered based on the effective concentration (EC3) value from the LLNA assay (Kimber et al., 2003). The RN was used as a representative of the moderate skin sensitizer. IG was selected as the strong skin sensitizer. The PPD and DNCB were selected for the extreme skin sensitizer. A vehicle (DMSO), a non-sensitizer (Gly), and a positive control, along with an UT, were included in the experiment. The cocktail of inflammatory cytokines, with or without T-cell activator, served as the positive control. After 24 hours of the treatment, ImmuSkin-MT was

frozen and prepared for the IF staining and H&E staining. The cells in the lower chambers were harvested for flow cytometry analysis.

The H&E results indicate that the ImmuSkin-MT has a three-layer structure comprising the stratified epidermis, the dermis, and the subdermal layer. The entire epidermis and the stratum corneum appeared dark pink, while the dermis and the subdermal layer had light pink characteristics. The cell nuclei were stained dark purple and found in all ImmuSkin-MT layers (**Figure 38A**).

The IF staining reveals that the appearance of the three-layer construct from the ImmuSkin-MT remains consistent between the treated and untreated conditions. The loricrin expression represents the stratum corneum, and CK10 expression marked the stratum granulosum and stratum spinosum. Lastly, the stratum basale was characterized by the expression of CK14. CD1a indicated the MoLC in the subdermal layer. Notably, CK10, CK14, CD1a, and loricrin are consistently present across all conditions. The CFSE signal, which is the signal of T-lymphocytes, is absent in the epidermal, dermal, and subdermal layers of every model, indicating that the T-lymphocytes did not migrate from the lower chamber to the three-layer construct. (**Figure 38B**).

To further assess the impact of treatment on ImmuSkin-MT, the epidermal thickness was measured and normalized to the untreated control. The results demonstrate no significant difference between the treated and untreated conditions, confirming that the treatments did not induce any observable changes in the appearance of the skin models (**Figure 38C**).

MoLC exhibited a significant increase in migration rate and upregulated CD86 in response to IG (1.4-times migration), DNCB (1.8-times migration and 1.5-times CD86 MFI upregulation), or PPD (2-times migration and 1.5-times CD86 MFI upregulation). The positive control resulted in the highest migration rate (3-times) and CD86 MFI upregulation (2.4-times) (**Figure 39A**). Moreover, analysis of the maturation marker of these migrated MoLC showed notable increases in CD86 MFI compared to baseline in the ImmuSkin-MT treated with DNCB (1.8-times), PPD (1.8-times), or the positive control (2.5-times) (**Figure 39B**). Thus, the results are consistent with the literature that the more potent skin sensitizers (DNCB and PPD) induce the highest migration and maturation of MoLC and therefore the influence on migration rate and CD86 upregulation of MoLC is reduced with decreasing sensitizing potential of the substances. Additionally, a viability analysis of the migrated cells demonstrated cell viability above 90% across all experimental conditions (**Figure 40A**). The results confirm that the observed effects are not due to cytotoxicity.

To assess T-lymphocyte response to treatments, the SI was calculated by normalizing proliferated T-lymphocytes of the treated ImmuSkin-MT to the untreated ImmuSkin-MT. The results showed significantly higher SI in ImmuSkin-MT treated with RN, IG, DNCB, PPD, or the positive control compared to the untreated control by 1.8, 2.1, 2.6, 2.4, and 3.1 times, respectively (**Figure 39C**). Thus, T-lymphocyte proliferation corresponds to the classification of sensitizing substances found in the literature; the most sensitizing substances (PPD and DNCB) lead to the highest T-lymphocyte proliferation. Furthermore, T-lymphocyte viability remained over 90% after every treatment (**Figure 40B**). These findings again indicate that the observed effects at these concentrations are not caused by cytotoxicity.

Interestingly, a comparable proportion of response was observed in ImmuSkin-M, where MoLC significantly migrated out from the three-layer construct into the lower chamber in response to IG (1.4-times), DNCB (2-times), PPD (1.9-times), and the positive control (2.4-times) compared to the untreated control (**Figure 39D**). The migrated MoLC also significantly upregulated CD86 MFI when ImmuSkin-M was treated with DNCB (1.9-times), PPD (1.8-times), and the positive control (2.5-times) (**Figure 39E**). In contrast to the results from ImmuSkin-MT, the response of T-lymphocytes from ImmuSkin-T, where MoLC were absent, measured by the SI, did not increase from any treatment except for the positive control, confirming the importance of MoLC in the T-lymphocytes response to skin sensitizers (**Figure 39F**). Analogous to the results from ImmuSkin-MT, the treatments appear to have no negative effect on the viability of MoLC from ImmuSkin-M and T-lymphocytes from ImmuSkin-T (**Figure 40C&D**).

These results demonstrate that the migration and maturation of MoLC and the proliferation of T-lymphocytes in ImmuSkin-MT correspond to different potencies of skin sensitizers. The positive control showed the most substantial effects, followed by the extreme sensitizer PPD and DNCB, the moderate sensitizer IG, and the weak sensitizer RN. The ImmuSkin-M also showed similar responses of MoLC to the treatments. In contrast, the ImmuSkin-T did not show any significant response of T-lymphocytes to the treatments, except for the positive control, confirming the importance of MoLC in the process of T-lymphocyte activation by skin sensitizers.

In conclusion, the results confirm that the ImmuSkin-MT demonstrates a remarkable capacity to faithfully recapitulate the intricate skin sensitization phase observed in physiological skin. Notably, this includes the migration and maturation of LCs, along with the dynamic cross-talk between LCs and T-lymphocytes in response to skin sensitizers. Accompanied by the results from ImmuSkin-M and ImmuSkin-T, the immunocompetent skin models can simulate the immunological response events that occur in physiological skin.

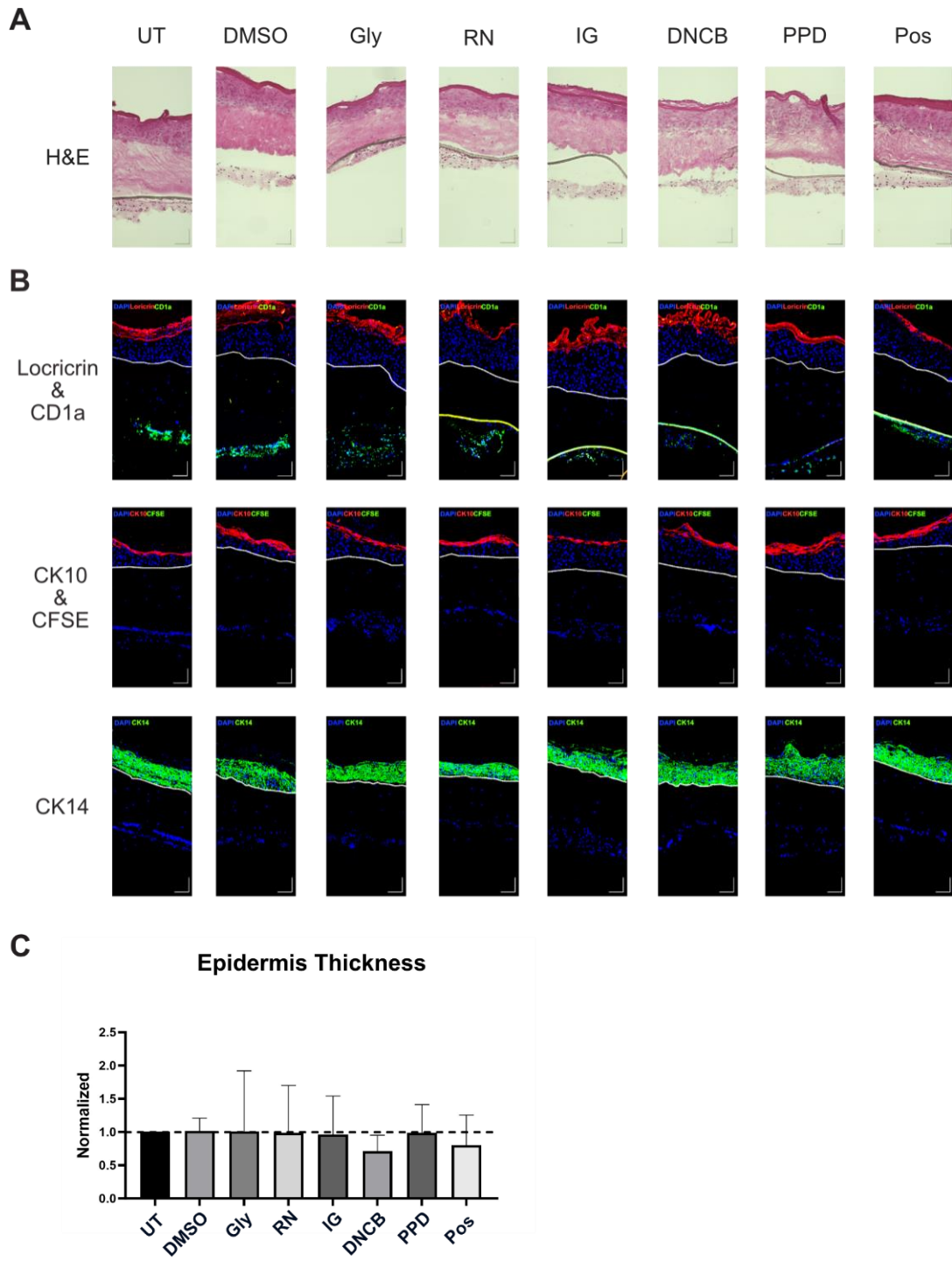


**Figure 38.** The characterization of the three-layer construct of the ImmuSkin-MT after treatment with various skin sensitizers.

**Figure 38.** (continue from the previous page). **The characterization of the three-layer construct of the ImmuSkin-MT after treatment with various skin sensitizers.** ImmuSkin-MT was treated with one of the following compounds for 24 hours, 0.1% DMSO, 500 $\mu$ M Glycerol (Gly), 250 $\mu$ M Resorcinol (RN), 300 $\mu$ M Isoeugenol (IG), 5 $\mu$ M 2,4-Dinitrochlorobenzene (DNCB), 10 $\mu$ M P-Paraphenylenediamine (PPD), and a positive control (TNF- $\alpha$  + IL-1 $\beta$ ). The untreated control (UT) was included. 4',6-diamidino-2-phenylindole (DAPI-blue) was used as a nucleus counter-staining. Cytokeratin 14 (CK14) signified stratum basale. Cytokeratin 10 (CK10) is the marker for stratum spinosum and granulosum. Stratum corneum is indicated by loricrin. CD1a is an indicator for dendritic cells. **A)** Hematoxylin and eosin (H&E) staining results. **B)** Immunofluorescent (IF) staining results against loricrin (red), CD1a (green), CK10-red, and CK14-green. The carboxyfluorescein succinimidyl ester (CFSE-green) is an indicator of T-lymphocytes, which are absent from the epidermis, dermis, and subdermal layer. **C)** Epidermal thickness was normalized to the untreated control. The bright yellow-green strip indicates the transwell insert membrane. The white dotted line represents the border between the epidermis and the dermis. Scale bar = 100 $\mu$ m. Data are presented as mean  $\pm$  SD. Statistical significance is indicated as \*p-value  $\leq$  0.05, assessed using Ordinary One-Way ANOVA with Dunnette correction for multiple comparisons. The black dotted line in the graph represents the baseline. n = 3.

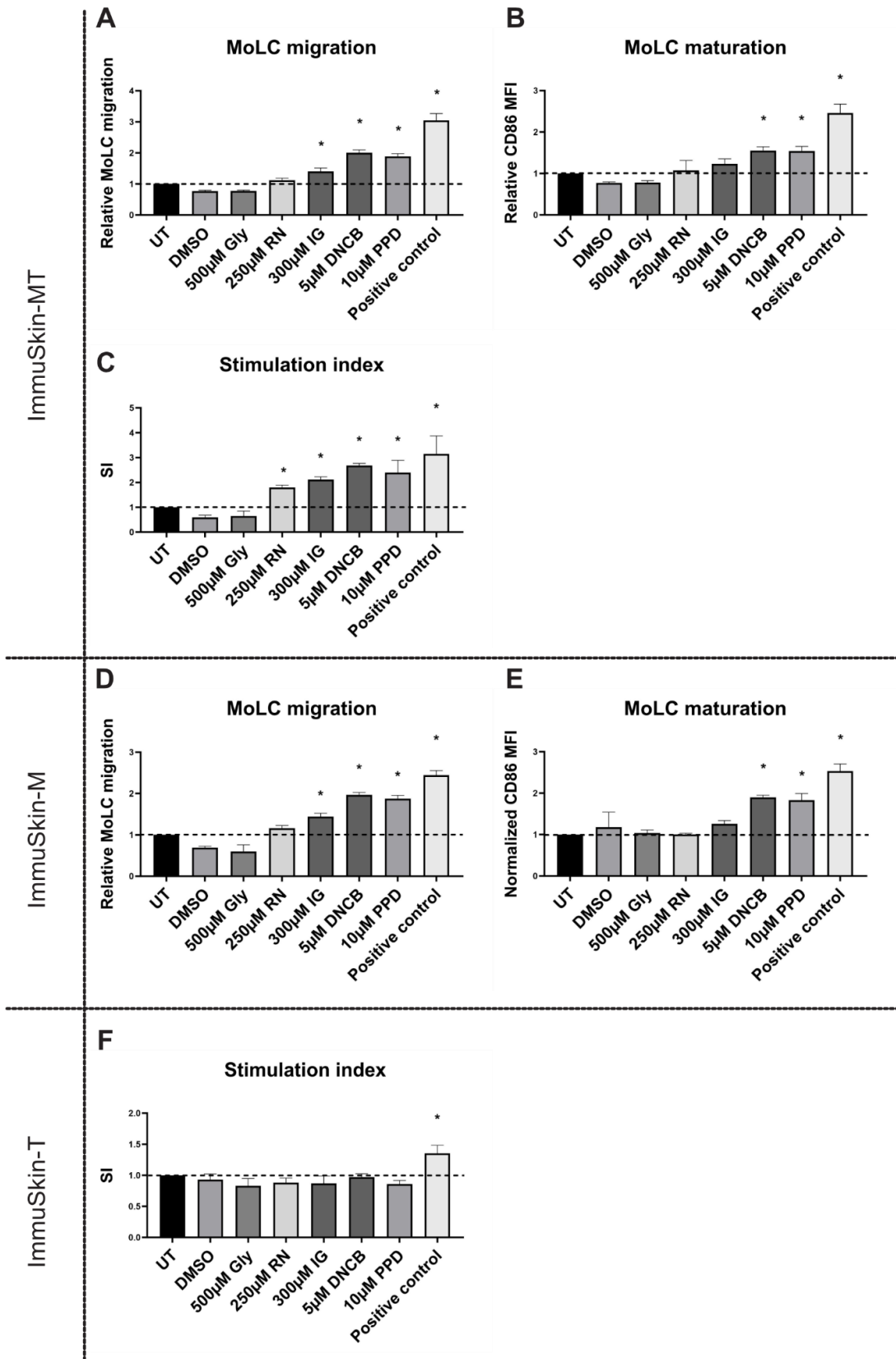
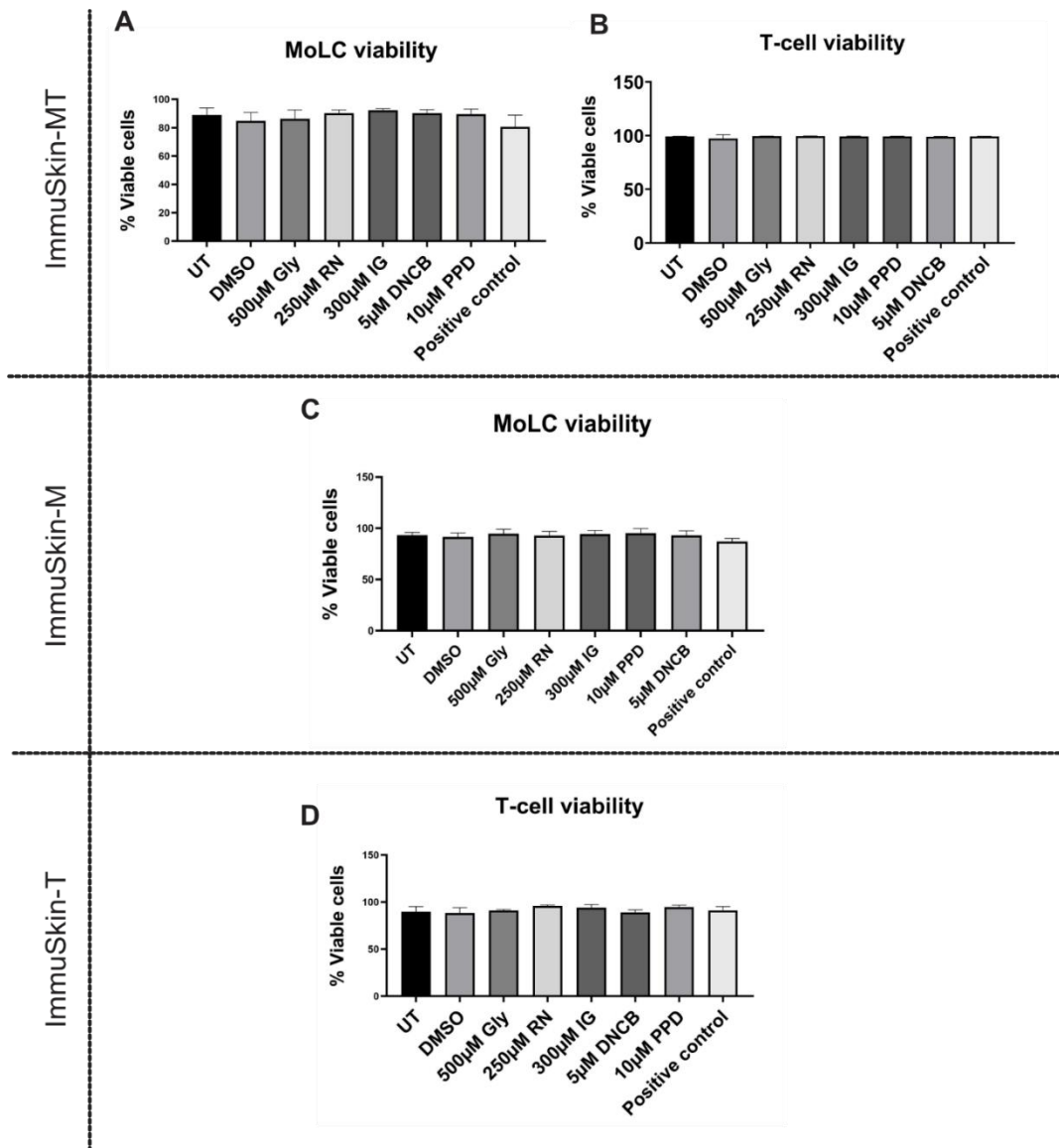


Figure 39. Skin sensitizers induce migration, maturation, and T-lymphocyte activation in Immuskins. Immuskins comprise three variants, which are Immuskin-M, Immuskin-T, and Immuskin-MT.

**Figure 39.** (continue from the previous page) **Skin sensitizers induce migration, maturation, and T-lymphocyte activation in ImmuSkins. ImmuSkins comprise three variants, which are ImmuSkin-M, ImmuSkin-T, and ImmuSkin-MT.** These variants were exposed to 0.1% DMSO (vehicle control), 500 $\mu$ M Glycerol (Gly), 250 $\mu$ M Resorcinol (RN), 300 $\mu$ M Isoeugenol (IG), 5 $\mu$ M 2,4-Dinitrochlorobenzene (DNCB), and 10 $\mu$ M Paraphenylenediamine (PPD) for 24 hours. For ImmuSkin-MT and ImmuSkin-T, IL-1 $\beta$ , TNF- $\alpha$ , and a T-cell activator were used as positive controls, whereas for ImmuSkin-M, only IL-1 $\beta$  and TNF- $\alpha$  served as positive controls. Cells collected from the lower chamber of each ImmuSkin variant were subjected to flow cytometry analysis staining against CD86, CD1a, and CD4. The response to treatment was assessed by measuring the migration and maturation of monocyte-derived Langerhans cells (MoLC) and the stimulation index (SI) of T-lymphocytes. The MoLC migration rate was determined using flow cytometry. The SI was calculated from the proliferation rate of T-lymphocytes. **A)** MoLC migration normalized to the untreated control (UT) in ImmuSkin-MT. **B)** CD86 mean fluorescence intensity (MFI) normalized to the UT in ImmuSkin-MT. **C)** SI of T-lymphocytes in ImmuSkin-MT. **D)** MoLC migration normalized to UT in ImmuSkin-M. **E)** MoLC maturation normalized to UT in ImmuSkin-M. **F)** SI of T-lymphocytes in ImmuSkin-T. Data are presented as mean  $\pm$  SD. Statistical significance is indicated as \*p-value  $\leq$  0.05, assessed using Ordinary One-Way ANOVA with Dunnett correction for multiple comparisons. The dotted line represents the baseline. n = 3.



**Figure 40. Viability of the cells from ImmuSkin-M, ImmuSkin-T and ImmuSkin-MT.** ImmuSkin-M, ImmuSkin-T, and ImmuSkin-MT were exposed to 0.1% DMSO, 500 µM Glycerol (Gly), 250 µM Resorcinol (RN), 300 µM Isoeugenol (IG), 5 µM 2-4 Dinitrochlorobenzene (DNCB), and 10 µM Paraphenylenediamine (PPD) for 24 hours. Cells collected from the lower chamber of each ImmuSkin variant were subjected to flow cytometry analysis and stained with 7-AAD to determine viability. **A)** The viability of monocyte-derived Langerhans cells (MoLC) from ImmuSkin-MT. **B)** The viability of T-lymphocytes from ImmuSkin-MT. **C)** MoLC viability from ImmuSkin-M. **D)** The viability of T-lymphocytes from ImmuSkin-T. Statistical significance is indicated as \* $p$ -value  $\leq 0.05$ , assessed using Ordinary One-Way ANOVA with Dunnette's correction for multiple comparisons.

The study successfully developed immunocompetent skin models, known as ImmuSkin-MT, which incorporate both MoLC and T-lymphocytes. These models aim to bridge the gap between *in vitro* and *in vivo* skin sensitization assays, providing a more complex and biologically relevant platform for assessing skin sensitization. In experiments using these models, various skin sensitizers of different potencies were applied topically, revealing significant MoLC migration and CD86 expression as a response to the treatment. The highest responses were observed with extreme sensitizers, followed by moderate and weak sensitizers. Notably, the ImmuSkin-MT models also demonstrated T-lymphocyte proliferation in response to these sensitizers, highlighting the

importance of MoLC in the activation of T-lymphocytes. Comparatively, ImmuSkin-M, the ImmuSkin without T-lymphocytes, exhibited similar MoLC responses to the treatments. In contrast, ImmuSkin-T models, lacking MoLC, showed minimal T-lymphocyte activation, except for positive control.

Overall, these results confirm the capacity of ImmuSkin-MT models to faithfully replicate the complex events of skin sensitization, including MoLC migration, maturation, and dynamic cross-talk with T-lymphocytes in response to sensitizers. Together with ImmuSkin-M and ImmuSkin-T, these immunocompetent skin models can simulate the immunological response in physiological skin, offering a valuable tool for studying skin sensitization processes.

## CHAPTER 5 DISCUSSION

As we advance in chemistry, pharmacology, and biology, the synthesis of new chemical compounds has increased significantly. This surge highlights continual innovation, as evidenced by studies like Llanos et al. (Llanos et al., 2019), which demonstrate the frequent introduction of novel compounds. However, this rapid development necessitates stringent risk assessments to mitigate economic and health impacts, particularly concerning skin sensitization. The effective evaluation of skin sensitizers is crucial for preventing health issues and minimizing medical costs while ensuring safety and regulatory compliance. The OECD and GHS have established guidelines to identify critical events in the AOP for skin sensitization (OECD, 2014). These guidelines aid in clarifying complex mechanisms—from protein binding to T-lymphocyte responses—and integrate various assays like the DPRA and KeratinoSens™. Nonetheless, gaps remain due to the lack of official recognition for several promising assays, underscoring the need for more comprehensive and physiologically relevant models. The immunocompetent skin models discussed aim to better replicate human skin physiology and provide a robust framework for evaluating the sensitization potential of new compounds, which could significantly improve risk prediction and management.

### 5.1 Hair Follicles as an Alternative Source for Keratinocytes and Fibroblasts

While juvenile foreskin has been a reliable source of fibroblasts and keratinocytes, it does come with limitations. It is primarily restricted to male donors and involves invasive methods. In contrast, hair follicles have emerged as a promising alternative source for these cells, offering a less invasive acquisition method. Hair follicle-derived cells (HFDs) can be sampled from each donor multiple times, collected from both male and female donors, and they do not require specialized equipment, making them more accessible.

Keratinocytes, as evidenced by various studies, are commonly derived from the outer root sheath, a component of hair follicles containing undifferentiated keratinocytes (Limat & Hunziker, 1996). The process of isolating keratinocytes from the hair follicles is well-established, allowing these cells to proliferate beyond the outer root sheath region when cultured on feeder cells (Bak et al., 2020; Lenoir-Viale et al., 1993; Limat & Hunziker, 1996; Wagner et al., 2018). Noteworthy is the substantial characterization dedicated to these cells, particularly emphasizing the unique properties of HFDC (Fusenig et al., 1994; Limat et al., 1991; Limat & Hunziker, 2002).

While the origin of HFDC is extensively documented, the same cannot be said for HFDF. The precise location within the hair follicle where fibroblasts originate remains unclear, yet studies propose the pivotal involvement of the dermal papilla and the dermal sheath in hosting these

cells (Ganier et al., 2022; Zhou et al., 2016). Historically, researchers initially referred to cells from the dermal papilla region as dermal papilla cells (Messenger, 1984). Subsequent investigations revealed these cells to exhibit a spindle-shaped morphology reminiscent of dermal fibroblasts, albeit with more prominent cytoplasm (J. J. Wu et al., 2005). Notably, *in vitro* cultivation of dermal papilla cells has demonstrated their ability to support the development of epidermis, akin to the functions performed by fibroblasts (Oliver & Jahoda, 1988).

Studies on rat dermal papilla cells have highlighted distinct molecular characteristics when compared to fibroblasts (Sleeman et al., 2000). Despite these differences, other research indicates a shared origin from progenitor cells for fibroblasts and dermal papilla (Yu et al., 2001; Zhao et al., 2019). Amidst the elusive evidence regarding the relationship between dermal papilla and fibroblasts, studies have successfully isolated fibroblasts by specifically extracting the dermal papilla from hair follicles and cultivating them on cell culture vessels (Topouzi et al., 2017, 2020; Williams & Thornton, 2020). Considering the cumulative evidence, the dermal papilla emerges as a potential source of fibroblasts.

In this thesis, HFDK and HFDF have been extensively characterized compared to NHEK and NHDF sourced from anonymous juvenile foreskin donors. Using immunofluorescence staining and flow cytometry techniques, the results indicate that these cells exhibit comparable characteristics in terms of the expression of CK14, CK5, CD29, and CD49f. However, a significant difference in cytokeratin 10 (CK10) levels was observed, with HFDK showing higher levels compared to NHEK. Cytokeratin 14 (CK14) and cytokeratin 5 (CK5), known as markers for undifferentiated keratinocytes, are also discussed (Alam et al., 2011; Dmello et al., 2019).

CD29, also known as  $\beta$ 1 integrin, is a transmembrane receptor primarily involved in cell-cell adhesion, typically localized to regions where cells make contact with one another (Larjava et al., 1990).  $\beta$ 1 integrin expressed the highest in basal keratinocytes. Furthermore, the synthesis of  $\beta$ 1 integrin is suppressed during the differentiation of keratinocytes (Hotchin et al., 1995; Levy et al., 2000). In light of this information, the results strongly suggest that both HFDK and NHEK can effectively maintain an undifferentiated state.

CD49f, or integrin  $\alpha$ 6, serves as a marker for identifying keratinocyte progenitors and characterizing the stem cell properties of these cells (Kligys et al., 2012; Krebsbach & Villa-Diaz, 2017; Xu et al., 2019). Studies have demonstrated that higher levels of CD49f correlate with increased pluripotency in cells. Notably, both HFDK and NHEK exhibit similar levels of CD49f, indicating that one is not more differentiated than the other.

In contrast, the increase of CK10 levels, a recognized marker for early keratinocyte differentiation, reveals a notable disparity (L. Zhang & Zhang, 2018). HFDK exhibit significantly higher CK10 levels than NHEK. This outcome diverges from findings related to other markers and the results of other studies comparing NHEK and HFDK (Löwa et al., 2018; Sasahara et al., 2009). It is essential to consider that CK10 primarily signifies early differentiation reflecting that the HFDK start to differentiate earlier than NHEK. Interestingly, the HFDK are found to be proliferating much slower than the NHEK, which such observance contradicted by the another study (Sasahara et al., 2009). However, this problem was overcome by optimizing the cultivation method by switching from a standard keratinocyte medium (KGM-2) to DermaCult™, resulting in a much higher proliferation rate and preserving the undifferentiated state of the cells.

The comparison between HFDF and NHDF isolated from foreskin donors is discussed. Characterization was carried out using flow cytometry and immunofluorescence staining. Additionally, the proliferation rates of HFDF and NHDF were compared. It was observed that HFDF required more time for proliferation compared to NHDF. This result is consistent with findings in previous studies, confirming it as one of the characteristic traits of HFDF (Arai et al., 1989; Pisansarakit et al., 1991; J. J. Wu et al., 2005). The results indicated comparable levels of Vimentin and Collagen IV in both types of fibroblasts, aligning with findings from Löwa et al. (Löwa et al., 2018). Notably, NHDF exhibited a higher collagen type I level than HFDF. While this might be the first time this has been observed, the inherent cell heterogeneity may provide a plausible explanation. As a case in point, papillary and reticular fibroblasts, though residing in the same organ, serve distinct functions and exhibit varying levels of collagen type I secretion because they serve different purposes (Nolte et al., 2008; Sorrell & Caplan, 2004). This difference in collagen type I secretion can be attributed to the inherent cell heterogeneity and the primary function of dermal papilla fibroblasts, which is not focused on maintaining a cellular scaffold but rather on engaging in signaling interactions with overlying epithelial cells to regulate hair growth and cycling. As a result, they are naturally less predisposed to produce collagen type I to the same extent as skin fibroblasts despite having the capacity to synthesize it (Sorrell & Caplan, 2004).

The differences between reticular and papillary fibroblasts can be determined by the level of CD90 expression, where papillary fibroblasts express CD90 and the reticular fibroblasts do not (Korosec et al., 2019; Rogovaya et al., 2021). However, it is essential to note that the prolonged culture of the papillary fibroblasts *in vitro* can lead to differentiation into the reticular type (Janson et al., 2013). Interestingly, more HFDF are CD90<sup>+</sup> than NHDF. Taking the high expression of CD90 and the less collagen I secretion in HFDF in comparison to NHDF into consideration, the

results suggest that the HFDF has a higher resemblance to papillary fibroblasts and might be able to retain the undifferentiated state when cultured *in vitro* for longer than NHDF.

Some additional common markers were used to detect fibroblasts, vimentin, CD10 and CD44. The HFDF and NHDF express similar levels of vimentin. Vimentin is an intermediate filament protein that is widely recognized as a marker of fibroblasts (Nomura, 2019; Tarbit et al., 2018). It contributes to cellular mechano-protection, which means it helps cells withstand mechanical stress. Vimentin is also involved in the regulation of cell migration and matrix remodeling (Ostrowska-Podhorodecka et al., 2022).

CD44 is surface glycoprotein that involves in the regulation of extra cellular matrix production in fibroblasts (Tsuneki & Madri, 2016). Moreover, it has also been proposed as a robust marker of fibroblasts (Quintanilla et al., 2014). CD10 is a cell surface enzyme with neutral metalloendopeptidase activity which can also be found expressing in skin appendages such as dermal sheath cells of hair follicles and is widely accepted as a fibroblasts marker (Itoh et al., 2013; Xie, Moroi, et al., 2011; Xie, Takahara, et al., 2011). Moreover, the heterogeneity of fibroblasts is an emerging topic which has been thoroughly reviewed elsewhere (Griffin et al., 2020; Sorrell & Caplan, 2004). Therefore, it is important to use a combination of markers to identify and characterize fibroblasts in the dermis accurately.

While deeper characterization of hair follicles is suggested for studies beyond the scope of this thesis, hair follicles present a robust alternative source for keratinocytes and fibroblasts. The noninvasive nature of the method allows for multiple sampling from the same donor. Moreover, this approach eliminates the restriction to male donors, which is a limitation when using foreskin as a source. According to the characterization done in this thesis and other studies regarding the function of the cells, evidence has pointed out that HFDs can be used interchangeably with foreskin-derived cells within the scope of this thesis.

## 5.2 Comparative Study of Autologous and Allogeneic Co-Cultures

Using HFDs offers distinct advantages in terms of donor selection. Moreover, accessibility to the donor also opens the door to acquiring the blood sample from the hair follicle donor, leading to the feasibility of personalized autologous assays. However, allogeneic assays also hold their unique advantage of flexibility and do not necessitate donor matching for their components. Nevertheless, it is worth noting that the idea of comparing autologous and allogeneic cell culture derived from the transplant rejection and graft-versus-host disease. The central theme of this disease is the interactions between donors and recipient immune cells, specifically LC, DC, and

naïve T-lymphocytes. Given that these cells are also the main players in skin sensitization, the question arises about whether allogenic assays can perform as effectively as autologous assays. Thus, part of this thesis aims to compare autologous and allogenic co-culture.

The initial experiment involved the co-culture of keratinocytes and naïve CD4<sup>+</sup> T-lymphocytes in both autologous and allogeneic settings. It is essential to mention that CD69 serves as an early activation marker for CD4<sup>+</sup> T-lymphocytes, detectable as early as three hours after activation (Borges et al., 2007), and T-lymphocyte characterization markers, including CD45RA and CCR7, were used as readouts. The results revealed that co-cultivating keratinocytes and naïve CD4<sup>+</sup> T-lymphocytes from different donors did not lead to changes in the presentation of characterization markers or activation markers when compared to co-cultures using cells from the same donor. This finding is consistent with existing literature indicating that, under normal circumstances, keratinocytes do not trigger responses from naïve CD4<sup>+</sup> T-lymphocytes, and they can only act as major histocompatibility complex class II (MHC-II) presenters after being treated with interferon-gamma (IFN- $\gamma$ ) (Black et al., 2007; X.-W. Cai et al., 2017; Skov & Baadsgaard, 1996). Furthermore, professional APCs, which play a significant role in T-lymphocyte activation, were absent in this design. It has also been reported that LC can pick up keratinocyte-derived proteins or mRNA, process them into antigens, and present them to T-lymphocytes later (De La Cruz Diaz & Kaplan, 2019; Rentzsch et al., 2021; Stoitzner et al., 2006; Su & Igyártó, 2019). Therefore, MoLC were included in the co-culture.

The monocytes were differentiated into LC using a cocktail mix of transforming growth factor beta (TGF- $\beta$ ), granulocyte-macrophage colony-stimulating factor (GM-CSF), and IL-4. GM-CSF and IL-4 have been shown to steer monocytes toward DC fate by upregulating TNF- $\alpha$ , thereby disrupting macrophage colony-stimulating factor (M-CSF) signaling, which could lead to macrophage differentiation instead (Hiasa et al., 2009). TGF- $\beta$  has been reported to steer the monocytes into the LC (Geissmann et al., 1998; Kel et al., 2010). In animal experiments, mice lacking TGF- $\beta$  showed an absence of LC (Borkowski et al., 1996). Moreover, it has been extensively discussed that TGF- $\beta$  is involved in several pathways, such as signal transducer and activator of transcription 5 (STAT5) and purine-rich Box-1 (PU1), which are crucial for Langerhans cell development and maintenance. The source of TGF- $\beta$  in the skin are both dermis and epidermis (Gunin & Golubtzova, 2019; Liarte et al., 2020; Seeger et al., 2015; X. Zhang et al., 2016). It has been proposed that the use of Notch ligand DLL4 in combination with GM-CSF and TGF- $\beta$  can also give rise to LCs from hematopoietic monocytes as well (Bellmann et al., 2021). Although other methods exist for differentiating LC from monocytes *in vitro*, the classical combination of GM-CSF, TGF- $\beta$ , and IL-4 is widely accepted and well-validated for MoLC differentiation.

The MoLC from the same donor as T-lymphocytes (autologous), or different donor from the T-lymphocytes (allogenic), were co-cultured together with the T-lymphocytes for three days. Although the alloreactivity between MoLC and T-lymphocytes was expected, none could be observed within the readouts of the experiment. Another study has also demonstrated that autologous and allogenic cultivation methods can be used interchangeably when cultivating T-lymphocytes with monocytes (Hollister & Jarrett, 1978). However, another study cultivating HIV-1 pulsed DC with T-lymphocytes in an autologous or allogenic system has found that the allogenic system leads to stronger activation of T-lymphocyte suggesting the additional foreign substance carry by the DC (Silva et al., 2013). Moreover, another study has highlighted lower immunoreactivity in the autologous system (Hill & Cuturi, 2010). Despite the lack of further investigation, the presumption of the result in this thesis could be thought of as the MoLC were immature and do not carry any antigen that could be presented to T-lymphocytes.

A further comparison experiment between autologous and allogenic was performed by including HFDK in the culture because keratinocytes are significant in skin sensitization. In autologous co-culture, MoLC, T-lymphocytes, and HFDK are derived from the same donor, while in allogenic co-culture, each cell type comes from different donors. The expectation was that MoLC would pick up proteins produced by allogeneic keratinocytes and present them to T-lymphocytes, leading to T-lymphocyte activation. However, the experiment's results ran contrary to these expectations. In this experimental design, neither MoLC nor naïve CD4<sup>+</sup> T-lymphocytes react differently to allogenic keratinocytes compared to autologous keratinocytes. It is important to note that another experiment comparing the single culture of immune cells to the co-culture of immune cells and to the co-culture of immune cells and HFDK has revealed interesting results. The result from the experiment showed that MoLC have matured in the presence of HFDK. This indicates that MoLC are able to pick up protein from HFDK, although it does not appear that the protein from allogenic HFDK will lead to higher maturation of MoLC. Although there are limited existing studies with a similar experimental setup, some literature suggests that autologous skin grafting does not always outperform allogenic skin grafting (Goyer et al., 2019; Kitala et al., 2016; Otto et al., 1995).

One plausible explanation for these results may be that the human leukocyte antigen (HLA) of the donors used in the experiment happened to match. The HLA system, a complex of genes encoding MHC proteins, plays a pivotal role in regulating the immune system. In the context of transplantation, such as skin transplants, the immune system identifies foreign entities within the body by detecting proteins that differ from those normally produced by the patient's cells. Key among these proteins is the HLA molecules, which the immune system uses to distinguish self from non-self (Ayala García et al., 2012; Montgomery et al., 2018).

In theory, the autologous system should offer a more suitable platform for co-cultivation experiments, the results from this thesis and other studies have demonstrated otherwise (Braye et al., 2000; Chevallier et al., 2010; Udehiya et al., 2013). In conclusion, within the scope of this thesis, the autologous co-culture of the three cell types does not demonstrate an advantage over the allogenic co-culture system. This suggests the potential for more versatile experimental designs involving these cell types within a donor pool.

## 5.3 Development of a Co-Culture-Based Skin Sensitization Assay

### 5.3.1 Response Patterns of T-Lymphocytes in the Co-Culture to DNCB

The intricate interplay between epidermal keratinocytes and CD4<sup>+</sup> T-lymphocytes in skin immunity is widely recognized. Many studies have explored co-cultures of T-lymphocytes and keratinocytes, mainly within the context of skin inflammation in conditions like psoriasis and atopic dermatitis (Humeau et al., 2022; Martin et al., 2012; Willis et al., 1991), but fewer have studied the interaction of keratinocytes and T-lymphocytes in the context of skin sensitization. Even though both keratinocytes and T-lymphocytes are central to the skin sensitization process, especially during the elicitation phase (Rustemeyer et al., 2011).

Keratinocytes play a dual role in initiating immune responses by recognizing pathogens through pattern recognition receptors like Toll-like receptors, leading to the release of pro-inflammatory cytokines. This, in turn, recruits CD4<sup>+</sup> T-lymphocytes to the site, where they are activated by DC through antigen presentation (Klicznik et al., 2018). Moreover, keratinocytes themselves can act as APCs, expressing MHC-II molecules and the co-stimulatory molecule CD80, which binds to CD28 and CTLA-4 on T-lymphocytes (Fan et al., 2003; Scheynius & Tjernlund, 1984; Tamoutounour et al., 2019a; Wakem et al., 2000). This raises questions about their efficacy in antigen presentation compared to traditional APCs and their specific role in skin sensitization reactions (Orlik et al., 2020).

*In vitro* co-culture systems face challenges due to the different nutrient requirements of immune cells and epithelial cells. While RPMI1640 complete is a standard medium supporting immune cell growth, it induces early terminal differentiation in keratinocytes, affecting cell viability due to high calcium content. Conversely, KGM-2, a standard medium for epithelial cells, leads to highly activated T-lymphocytes. Finding a suitable medium for co-culturing these cells is essential, with Mix2 emerging as a promising option in this study (Geisendörfer, 2022).

In this study, naïve CD4<sup>+</sup> T-lymphocytes were co-cultured with HFDK and exposed to the potent skin sensitizer 2,4 dinitrochlorobenzene (DNCB). Despite known cross-talk between keratinocytes

and T-lymphocytes in other inflammatory contexts than skin sensitization, no response to DNCB was observed from the T-lymphocytes in the co-culture.

While some research suggests keratinocytes can directly stimulate naïve T-lymphocytes, the mechanisms differ from those induced by typical skin sensitizers like DNCB. For instance, *Staphylococcus aureus* protein A induces autophagy in keratinocytes, leading to cytokine secretion (X. W. Cai et al., 2017), while skin sensitizers trigger oxidative stress pathways. Although keratinocytes can secrete inflammatory cytokines in response to skin sensitizers, these alone cannot activate naïve T-lymphocytes. Activation requires direct binding of MHC-II to T-lymphocyte receptors and interaction with co-stimulatory molecules.

These observations underscore the complexity of skin sensitization and the potential limitations of current *in vitro* models to fully capture the dynamics of immune response. Future studies should explore the incorporation of other immune components, such as professional APCs or a more physiologically relevant mix of cytokines, to enhance the model's predictive power for skin sensitization. This research not only illuminates the specific challenges in modeling skin sensitization but also highlights the need for refined *in vitro* systems that better mimic the intricate immune interactions occurring in human skin.

### 5.3.2 Sensitivity to DNCB of the Three-Cell Culture

Professional APCs, such as DC and LC, are known to be pivotal in detecting hapten-protein complexes and converting them into antigens before presenting them to naïve T-lymphocytes. However, this crucial aspect was lacking in the previous setup. To address this gap, MoLC were introduced into the co-culture, which was subsequently challenged by DNCB.

The co-cultivation of three cell types has yielded intriguing insights, particularly when HFDK are present, resulting in a significant upregulation of maturation markers in MoLC. This suggests a nuanced interaction between MoLC and HFDK. Notably, this maturation, while evident, does not translate into the activation of T-lymphocytes, as indicated by the absence of CD69 expression. A parallel can be drawn with findings from Geisendörfer's work, where MoLC demonstrated auto-activation, marked by a notable upregulation of CD86 and CD83 in the presence of HFDK (Geisendörfer, 2022). This supports the notion that proteins from HFDK are assimilated by MoLC, influencing their maturation.

However, a critical aspect lies in the temporal dynamics of this interaction. Within the 72-hour co-cultivation period, pinpointing when the cross-talk between HFDK and MoLC occurs remains

elusive. Two plausible scenarios may explain the absence of CD69 activation. First, CD69 may have already been downregulated during the differentiation of T-lymphocytes. Alternatively, the cross-talk between MoLC and T-lymphocytes might not have been initiated by the analysis point. CD69 is known to be an early activation marker of T-lymphocytes that can be detected as early as one hour before fading by 72 hours after activation (Beltman et al., 2007; Borges et al., 2007; Hommel & Kyewski, 2003; Simms & Ellis, 1996).

While the co-culture experiment produced unexpected outcomes, its results do not significantly impact the decision to treat the system with DNCB. In a situation where the co-culture responds to the treatment, the point of activation for analysis would naturally be at the treatment initiation. This strategic choice allows for an examination of interactions among the three cell types and DNCB, including the MoLC maturation, CD69 expression, and other responses beyond the treatment start. Therefore, the unexpected co-culture results do not hinder the rationale for focusing on the impact of DNCB on the system.

The result indicates that even with the inclusion of APCs, the co-culture system failed to respond to DNCB. This outcome contrasts with research indicating that co-cultures involving at least all three cell types -HFDK, MoLC, and T-lymphocytes - can respond to skin sensitizers, including DNCB (Frombach et al., 2018; Sonnenburg et al., 2023). It is essential to note that there are relatively few studies that have explored three cell co-cultures, or even co-culturing keratinocytes with PBMC, apart from the studies mentioned earlier. Most studies tend to focus on either co-culturing APCs with keratinocytes or co-culturing APCs with T-lymphocytes (Bechara et al., 2019; Betts et al., 2017; Cao et al., 2012; Galbiati et al., 2020; Hennen et al., 2011; Richter et al., 2013; Sawada et al., 2022). The results from these studies, especially when APCs were co-cultured directly with T-lymphocytes, have been successful in identifying skin sensitizers.

Furthermore, the contradictions in the findings may also be attributed to the varied readouts used in different studies. For instance, one study employed CD44, CD124, and CD119 expression on T-lymphocytes as readouts (Frombach et al., 2018), while some studies incorporated CD69 expression into their readout criteria (Almeida TLP, 2013; Hou et al., 2020). Others opted for IFN- $\gamma$  secretion from T-lymphocytes as a readout (Bechara et al., 2019; Betts et al., 2017; Richter et al., 2013), and several relied on T-lymphocyte proliferation as a readout, including the LLNA (Gerberick et al., 2007; Jenkinson et al., 2010; Oakes et al., 2017). This variance raises the question of whether CD69 serves as an appropriate readout for T-lymphocytes in the specific experiment.

In theory, CD69 should suffice for detecting T-lymphocyte activation. However, the results reveal that while CD69 is upregulated when T-lymphocytes are activated with T-cell activator (positive

control for T-lymphocyte activation), DNCB treatment did not induce a similar upregulation of CD69 in the co-culture with either HFDK, MoLC, or both. This suggests that CD69 may indeed be a suitable marker, but the co-culture system might have limitations in recognizing skin sensitizers effectively.

It is worth noting that the 2D co-culture environment may not be the ideal setting for cultivating all three cell types together. In the physiological skin, keratinocytes coexist with APCs, followed by interactions between APCs and T-lymphocytes. Moreover, the type of keratinocytes typically present in 2D co-culture settings primarily comprises basal keratinocytes, which cannot fully represent the diverse keratinocyte populations found in the complex structure of physiological skin, where keratinocytes have different differentiation states. In a related report, monolayer cultivation of keratinocytes was found to lack approximately 10% of the gene expression profile observed in human skin explants or human reconstructed epidermis (Bernard et al., 2002). This suggests that the 2D co-culture model may have inherent limitations when attempting to mimic the intricacies of physiological skin.

Balancing the convenience of 2D assays with their ability to faithfully represent real-life data is a critical consideration when conducting such experiments. Although 2D assays offer simplicity and robustness, they may not fully capture the complexity of *in vivo* scenarios, especially in the absence of well-accepted *in vitro* assays for T-lymphocytes. This thesis initially aimed to develop skin sensitization assays based on T-lymphocytes, which subsequently evolved to include MoLC in the co-culture setup. Ultimately, the research has progressed towards the development of immunocompetent skin models.

## 5.4 Advances in Immunocompetent Skin Models

RHS are pivotal in a broad spectrum of research areas due to their versatility and the flexibility offered by their primary components—a collagen-embedded dermal layer populated with fibroblasts and an overlying epidermal layer of keratinocytes. The choice of cell sources, extending beyond healthy cells, enables the emulation of specific skin conditions. For example, the utilization of cells from diabetic patients and filaggrin-deficient keratinocytes has successfully replicated the environments of diabetic wounds and atopic dermatitis, respectively (Barker et al., 2004; Küchler et al., 2011; Maione et al., 2015; Ozdogan et al., 2020). These models replicate key disease characteristics, offering a platform for targeted therapeutic interventions.

Moreover, researchers have augmented the utility of skin models by integrating supplementary components, enhancing their physiological relevance. Noteworthy endeavors include the integration of vascularized human skin models to investigate fibrosis and assess anti-fibrotic drugs

(Matei et al., 2019) as well as the development of perfusable vascularized skin models incorporating melanocytes to explore intricate cell-cell interactions (Duval et al., 2012; Rimal et al., 2021; Salameh et al., 2021; Zoio et al., 2021). These developments have further extended to the incorporation of melanoma spheroids into skin models, providing valuable insights into their behavior, particularly in the context of skin cancer research (I. Müller & Kulms, 2018; Vörsmann et al., 2013).

Despite the notable successes of RHS models across diverse applications, a significant limitation persists—the absence of multiple immune cells within these models. Immune cells are integral to the skin function, playing a central role in inflammatory responses and skin-related disease symptoms. Common skin diseases, including atopic dermatitis and psoriasis, are fundamentally immune-mediated, with immune cells driving the associated symptoms. For example, in atopic dermatitis, cytokines such as IL-4, IL-13, and IL-22 produced by T-lymphocytes and B-cells play a crucial role (Guttman-Yassky & Krueger, 2017). Similarly, psoriasis symptomatology is amplified by IL-17 produced by T-lymphocytes (Schön, 2019). Even in cases of contact dermatitis or skin sensitization, where LC recognize and present antigens to T-lymphocytes, the inflammatory response primarily rests on T-lymphocytes. Hence, the inclusion of immune cells in skin models, particularly for establishing humane alternatives to animal models, is imperative. Notably, skin models have shown promise in testing skin sensitizers (Chau et al., 2013; Galbiati et al., 2017; Schellenberger et al., 2019).

This brings us to the central objective of this thesis, the development of a more intricate immunocompetent reconstructed human skin model that seamlessly integrates two distinct immune cell types, MoLC and naïve T-lymphocytes (ImmuSkin-MT). These immune cells, sourced from buffy coat, are integrated into the same culture setting with existing RHS. A minimally invasive method is employed for the isolation of keratinocytes and fibroblasts from the hair follicles of both male and female donors. These HFDs form the foundation of the ImmuSkin-MT. The ultimate objective of this immunocompetent skin model is to facilitate the precise prediction of the sensitizing potential of various chemical substances.

In most RHS, the source of keratinocytes and fibroblasts is the juvenile or neonatal foreskin (Matei et al., 2019; Reijnders et al., 2015; Salameh et al., 2021; Schmidt et al., 2020; Zoio et al., 2021). Although skin models generated from these cell sources are well characterized, they have several crucial limitations, which are as follows: an invasive method due to the surgical procedure, a limitation to only male donors, and the cells from the same donor not being accessible for multiple acquires. By using HFDs it is possible to overcome these limitations, since it is now possible, to

develop *in vitro* RHS from both, male and female donors in a minimally invasive way (Löwa et al., 2018; Matsuzawa et al., 2019).

It was shown that in both RHS-FD and RHS-HFD, HFDK have organized themselves into different layers and the outmost layer where the cells are exposed to the air is fully stratified. In the dermis layer, fibroblasts can be seen embedded in collagen. Such results align with another study where the RHS was built from HFDs (Löwa et al., 2018). Moreover, the comparison of the epidermis thickness of RHS-FD or RHS-HFD has shown that the epidermal thickness of the RHS from the two cell sources is comparable. The result confirmed that HFDs can be used to build the RHS as well as foreskin-derived cells.

Prior to model development, extensive investigations were conducted to identify a suitable medium for ImmuSkin-MT. Traditional base media, rich in glucose and deficient in essential amino acids crucial for immune cell functions, posed challenges. Studies have highlighted the significant impact of medium selection on immune cell functionality and survival (Glaczynska et al., 2021; Griffoni et al., 2021; Koh et al., 2022). Additionally, KDM includes components such as cholera toxin, hydrocortisone, adenine, insulin, and EGF, which negatively affect immune cell viability.

Specifically, cholera toxin and hydrocortisone promote keratinocyte proliferation but may inhibit immune cell activation, with hydrocortisone exhibiting anti-inflammatory effects primarily at high concentrations (Ghio et al., 2018; N. Okada & Kitano, 1982; Rheinwald, 1975). Insulin stimulates keratinocyte migration and potentially supports DC maturation, although its direct impact on LC is not well documented (Benoliel et al., 1997; Lu et al., 2015; Xuan et al., 2017). EGF promotes keratinocyte growth but may dampen the immune response, relevant for MoLC viability in experimental setups (J. Chen et al., 2016; Y. J. Kim et al., 2018).

Experimental results indicated that media combinations such as KDM and RKD1 (50% RPMI1640 + 50% KDM) facilitate MoLC maturation but show higher mortality rates compared to other media like Mix2. The DC generation medium, in contrast, proved most effective for MoLC viability, underscoring the need to balance the stimulatory and inhibitory effects of KDM components on immune cells.

The response of T-lymphocytes in these media experiments showed no upregulation of activation markers, suggesting an inhibition possibly due to KDM components like cholera toxin, which can suppress T-lymphocyte proliferation unless counteracted by specific stimulations (Eriksson et al., 2000). Hydrocortisone modifies T-lymphocyte receptors, reducing essential cytokine production

(Olmes et al., 2016; Palacios & Sugawara, 1982), while insulin can enhance T-lymphocyte function under certain conditions (Fischer et al., 2017; Marchingo et al., 2020; Tsai et al., 2018).

In conclusion, while KDM supports keratinocyte growth, its components are not ideal for immune function, highlighting the importance of selecting the appropriate medium for developing an immunocompetent ImmuSkin-MT. The findings suggest that DC generation medium is most conducive for cultivating immune cells, crucial for the accurate modeling of immune responses in skin models.

After the careful consideration of medium and cultivation time, immunocompetent skin models containing MoLC (ImmuSkin-M), naïve T-lymphocytes (ImmuSkin-T), and both MoLC and naïve T-lymphocytes (ImmuSkin-MT) were developed.

Although accurately positioning MoLC to fully emulate the natural arrangement of LC in the epidermis alongside dermal DC in the dermis presents challenges, progress is being made. Several efforts by a collaborator to embed MoLC within the epidermal layer of RHS and maintain them for 14 days faced difficulties (Geisendörfer, 2022). Importantly, other studies suggested that even if immune cells are not perfectly placed within the RHS, it does not necessarily compromise the functional integrity of these advanced skin models. For instance, the addition of T-lymphocytes beneath skin models to study skin inflammation has been successfully demonstrated (Van Den Bogaard et al., 2014; Wallmeyer et al., 2017). Another study showed that THP-1 co-cultured with RHS, placed beneath the RHS, were able to responses to test substances (Schellenberger et al., 2019). Furthermore, a study that introduced an immune-cells-containing extracellular matrix layer within the skin models confirmed the functionality and responsiveness of DC to test substances in such an environment (Chau et al., 2013). It is noteworthy that cultivating DC in collagen type I does not alter their function (Sapudom et al., 2020). This ongoing progress underscores the potential of ImmuSkin-MT to enhance the simulation of skin immunology in a controlled setting.

The presence of CD1a+ cells in the subdermal layers of ImmuSkin-MT and ImmuSkin-M, but not in ImmuSkin-T or RHS, supports the models' ability to differentially support MoLC integration and survival. The absence of T-lymphocytes in all variants of ImmuSkin and RHS aligns with the designed constraints of these physical skin models, indicating that they do not migrate into these systems.

The consistent detection of epidermal markers across various ImmuSkin suggests that the presence of immune cells does not inhibit keratinocyte differentiation, maintaining keratinocyte function and the structural integrity of these models.

MoLC migration from the subdermal layer into the well in both ImmuSkin-M and ImmuSkin-MT, expressing CD86 even without external stimuli, suggests a basal level of maturation. Langerhans cell migration is a known marker of their maturation, which could be triggered by TGF- $\beta$  and IL-1 $\beta$ , secreted by keratinocytes (Bobr et al., 2012; Cumberbatch et al., 2003; Hemmi et al., 2001).

CD86 serves as a reliable marker of MoLC maturation due to its early and robust upregulation upon encountering antigens or maturation signals, distinguishing it as a dependable indicator of LC maturation. Functionally, CD86 is crucial for facilitating effective T-lymphocyte priming, underpinning the initiation of adaptive immune responses. The positive correlation between CD86 expression on LCs and other maturation markers, such as HLA-DR, further underscores its suitability as a maturation marker (Grosche et al., 2020; Z. Li et al., 2019; Prechtel & Steinkasserer, 2007; Tai et al., 2018).

From the aspect of the T-lymphocytes, a comparison between ImmuSkin-MT and ImmuSkin-T revealed a significant increase in T-lymphocytes count in the former, suggesting T-lymphocyte activation by migrated MoLC. In ImmuSkin-T, where MoLC were absent, only basal-level T-lymphocyte proliferation was observed. These results underscore the importance of MoLC in the modulation of immune responses, potentially through the facilitation of antigen presentation to T-lymphocytes.

T-lymphocyte proliferation is a widely recognized marker for T-lymphocyte activation, reflecting the clonal expansion of antigen-specific T-lymphocytes essential for effective immune responses. When T-lymphocytes encounter their specific antigens presented by APC, they undergo a series of complex signaling cascades leading to activation. This activation triggers the T-lymphocytes to enter the cell cycle, resulting in multiple rounds of division that amplify their population, thereby bolstering the body's capacity to combat specific antigens (Meraviglia et al., 2019). The significant expansion of T-lymphocyte numbers following activation not only provides a robust measure of immune response but also serves as a sensitive and specific indicator of immune system engagement (Zhan et al., 2017).

In summary, T-lymphocyte proliferation is a robust and informative readout for T-lymphocyte activation due to its fundamental role in immune defense, its sensitivity and specificity in antigen recognition, and its quantifiable and time-dependent nature.

## 5.5 Application of Immunocompetent Skin Models in Sensitizer Detection

After the ImmuSkin-MT was successfully developed and the function of the immune cells was well characterized, the ImmuSkin-M, ImmuSkin-T and ImmuSkin-MT were subject to the test if they

could discriminate between non-sensitizers and the skin sensitizers in the yes and no manner, and if it was sensitive enough to detect if the sensitizer is extreme, strong, or moderate. All three types of ImmuSkin were treated with glycerol, 0.1% DMSO (vehicle), RN (moderate skin sensitizer), IG (strong skin sensitizer), DNCB (extreme skin sensitizer), PPD (extreme skin sensitizer), and positive control (inflammatory cytokines cocktail and T-cell activator).

The result has shown that using the migration and maturation of MoLC as readouts, ImmuSkin-M and ImmuSkin-MT appear to be able to distinguish between the non-sensitizer from the sensitizer. The maturation and migration rate of the MoLC significantly increased after the ImmuSkin-M or ImmuSkin-MT were exposed to moderate or strong skin sensitizers, suggesting a response to the treatment. These results from this thesis are similar to other studies that have used Langerhans cell migration and maturation as an indicator of the response to contact skin sensitizers (Azam et al., 2006; Bock et al., 2018; Gibbs et al., 2013; Jacobs et al., 2006; Rees et al., 2011; Sakaguchi et al., 2009b; Villablanca & Mora, 2008). Furthermore, it is widely accepted to use CD86 upregulation and migration of MoLC as a readout for skin sensitization testing. h-CLAT, and U937 Cell Line Activation test (U-SENS™), two of the assays focusing on the KE 3 accepted into the OECD guideline, use the expression of CD86 as the parameters to test the skin sensitizers (OECD, 2023d; Piroird et al., 2015; Sakaguchi et al., 2009b).

In addition to the readout addressing KE 3, ImmuSkin-MT can provide an additional readout addressing KE 4. The SI based on the proliferation of T-lymphocytes was used as a readout addressing KE 4. The findings demonstrate that T-lymphocytes in ImmuSkin-T exhibited limited responsiveness to all treatments except the positive control. In contrast, T-lymphocytes in ImmuSkin-MT demonstrated robust responses to all sensitizers. The cross-talk of the interaction between MoLC and T-lymphocytes is well portrayed in this skin model. The result aligns with other studies where T-lymphocyte proliferation was used as an indicator for T-lymphocytes response to skin sensitizers (Bennett et al., 2007; Betts et al., 2017; Hunger et al., 2004; C.-H. Lee et al., 2012; Peiser et al., 2004). ImmuSkin-T only responds to the positive control, which is as expected. The T-lymphocytes in UT ImmuSkin-T have appeared to be proliferating, despite the absence of APC and the T-cell activator. Classically, naïve T-lymphocytes require direct activation to proliferate, but it has also been reported that the combination of IL-7 and IL-2 can induce the proliferation of the cells which can be enhanced by the pro-inflammatory cytokines like IL-1 $\beta$  and TNF- $\alpha$  (Ben-Sasson et al., 2009; Jaleco et al., 2003; Skartsis et al., 2022; Van Den Eeckhout et al., 2020). It can be explained that keratinocytes could be the source of IL-7, and T-lymphocytes itself as a source of IL-2 (D. Chen et al., 2021). It is important to note that the DC generation medium is a defined medium for DC generation where the component of the medium is unknown to the consumer, so the

possibility that the medium itself contains certain components that can affect naïve T-lymphocytes response to the pro-inflammatory cytokines should not be prematurely excluded.

The skin sensitizing potency classification defined based on EC3 LLNA data categorized substances into extreme, strong, and moderate sensitizers (Basketter et al., 2014; Gerberick et al., 2004; Natsch et al., 2013).

The ImmuSkin-MT represents a promising innovation in assessing skin sensitizers through a straightforward yes/no format. Although the results did not reach statistical significance, there is a clear trend showing that ImmuSkin-MT might have the potential to distinguish varying levels of sensitization. Despite the constraints of a limited number of sensitizers tested and experimental repeats, ImmuSkin-MT has successfully outlined a preliminary framework for categorization. Under this schema, substances that prompt substantial migration of MoLC, elevate CD86 expression, and enhance T-lymphocyte proliferation are classified as extreme sensitizers. Notably, substances like DNCB and PPD fall into this category. Meanwhile, substances like IG, which increase MoLC migration and SI but do not significantly boost CD86 expression, are considered strong sensitizers. Lastly, substances that solely exhibit increased SI, such as RN, are categorized as moderate sensitizers. This way of categorization aligns well with traditional classifications, adding a valuable layer of verification to the results obtained through ImmuSkin-MT.

In this experimental setup, ImmuSkin-MT represents a significant advancement toward replicating the complex milieu of physiological skin, where key immune cells coexist in a dynamic environment. This novel and intricate immunocompetent skin model showcases the potential to enhance the identification of skin sensitizers by effectively capturing KE 3 and 4 from the AOP. The co-culture setup successfully mirrors the important interaction between MoLC and T-lymphocytes, marking a vital step forward in skin sensitization research.

Despite this progress, one limitation of the ImmuSkin-MT is the absence of a direct readout from keratinocytes, which are involved in KE 2. Ideally, it should be possible to detect cytokine secretion from the RHS, although this is not the most established readout for skin sensitization in such a complex system. The current OECD-approved methods for detecting KE 2, such as KeratinoSense, LuSens, and EpiSensA, focus on changes in gene expression related to the Keap1-Nrf-ARE pathway rather than cytokine secretion (Natch, 2017; Ramirez et al., 2014; Saito et al., 2013). There are more assays that have been developed, but have not made it to the OECD guidelines, such as the IL-18 RhE assay that uses the secretion of IL-18 from RHE and cytotoxicity as readouts (Andres et al., 2017; Galbiati et al., 2018), or the measurement of IL-18 secreted from NCTC 2544 (Corsini et al., 2013). These assays, while robust and reliable, are optimized for simpler test systems.

Nevertheless, the performance of ImmuSkin-MT in classifying skin sensitizing potency, while showing preliminary trends, calls for further refinement. The model has demonstrated the ability to preliminarily categorize sensitizers based on the robustness of MoLC migration, CD86 expression, and T-lymphocyte proliferation, correlating with known classifications of extreme, strong, and moderate sensitizers. To improve the relevance and accuracy of ImmuSkin-MT, further development should focus on optimizing the placement of MoLC to more accurately mimic their physiological locations. Additionally, expanding the range of tested known sensitizers and conducting ring validation studies will strengthen the model's reliability and its capability to detect various key events simultaneously.

Overall, ImmuSkin-MT stands as a promising tool in the advancement of *in vitro* assays capable of predicting and identifying skin sensitization events concurrently. This model is not only a testament to the potential for significant strides in dermatological research but also highlights the ongoing need for innovative approaches to better assessing complex biological interactions in skin sensitization.

## 5.6 Outlook

The next crucial step is the integration of induced pluripotent stem cells (iPSCs) into these models. iPSCs, with their ability to differentiate into various skin cells and immune cells, offer a transformative potential for skin sensitization assays. By providing a standardized and potentially unlimited source of diverse skin cells, iPSCs can enhance the complexity and clinical relevance of skin models. This approach ensures a rich, varied cellular environment that closely mimics human skin, setting the stage for more accurate and personalized testing.

Building on the foundation provided by iPSC technology, skin-on-chip platforms can further advance the field. These platforms typically feature distinct types of chips, some allowing for cell culture at a microscale, while others enable the placement of static skin models in separate chambers connected by channels simulating blood vessels. Although achieving a fully functional perfusion system for the cells is currently challenging, incorporating iPSC-derived skin cells into these setups could bring models like ImmuSkin-MT closer to mimicking physiological skin. This could be achieved by incorporating a lymph node model with T-lymphocytes in one chamber and MoLC in another, with a perfusion system running between them.

The envisioned process involves exposing the skin models to a skin sensitizer and monitoring the migration of MoLC from the RHS chamber to the lymph node model, where they present antigens to T-lymphocytes. Subsequently, the T-lymphocytes migrate from the lymph node and remain

within the perfusion system. In a subsequent exposure, the migration of T-lymphocytes to the skin models should be observed. This setup, supported by the cellular diversity provided by iPSCs, could significantly enhance the physiological relevance and predictive accuracy of skin-on-chip technologies.

The idea of integrating iPSCs into skin-on-chip models is supported by current advancements in the field. Reports have indicated the utility of skin-on-chip for testing chemical toxicity and for incorporating immune responses, demonstrating the capability of these systems to support complex biological interactions and responses to external stimuli (J. S. Lee et al., 2022; Spagolla Napoleão Tavares et al., 2020; Varga-Medveczky et al., 2021; Wufuer et al., 2016). Moreover, studies like those by Kwak et al. (Kwak et al., 2020) and J. J. Kim et al. (J. J. Kim et al., 2019) show that skin-on-chip can effectively incorporate immune cells and respond dynamically to environmental challenges such as UV irradiation and bacterial infection. Another study has also shown the success of skin-on-chip containing DC (Ramadan & Ting, 2016). Interestingly, it has also been reported that culturing skin models with the perfusion system resulted in improved epidermal morphogenesis and barrier function (Sriram et al., 2018). Therefore, the skin-on-chip in combination with the microfluidic system might be the future of the fast, high-throughput, and biologically relevant skin sensitization assay.

In summary, this development positions ImmuSkin-MT as a promising and innovative method to test skin sensitizers, providing a more biologically relevant alternative to traditional *in vitro* models and potentially reducing reliance on animal testing. With its ability to emulate key events of skin sensitization while incorporating two crucial immune cell types, ImmuSkin-MT stands as a potent tool for future research in dermatotoxicology. The enhanced physiological relevance of this model holds the potential to offer a more reliable and ethical approach to assessing the sensitizing potential of chemical substances. By promoting the adoption of ImmuSkin-MT and other advanced *in vitro* models, a significant step towards fulfilling the vision of reducing and eventually replacing animal testing in the realm of skin sensitization research has been taken.

## CHAPTER 6 CONCLUSION

Skin sensitization presents a pressing challenge in dermatotoxicology, underscoring the necessity for advanced and biologically relevant testing approaches. Conventional *in vitro* models and animal studies, traditionally used to predict skin sensitization, are powerful but have significant limitations that compromise their effectiveness in accurately predicting skin sensitization in humans. The *in vitro* models, while convenient, frequently fall short in capturing the intricate interplay of skin sensitization, thus lacking the representation of essential interactions among immune cells, keratinocytes, and chemical sensitizers. Moreover, animal testing, despite its higher biological relevance, substantially deviates from human skin physiology, undermining its predictive value when applied to human responses and reducing overall reliability. The pressing ethical concerns surrounding animal testing have catalyzed a global movement towards more humane and efficient alternatives. Regulatory pressures have further accentuated the demand for alternative testing approaches that align with the objectives of regulatory agencies such as ECHA and the United Nations Globally Harmonized System of Classification and Labelling of Chemicals (UN GHS).

Recognizing these shortcomings and the growing need for improved skin sensitization testing, this thesis aimed to develop an immunocompetent skin model (ImmuSkin-MT). The model was designed to replicate the intricate cellular interactions and physiological environment of human skin, addressing the limitations of existing *in vitro* models while respecting ethical concerns. There are three key players in skin sensitization; keratinocytes, being the most abundant cell type in the epidermis, serve as the primary targets for sensitization events, MoLC, which closely resemble LCs, function as APC that interact with sensitizers, and T-lymphocytes complete the picture, representing the effector cells that respond to sensitizing agents.

In summary, hair follicles were chosen as the source of skin cells for the development of ImmuSkins. Despite minor differences compared to foreskin-derived cells, hair follicle-derived cells proved to be a suitable alternative. The initial phase of the thesis involved 2D co-culture, where cells involved in the skin sensitization process were co-cultured. This intricate assembly of cell types reflects the complexity of immune responses in the skin and underpins the biological relevance of the model. However, this approach proved ineffective in detecting skin sensitizers, likely due to MoLC auto-activation. Additionally, this approach revealed that the autologous culture of different cell types is not superior to the allogeneic co-culture, facilitating the choice of cells. Subsequently, ImmuSkins were developed and characterized, demonstrating that immune cells do not compromise the integrity of the RHS.

ImmuSkins were then subjected to various skin sensitizers and non-sensitizers. Results indicated that the treatment did not affect the appearance of ImmuSkins. The ImmuSkin-MT can measure two key events in the AOP of skin sensitization, which were KE 3 (the maturation and migration of MoLC), and KE 4, (the activation of T-lymphocytes). The ImmuSkin-MT can differentiate between skin sensitizers and non-sensitizers based on these KEs. This evidence suggests the potential of ImmuSkin-MT as a reliable tool for skin sensitization assessment. Furthermore, ImmuSkin-MT assessment methods align with the principles of 3R (Replace, Reduce, and Refine animal testing) to minimize animal testing. By filling the gap in traditional *in vitro* models, ImmuSkin-MT offers a more physiologically relevant platform and is also an ethical alternative that reduces the need for animal experimentation.

This comprehensive approach, combining biologically relevant cell types and advanced methods, positions ImmuSkin-MT as a promising solution for more accurate and ethical skin sensitization testing, with the potential to reshape the landscape of dermatotoxicology research. This thesis introduces ImmuSkin-MT as an innovative solution, effectively bridging these constraints and providing a promising, ethically sound, and biologically realistic avenue for skin sensitization research.

## REFERENCES

- Adams, M. P., Mallet, D. G., & Pettet, G. J. (2015). Towards a Quantitative Theory of Epidermal Calcium Profile Formation in Unwounded Skin. *PLOS ONE*, *10*(1), e0116751. <https://doi.org/10.1371/JOURNAL.PONE.0116751>
- Adhikary, G., Crish, J., Lass, J., & Eckert, R. L. (2004). Regulation of Involucrin Expression in Normal Human Corneal Epithelial Cells: A Role for Activator Protein One. *Investigative Ophthalmology & Visual Science*, *45*(4), 1080–1087. <https://doi.org/10.1167/IOVS.03-1180>
- Agonia, A. S., Palmeira-de-Oliveira, A., Cardoso, C., Augusto, C., Pellevoisin, C., Videau, C., Dinis-Oliveira, R. J., & Palmeira-de-Oliveira, R. (2022). Reconstructed Human Epidermis: An Alternative Approach for In Vitro Bioequivalence Testing of Topical Products. *Pharmaceutics*, *14*(8), 1554. <https://doi.org/10.3390/PHARMACEUTICS14081554/S1>
- Ahmed, S. S., Wang, X. N., Fielding, M., Kerry, A., Dickinson, I., Munuswamy, R., Kimber, I., & Dickinson, A. M. (2015). An in vitro human skin test for assessing sensitization potential. *Journal of Applied Toxicology*, *36*(5), 669–684. <https://doi.org/10.1002/JAT.3197>
- Akinduro, O., Sully, K., Patel, A., Robinson, D. J., Chikh, A., McPhail, G., Braun, K. M., Philpott, M. P., Harwood, C. A., Byrne, C., O'Shaughnessy, R. F. L., & Bergamaschi, D. (2016). Constitutive Autophagy and Nucleophagy during Epidermal Differentiation. *Journal of Investigative Dermatology*, *136*(7), 1460–1470. <https://doi.org/10.1016/J.JID.2016.03.016>
- Alam, H., Sehgal, L., Kundu, S. T., Dalal, S. N., & Vaidya, M. M. (2011). Novel function of keratins 5 and 14 in proliferation and differentiation of stratified epithelial cells. *Molecular Biology of the Cell*, *22*(21), 4068. <https://doi.org/10.1091/MBC.E10-08-0703>
- Aleksic, M., Pease, C. K., Basketter, D. A., Panico, M., Morris, H. R., & Dell, A. (2007). Investigating protein haptentation mechanisms of skin sensitizers using human serum albumin as a model protein. *Toxicology in Vitro: An International Journal Published in Association with BIBRA*, *21*(4), 723–733. <https://doi.org/10.1016/j.tiv.2007.01.008>
- Aleksic, M., Thain, E., Roger, D., Saib, O., Davies, M., Li, J., Aptula, A., & Zazzeroni, R. (2009). Reactivity profiling: covalent modification of single nucleophile peptides for skin sensitization risk assessment. *Toxicological Sciences: An Official Journal of the Society of Toxicology*, *108*(2), 401–411. <https://doi.org/10.1093/toxsci/kfp030>
- Almeida TLP, V. L. (2013). Association of CD69 and CD 25 Activation Markers on CD4 and CD8 Cells with Skin Tests in Drug Allergy. *Journal of Pharmacovigilance*, *01*(03), 1–5. <https://doi.org/10.4172/2329-6887.1000111>
- Andres, E., Barry, M., Hundt, A., Dini, C., Corsini, E., Gibbs, S., Roggen, E. L., & Ferret, P. J. (2017). Preliminary performance data of the RHE/IL-18 assay performed on SkinEthic™ RHE for the identification of contact sensitizers. *International Journal of Cosmetic Science*, *39*(2), 121–132. <https://doi.org/10.1111/ICS.12355>
- Aptula, A. O., Roberts, D. W., & Pease, C. K. (2007). Haptens, prohaptens and prehaptens, or electrophiles and proelectrophiles. *Contact Dermatitis*, *56*(1), 54–56. <https://doi.org/10.1111/J.1600-0536.2007.00944.X>
- Arai, A., Katsuoka, K., Kiesewetter, F., Schell, H., & Hornstein, O. (1989). Effects of testosterone, dihydrotestosterone and estradiol on the growth behavior of cultured hair bulb papilla cells and root sheath fibroblasts. In J. M. L. and J. L. A. D. Van Neste (Ed.), *Trends in Human Hair Growth and Alopecia Research* (pp. 99–104). Kluwer Academic Publishers. <https://doi.org/10.1007/978-94-011-7873-0>
- Ashikaga, T., Yoshida, Y., Hirota, M., Yoneyama, K., Itagaki, H., Sakaguchi, H., Miyazawa, M., Ito, Y., Suzuki, H., & Toyoda, H. (2006). Development of an in vitro skin sensitization test using human cell lines: The human Cell Line Activation Test (h-CLAT). I. Optimization of the h-CLAT protocol. *Toxicology in Vitro*, *20*(5), 767–773. <https://doi.org/10.1016/J.TIV.2005.10.012>
- Ayala García, M. A., González Yebra, B., López Flores, A. L., & Guaní Guerra, E. (2012). The Major Histocompatibility Complex in Transplantation. *Journal of Transplantation*, *2012*, 1–7. <https://doi.org/10.1155/2012/842141>
- Azam, P., Peiffer, J.-L., Chamousset, D., Tissier, M.-H., Bonnet, P.-A., Vian, L., Fabre, I., & Ourlin, J.-C. (2006). The cytokine-dependent MUTZ-3 cell line as an in vitro model for the screening of contact sensitizers. *Toxicology and Applied Pharmacology*, *212*(1), 14–23. <https://doi.org/10.1016/j.taap.2005.06.018>
- Bak, S. S., Park, J. M., Oh, J. W., Kim, J. C., Kim, M. K., & Sung, Y. K. (2020). Knockdown of FOXA2 Impairs Hair-Inductive Activity of Cultured Human Follicular Keratinocytes. *Frontiers in Cell and Developmental Biology*, *8*(October), 2–9. <https://doi.org/10.3389/fcell.2020.575382>
- Barker, C. L., McHale, M. T., Gillies, A. K., Waller, J., Pearce, D. M., Osborne, J., Hutchinson, P. E., Smith, G. M., & Pringle, J. H. (2004).

- The development and characterization of an in vitro model of psoriasis. *Journal of Investigative Dermatology*, 123(5), 892–901. <https://doi.org/10.1111/j.0022-202X.2004.23435.x>
- Basketter, D. A., Alépée, N., Ashikaga, T., Barroso, J., Gilmour, N., Goebel, C., Hibatallah, J., Hoffmann, S., Kern, P., Martinuzzi-Teissier, S., Maxwell, G., Reisinger, K., Sakaguchi, H., Schepky, A., Tailhardat, M., & Templier, M. (2014). Categorization of chemicals according to their relative human skin sensitizing potency. *Dermatitis : Contact, Atopic, Occupational, Drug*, 25(1), 11–21. <https://doi.org/10.1097/DER.0000000000000003>
- Basketter, D. A., Clapp, C., Jefferies, D., Safford, B., Ryan, C. A., Gerberick, F., Dearman, R. J., & Kimber, I. (2005). Predictive identification of human skin sensitization thresholds. *Contact Dermatitis*, 53(5), 260–267. <https://doi.org/10.1111/j.0105-1873.2005.00707.x>
- Bauch, C., Kolle, S. N., Fabian, E., Pachel, C., Ramirez, T., Wiench, B., Wruck, C. J., Ravenzwaay, B. van, & Landsiedel, R. (2011). Intralaboratory validation of four in vitro assays for the prediction of the skin sensitizing potential of chemicals. *Toxicology in Vitro : An International Journal Published in Association with BIBRA*, 25(6), 1162–1168. <https://doi.org/10.1016/J.TIV.2011.05.030>
- Bauch, C., Kolle, S. N., Ramirez, T., Eltze, T., Fabian, E., Mehling, A., Teubner, W., van Ravenzwaay, B., & Landsiedel, R. (2012). Putting the parts together: Combining in vitro methods to test for skin sensitizing potentials. *Regulatory Toxicology and Pharmacology*, 63(3), 489–504. <https://doi.org/10.1016/J.YRTPH.2012.05.013>
- Bechara, R., Pollastro, S., Azoury, M. E., Szely, N., Maillère, B., De Vries, N., & Pallardy, M. (2019). Identification and characterization of circulating naïve CD4+ and CD8+ T cells recognizing nickel. *Frontiers in Immunology*, 10(JUN), 1–12. <https://doi.org/10.3389/fimmu.2019.01331>
- Bechetoille, N., Dezutter-Dambuyant, C., Damour, O., André, V., Orly, I., & Perrier, E. (2007). Effects of solar ultraviolet radiation on engineered human skin equivalent containing both Langerhans cells and dermal dendritic cells. *Tissue Engineering*, 13(11), 2667–2679. <https://doi.org/10.1089/ten.2006.0405>
- Bell, E., Ehrlich, H. P., Buttle, D. J., & Nakatsuji, T. (1981a). Living tissue formed in vitro and accepted as skin-equivalent tissue of full thickness. *Science*, 211(4486), 1052–1054. <https://doi.org/10.1126/SCIENCE.7008197>
- Bell, E., Ehrlich, H. P., Buttle, D. J., & Nakatsuji, T. (1981b). Living Tissue Formed in Vitro and Accepted as Skin-Equivalent Tissue of Full Thickness. *Science*, 211(4486), 1052–1054. <https://doi.org/10.1126/SCIENCE.7008197>
- Bella, J., & Hulmes, D. J. S. (2017). Fibrillar Collagens. *Sub-Cellular Biochemistry*, 82, 457–490. [https://doi.org/10.1007/978-3-319-49674-0\\_14](https://doi.org/10.1007/978-3-319-49674-0_14)
- Bellmann, L., Zelle-Rieser, C., Milne, P., Resteu, A., Tripp, C. H., Hermann-Kleiter, N., Zaderer, V., Wilflingseder, D., Hörtnagl, P., Theochari, M., Schulze, J., Rentzsch, M., Del Frari, B., Collin, M., Rademacher, C., Romani, N., & Stoitzner, P. (2021). Notch-Mediated Generation of Monocyte-Derived Langerhans Cells: Phenotype and Function. *Journal of Investigative Dermatology*, 141(1), 84–94.e6. <https://doi.org/10.1016/j.jid.2020.05.098>
- Beltman, J. B., Marée, A. F. M., & De Boer, R. J. (2007). Spatial modelling of brief and long interactions between T cells and dendritic cells. *Immunology and Cell Biology*, 85(4), 306–314. <https://doi.org/10.1038/SJ.ICB.7100054>
- Ben-Sasson, S. Z., Hu-Li, J., Quiel, J., Cauchetaux, S., Ratner, M., Shapira, I., Dinarello, C. A., & Paul, W. E. (2009). IL-1 acts directly on CD4 T cells to enhance their antigen-driven expansion and differentiation. *Proceedings of the National Academy of Sciences of the United States of America*, 106(17), 7119–7124. <https://doi.org/10.1073/pnas.0902745106>
- Bennett, C. L., Noordegraaf, M., Martina, C. A. E., & Clausen, B. E. (2007). Langerhans Cells Are Required for Efficient Presentation of Topically Applied Hapten to T Cells. *The Journal of Immunology*, 179(10), 6830–6835. <https://doi.org/10.4049/jimmunol.179.10.6830>
- Benoiel, A. M., Kahn-Perles, B., Imbert, J., & Verrando, P. (1997). Insulin stimulates haptotactic migration of human epidermal keratinocytes through activation of NF-kappa B transcription factor. *Journal of Cell Science*, 110 ( Pt 17)(17), 2089–2097. <https://doi.org/10.1242/JCS.110.17.2089>
- Bergström, M. A., Ott, H., Carlsson, A., Neis, M., Zwadlo-Klarwasser, G., Jonsson, C. A. M., Merk, H. F., Karlberg, A.-T., & Baron, J. M. (2007). A skin-like cytochrome P450 cocktail activates prohaptens to contact allergenic metabolites. *The Journal of Investigative Dermatology*, 127(5), 1145–1153. <https://doi.org/10.1038/sj.jid.5700638>
- BERMAN, B., CHEN, V. L., FRANCE, D. S., DOTZ, W. I., & PETRONI, G. (1983). Anatomical mapping of epidermal Langerhans cell densities in adults. *British Journal of Dermatology*, 109(5), 553–558. <https://doi.org/10.1111/j.1365-2133.1983.tb07678.x>

- Bernard, F. X., Pedretti, N., Rosdy, M., & Deguercy, A. (2002). Comparison of gene expression profiles in human keratinocyte mono-layer cultures, reconstituted epidermis and normal human skin; Transcriptional effects of retinoid treatments in reconstituted human epidermis. *Experimental Dermatology*, *11*(1), 59–74. <https://doi.org/10.1034/j.1600-0625.2002.110107.x>
- Betts, R. J., Perkovic, A., Mahapatra, S., Del Bufalo, A., Camara, K., Howell, A. R., Martinuzzi Teissier, S., De Libero, G., & Mori, L. (2017). Contact sensitizers trigger human CD1-autoreactive T-cell responses. *European Journal of Immunology*, *47*(7), 1171–1180. <https://doi.org/10.1002/eji.201746939>
- Bikle, D. D., Xie, Z., & Tu, C. L. (2012). Calcium regulation of keratinocyte differentiation. *Expert Review of Endocrinology & Metabolism*, *7*(4), 461. <https://doi.org/10.1586/EEM.12.34>
- Black, A. P. B., Ardern-Jones, M. R., Kasproiwicz, V., Bowness, P., Jones, L., Bailey, A. S., & Ogg, G. S. (2007). Human keratinocyte induction of rapid effector function in antigen-specific memory CD4+ and CD8+ T cells. *European Journal of Immunology*, *37*(6), 1485–1493. <https://doi.org/10.1002/EJI.200636915>
- Blander, J. M., & Medzhitov, R. (2006). On regulation of phagosome maturation and antigen presentation. *Nature Immunology* *2005* *7*:10, *7*(10), 1029–1035. <https://doi.org/10.1038/ni1006-1029>
- Blum, J. S., Wearsch, P. A., & Cresswell, P. (2013). Pathways of antigen processing. *Annu. Rev. Immunol.*, *31*, 443–473. <https://doi.org/10.1146/annurev-immunol-032712-095910>
- Bobr, A., Igyarto, B. Z., Haley, K. M., Li, M. O., Flavell, R. A., & Kaplan, D. H. (2012). Autocrine/paracrine TGF- $\beta$ 1 inhibits Langerhans cell migration. *Proceedings of the National Academy of Sciences*, *109*(26), 10492–10497. <https://doi.org/10.1073/pnas.1119178109>
- Bock, S., Said, A., Müller, G., Schäfer-Korting, M., Zoschke, C., & Weindl, G. (2018). Characterization of reconstructed human skin containing Langerhans cells to monitor molecular events in skin sensitization. *Toxicology in Vitro*, *46*(December 2016), 77–85. <https://doi.org/10.1016/j.tiv.2017.09.019>
- Bonnet, C., Brahmabhatt, A., Deng, S. X., & Zheng, J. J. (2021). Wnt signaling activation: targets and therapeutic opportunities for stem cell therapy and regenerative medicine. *RSC Chemical Biology*, *2*(4), 1144–1157. <https://doi.org/10.1039/D1CB00063B>
- Borges, O., Borchard, G., de Sousa, A., Junginger, H. E., & Cordeiro-da-Silva, A. (2007). Induction of lymphocytes activated marker CD69 following exposure to chitosan and alginate biopolymers. *International Journal of Pharmaceutics*, *337*(1–2), 254–264. <https://doi.org/10.1016/j.ijpharm.2007.01.021>
- Borkowski, T. A., Letterio, J. J., Farr, A. G., & Udey, M. C. (1996). A Role for Endogenous Transforming Growth Factor  $\beta$ 1 in Langerhans Cell Biology: The Skin of Transforming Growth Factor  $\beta$ 1 Null Mice Is Devoid of Epidermal Langerhans Cells. *The Journal of Experimental Medicine*, *184*(6), 2417. <https://doi.org/10.1084/JEM.184.6.2417>
- Bozso, S. J., Kang, J. J. H., & Nagendran, J. (2020). The role of competing mechanisms on Lck regulation. *Immunologic Research*, *68*(5), 289–295. <https://doi.org/10.1007/S12026-020-09148-2/FIGURES/1>
- Braye, F., Pascal, P., Bertin-Maghit, M., Colpart, J. J., Tissot, E., & Damour, O. (2000). Advantages of using a bank of allogenic keratinocytes for the rapid coverage of extensive and deep second-degree burns. *Medical and Biological Engineering and Computing*, *38*(2), 248–252. <https://doi.org/10.1007/BF02344784/METRICS>
- Breloer, M., & Fleischer, B. (2008). CD83 regulates lymphocyte maturation, activation and homeostasis. *Trends in Immunology*, *29*(4), 186–194. <https://doi.org/10.1016/j.it.2008.01.009>
- Britschgi, M. R., Link, A., Lissandrin, T. K. A., & Luther, S. A. (2008). Dynamic modulation of CCR7 expression and function on naive T lymphocytes in vivo. *Journal of Immunology (Baltimore, Md. : 1950)*, *181*(11), 7681–7688. <https://doi.org/10.4049/JIMMUNOL.181.11.7681>
- Bromley, S. K., Thomas, S. Y., & Luster, A. D. (2005). Chemokine receptor CCR7 guides T cell exit from peripheral tissues and entry into afferent lymphatics. *Nature Immunology* *2005* *6*:9, *6*(9), 895–901. <https://doi.org/10.1038/ni1240>
- Cai, X.-W., Zhu, R., Ran, L., Li, Y.-Q. Q., Huang, K., Peng, J., He, W., Zhou, C.-L. L., & Wang, R.-P. P. (2017). A novel non-contact communication between human keratinocytes and T cells: Exosomes derived from keratinocytes support superantigen-induced proliferation of resting T cells. *Molecular Medicine Reports*, *16*(5), 7032–7038. <https://doi.org/10.3892/mmr.2017.7492>
- Cai, X. W., Zhu, R., Ran, L., Li, Y. Q., Huang, K., Peng, J., He, W., Zhou, C. L., & Wang, R. P. (2017). A novel non-contact communication between human keratinocytes and T cells: Exosomes derived from keratinocytes support superantigen-induced proliferation of resting T cells. *Molecular Medicine Reports*, *16*(5), 7032–7038. <https://doi.org/10.3892/mmr.2017.7492>

- Candi, E., Schmidt, R., & Melino, G. (2005). The cornified envelope: a model of cell death in the skin. *Nature Reviews Molecular Cell Biology* 2005 6:4, 6(4), 328–340. <https://doi.org/10.1038/nrm1619>
- Cao, Y. P., Ma, P. C., Liu, W. Da, Zhou, W. Q., Tao, Y., Zhang, M. L., Li, L. J., & Chen, Z. Y. (2012). Evaluation of the skin sensitization potential of chemicals in THP-1/keratinocyte co-cultures. *Immunopharmacology and Immunotoxicology*, 34(2), 196–204. <https://doi.org/10.3109/08923973.2011.591800>
- Casati, S., Aschberger, K., Asturiol, D., Basketter, D., Dimitrov, S., Dumont, C., Karlberg, A.-T., Lepoittevin, J.-P., Patlewicz, G., Roberts, D. W., Worth, A., & Institute for Health and Consumer Protection. (2016). *Ability of non-animal methods for skin sensitisation to detect pre- and pro-haptens report and recommendations of an EURL ECVAM expert meeting*. 23. <https://doi.org/10.2788/01803>
- Chau, D. Y. S., Johnson, C., MacNeil, S., Haycock, J. W., & Ghaemmaghami, A. M. (2013). The development of a 3D immunocompetent model of human skin. *Biofabrication*, 5(3), 035011. <https://doi.org/10.1088/1758-5082/5/3/035011>
- Chen, D., Tang, T. X., Deng, H., Yang, X. P., & Tang, Z. H. (2021). Interleukin-7 Biology and Its Effects on Immune Cells: Mediator of Generation, Differentiation, Survival, and Homeostasis. *Frontiers in Immunology*, 12, 747324. <https://doi.org/10.3389/FIMMU.2021.747324/BIBTEX>
- Chen, J., Zeng, F., Forrester, S. J., Eguchi, S., Zhang, M. Z., & Harris, R. C. (2016). Expression and function of the epidermal growth factor receptor in physiology and disease. *Physiological Reviews*, 96(3), 1025–1069. <https://doi.org/10.1152/PHYSREV.00030.2015/ASSET/IMAGES/LARGE/Z9J0031627690008.JPEG>
- Chen, X., Lloyd, S. M., Kweon, J., Gamalong, G. M., & Bao, X. (2021). Epidermal progenitors suppress GRHL3-mediated differentiation through intronic polyadenylation promoted by CPSF-HNRNPA3 collaboration. *Nature Communications* 2021 12:1, 12(1), 1–15. <https://doi.org/10.1038/s41467-020-20674-3>
- Chen, Y., Fang, Q., Wang, Z., Zhang, J. Y., MacLeod, A. S., Hall, R. P., & Liedtke, W. B. (2016). Transient Receptor Potential Vanilloid 4 Ion Channel Functions as a Pruriceptor in Epidermal Keratinocytes to Evoke Histaminergic Itch. *The Journal of Biological Chemistry*, 291(19), 10252–10262. <https://doi.org/10.1074/JBC.M116.716464>
- Chevallier, N., Anagnostou, F., Zilber, S., Bodivit, G., Maurin, S., Barrault, A., Bierling, P., Hernigou, P., Layrolle, P., & Rouard, H. (2010). Osteoblastic differentiation of human mesenchymal stem cells with platelet lysate. *Biomaterials*, 31(2), 270–278. <https://doi.org/10.1016/J.BIOMATERIALS.2009.09.043>
- Chieosilapatham, P., Kiatsurayanon, C., Umehara, Y., Trujillo-Paez, J. V., Peng, G., Yue, H., Nguyen, L. T. H., & Niyonsaba, F. (2021). Keratinocytes: innate immune cells in atopic dermatitis. *Clinical and Experimental Immunology*, 204(3), 296–309. <https://doi.org/10.1111/CEI.13575>
- Chipinda, I., Hettick, J. M., & Siegel, P. D. (2011). Haptenation: chemical reactivity and protein binding. *J Allergy (Cairo)*, 2011, 839682. <https://doi.org/10.1155/2011/839682>
- Clark, R. A. (2010). Skin-resident T cells: The ups and downs of on site immunity. *Journal of Investigative Dermatology*, 130(2), 362–370. <https://doi.org/10.1038/jid.2009.247>
- Clayton, K., Vallejo, A. F., Davies, J., Sirvent, S., & Polak, M. E. (2017). Langerhans Cells—Programmed by the Epidermis. *Frontiers in Immunology*, 8(NOV). <https://doi.org/10.3389/fimmu.2017.01676>
- Cordani, N., Pozzi, S., Martynova, E., Fanoni, D., Borrelli, S., Alotto, D., Castagnoli, C., Berti, E., Viganò, M. A., & Mantovani, R. (2010). Mutant p53 subverts p63 control over KLF4 expression in keratinocytes. *Oncogene* 2011 30:8, 30(8), 922–932. <https://doi.org/10.1038/onc.2010.474>
- Corsini, E., Galbiati, V., Mitjans, M., Galli, C. L., & Marinovich, M. (2013). NCTC 2544 and IL-18 production: A tool for the identification of contact allergens. *Toxicology in Vitro*, 27(3), 1127–1134. <https://doi.org/10.1016/j.tiv.2012.05.018>
- Cumberbatch, M., Bhushan, M., Dearman, R. J., Kimber, I., & Griffiths, C. E. M. (2003). IL-1beta-induced Langerhans' cell migration and TNF-alpha production in human skin: regulation by lactoferrin. *Clinical and Experimental Immunology*, 132(2), 352–359. <https://doi.org/10.1046/j.1365-2249.2003.02146.x>
- Darby, W. G., Grace, M. S., Baratchi, S., & McIntyre, P. (2016). Modulation of TRPV4 by diverse mechanisms. *The International Journal of Biochemistry & Cell Biology*, 78, 217–228. <https://doi.org/10.1016/J.BIOCEL.2016.07.012>
- De La Cruz Diaz, J. S., & Kaplan, D. H. (2019). Langerhans Cells Spy on Keratinocytes. *The Journal of Investigative Dermatology*, 139(11), 2260. <https://doi.org/10.1016/J.JID.2019.06.120>
- Divkovic, M., Pease, C. K., Gerberick, G. F., & Basketter, D. A. (2005). Hapten-protein binding: from theory to practical application in

- the in vitro prediction of skin sensitization. *Contact Dermatitis*, 53(4), 189–200. <https://doi.org/10.1111/j.0105-1873.2005.00683.x>
- Dmello, C., Srivastava, S. S., Tiwari, R., Chaudhari, P. R., Sawant, S., & Vaidya, M. M. (2019). Multifaceted role of keratins in epithelial cell differentiation and transformation. *Journal of Biosciences*, 44(2), 1–16. <https://doi.org/10.1007/S12038-019-9864-8/FIGURES/4>
- Driskell, R. R., Lichtenberger, B. M., Hoste, E., Kretzschmar, K., Simons, B. D., Charalambous, M., Ferron, S. R., Heralut, Y., Pavlovic, G., Ferguson-Smith, A. C., & Watt, F. M. (2013). Distinct fibroblast lineages determine dermal architecture in skin development and repair. *Nature*, 504(7479), 277. <https://doi.org/10.1038/NATURE12783>
- Duval, C., Chagnoleau, C., Pouradier, F., Sextius, P., Condom, E., & Bernerd, F. (2012). Human skin model containing melanocytes: essential role of keratinocyte growth factor for constitutive pigmentation-functional response to  $\alpha$ -melanocyte stimulating hormone and forskolin. *Tissue Engineering. Part C, Methods*, 18(12), 947–957. <https://doi.org/10.1089/ten.TEC.2011.0676>
- El Ali, Z., Gerbeix, C., Hemon, P., Esser, P. R., Martin, S. F., Pallardy, M., & Kerdine-Römer, S. (2013). *Allergic Skin Inflammation Induced by Chemical Sensitizers Is Controlled by the Transcription Factor Nrf2*. <https://doi.org/10.1093/toxsci/kft084>
- Elahi, E. N., Wright, Z., Hinselwood, D., Hotchkiss, S. A. M., Basketter, D. A., & Pease, C. K. S. (2004). Protein binding and metabolism influence the relative skin sensitization potential of cinnamic compounds. *Chemical Research in Toxicology*, 17(3), 301–310. <https://doi.org/10.1021/TX0341456>
- Elias, P. M., Ahn, S. K., Brown, B. E., Crumrine, D., & Feingold, K. R. (2002). Origin of the epidermal calcium gradient: regulation by barrier status and role of active vs passive mechanisms. *The Journal of Investigative Dermatology*, 119(6), 1269–1274. <https://doi.org/10.1046/J.1523-1747.2002.19622.X>
- Engel, M. A., Leffler, A., Niedermirtl, F., Babes, A., Zimmermann, K., Filipovi, M. R., Izydorczyk, I., Eberhardt, M., Kichko, T. I., Muellertribbensee, S. M., Khalil, M., Siklosi, N., Nau, C., Ivanoviburmazovi, I., Neuhuber, W. L., Becker, C., Neurath, M. F., & Reeh, P. W. (2011). TRPA1 and substance P mediate colitis in mice. *Gastroenterology*, 141(4), 1346–1358. <https://doi.org/10.1053/J.GASTRO.2011.07.002>
- Engelhart, K., El Hindi, T., Biesalski, H. K., & Pfitzner, I. (2005). In vitro reproduction of clinical hallmarks of eczematous dermatitis in organotypic skin models. *Archives of Dermatological Research*, 297(1), 1–9. <https://doi.org/10.1007/s00403-005-0575-7>
- Erdogmus, S., Concepcion, A. R., Yamashita, M., Sidhu, I., Tao, A. Y., Li, W., Rocha, P. P., Huang, B., Garippa, R., Lee, B., Lee, A., Hell, J. W., Lewis, R. S., Prakriya, M., & Feske, S. (2022). Cav $\beta$ 1 regulates T cell expansion and apoptosis independently of voltage-gated Ca $^{2+}$  channel function. *Nature Communications* 2022 13:1, 13(1), 1–19. <https://doi.org/10.1038/s41467-022-29725-3>
- Eriksson, K., Nordström, I., Czerkinsky, C., & Holmgren, J. (2000). Differential effect of cholera toxin on CD45RA $^{+}$  and CD45RO $^{+}$  T cells: specific inhibition of cytokine production but not proliferation of human naive T cells. *Clinical and Experimental Immunology*, 121(2), 283–288. <https://doi.org/10.1046/J.1365-2249.2000.01282.X>
- Erkes, D. A., & Selvan, S. R. (2014). Hapten-induced contact hypersensitivity, autoimmune reactions, and tumor regression: plausibility of mediating antitumor immunity. *J Immunol Res*, 2014, 175265. <https://doi.org/10.1155/2014/175265>
- Farage, M. A. (2019). The Prevalence of Sensitive Skin. *Frontiers in Medicine*, 6, 456643. <https://doi.org/10.3389/FMED.2019.00098/BIBTEX>
- Fischer, H. J., Sie, C., Schumann, E., Witte, A.-K., Dressel, R., van den Brandt, J., & Reichardt, H. M. (2017). The Insulin Receptor Plays a Critical Role in T Cell Function and Adaptive Immunity. *Journal of Immunology (Baltimore, Md. : 1950)*, 198(5), 1910–1920. <https://doi.org/10.4049/JIMMUNOL.1601011>
- Frombach, J., Sonnenburg, A., Krapohl, B.-D., Zuberbier, T., Peiser, M., Stahlmann, R., & Schreiner, M. (2018). Lymphocyte surface markers and cytokines are suitable for detection and potency assessment of skin-sensitizing chemicals in an in vitro model of allergic contact dermatitis: the LCSA-Iy. *Archives of Toxicology*, 92(4), 1495–1505. <https://doi.org/10.1007/s00204-018-2164-5>
- Fusenig, N. E., Limat, A., Stakr, H. J., & Breitkreutz, D. (1994). Modulation of the differentiated phenotype of keratinocytes of the hair follicle and from epidermis. *Journal of Dermatological Science*, 7(SUPPL. 1). [https://doi.org/10.1016/0923-1811\(94\)90045-0](https://doi.org/10.1016/0923-1811(94)90045-0)
- Galbiati, V., Gibbs, S., Roggen, E., & Corsini, E. (2018). Development of an In Vitro Method to Estimate the Sensitization Induction Level of Contact Allergens. *Current Protocols in Toxicology*, 75(1), 20.15.1-20.15.20. <https://doi.org/10.1002/cptx.44>
- Galbiati, V., Maddalon, A., Iulini, M., Marinovich, M., & Corsini, E. (2020). Human keratinocytes and monocytes co-culture cell system: An important contribution for the study of moderate and weak sensitizers. *Toxicology in Vitro*, 68. <https://doi.org/10.1016/j.tiv.2020.104929>

- Galbiati, V., Papale, A., Marinovich, M., Gibbs, S., Roggen, E., & Corsini, E. (2017). Development of an in vitro method to estimate the sensitization induction level of contact allergens. *Toxicology Letters*, 271, 1–11. <https://doi.org/10.1016/J.TOXLET.2017.01.016>
- Gallego, C., Vétillard, M., Calmette, J., Roriz, M., Marin-Esteban, V., Evrard, M., Aknin, M. L., Pionnier, N., Lefrançois, M., Mercier-Nomé, F., Bertrand, Y., Suarez, F., Donadieu, J., Ng, L. G., Balabanian, K., Bachelerie, F., & Schlecht-Louf, G. (2021). CXCR4 signaling controls dendritic cell location and activation at steady state and in inflammation. *Blood*, 137(20), 2770–2784. <https://doi.org/10.1182/BLOOD.2020006675>
- Ganier, C., Rognoni, E., Goss, G., Lynch, M., & Watt, F. M. (2022). Fibroblast Heterogeneity in Healthy and Wounded Skin. *Cold Spring Harbor Perspectives in Biology*, a041238. <https://doi.org/10.1101/cshperspect.a041238>
- Gdula, M. R., Poterlowicz, K., Mardaryev, A. N., Sharov, A. A., Peng, Y., Fessing, M. Y., & Botchkarev, V. A. (2013). Remodeling of Three-Dimensional Organization of the Nucleus during Terminal Keratinocyte Differentiation in the Epidermis. *Journal of Investigative Dermatology*, 133(9), 2191–2201. <https://doi.org/10.1038/JID.2013.66>
- Geisendörfer, B. (2022). *Autologer Ansatz zur Entwicklung von 2D- und 3D-Kokultivierungsmethoden für die Bestimmung des sensibilisierenden Potenzials von Xenobiotika* (Issue April) [Universität Potsdam]. <https://publishup.uni-potsdam.de/frontdoor/index/index/docId/56778>
- Geissmann, F., Prost, C., Monnet, J. P., Dy, M., Brousse, N., & Hermine, O. (1998). Transforming growth factor beta1, in the presence of granulocyte/macrophage colony-stimulating factor and interleukin 4, induces differentiation of human peripheral blood monocytes into dendritic Langerhans cells. *The Journal of Experimental Medicine*, 187(6), 961–966. <https://doi.org/10.1084/jem.187.6.961>
- Gerberick, G. F., Ryan, C. A., Dearman, R. J., & Kimber, I. (2007). Local lymph node assay (LLNA) for detection of sensitization capacity of chemicals. *Methods (San Diego, Calif.)*, 41(1), 54–60. <https://doi.org/10.1016/j.ymeth.2006.07.006>
- Gerberick, G. F., Ryan, C. A., Kern, P. S., Dearman, R. J., Kimber, I., Patlewicz, G. Y., & Basketter, D. A. (2004). A chemical dataset for evaluation of alternative approaches to skin-sensitization testing. *Contact Dermatitis*, 50(5), 274–288. <https://doi.org/10.1111/j.0105-1873.2004.00290.x>
- Gerberick, G. F., Troutman, J. A., Foertsch, L. M., Vassallo, J. D., Quijano, M., Dobson, R. L. M., Goebel, C., & Lepoittevin, J.-P. (2009). Investigation of peptide reactivity of pro-hapten skin sensitizers using a peroxidase-peroxide oxidation system. *Toxicological Sciences : An Official Journal of the Society of Toxicology*, 112(1), 164–174. <https://doi.org/10.1093/toxsci/kfp192>
- Ghio, S. C., Cantin-Warren, L., Guignard, R., Larouche, D., & Germain, L. (2018). Are the effects of the cholera toxin and isoproterenol on human keratinocytes' proliferative potential dependent on whether they are co-cultured with human or murine fibroblast feeder layers? *International Journal of Molecular Sciences*, 19(8). <https://doi.org/10.3390/ijms19082174>
- Gibbs, S., Spiekstra, S., Corsini, E., McLeod, J., & Reinders, J. (2013). Dendritic cell migration assay: a potential prediction model for identification of contact allergens. *Toxicology in Vitro : An International Journal Published in Association with BIBRA*, 27(3), 1170–1179. <https://doi.org/10.1016/j.tiv.2012.05.016>
- Glaczynska, M., MacHcinska, M., & Donskow-Lysoniewska, K. (2021). Effects of Different Media on Human T Regulatory Cells Phenotype. *In Vivo*, 35(1), 283. <https://doi.org/10.21873/INVIVO.12257>
- Goebeler, M., Trautmann, A., Voss, A., Bröcker, E. B., Toksoy, A., & Gillitzer, R. (2001). Differential and sequential expression of multiple chemokines during elicitation of allergic contact hypersensitivity. *American Journal of Pathology*, 158(2), 431–440. [https://doi.org/10.1016/S0002-9440\(10\)63986-7](https://doi.org/10.1016/S0002-9440(10)63986-7)
- Golden, E., Macmillan, D. S., Dameron, G., Kern, P., Hartung, T., & Maertens, A. (2021). Evaluation of the Global Performance of Eight In Silico Skin Sensitization Models Using Human Data. *Altex*, 38(1), 33–48. <https://doi.org/10.14573/altex.1911261>
- Goletz, S., Zillikens, D., & Schmidt, E. (2017). Structural proteins of the dermal-epidermal junction targeted by autoantibodies in pemphigoid diseases. *Experimental Dermatology*, 26(12), 1154–1162. <https://doi.org/10.1111/EXD.13446>
- Gomes, R. N., Manuel, F., & Nascimento, D. S. (2021). The bright side of fibroblasts: molecular signature and regenerative cues in major organs. *Npj Regenerative Medicine* 2021 6:1, 6(1), 1–12. <https://doi.org/10.1038/s41536-021-00153-z>
- Goyer, B., Larouche, D., Kim, D. H., Veillette, N., Pruneau, V., Bernier, V., Auger, F. A., & Germain, L. (2019). Immune tolerance of tissue-engineered skin produced with allogeneic or xenogeneic fibroblasts and syngeneic keratinocytes grafted on mice. *Acta Biomaterialia*, 90, 192–204. <https://doi.org/10.1016/J.ACTBIO.2019.04.010>
- Griffin, M. F., desJardins-Park, H. E., Mascharak, S., Borrelli, M. R., & Longaker, M. T. (2020). Understanding the impact of fibroblast

- heterogeneity on skin fibrosis. *DMM Disease Models and Mechanisms*, 13(6). <https://doi.org/10.1242/DMM.044164/225248>
- Griffoni, C., Neidhart, B., Yang, K., Groeber-Becker, F., Maniura-Weber, K., Dandekar, T., Walles, H., & Rottmar, M. (2021). In vitro skin culture media influence the viability and inflammatory response of primary macrophages. *Scientific Reports* 2021 11:1, 11(1), 1–11. <https://doi.org/10.1038/s41598-021-86486-7>
- Grosche, L., Knippertz, I., König, C., Royzman, D., Wild, A. B., Zinser, E., Sticht, H., Müller, Y. A., Steinkasserer, A., & Lechmann, M. (2020). The CD83 Molecule – An Important Immune Checkpoint. *Frontiers in Immunology*, 11. <https://doi.org/10.3389/FIMMU.2020.00721/FULL>
- Gunin, A. G., & Golubtzova, N. N. (2019). Transforming Growth Factor- $\beta$  (TGF- $\beta$ ) in Human Skin during Aging. *Advances in Gerontology*, 9(3), 267–273. <https://doi.org/10.1134/S2079057019030068/FIGURES/4>
- Gutowska-Owsiak, D., Podobas, E. I., Eggeling, C., Ogg, G. S., & Bernardino de la Serna, J. (2020). Addressing Differentiation in Live Human Keratinocytes by Assessment of Membrane Packing Order. *Frontiers in Cell and Developmental Biology*, 8, 573230. <https://doi.org/10.3389/FCELL.2020.573230/BIBTEX>
- Guttman-Yassky, E., & Krueger, J. G. (2017). Atopic dermatitis and psoriasis: two different immune diseases or one spectrum? *Current Opinion in Immunology*, 48, 68–73. <https://doi.org/10.1016/j.coi.2017.08.008>
- Hansson, C., Ezzelarab, M., & Sterner, O. (1995). Oxidative activation of the propolis hapten isoprenyl caffeate. *Acta Dermatovenereologica*, 75(1), 34–36. <https://doi.org/10.2340/0001555753436>
- Hemmi, H., Yoshino, M., Yamazaki, H., Naito, M., Iyoda, T., Omatsu, Y., Shimoyama, S., Letterio, J. J., Nakabayashi, T., Tagaya, H., Yamane, T., Ogawa, M., Nishikawa, S. I., Ryoike, K., Inaba, K., Hayashi, S. I., & Kunisada, T. (2001). Skin antigens in the steady state are trafficked to regional lymph nodes by transforming growth factor- $\beta$ 1-dependent cells. *International Immunology*, 13(5), 695–704. <https://doi.org/10.1093/intimm/13.5.695>
- Hennen, J., Aeby, P., Goebel, C., Schettgen, T., Oberli, A., Kalmes, M., & Blömeke, B. (2011). Cross talk between keratinocytes and dendritic cells: impact on the prediction of sensitization. *Toxicological Sciences: An Official Journal of the Society of Toxicology*, 123(2), 501–510. <https://doi.org/10.1093/toxsci/kfr174>
- Hiasa, M., Abe, M., Nakano, A., Oda, A., Amou, H., Kido, S., Takeuchi, K., Kagawa, K., Yata, K., Hashimoto, T., Ozaki, S., Asaoka, K., Tanaka, E., Moriyama, K., & Matsumoto, T. (2009). GM-CSF and IL-4 induce dendritic cell differentiation and disrupt osteoclastogenesis through M-CSF receptor shedding by up-regulation of TNF- $\alpha$  converting enzyme (TACE). *Blood*, 114(20), 4517–4526. <https://doi.org/10.1182/BLOOD-2009-04-215020>
- Hill, M., & Cuturi, M. C. (2010). Negative vaccination by tolerogenic dendritic cells in organ transplantation. *Current Opinion in Organ Transplantation*, 15(6), 738–743. <https://doi.org/10.1097/MOT.0b013e32833f7114>
- Ho, A. W., & Kupper, T. S. (2019). T cells and the skin: from protective immunity to inflammatory skin disorders. *Nature Reviews Immunology* 2019 19:8, 19(8), 490–502. <https://doi.org/10.1038/s41577-019-0162-3>
- Hollister, J. R., & Jarrett, C. E. W. (1978). Monocyte enhancement of mitogen-induced lymphocyte proliferation in a human co-culture system. *Cellular Immunology*, 41(2), 330–337. [https://doi.org/10.1016/0008-8749\(78\)90230-7](https://doi.org/10.1016/0008-8749(78)90230-7)
- Hommel, M., & Kyewski, B. (2003). Dynamic Changes During the Immune Response in T Cell–Antigen-presenting Cell Clusters Isolated from Lymph Nodes. *Journal of Experimental Medicine*, 197(3), 269–280. <https://doi.org/10.1084/JEM.20021512>
- Hotchin, N. A., Gandarillas, A., & Watt, F. M. (1995). Regulation of cell surface beta 1 integrin levels during keratinocyte terminal differentiation. *The Journal of Cell Biology*, 128(6), 1209–1219. <https://doi.org/10.1083/jcb.128.6.1209>
- Hou, F., Xing, C., Li, B., Cheng, J., & Chen, W. (2020). Performance of a novel in vitro assay for skin sensitization based on activation of T lymphocytes. *ALTEX*, 37(3), 451–468. <https://doi.org/10.14573/altex.2001312>
- Huang, X., Huang, Z., Gao, W., Gao, W., He, R., Li, Y., Crawford, R., Zhou, Y., Xiao, L., & Xiao, Y. (2022). Current Advances in 3D Dynamic Cell Culture Systems. *Gels* 2022, Vol. 8, Page 829, 8(12), 829. <https://doi.org/10.3390/GELS8120829>
- Humeau, M., Boniface, K., & Bodet, C. (2022). Cytokine-Mediated Crosstalk Between Keratinocytes and T Cells in Atopic Dermatitis. *Frontiers in Immunology*, 13, 801579. <https://doi.org/10.3389/FIMMU.2022.801579/BIBTEX>
- Hunger, R. E., Sieling, P. A., Ochoa, M. T., Sugaya, M., Burdick, A. E., Rea, T. H., Brennan, P. J., Belisle, J. T., Blauvelt, A., Porcelli, S. A., & Modlin, R. L. (2004). Langerhans cells utilize CD1a and langerin to efficiently present nonpeptide antigens to T cells. *Journal of Clinical Investigation*, 113(5), 701–708. <https://doi.org/10.1172/JCI200419655>
- Ishibashi, T., Takumida, M., Akagi, N., Hirakawa, K., & Anniko, M. (2008). Expression of transient receptor potential vanilloid (TRPV) 1, 2, 3, and 4 in mouse inner ear. *Acta Oto-Laryngologica*, 128(12), 1286–1293. <https://doi.org/10.1080/00016480801938958>

- Itoh, M., Umegaki-Arao, N., Guo, Z., Liu, L., Higgins, C. A., & Christiano, A. M. (2013). Generation of 3D Skin Equivalents Fully Reconstituted from Human Induced Pluripotent Stem Cells (iPSCs). *PLoS ONE*, *8*(10).  
<https://doi.org/10.1371/journal.pone.0077673>
- Jacobs, J. J. L. L., Lehe, C. L., Hasegawa, H., Elliott, G. R., & Das, P. K. (2006). Skin irritants and contact sensitizers induce Langerhans cell migration and maturation at irritant concentration. *Experimental Dermatology*, *15*(6), 432–440.  
<https://doi.org/10.1111/j.0906-6705.2006.00420.x>
- Jaleco, S., Swainson, L., Dardalhon, V., Burjanadze, M., Kinet, S., & Taylor, N. (2003). Homeostasis of Naive and Memory CD4+ T Cells: IL-2 and IL-7 Differentially Regulate the Balance Between Proliferation and Fas-Mediated Apoptosis. *The Journal of Immunology*, *171*(1), 61–68. <https://doi.org/10.4049/JIMMUNOL.171.1.61>
- Janson, D., Saintigny, G., Mahé, C., & Ghalbzouri, A. El. (2013). Papillary fibroblasts differentiate into reticular fibroblasts after prolonged in vitro culture. *Experimental Dermatology*, *22*(1), 48–53. <https://doi.org/10.1111/exd.12069>
- Jenkinson, C., Jenkins, R. E., Aleksic, M., Pirmohamed, M., Naisbitt, D. J., & Park, B. K. (2010). Characterization of p-Phenylenediamine–Albumin Binding Sites and T-Cell Responses to Hapten-Modified Protein. *Journal of Investigative Dermatology*, *130*(3), 732–742. <https://doi.org/10.1038/jid.2009.271>
- Jiang, Y., Tsoi, L. C., Billi, A. C., Ward, N. L., Harms, P. W., Zeng, C., Maverakis, E., Kahlenberg, J. M., & Gudjonsson, J. E. (2020). Cytokines: the diverse contribution of keratinocytes to immune responses in skin. *JCI Insight*, *5*(20).  
<https://doi.org/10.1172/jci.insight.142067>
- Joglekar, A. V., & Li, G. (2021). T cell antigen discovery. *Nature Methods*, *18*(8), 873–880. <https://doi.org/10.1038/S41592-020-0867-Z>
- Johnson, C., Ahlberg, E., Anger, L. T., Beilke, L., Benigni, R., Bercu, J., Bobst, S., Bower, D., Brigo, A., Campbell, S., Cronin, M. T. D., Crooks, I., Cross, K. P., Doktorova, T., Exner, T., Faulkner, D., Fearon, I. M., Fehr, M., Gad, S. C., ... Myatt, G. J. (2020). Skin sensitization in silico protocol. *Regulatory Toxicology and Pharmacology : RTP*, *116*, 104688.  
<https://doi.org/10.1016/J.YRTPH.2020.104688>
- Joshi, R. S. (2011). The Inner Root Sheath and the Men Associated with it Eponymically. *International Journal of Trichology*, *3*(1), 57.  
<https://doi.org/10.4103/0974-7753.82119>
- Joulai Veijouye, S., Yari, A., Heidari, F., Sajedi, N., Ghoroghi Moghani, F., & Nobakht, M. (2017). Bulge Region as a Putative Hair Follicle Stem Cells Niche: A Brief Review. *Iranian Journal of Public Health*, *46*(9), 1167. /pmc/articles/PMC5632317/
- Kadler, K. E., Baldock, C., Bella, J., & Boot-Handford, R. P. (2007). Collagens at a glance. *Journal of Cell Science*, *120*(Pt 12), 1955–1958.  
<https://doi.org/10.1242/jcs.03453>
- Kageyama, T., Seo, J., Yan, L., & Fukuda, J. (2023). Effects of oxytocin on the hair growth ability of dermal papilla cells. *Scientific Reports*, *13*(1), 1–8. <https://doi.org/10.1038/s41598-023-40521-x>
- Karamanos, N. K., Theocharis, A. D., Piperigkou, Z., Manou, D., Passi, A., Skandalis, S. S., Vynios, D. H., Orian-Rousseau, V., Ricard-Blum, S., Schmelzer, C. E. H., Duca, L., Durbeej, M., Afratis, N. A., Troeberg, L., Franchi, M., Masola, V., & Onisto, M. (2021). A guide to the composition and functions of the extracellular matrix. *FEBS Journal*, *288*(24), 6850–6912.  
<https://doi.org/10.1111/febs.15776>
- Karlberg, A. T., Börje, A., Duus Johansen, J., Lidén, C., Rastogi, S., Roberts, D., Uter, W., & White, I. R. (2013). Activation of non-sensitizing or low-sensitizing fragrance substances into potent sensitizers – prehaptens and prohaptens. *Contact Dermatitis*, *69*(6), 323–334. <https://doi.org/10.1111/COD.12127>
- Kathamuthu, G. R., Sridhar, R., Baskaran, D., & Babu, S. (2022). Dominant expansion of CD4+, CD8+ T and NK cells expressing Th1/Tc1/Type 1 cytokines in culture-positive lymph node tuberculosis. *PLOS ONE*, *17*(5), e0269109.  
<https://doi.org/10.1371/JOURNAL.PONE.0269109>
- Kel, J. M., Girard-Madoux, M. J. H., Reizis, B., & Clausen, B. E. (2010). TGF-beta is required to maintain the pool of immature Langerhans cells in the epidermis. *Journal of Immunology (Baltimore, Md. : 1950)*, *185*(6), 3248–3255.  
<https://doi.org/10.4049/jimmunol.1000981>
- Kessner, D., Kiselev, M., Dante, S., Hauß, T., Lersch, P., Wartewig, S., & Neubert, R. H. H. (2008). Arrangement of ceramide [EOS] in a stratum corneum lipid model matrix: New aspects revealed by neutron diffraction studies. *European Biophysics Journal*, *37*(6), 989–999. <https://doi.org/10.1007/s00249-008-0328-6>
- Kiani, M. T., Higgins, C. A., & Almquist, B. D. (2018). The Hair Follicle: An Underutilized Source of Cells and Materials for Regenerative Medicine. *ACS Biomaterials Science and Engineering*, *4*(4), 1193–1207. <https://doi.org/10.1021/acsbomaterials.7b00072>

- Kiesewetter, F., Arai, A., & Schell, H. (1993). Sex hormones and antiandrogens influence in vitro growth of dermal papilla cells and outer root sheath keratinocytes of human hair follicles. *The Journal of Investigative Dermatology*, *101*(1 Suppl), 98S-105S. <https://doi.org/10.1111/1523-1747.ep12363015>
- Kim, J. J., Ellett, F., Thomas, C. N., Jalali, F., Anderson, R. R., Irimia, D., & Raff, A. B. (2019). A microscale, full-thickness, human skin on a chip assay simulating neutrophil responses to skin infection and antibiotic treatments. *Lab on a Chip*, *19*(18), 3094–3103. <https://doi.org/10.1039/C9LC00399A>
- Kim, Y. J., Choi, M. J., Bak, D. H., Lee, B. C., Ko, E. J., Ahn, G. R., Ahn, S. W., Kim, M. J., Na, J., & Kim, B. J. (2018). Topical administration of EGF suppresses immune response and protects skin barrier in DNCB-induced atopic dermatitis in NC/Nga mice. *Scientific Reports* *2018* *8*:1, *8*(1), 1–11. <https://doi.org/10.1038/s41598-018-30404-x>
- Kimber, I., Basketter, D. A., Butler, M., Gamer, A., Garrigue, J. L., Gerberick, G. F., Newsome, C., Steiling, W., & Vohr, H. W. (2003). Classification of contact allergens according to potency: proposals. *Food and Chemical Toxicology*, *41*(12), 1799–1809. [https://doi.org/10.1016/S0278-6915\(03\)00223-0](https://doi.org/10.1016/S0278-6915(03)00223-0)
- Kimber, I., Mitchell, J. A., & Griffin, A. C. (1986). Development of a murine local lymph node assay for the determination of sensitizing potential. *Food and Chemical Toxicology*, *24*(6–7), 585–586. [https://doi.org/10.1016/0278-6915\(86\)90124-9](https://doi.org/10.1016/0278-6915(86)90124-9)
- Kitala, D., Kaweckı, M., Klama-Baryła, A., ıbuś, W., Kraut, M., Glik, J., Ryszkiel, I., Kaweckı, M. P., & Nowak, M. (2016). Allogeneic vs. Autologous Skin Grafts in the Therapy of Patients with Burn Injuries: A Restrospective, Open-label Clinical Study with Pair Matching. *Advances in Clinical and Experimental Medicine : Official Organ Wroclaw Medical University*, *25*(5), 923–929. <https://doi.org/10.17219/ACEM/61961>
- Klein, R. H., Lin, Z., Hopkin, A. S., Gordon, W., Tsoi, L. C., Liang, Y., Gudjonsson, J. E., & Andersen, B. (2017). GRHL3 binding and enhancers rearrange as epidermal keratinocytes transition between functional states. *PLOS Genetics*, *13*(4), e1006745. <https://doi.org/10.1371/JOURNAL.PGEN.1006745>
- Klicznik, M. M., Szenes-Nagy, A. B., Campbell, D. J., & Gratz, I. K. (2018). Taking the lead – how keratinocytes orchestrate skin T cell immunity. *Immunology Letters*, *200*, 43. <https://doi.org/10.1016/J.IMLET.2018.06.009>
- Kligys, K. R., Wu, Y., Hopkinson, S. B., Kaur, S., Platanias, L. C., & Jones, J. C. R. (2012).  $\alpha 6 \beta 4$  Integrin, a Master Regulator of Expression of Integrins in Human Keratinocytes. *The Journal of Biological Chemistry*, *287*(22), 17975. <https://doi.org/10.1074/JBC.M111.310458>
- Koh, S. K., Park, J., Kim, S.-E., Lim, Y., Phan, M.-T. T., Kim, J., Hwang, I., Ahn, Y.-O., Shin, S., Doh, J., & Cho, D. (2022). Natural Killer Cell Expansion and Cytotoxicity Differ Depending on the Culture Medium Used. *Annals of Laboratory Medicine*, *42*(6), 638–649. <https://doi.org/10.3343/alm.2022.42.6.638>
- Korosec, A., Frech, S., Gesslbauer, B., Vierhapper, M., Radtke, C., Petzelbauer, P., & Lichtenberger, B. M. (2019). Lineage Identity and Location within the Dermis Determine the Function of Papillary and Reticular Fibroblasts in Human Skin. *Journal of Investigative Dermatology*, *139*(2), 342–351. <https://doi.org/10.1016/j.jid.2018.07.033>
- Koster, M. I. M. I., Kim, S., Mills, A. A. A., DeMayo, F. J. F. J., & Roop, D. R. D. R. (2004). p63 is the molecular switch for initiation of an epithelial stratification program. *Genes & Development*, *18*(2), 126. <https://doi.org/10.1101/GAD.1165104>
- Kouwenhoven, E. N., Oti, M., Niehues, H., van Heeringen, S. J., Schalkwijk, J., Stunnenberg, H. G., van Bokhoven, H., & Zhou, H. (2015). Transcription factor p63 bookmarks and regulates dynamic enhancers during epidermal differentiation. *EMBO Reports*, *16*(7), 863–878. <https://doi.org/10.15252/embr.201439941>
- Koyama-Nasu, R., Wang, Y., Hasegawa, I., Endo, Y., Nakayama, T., & Kimura, M. Y. (2022). The cellular and molecular basis of CD69 function in anti-tumor immunity. *International Immunology*, *34*(11), 555–561. <https://doi.org/10.1093/INTIMM/DXAC024>
- Krebsbach, P. H., & Villa-Diaz, L. G. (2017). The Role of Integrin  $\alpha 6$  (CD49f) in Stem Cells: More than a Conserved Biomarker. *Stem Cells and Development*, *26*(15), 1090. <https://doi.org/10.1089/SCD.2016.0319>
- Küchler, S., Henkes, D., Eckl, K. M., Ackermann, K., Plendl, J., Korting, H. C., Hennies, H. C., & Schäfer-Korting, M. (2011). Hallmarks of atopic skin mimicked in vitro by means of a skin disease model based on FLG knock-down. *Alternatives to Laboratory Animals : ATLA*, *39*(5), 471–480. <https://doi.org/10.1177/026119291103900508>
- Kühbacher, A., Henkel, H., Stevens, P., Grumaz, C., Finkemeier, D., Burger-Kentischer, A., Sohn, K., & Rupp, S. (2017). Central Role for Dermal Fibroblasts in Skin Model Protection against *Candida albicans*. *The Journal of Infectious Diseases*, *215*(11), 1742–1752. <https://doi.org/10.1093/infdis/jix153>
- Kusharyoto, W., Pleiss, J., Bachmann, T. T., & Schmid, R. D. (2002). Mapping of a hapten-binding site: molecular modeling and site-

- directed mutagenesis study of an anti-atrazine antibody. *Protein Engineering, Design and Selection*, 15(3), 233–241.  
<https://doi.org/10.1093/PROTEIN/15.3.233>
- Kwak, B. S., Jin, S.-P., Kim, S. J., Kim, E. J., Chung, J. H., & Sung, J. H. (2020). Microfluidic skin chip with vasculature for recapitulating the immune response of the skin tissue. *Biotechnology and Bioengineering*, 117(6), 1853–1863.  
<https://doi.org/10.1002/bit.27320>
- Larbi, A., & Fulop, T. (2014). From “truly naïve” to “exhausted senescent” T cells: When markers predict functionality. *Cytometry Part A*, 85(1), 25–35. <https://doi.org/10.1002/cyto.a.22351>
- Larjava, H., Peltonen, J., Akiyama, S. K., Yamada, S. S., Gralnick, H. R., Uitto, J., & Yamada, K. M. (1990). Novel function for beta 1 integrins in keratinocyte cell-cell interactions. *The Journal of Cell Biology*, 110(3), 803–815.  
<https://doi.org/10.1083/JCB.110.3.803>
- Laubach, V., Zöller, N., Rossberg, M., Görg, K., Kippenberger, S., Bereiter-Hahn, J., Kaufmann, R., & Bernd, A. (2011). Integration of Langerhans-like cells into a human skin equivalent. *Archives of Dermatological Research*, 303(2), 135–139.  
<https://doi.org/10.1007/s00403-010-1092-x>
- le Riche, A., Aberdam, E., Marchand, L., Frank, E., Jahoda, C., Petit, I., Bordes, S., Closs, B., & Aberdam, D. (2019). Extracellular Vesicles from Activated Dermal Fibroblasts Stimulate Hair Follicle Growth Through Dermal Papilla-Secreted Norrin. *Stem Cells*, 37(9), 1166–1175. <https://doi.org/10.1002/STEM.3043>
- Lee, C.-H., Hong, C.-H., Yu, C.-L., Wang, L.-F., Clausen, B. E., Liao, W.-T., Huang, S.-K., Chen, G.-S., & Yu, H.-S. (2012). Arsenic mobilizes Langerhans cell migration and induces Th1 response in epicutaneous protein sensitization via CCL21: a plausible cause of decreased Langerhans cells in arsenic-induced intraepithelial carcinoma. *Biochemical Pharmacology*, 83(9), 1290–1299.  
<https://doi.org/10.1016/j.bcp.2012.01.028>
- Lee, J. S., Kim, J., Cui, B., Kim, S. K., Cho, S.-A., An, S., & Cho, S.-W. (2022). Hybrid skin chips for toxicological evaluation of chemical drugs and cosmetic compounds. *Lab on a Chip*, 22(2), 343–353. <https://doi.org/10.1039/d1lc00550b>
- Lee, J. U., Kim, L. K., & Choi, J. M. (2018). Revisiting the concept of targeting NFAT to control T cell immunity and autoimmune diseases. *Frontiers in Immunology*, 9(NOV), 422248. <https://doi.org/10.3389/FIMMU.2018.02747/BIBTEX>
- Lemus, R., & Karol, M. H. (1985). Conjugation of haptens. *Laboratory Techniques in Biochemistry and Molecular Biology*, 15(C), 279–296. [https://doi.org/10.1016/S0075-7535\(08\)70142-6](https://doi.org/10.1016/S0075-7535(08)70142-6)
- Lenoir-Viale, M. C., Galup, C., Darmon, M., & Bernard, B. A. (1993). Epidermis reconstructed from the outer root sheath of human hair follicle. Effect of retinoic acid. *Archives of Dermatological Research*, 285(4), 197–204.  
<https://doi.org/10.1007/BF00372009>
- Levy, L., Broad, S., Diekmann, D., Evans, R. D., & Watt, F. M. (2000).  $\beta$ 1 Integrins regulate keratinocyte adhesion and differentiation by distinct mechanisms. *Molecular Biology of the Cell*, 11(2), 453–466.  
<https://doi.org/10.1091/MBC.11.2.453/ASSET/IMAGES/LARGE/MK0201107007.JPEG>
- Li, J., Chen, S., Li, Y., Zhu, Z., Huang, H., Wang, W., Yang, Y., Liang, Y., & Shu, L. (2022). Comprehensive Profiling Analysis of CD209 in Malignancies Reveals the Therapeutic Implication for Tumor Patients Infected With SARS-CoV-2. *Frontiers in Genetics*, 13, 883234. <https://doi.org/10.3389/FGENE.2022.883234/BIBTEX>
- Li, Z., Ju, X., Silveira, P. A., Abadir, E., Hsu, W. H., Hart, D. N. J., & Clark, G. J. (2019). CD83: Activation marker for antigen presenting cells and its therapeutic potential. *Frontiers in Immunology*, 10(JUN), 460131.  
<https://doi.org/10.3389/FIMMU.2019.01312/BIBTEX>
- Liarte, S., Bernabé-García, Á., & Nicolás, F. J. (2020). Role of TGF- $\beta$  in Skin Chronic Wounds: A Keratinocyte Perspective. *Cells*, 9(2).  
<https://doi.org/10.3390/CELLS9020306>
- Lim, J., Ng, K. J., & Clavel, C. (2019). Dermal papilla regulation of hair growth and pigmentation. In *Advances in Stem Cells and their Niches* (1st ed., Vol. 3). Elsevier Inc. <https://doi.org/10.1016/bs.asn.2019.06.002>
- Limat, A., Breitkreutz, D., Stark, H. J., Hunziker, T., Thikoetter, G., Noser, F., & Fusenig, N. E. (1991). Experimental modulation of the differentiated phenotype of keratinocytes from epidermis and hair follicle outer root sheath and matrix cells. *Annals of the New York Academy of Sciences*, 642(1), 125–146; discussion 146–7. <https://doi.org/10.1111/j.1749-6632.1991.tb24385.x>
- Limat, A., & Hunziker, T. (1996). Cultivation of keratinocytes from the outer root sheath of human hair follicles. *Methods Mol Med*, 2, 21–31. <https://doi.org/10.1385/0-89603-335-X:21>
- Limat, A., & Hunziker, T. (2002). Use of Epidermal Equivalents Generated from Follicular Outer Root Sheath Cells in vitro and for

- Autologous Grafting of Chronic Wounds. *Cells Tissues Organs*, 172(2), 79–85. <https://doi.org/10.1159/000065615>
- Llanos, E. J., Leal, W., Luu, D. H., Jost, J., Stadler, P. F., & Restrepo, G. (2019). Exploration of the chemical space and its three historical regimes. *Proceedings of the National Academy of Sciences of the United States of America*, 116(26), 12660–12665. [https://doi.org/10.1073/PNAS.1816039116/SUPPL\\_FILE/PNAS.1816039116.SAPP.PDF](https://doi.org/10.1073/PNAS.1816039116/SUPPL_FILE/PNAS.1816039116.SAPP.PDF)
- López-Cabrera, M., Santis, A. G., Fernández-Ruiz, E., Blacher, R., Esch, F., Sánchez-Mateos, P., & Sánchez-Madrid, F. (1993). Molecular cloning, expression, and chromosomal localization of the human earliest lymphocyte activation antigen AIM/CD69, a new member of the C-type animal lectin superfamily of signal-transmitting receptors. *Journal of Experimental Medicine*, 178(2), 537–547. <https://doi.org/10.1084/JEM.178.2.537>
- Löwa, A., Vogt, A., Kaessmeyer, S., & Hedtrich, S. (2018). Generation of full-thickness skin equivalents using hair follicle-derived primary human keratinocytes and fibroblasts. *Journal of Tissue Engineering and Regenerative Medicine*, 12(4), e2134–e2146. <https://doi.org/10.1002/term.2646>
- Lozano-Ojalvo, D., López-Fandiño, R., & López-Expósito, I. (2015). PBMC-Derived T Cells. *The Impact of Food Bioactives on Health: In Vitro and Ex Vivo Models*, 169–180. [https://doi.org/10.1007/978-3-319-16104-4\\_16](https://doi.org/10.1007/978-3-319-16104-4_16)
- Lu, H., Huang, D., Yao, K., Li, C., Chang, S., Dai, Y., Sun, A., Zou, Y., Qian, J., & Ge, J. (2015). Insulin enhances dendritic cell maturation and scavenger receptor-mediated uptake of oxidised low-density lipoprotein. *Journal of Diabetes and Its Complications*, 29(4), 465–471. <https://doi.org/10.1016/J.JDIACOMP.2015.03.005>
- Mahnke, Y. D., Brodie, T. M., Sallusto, F., Roederer, M., & Lugli, E. (2013). The who's who of T-cell differentiation: human memory T-cell subsets. *Eur J Immunol*, 43(11), 2797–2809. <https://doi.org/10.1002/eji.201343751>
- Maione, A. G., Brudno, Y., Stojadinovic, O., Park, L. K., Smith, A., Tellechea, A., Leal, E. C., Kearney, C. J., Veves, A., Tomic-Canic, M., Mooney, D. J., & Garlick, J. A. (2015). Three-Dimensional Human Tissue Models That Incorporate Diabetic Foot Ulcer-Derived Fibroblasts Mimic In Vivo Features of Chronic Wounds. *Tissue Engineering. Part C, Methods*, 21(5), 499. <https://doi.org/10.1089/TEN.TEC.2014.0414>
- Maney, N. J., Reynolds, G., Krippner-Heidenreich, A., & Hilkens, C. M. U. (2014). Dendritic cell maturation and survival are differentially regulated by TNFR1 and TNFR2. *Journal of Immunology (Baltimore, Md. : 1950)*, 193(10), 4914–4923. <https://doi.org/10.4049/JIMMUNOL.1302929>
- Mann, A., Breuhahn, K., Schirmacher, P., & Blessing, M. (2001). Keratinocyte-derived granulocyte-macrophage colony stimulating factor accelerates wound healing: Stimulation of keratinocyte proliferation, granulation tissue formation, and vascularization. *The Journal of Investigative Dermatology*, 117(6), 1382–1390. <https://doi.org/10.1046/j.0022-202x.2001.01600.x>
- Marchingo, J. M., Sinclair, L. V., Howden, A. J., & Cantrell, D. A. (2020). Quantitative analysis of how myc controls t cell proteomes and metabolic pathways during t cell activation. *ELife*, 9. <https://doi.org/10.7554/ELIFE.53725>
- Martel, J. L., Miao, J. H., & Badri, T. (2023). Anatomy, Hair Follicle. In *StatPearls*. StatPearls Publishing. <https://www.ncbi.nlm.nih.gov/books/NBK470321/>
- Martin, G., Guérard, S., Fortin, M. M. R., Rusu, D., Soucy, J., Poubelle, P. E., & Pouliot, R. (2012). Pathological crosstalk in vitro between T lymphocytes and lesional keratinocytes in psoriasis: Necessity of direct cell-to-cell contact. *Laboratory Investigation*, 92(7), 1058–1070. <https://doi.org/10.1038/labinvest.2012.69>
- Martinez-Sanchez, M. E., Huerta, L., Alvarez-Buylla, E. R., & Luján, C. V. (2018). Role of cytokine combinations on CD4+ T cell differentiation, partial polarization, and plasticity: Continuous network modeling approach. *Frontiers in Physiology*, 9(AUG), 339229. <https://doi.org/10.3389/FPHYS.2018.00877/BIBTEX>
- Martino, P. A., Heitman, N., & Rendl, M. (2021). The dermal sheath: An emerging component of the hair follicle stem cell niche. *Experimental Dermatology*, 30(4), 512–521. <https://doi.org/10.1111/EXD.14204>
- Matei, A. E., Chen, C. W., Kiesewetter, L., Györfi, A. H., Li, Y. N., Trinh-Minh, T., Xu, X., Tran Manh, C., Van Kuppevelt, T., Hansmann, J., Jüngel, A., Schett, G., Groeber-Becker, F., & Distler, J. H. W. (2019). Vascularised human skin equivalents as a novel in vitro model of skin fibrosis and platform for testing of antifibrotic drugs. *Annals of the Rheumatic Diseases*, 78(12), 1686–1692. <https://doi.org/10.1136/ANNRHEUMDIS-2019-216108>
- Matsui, T., & Amagai, M. (2015). Dissecting the formation, structure and barrier function of the stratum corneum. *International Immunology*, 27(6), 269–280. <https://doi.org/10.1093/INTIMM/DXV013>
- Matsuzawa, T., Nakano, M., Oikawa, A., Nakamura, Y., & Matsue, H. (2019). Three-Dimensional Epidermal Model from Human Hair Follicle-Derived Keratinocytes. In *Methods in molecular biology (Clifton, N.J.)* (Vol. 1993, pp. 123–137). Methods Mol Biol.

[https://doi.org/10.1007/978-1-4939-9473-1\\_10](https://doi.org/10.1007/978-1-4939-9473-1_10)

- Mayer, R. L. (1956). The significance of cross-links in the formation of hapten-carrier complexes. *International Archives of Allergy and Immunology*, 8(3), 115–129. <https://doi.org/10.1159/000228275>
- Maytin, E. V., Lin, J. C., Krishnamurthy, R., Batchvarova, N., Ron, D., Mitchell, P. J., & Habener, J. F. (1999). Keratin 10 gene expression during differentiation of mouse epidermis requires transcription factors C/EBP and AP-2. *Developmental Biology*, 216(1), 164–181. <https://doi.org/10.1006/dbio.1999.9460>
- Mbongue, J., Nicholas, D., Firek, A., & Langridge, W. (2014). The role of dendritic cells in tissue-specific autoimmunity. In *Journal of Immunology Research* (Vol. 2014). Hindawi Publishing Corporation. <https://doi.org/10.1155/2014/857143>
- McCully, M. L., Ladell, K., Hakobyan, S., Mansel, R. E., Price, D. A., & Moser, B. (2012). Epidermis instructs skin homing receptor expression in human T cells. *Blood*, 120(23), 4591–4598. <https://doi.org/10.1182/blood-2012-05-433037>
- Menon, G. K., Cleary, G. W., & Lane, M. E. (2012). The structure and function of the stratum corneum. *International Journal of Pharmaceutics*, 435(1), 3–9. <https://doi.org/10.1016/j.ijpharm.2012.06.005>
- Merad, M., Ginhoux, F., & Collin, M. (2008). Origin, homeostasis and function of Langerhans cells and other langerin-expressing dendritic cells. *Nature Reviews. Immunology*, 8(12), 935–947. <https://doi.org/10.1038/nri2455>
- Meraviglia, S., Di Carlo, P., Pampinella, D., Guadagnino, G., Presti, E. Lo, Orlando, V., Marchetti, G., Dieli, F., & Sergi, C. (2019). T-Cell Subsets (TCM, TEM, TEMRA) and Poly-Functional Immune Response in Patients with Human Immunodeficiency Virus (HIV) Infection and Different T-CD4 Cell Response. *Annals of Clinical and Laboratory Science*, 49(4), 519–528.
- Messenger, A. G. (1984). The culture of dermal papilla cells from human hair follicles. *The British Journal of Dermatology*, 110(6), 685–689. <https://doi.org/10.1111/j.1365-2133.1984.tb04705.x>
- Mestrallet, G., Rouas-Freiss, N., LeMaout, J., Fortunel, N. O., & Martin, M. T. (2021). Skin Immunity and Tolerance: Focus on Epidermal Keratinocytes Expressing HLA-G. *Frontiers in Immunology*, 12, 772516. <https://doi.org/10.3389/FIMMU.2021.772516/BIBTEX>
- Mita, Y., Kimura, M. Y., Hayashizaki, K., Koyama-Nasu, R., Ito, T., Motohashi, S., Okamoto, Y., & Nakayama, T. (2018). Crucial role of CD69 in anti-tumor immunity through regulating the exhaustion of tumor-infiltrating T cells. *International Immunology*, 30(12), 559–567. <https://doi.org/10.1093/INTIMM/DXY050>
- Mizumoto, N., & Takashima, A. (2004). CD1a and langerin: acting as more than Langerhans cell markers. *The Journal of Clinical Investigation*, 113(5), 658–660. <https://doi.org/10.1172/JCI21140>
- Montgomery, R. A., Tatapudi, V. S., Leffell, M. S., & Zachary, A. A. (2018). HLA in transplantation. *Nature Reviews Nephrology*, 14(9), 558–570. <https://doi.org/10.1038/s41581-018-0039-x>
- Moreci, R. S., & Lechler, T. (2020). Epidermal structure and differentiation. *Current Biology : CB*, 30(4), R144–R149. <https://doi.org/10.1016/j.cub.2020.01.004>
- Morgner, B., Tittelbach, J., & Wiegand, C. (2023). Induction of psoriasis- and atopic dermatitis-like phenotypes in 3D skin equivalents with a fibroblast-derived matrix. *Scientific Reports*, 13(1), 1–17. <https://doi.org/10.1038/s41598-023-28822-7>
- Mori, N., Morimoto, Y., & Takeuchi, S. (2017). Skin integrated with perfusable vascular channels on a chip. *Biomaterials*, 116, 48–56. <https://doi.org/10.1016/J.BIOMATERIALS.2016.11.031>
- Müller, I., & Kulms, D. (2018). A 3D Organotypic Melanoma Spheroid Skin Model. *Journal of Visualized Experiments : JoVE*, 2018(135), 57500. <https://doi.org/10.3791/57500>
- Müller, L., Hatzfeld, M., & Keil, R. (2021). Desmosomes as Signaling Hubs in the Regulation of Cell Behavior. *Frontiers in Cell and Developmental Biology*, 9, 745670. <https://doi.org/10.3389/FCELL.2021.745670/BIBTEX>
- Nair, R. P., & Krishnan, L. K. (2013). Identification of p63+ keratinocyte progenitor cells in circulation and their matrix-directed differentiation to epithelial cells. *Stem Cell Research & Therapy*, 4(2), 38. <https://doi.org/10.1186/scrt186>
- Nakajima, S., Igyártó, B. Z., Honda, T., Egawa, G., Otsuka, A., Hara-Chikuma, M., Watanabe, N., Ziegler, S. F., Tomura, M., Inaba, K., Miyachi, Y., Kaplan, D. H., & Kabashima, K. (2012). Langerhans cells are critical in epicutaneous sensitization with protein antigen via thymic stromal lymphopoietin receptor signaling. *The Journal of Allergy and Clinical Immunology*, 129(4), 1048. <https://doi.org/10.1016/J.JACI.2012.01.063>
- Natch, A. (2017). The KeratinoSens– assay for skin sensitization screening. *Alternatives for Dermal Toxicity Testing*, 235–248. [https://doi.org/10.1007/978-3-319-50353-0\\_17/COVER](https://doi.org/10.1007/978-3-319-50353-0_17/COVER)
- Natsch, A., Ryan, C. A., Foertsch, L., Emter, R., Jaworska, J., Gerberick, F., & Kern, P. (2013). A dataset on 145 chemicals tested in

- alternative assays for skin sensitization undergoing prevalidation. *Journal of Applied Toxicology : JAT*, 33(11), 1337–1352. <https://doi.org/10.1002/jat.2868>
- Ng, D. C., Shafae, S., Lee, D., & Bikle, D. D. (2000). Requirement of an AP-1 Site in the calcium response region of the involucrin promoter. *Journal of Biological Chemistry*, 275(31), 24080–24088. <https://doi.org/10.1074/jbc.M002508200>
- Nguyen, B. C., Lefort, K., Mandinova, A., Antonini, D., Devgan, V., Gatta, G. Della, Koster, M. I., Zhang, Z., Wang, J., Di Vignano, A. T., Kitajewski, J., Chiorino, G., Roop, D. R., Missero, C., & Dotto, G. P. (2006). Cross-regulation between Notch and p63 in keratinocyte commitment to differentiation. *Genes & Development*, 20(8), 1028–1042. <https://doi.org/10.1101/GAD.1406006>
- Niehues, H., Bouwstra, J. A., El Ghalbzouri, A., Brandner, J. M., Zeeuwen, P. L. J. M., & van den Bogaard, E. H. (2018). 3D skin models for 3R research: The potential of 3D reconstructed skin models to study skin barrier function. *Experimental Dermatology*, 27(5), 501–511. <https://doi.org/10.1111/EXD.13531>
- Nolte, S. V., Xu, W., Rennekampff, H. O., & Rodemann, H. P. (2008). Diversity of fibroblasts--a review on implications for skin tissue engineering. *Cells, Tissues, Organs*, 187(3), 165–176. <https://doi.org/10.1159/000111805>
- Oakes, T., Popple, A. L., Williams, J., Best, K., Heather, J. M., Ismail, M., Maxwell, G., Gellatly, N., Dearman, R. J., Kimber, I., & Chain, B. (2017). The T Cell Response to the Contact Sensitizer Paraphenylenediamine Is Characterized by a Polyclonal Diverse Repertoire of Antigen-Specific Receptors. *Frontiers in Immunology*, 8(FEB). <https://doi.org/10.3389/FIMMU.2017.00162>
- OECD. (2010). *Test No. 429: Skin Sensitisation : Local Lymph Node Assay*. OECD. <https://doi.org/10.1787/9789264071100-en>
- OECD. (2014). *The Adverse Outcome Pathway for Skin Sensitisation Initiated by Covalent Binding to Proteins*. OECD. <https://doi.org/10.1787/9789264221444-en>
- OECD. (2022). *Test No. 442D: In Vitro Skin Sensitisation: ARE-Nrf2 Luciferase Test Method*. OECD. <https://doi.org/10.1787/9789264229822-en>
- OECD. (2023a). Guideline No. 497: Defined Approaches on Skin Sensitisation. In *OECD Guidelines for the Testing of Chemicals, Section 4, OECD Publishing, Paris*. OECD. <https://doi.org/10.1787/b92879a4-en>
- OECD. (2023b). *Test No. 442C: In Chemico Skin Sensitisation: DPRA*. OECD. <https://doi.org/10.1787/9789264229709-en>
- OECD. (2023c). *Test No. 442C: In Chemico Skin Sensitisation*. OECD. <https://doi.org/10.1787/9789264229709-en>
- OECD. (2023d). *Test No. 442E: In Vitro Skin Sensitisation: Addressing the Adverse Outcome Pathway Key Event on Activation of Dendritic Cells* (Issue 442). OECD. <https://doi.org/10.1787/9789264264359-en>
- Ohl, L., Mohaupt, M., Czeloth, N., Hintzen, G., Kiafard, Z., Zwirner, J., Blankenstein, T., Henning, G., & Förster, R. (2004). CCR7 Governs Skin Dendritic Cell Migration under Inflammatory and Steady-State Conditions. *Immunity*, 21(2), 279–288. <https://doi.org/10.1016/j.immuni.2004.06.014>
- Okada, N., & Kitano, Y. (1982). Effects of Cholera Toxin on Proliferation of Cultured Human Keratinocytes in Relation to Intracellular Cyclic AMP Level. *Journal of Investigative Dermatology*, 79(1), 42–47. <https://doi.org/10.1111/1523-1747.ep12510580>
- Okada, R., Kondo, T., Matsuki, F., Takata, H., & Takiguchi, M. (2008). Phenotypic classification of human CD4+ T cell subsets and their differentiation. *Int Immunol*, 20(9), 1189–1199. <https://doi.org/10.1093/intimm/dxn075>
- Okuyama, R., Nguyen, B. C., Talora, C., Ogawa, E., Tommasi di Vignano, A., Lioumi, M., Chiorino, G., Tagami, H., Woo, M., & Dotto, G. P. (2004). High commitment of embryonic keratinocytes to terminal differentiation through a Notch1-caspase 3 regulatory mechanism. *Developmental Cell*, 6(4), 551–562. [https://doi.org/10.1016/S1534-5807\(04\)00098-X](https://doi.org/10.1016/S1534-5807(04)00098-X)
- Oliver, R. F., & Jahoda, C. A. B. (1988). Dermal-epidermal interactions. *Clinics in Dermatology*, 6(4), 74–82. [https://doi.org/10.1016/0738-081X\(88\)90069-7](https://doi.org/10.1016/0738-081X(88)90069-7)
- Olnes, M. J., Kotliarov, Y., Biancotto, A., Cheung, F., Chen, J., Shi, R., Zhou, H., Wang, E., Tsang, J. S., & Nussenblatt, R. (2016). Effects of Systemically Administered Hydrocortisone on the Human Immunome. *Scientific Reports 2016 6:1*, 6(1), 1–15. <https://doi.org/10.1038/srep23002>
- Onursal, C., Dick, E., Angelidis, I., Schiller, H. B., & Staab-Weijnitz, C. A. (2021). Collagen Biosynthesis, Processing, and Maturation in Lung Ageing. In *Frontiers in Medicine* (Vol. 8, p. 593874). Frontiers Media S.A. <https://doi.org/10.3389/fmed.2021.593874>
- Orlik, C., Deibel, D., Küblbeck, J., Balta, E., Ganskih, S., Habicht, J., Niesler, B., Schröder-Braunstein, J., Schäkel, K., Wabnitz, G., & Samstag, Y. (2020). Keratinocytes costimulate naive human T cells via CD2: a potential target to prevent the development of proinflammatory Th1 cells in the skin. *Cellular & Molecular Immunology*, 17(4), 380–394. <https://doi.org/10.1038/s41423-019-0261-x>
- Ostrowska-Podhorodecka, Z., Ding, I., Norouzi, M., & McCulloch, C. A. (2022). Impact of Vimentin on Regulation of Cell Signaling and

- Matrix Remodeling. *Frontiers in Cell and Developmental Biology*, 10, 869069.  
<https://doi.org/10.3389/FCELL.2022.869069/BIBTEX>
- Otto, W. R., Nanchahal, J., Lu, Q. L., Boddy, N., & Dover, R. (1995). Survival of allogeneic cells in cultured organotypic skin grafts. *Plastic and Reconstructive Surgery*, 96(1), 166–176. <https://doi.org/10.1097/00006534-199507000-00025>
- Ouwehand, K., Spiekstra, S. W., Waaijman, T., Scheper, R. J., de Gruijl, T. D., & Gibbs, S. (2011). Technical advance: Langerhans cells derived from a human cell line in a full-thickness skin equivalent undergo allergen-induced maturation and migration. *Journal of Leukocyte Biology*, 90(5), 1027–1033. <https://doi.org/10.1189/jlb.0610374>
- Ozdogan, C. Y., Kenar, H., Davun, K. E., Yucel, D., Doger, E., & Alagoz, S. (2020). An in vitro 3D diabetic human skin model from diabetic primary cells. *Biomedical Materials*, 16(1), 015027. <https://doi.org/10.1088/1748-605X/ABC1B1>
- Palacios, R., & Sugawara, I. (1982). Hydrocortisone abrogates proliferation of T cells in autologous mixed lymphocyte reaction by rendering the interleukin-2 Producer T cells unresponsive to interleukin-1 and unable to synthesize the T-cell growth factor. *Scandinavian Journal of Immunology*, 15(1), 25–31. <https://doi.org/10.1111/j.1365-3083.1982.tb00618.x>
- Peiser, M., Wanner, R., & Kolde, G. (2004). Human epidermal Langerhans cells differ from monocyte-derived Langerhans cells in CD80 expression and in secretion of IL-12 after CD40 cross-linking. *Journal of Leukocyte Biology*, 76(3), 616–622. <https://doi.org/10.1189/jlb.0703327>
- Pellegrini, G., Dellambra, E., Golisano, O., Martinelli, E., Fantozzi, I., Bondanza, S., Ponzin, D., McKeon, F., & De Luca, M. (2001). p63 identifies keratinocyte stem cells. *Proceedings of the National Academy of Sciences*, 98(6), 3156–3161. <https://doi.org/10.1073/pnas.061032098>
- Pfisterer, K., Shaw, L. E., Symmank, D., & Weninger, W. (2021). The Extracellular Matrix in Skin Inflammation and Infection. *Frontiers in Cell and Developmental Biology*, 9, 682414. <https://doi.org/10.3389/FCELL.2021.682414/BIBTEX>
- Piroid, C., Ovigne, J. M., Rousset, F., Martinozzi-Teissier, S., Gomes, C., Cotovio, J., & Alépée, N. (2015). The Myeloid U937 Skin Sensitization Test (U-SENS) addresses the activation of dendritic cell event in the adverse outcome pathway for skin sensitization. *Toxicology in Vitro*, 29(5), 901–916. <https://doi.org/10.1016/j.tiv.2015.03.009>
- Pisansarakit, P., du Cros, D. L., & Moore, G. P. M. (1991). Cultivation of mesenchymal cells derived from the skin and hair follicles of the sheep: The involvement of peptide factors in growth regulation. *Archives of Dermatological Research*, 283(5), 321–327. <https://doi.org/10.1007/BF00376621>
- Prechtel, A. T., & Steinkasserer, A. (2007). CD83: An update on functions and prospects of the maturation marker of dendritic cells. *Archives of Dermatological Research*, 299(2), 59–69. <https://doi.org/10.1007/S00403-007-0743-Z/FIGURES/4>
- Prockop, D. J. (1982). How Does a Skin Fibroblast Make Type I Collagen Fibers? *Journal of Investigative Dermatology*, 79(Suppl. 1), 3–6. <https://doi.org/10.1038/JID.1982.2>
- Quintanilla, R. H., Asprer, J. S. T., Vaz, C., Tanavde, V., & Lakshmiathy, U. (2014). CD44 Is a Negative Cell Surface Marker for Pluripotent Stem Cell Identification during Human Fibroblast Reprogramming. *PLOS ONE*, 9(1), e85419. <https://doi.org/10.1371/JOURNAL.PONE.0085419>
- Rahimi, N. (2020). C-type Lectin CD209L/L-SIGN and CD209/DC-SIGN: Cell Adhesion Molecules Turned to Pathogen Recognition Receptors. *Biology 2021*, Vol. 10, Page 1, 10(1), 1. <https://doi.org/10.3390/BIOLOGY10010001>
- Ramadan, Q., & Ting, F. C. W. (2016). In vitro micro-physiological immune-competent model of the human skin. *Lab on a Chip*, 16(10), 1899–1908. <https://doi.org/10.1039/C6LC00229C>
- Ramirez, T., Mehling, A., Kolle, S. N., Wruck, C. J., Teubner, W., Eltze, T., Aumann, A., Urbisch, D., van Ravenzwaay, B., & Landsiedel, R. (2014). LuSens: a keratinocyte based ARE reporter gene assay for use in integrated testing strategies for skin sensitization hazard identification. *Toxicology in Vitro : An International Journal Published in Association with BIBRA*, 28(8), 1482–1497. <https://doi.org/10.1016/J.TIV.2014.08.002>
- Rees, B., Spiekstra, S. W., Carfi, M., Ouwehand, K., Williams, C. A., Corsini, E., McLeod, J. D., & Gibbs, S. (2011). Inter-laboratory study of the in vitro dendritic cell migration assay for identification of contact allergens. *Toxicology in Vitro*, 25(8), 2124–2134. <https://doi.org/10.1016/j.tiv.2011.09.021>
- Reijnders, C. M. A., van Lier, A., Roffel, S., Kramer, D., Scheper, R. J., & Gibbs, S. (2015). Development of a Full-Thickness Human Skin Equivalent In Vitro Model Derived from TERT-Immortalized Keratinocytes and Fibroblasts. *Tissue Engineering. Part A*, 21(17–18), 2448–2459. <https://doi.org/10.1089/ten.TEA.2015.0139>
- Rentsch, M., Wawrzinek, R., Zelle-Rieser, C., Strandt, H., Bellmann, L., Fuchsberger, F. F., Schulze, J., Busmann, J., Rademacher, J.,

- Sigl, S., Del Frari, B., Stoitzner, P., & Rademacher, C. (2021). Specific Protein Antigen Delivery to Human Langerhans Cells in Intact Skin. *Frontiers in Immunology*, *12*, 732298. <https://doi.org/10.3389/FIMMU.2021.732298/BIBTEX>
- Rheinwald, G. (1975). *Rheinwald, Green 1975b, Cell, Serial.pdf*.
- Richter, A., Schmucker, S. S., Esser, P. R., Traska, V., Weber, V., Dietz, L., Thierse, H. J., Pennino, D., Cavani, A., & Martin, S. F. (2013). Human T cell priming assay (hTCPA) for the identification of contact allergens based on naive T cells and DC – IFN- $\gamma$  and TNF- $\alpha$  readout. *Toxicology in Vitro*, *27*(3), 1180–1185. <https://doi.org/10.1016/J.TIV.2012.08.007>
- Rimal, R., Marquardt, Y., Nevolianis, T., Djeljadini, S., Marquez, A. B., Huth, S., Chigrin, D. N., Wessling, M., Baron, J. M., Möller, M., & Singh, S. (2021). Dynamic flow enables long-term maintenance of 3-D vascularized human skin models. *Applied Materials Today*, *25*, 101213. <https://doi.org/10.1016/J.APMT.2021.101213>
- Roche, P. A., & Furuta, K. (2015). The ins and outs of MHC class II-mediated antigen processing and presentation. *Nature Reviews Immunology* *2015 15:4*, *15*(4), 203–216. <https://doi.org/10.1038/nri3818>
- Rogovaya, O. S., Zupnik, A. O., Izmailova, L. S., & Vorotelyak, E. A. (2021). Morphofunctional Characteristics of Fibroblasts of the Papillary and Reticular Layers of Human Skin Dermis. *Moscow University Biological Sciences Bulletin*, *76*(4), 225–231. <https://doi.org/10.3103/S0096392521040106>
- Ross, S. H., & Cantrell, D. A. (2018). Signaling and Function of Interleukin-2 in T Lymphocytes. *Annual Review of Immunology*, *36*, 411. <https://doi.org/10.1146/ANNUREV-IMMUNOL-042617-053352>
- Rousi, E., Malheiro, A., Harichandan, A., Mohren, R., Ana, ·, Lourenço, F., Carlos Mota, ·, Cillero-Pastor, B., Paul Wieringa, ·, & Moroni, · Lorenzo. (2022). An innervated skin 3D in vitro model for dermatological research. *In Vitro Models 2022*, *1*, 1–9. <https://doi.org/10.1007/S44164-022-00021-0>
- Russo, B., Brembilla, N. C., & Chizzolini, C. (2020). Interplay between keratinocytes and fibroblasts: A systematic review providing a new angle for understanding skin fibrotic disorders. *Frontiers in Immunology*, *11*, 535808. <https://doi.org/10.3389/FIMMU.2020.00648/BIBTEX>
- Rustemeyer, T. (2022). Immunological Mechanisms in Allergic Contact Dermatitis. *Current Treatment Options in Allergy*, *9*(2), 67–75. <https://doi.org/10.1007/S40521-022-00299-1/FIGURES/1>
- Rustemeyer, T., Van Hoogstraten, I. M. W., Von Blomberg, B. M. E., & Scheper, R. J. (2011). Mechanisms in allergic contact dermatitis. *Contact Dermatitis*, *11*–43. [https://doi.org/10.1007/3-540-31301-X\\_2](https://doi.org/10.1007/3-540-31301-X_2)
- Saito, K., Nukada, Y., Takenouchi, O., Miyazawa, M., Sakaguchi, H., & Nishiyama, N. (2013). Development of a new in vitro skin sensitization assay (Epidermal Sensitization Assay; EpiSensA) using reconstructed human epidermis. *Toxicology in Vitro: An International Journal Published in Association with BIBRA*, *27*(8), 2213–2224. <https://doi.org/10.1016/j.tiv.2013.08.007>
- Sakaguchi, H., Ashikaga, T., Miyazawa, M., Kosaka, N., Ito, Y., Yoneyama, K., Sono, S., Itagaki, H., Toyoda, H., & Suzuki, H. (2009a). The relationship between CD86/CD54 expression and THP-1 cell viability in an in vitro skin sensitization test - Human cell line activation test (h-CLAT). *Cell Biology and Toxicology*, *25*(2), 109–126. <https://doi.org/10.1007/s10565-008-9059-9>
- Sakaguchi, H., Ashikaga, T., Miyazawa, M., Kosaka, N., Ito, Y., Yoneyama, K., Sono, S., Itagaki, H., Toyoda, H., & Suzuki, H. (2009b). The relationship between CD86/CD54 expression and THP-1 cell viability in an in vitro skin sensitization test - Human cell line activation test (h-CLAT). *Cell Biology and Toxicology*, *25*(2), 109–126. <https://doi.org/10.1007/S10565-008-9059-9/FIGURES/4>
- Salameh, S., Tissot, N., Cache, K., Lima, J., Suzuki, I., Marinho, P. A., Rielland, M., Soeur, J., Takeuchi, S., Germain, S., & Breton, L. (2021). A perfusable vascularized full-thickness skin model for potential topical and systemic applications. *Biofabrication*, *13*(3), 035042. <https://doi.org/10.1088/1758-5090/abfca8>
- Sallusto, F., Geginat, J., & Lanzavecchia, A. (2004). Central memory and effector memory T cell subsets: Function, generation, and maintenance. *Annual Review of Immunology*, *22*, 745–763. <https://doi.org/10.1146/annurev.immunol.22.012703.104702>
- Sallusto, F., Lenig, D., Förster, R., Lipp, M., & Lanzavecchia, A. (1999). Two subsets of memory T lymphocytes with distinct homing potentials and effector functions. *Nature*, *401*(6754), 708–712. <https://doi.org/10.1038/44385>
- Sapudom, J., Alatoon, A., Mohamed, W. K. E., Garcia-Sabaté, A., McBain, I., Nasser, R. A., & Teo, J. C. M. (2020). Dendritic cell immune potency on 2D and in 3D collagen matrices. *Biomaterials Science*, *8*(18), 5106–5120. <https://doi.org/10.1039/d0bm01141j>
- Sarama, R., Matharu, P. K., Abduldaiem, Y., Corrêa, M. P., Gil, C. D., & Greco, K. V. (2022). In Vitro Disease Models for Understanding Psoriasis and Atopic Dermatitis. *Frontiers in Bioengineering and Biotechnology*, *10*(February), 1–8. <https://doi.org/10.3389/fbioe.2022.803218>

- Sasahara, Y., Yoshikawa, Y., Morinaga, T., Nakano, Y., Kanazawa, N., Kotani, J., Kawamata, S., Murakami, Y., Takeuchi, K., Inoue, C., Kitano, Y., & Hashimoto-Tamaoki, T. (2009). Human keratinocytes derived from the bulge region of hair follicles are refractory to differentiation. *International Journal of Oncology*, *34*(5), 1191–1199. [https://doi.org/10.3892/IJO\\_00000247/DOWNLOAD](https://doi.org/10.3892/IJO_00000247/DOWNLOAD)
- Sawada, Y., Tsukumo, H., Fukuda, J., Iijima, K., & Itagaki, H. (2022). Co-Culture of THP-1 Cells and Normal Human Epidermal Keratinocytes (NHEK) for Modified Human Cell Line Activation Test (h-CLAT). *Applied Sciences (Switzerland)*, *12*(12), 6207. <https://doi.org/10.3390/APP12126207/S1>
- Schellenberger, M. T., Bock, U., Hennen, J., Groeber-Becker, F., Walles, H., & Blömeke, B. (2019). A coculture system composed of THP-1 cells and 3D reconstructed human epidermis to assess activation of dendritic cells by sensitizing chemicals after topical exposure. *Toxicology in Vitro*, *57*, 62–66. <https://doi.org/10.1016/j.tiv.2019.02.002>
- Schmidt, F. F., Nowakowski, S., & Kluger, P. J. (2020). Improvement of a Three-Layered in vitro Skin Model for Topical Application of Irritating Substances. *Frontiers in Bioengineering and Biotechnology*, *8*, 388. <https://doi.org/10.3389/fbioe.2020.00388>
- Schön, M. P. (2019). Adaptive and Innate Immunity in Psoriasis and Other Inflammatory Disorders. *Frontiers in Immunology*, *10*, 1764. <https://doi.org/10.3389/fimmu.2019.01764>
- Seeger, P., Musso, T., & Sozzani, S. (2015). The TGF- $\beta$  superfamily in dendritic cell biology. *Cytokine and Growth Factor Reviews*, *26*(6), 647–657. <https://doi.org/10.1016/j.cytogfr.2015.06.002>
- Seppälä, I. J. T., & Mäkelä, O. (1998). Hapten. In P. J. D. and I. M. Roitt (Ed.), *Encyclopedia of Immunology* (Second, Vol. 1, pp. 1050–1052). Elsevier. <https://doi.org/10.1006/rwei.1999.0273>
- Sertznig, P., Seifert, M., Tilgen, W., & Reichrath, J. (2012). Peroxisome Proliferator-Activated Receptors (PPARs) and the Human Skin. *American Journal of Clinical Dermatology 2008 9:1*, *9*(1), 15–31. <https://doi.org/10.2165/00128071-200809010-00002>
- Shin, J. U., Abaci, H. E., Herron, L., Guo, Z., Sallee, B., Pappalardo, A., Jackow, J., Wang, E. H. C., Doucet, Y., & Christiano, A. M. (2020). Recapitulating T cell infiltration in 3D psoriatic skin models for patient-specific drug testing. *Scientific Reports*, *10*(1), 4123. <https://doi.org/10.1038/s41598-020-60275-0>
- Silva, L. T. Da, Pontillo, A., Da Silva, W. C., Almeida, A. De, Duarte, A. J. D. S., & Oshiro, T. M. (2013). Autologous and allogenic systems of HIV expansion: what is the better choice for clinical application in therapeutic vaccine? <https://doi.org/10.2217/IMT.13.136>, *5*(12), 1305–1311. <https://doi.org/10.2217/IMT.13.136>
- Simms, P. E., & Ellis, T. M. (1996). Utility of flow cytometric detection of CD69 expression as a rapid method for determining poly- and oligoclonal lymphocyte activation. *Clinical Diagnostic Laboratory Immunology*, *3*(3), 301–304. <https://doi.org/10.1128/CDLI.3.3.301-304.1996>
- Singleton, H., Popple, A., Gellatly, N., Maxwell, G., Williams, J., Friedmann, P. S., Kimber, I., & Dearman, R. J. (2016). Anti-hapten antibodies in response to skin sensitization. *Contact Dermatitis*, *74*(4), 197–204. <https://doi.org/10.1111/cod.12486>
- Sjaastad, L. E., Owen, D. L., Tracy, S. I., & Farrar, M. A. (2021). Phenotypic and Functional Diversity in Regulatory T Cells. *Frontiers in Cell and Developmental Biology*, *9*, 715901. <https://doi.org/10.3389/fcell.2021.715901/BIBTEX>
- Skartsis, N., Ferreira, L. M. R., & Tang, Q. (2022). The dichotomous outcomes of TNF $\alpha$  signaling in CD4+ T cells. *Frontiers in Immunology*, *13*, 1042622. <https://doi.org/10.3389/fimmu.2022.1042622/BIBTEX>
- Sköld, M., Börje, A., Harambasic, E., & Karlberg, A. T. (2004). Contact allergens formed on air exposure of linalool. Identification and quantification of primary and secondary oxidation products and the effect on skin sensitization. *Chemical Research in Toxicology*, *17*(12), 1697–1705. <https://doi.org/10.1021/TX049831Z/ASSET/IMAGES/MEDIUM/TX049831ZN00001.GIF>
- Skov, L., & Baadsgaard, O. (1996). MHC class II+ keratinocytes from IFN $\gamma$ -treated human skin activate T cells in the presence of staphylococcal superantigen despite UVB irradiation. *Archives of Dermatological Research*, *288*(5–6), 255–257. <https://doi.org/10.1007/BF02530095/METRICS>
- Sleeman, M. A., Murison, J. G., Strachan, L., Kumble, K., Glenn, M. P., McGrath, A., Grierson, A., Havukkala, I., Tan, P. L. J., & Watson, J. D. (2000). Gene Expression in Rat Dermal Papilla Cells: Analysis of 2529 ESTs. *Genomics*, *69*(2), 214–224. <https://doi.org/10.1006/GENO.2000.6300>
- Smith, M. M., & Melrose, J. (2015). Proteoglycans in Normal and Healing Skin. *Advances in Wound Care*, *4*(3), 152. <https://doi.org/10.1089/WOUND.2013.0464>
- Sonnenburg, A., Stahlmann, R., Kreutz, R., & Peiser, M. (2023). A new cell line based coculture system for skin sensitisation testing in one single assay using T cells, aryl hydrocarbon receptor knockout, and co-inhibitory blockage. *Archives of Toxicology*, *97*(6), 1677–1689. <https://doi.org/10.1007/s00204-023-03506-3>

- Sorrell, J. M., & Caplan, A. I. (2004). Fibroblast heterogeneity: More than skin deep. In *Journal of Cell Science* (Vol. 117, Issue 5, pp. 667–675). The Company of Biologists. <https://doi.org/10.1242/jcs.01005>
- Spagolla Napoleão Tavares, R., Stuchi Maria-Engler, S., Colepicolo, P., Debonsi, H. M., Schäfer-Korting, M., Marx, U., Rigo Gaspar, L., & Zoschke, C. (2020). Skin Irritation Testing beyond Tissue Viability: Fucoxanthin Effects on Inflammation, Homeostasis, and Metabolism. *Pharmaceutics*, *12*(2), 136. <https://doi.org/10.3390/pharmaceutics12020136>
- Sriram, G., Alberti, M., Dancik, Y., Wu, B., Wu, R., Feng, Z., Ramasamy, S., Bigliardi, P. L., Bigliardi-Qi, M., & Wang, Z. (2018). Full-thickness human skin-on-chip with enhanced epidermal morphogenesis and barrier function. *Materials Today*, *21*(4), 326–340. <https://doi.org/10.1016/J.MATTOD.2017.11.002>
- Steinert, P. M., & Marekov, L. N. (1995). The proteins elafin, filaggrin, keratin intermediate filaments, loricrin, and small proline-rich proteins 1 and 2 are isopeptide cross-linked components of the human epidermal cornified cell envelope. *Journal of Biological Chemistry*, *270*(30), 17702–17711. <https://doi.org/10.1074/jbc.270.30.17702>
- Stoitzner, P., Tripp, C. H., Eberhart, A., Price, K. M., Jung, J. Y., Bursch, L., Ronchese, F., & Romani, N. (2006). Langerhans cells cross-present antigen derived from skin. *Proceedings of the National Academy of Sciences of the United States of America*, *103*(20), 7783–7788. <https://doi.org/10.1073/pnas.0509307103>
- Strickland, J., Zang, Q., Kleinstreuer, N., Paris, M., Lehmann, D. M., Choksi, N., Matheson, J., Jacobs, A., Lowit, A., Allen, D., & Casey, W. (2016). Integrated decision strategies for skin sensitization hazard. *Journal of Applied Toxicology*, *36*(9), 1150–1162. <https://doi.org/10.1002/jat.3281>
- Su, Q., & Igyártó, B. Z. (2019). Keratinocytes Share Gene Expression Fingerprint with Epidermal Langerhans Cells via mRNA Transfer. *Journal of Investigative Dermatology*, *139*(11), 2313–2323.e8. <http://www.jidonline.org/article/S0022202X19315684/fulltext>
- Sun, Y. G., & Chen, Z. F. (2007). A gastrin-releasing peptide receptor mediates the itch sensation in the spinal cord. *Nature*, *448*(7154), 700–703. <https://doi.org/10.1038/NATURE06029>
- Sung, J. H., & Kim, J. J. (2023). Recent advances in in vitro skin-on-a-chip models for drug testing. *Expert Opinion on Drug Metabolism & Toxicology*, *19*(5), 249–267. <https://doi.org/10.1080/17425255.2023.2227379>
- Taghiabadi, E., Nilforoushzadeh, M. A., & Aghdami, N. (2020). Maintaining Hair Inductivity in Human Dermal Papilla Cells: A Review of Effective Methods. *Skin Pharmacology and Physiology*, *33*(5), 280–292. <https://doi.org/10.1159/000510152>
- Tai, Y., Wang, Q., Korner, H., Zhang, L., & Wei, W. (2018). Molecular mechanisms of T cells activation by dendritic cells in autoimmune diseases. *Frontiers in Pharmacology*, *9*(JUN), 360499. <https://doi.org/10.3389/FPHAR.2018.00642/BIBTEX>
- Talagas, M., & Misery, L. (2019). Role of Keratinocytes in Sensitive Skin. *Frontiers in Medicine*, *6*, 456180. <https://doi.org/10.3389/FMED.2019.00108/BIBTEX>
- Tamoutounour, S., Han, S. J., Deckers, J., Constantinides, M. G., Hurabielle, C., Harrison, O. J., Bouladoux, N., Linehan, J. L., Link, V. M., Vujkovic-Cvijin, I., Perez-Chaparro, P. J., Rosshart, S. P., Rehermann, B., Lazarevic, V., & Belkaid, Y. (2019). Keratinocyte-intrinsic MHCII expression controls microbiota-induced Th1 cell responses. *Proceedings of the National Academy of Sciences of the United States of America*, *116*(47), 23643–23652. <https://doi.org/10.1073/PNAS.1912432116>
- Tavares, R. S. N., Phuong-Tao, T., Maschmeyer, I., Maria-Engler, S. S., Schäfer-Korting, M., Winter, A., Zoschke, C., Lauster, R., Marx, U., & Gaspar, L. R. (2020). Toxicity of topically applied drugs beyond skin irritation: Static skin model vs. Two organs-on-a-chip. *International Journal of Pharmaceutics*, *589*(August), 119788. <https://doi.org/10.1016/j.ijpharm.2020.119788>
- Tewari, R., Shayahati, B., Fan, Y., & Akimzhanov, A. M. (2021). T cell receptor-dependent S-acylation of ZAP-70 controls activation of T cells. *Journal of Biological Chemistry*, *296*, 100311–100312. <https://doi.org/10.1016/j.jbc.2021.100311>
- Tharakan, S., Pontiggia, L., Biedermann, T., Böttcher-Haberzeth, S., Schiestl, C., Reichmann, E., & Meuli, M. (2010). Transglutaminases, involucrin, and loricrin as markers of epidermal differentiation in skin substitutes derived from human sweat gland cells. *Pediatric Surgery International*, *26*(1), 71–77. <https://doi.org/10.1007/S00383-009-2517-5/FIGURES/3>
- Tian, Y., Babor, M., Lane, J., Schulten, V., Patil, V. S., Seumois, G., Rosales, S. L., Fu, Z., Picarda, G., Burel, J., Zapardiel-Gonzalo, J., Tennekoon, R. N., De Silva, A. D., Premawansa, S., Premawansa, G., Wijewickrama, A., Greenbaum, J. A., Vijayanand, P., Weiskopf, D., ... Peters, B. (2017). Unique phenotypes and clonal expansions of human CD4 effector memory T cells re-expressing CD45RA. *Nature Communications*, *8*(1), 1473. <https://doi.org/10.1038/s41467-017-01728-5>
- Topouzi, H., Boyle, C. J., Williams, G., & Higgins, C. A. (2020). Harnessing the Secretome of Hair Follicle Fibroblasts to Accelerate Ex Vivo Healing of Human Skin Wounds. *Journal of Investigative Dermatology*, *140*(5), 1075–1084.e11. <https://doi.org/10.1016/J.JID.2019.09.019>

- Topouzi, H., Logan, N. J., Williams, G., & Higgins, C. A. (2017). Methods for the isolation and 3D culture of dermal papilla cells from human hair follicles. *Experimental Dermatology*, 26(6), 491. <https://doi.org/10.1111/EXD.13368>
- Törmä, H. (2011). *Regulation of keratin expression by retinoids*. 3(3). /pmc/articles/PMC3219164/
- Tourneix, F., Alépée, N., Detroyer, A., Eilstein, J., Martinuzzi Teissier, S., Nardelli, L., Noçairi, H., Pauloin, T., Piroird, C., & Del Bufalo, A. (2019). Assessment of a defined approach based on a stacking prediction model to identify skin sensitization hazard. *Toxicology in Vitro*, 60, 134–143. <https://doi.org/10.1016/j.tiv.2019.05.008>
- Trowbridge, I. S., & Thomas, M. L. (1994). CD45: An Emerging Role as a Protein Tyrosine Phosphatase Required for Lymphocyte Activation and Development. *Annual Review of Immunology*, 12(1), 85–116. <https://doi.org/10.1146/annurev.iy.12.040194.000505>
- Tsai, S., Clemente-Casares, X., Zhou, A. C., Lei, H., Ahn, J. J., Chan, Y. T., Choi, O., Luck, H., Woo, M., Dunn, S. E., Engleman, E. G., Watts, T. H., Winer, S., & Winer, D. A. (2018). Insulin Receptor-Mediated Stimulation Boosts T Cell Immunity during Inflammation and Infection. *Cell Metabolism*, 28(6), 922–934.e4. <https://doi.org/10.1016/J.CMET.2018.08.003>
- Tsuneki, M., & Madri, J. A. (2016). CD44 Influences Fibroblast Behaviors Via Modulation of Cell-Cell and Cell-Matrix Interactions, Affecting Survivin and Hippo Pathways. *Journal of Cellular Physiology*, 231(3), 731–743. <https://doi.org/10.1002/JCP.25123>
- Tze, L. E., Horikawa, K., Domaschew, H., Howard, D. R., Roots, C. M., Rigby, R. J., Way, D. A., Ohmura-Hoshino, M., Ishido, S., Andoniu, C. E., Degli-Esposti, M. A., & Goodnow, C. C. (2011). CD83 increases MHC II and CD86 on dendritic cells by opposing IL-10-driven MARCH1-mediated ubiquitination and degradation. *The Journal of Experimental Medicine*, 208(1), 149–165. <https://doi.org/10.1084/JEM.20092203>
- Udehiya, R. K., Amarpal, Aithal, H. P., Kinjavdekar, P., Pawde, A. M., Singh, R., & Taru Sharma, G. (2013). Comparison of autogenic and allogenic bone marrow derived mesenchymal stem cells for repair of segmental bone defects in rabbits. *Research in Veterinary Science*, 94(3), 743–752. <https://doi.org/10.1016/J.RVSC.2013.01.011>
- Urbisch, D., Becker, M., Honarvar, N., Kolle, S. N., Mehling, A., Teubner, W., Wareing, B., & Landsiedel, R. (2016). Assessment of Pre- and Pro-haptens Using Nonanimal Test Methods for Skin Sensitization. *Chemical Research in Toxicology*, 29(5), 901–913. <https://doi.org/10.1021/acs.chemrestox.6b00055>
- Urbisch, D., Mehling, A., Guth, K., Ramirez, T., Honarvar, N., Kolle, S., Landsiedel, R., Jaworska, J., Kern, P. S., Gerberick, F., Natsch, A., Emter, R., Ashikaga, T., Miyazawa, M., & Sakaguchi, H. (2015). Assessing skin sensitization hazard in mice and men using non-animal test methods. *Regulatory Toxicology and Pharmacology*, 71(2), 337–351. <https://doi.org/10.1016/J.YRTPH.2014.12.008>
- Van Den Bogaard, E. H., Tjabringa, G. S., Joosten, I., Vonk-Bergers, M., Van Rijssen, E., Tijssen, H. J., Erkens, M., Schalkwijk, J., & Koenen, H. J. P. M. (2014). Crosstalk between keratinocytes and T cells in a 3D microenvironment: A model to study inflammatory skin diseases. *Journal of Investigative Dermatology*, 134(3), 719–727. <https://doi.org/10.1038/jid.2013.417>
- Van Den Eeckhout, B., Tavernier, J., & Gerlo, S. (2020). Interleukin-1 as Innate Mediator of T Cell Immunity. *Frontiers in Immunology*, 11, 621931. <https://doi.org/10.3389/FIMMU.2020.621931/BIBTEX>
- van Huygevoort, T. (2017). The Murine Local Lymph Node Assay. *Molecular and Integrative Toxicology*, 99, 619–637. [https://doi.org/10.1007/978-3-319-47377-2\\_14](https://doi.org/10.1007/978-3-319-47377-2_14)
- Varga-Medveczky, Z., Kocsis, D., Naszlady, M. B., Fónagy, K., & Erdő, F. (2021). Skin-on-a-Chip Technology for Testing Transdermal Drug Delivery—Starting Points and Recent Developments. *Pharmaceutics*, 13(11), 1852. <https://doi.org/10.3390/pharmaceutics13111852>
- Vietri Rudan, M., & Watt, F. M. (2022). Mammalian Epidermis: A Compendium of Lipid Functionality. *Frontiers in Physiology*, 12(January). <https://doi.org/10.3389/fphys.2021.804824>
- Vilela De Sousa, I., Ferreira, M. J. S., Bebiano, L. B., Simões, S., Matos, A. F., Pereira, R. F., & Granja, P. L. (2023). Skin models of cutaneous toxicity, transdermal transport and wound repair. *Burns & Trauma*, 11. <https://doi.org/10.1093/BURNST/TKAD014>
- Villablanca, E. J., & Mora, J. R. (2008). A two-step model for Langerhans cell migration to skin-draining LN. *European Journal of Immunology*, 38(11), 2975–2980. <https://doi.org/10.1002/eji.200838919>
- Vörsmann, H., Groeber, F., Walles, H., Busch, S., Beisert, S., Walczak, H., & Kulms, D. (2013). Development of a human three-dimensional organotypic skin-melanoma spheroid model for in vitro drug testing. *Cell Death and Disease*, 4(7). <https://doi.org/10.1038/cddis.2013.249>
- Wagner, T., Gschwandtner, M., Strajeriu, A., Elbe-Bürger, A., Grillari, J., Grillari-Voglauer, R., Greiner, G., Golabi, B., Tschachler, E., &

- Mildner, M. (2018). Establishment of keratinocyte cell lines from human hair follicles. *Scientific Reports*, *8*(1), 13434. <https://doi.org/10.1038/s41598-018-31829-0>
- Wakabayashi, N., Dinkova-Kostova, A. T., Holtzclaw, W. D., Kang, M. I., Kobayashi, A., Yamamoto, M., Kensler, T. W., & Talalay, P. (2004). Protection against electrophile and oxidant stress by induction of the phase 2 response: fate of cysteines of the Keap1 sensor modified by inducers. *Proceedings of the National Academy of Sciences of the United States of America*, *101*(7), 2040–2045. <https://doi.org/10.1073/PNAS.0307301101>
- Wallmeyer, L., Dletert, K., Sochorová, M., Gruber, A. D., Kleuser, B., Vávrová, K., & Hedtrich, S. (2017). TSLP is a direct trigger for T cell migration in filaggrin-deficient skin equivalents. *Scientific Reports*, *7*(1), 1–12. <https://doi.org/10.1038/s41598-017-00670-2>
- Wang, M., Sun, Y., Li, L., Wu, P., DKW, O., & Shi, H. (2021). Calcium Channels: Noteworthy Regulators and Therapeutic Targets in Dermatological Diseases. *Frontiers in Pharmacology*, *12*, 702264. <https://doi.org/10.3389/FPHAR.2021.702264/BIBTEX>
- Wang, Y., Xiong, X., Wu, D., Wang, X., & Wen, B. (2011). Efficient activation of T cells by human monocyte-derived dendritic cells (HMDCs) pulsed with *Coxiella burnetii* outer membrane protein Com1 but not by HspB-pulsed HMDCs. *BMC Immunology* *2011 12:1*, *12*(1), 1–12. <https://doi.org/10.1186/1471-2172-12-52>
- Wanibuchi, S., Yamamoto, Y., Sato, A., Kasahara, T., & Fujita, M. (2019). The amino acid derivative reactivity assay with fluorescence detection and its application to multi-constituent substances. *Journal of Toxicological Sciences*, *44*(12), 821–832. <https://doi.org/10.2131/jts.44.821>
- Wass, U., & Belin, L. (1990). An in vitro method for predicting sensitizing properties of inhaled chemicals. *Scandinavian Journal of Work, Environment & Health*, *16*(3), 208–214. <https://doi.org/10.5271/SJWEH.1802>
- Wiese, A. K., Burdine, M. S., Turnage, R. H., Tackett, A. J., & Burdine, L. J. (2017). DNA-PKcs controls calcineurin mediated IL-2 production in T lymphocytes. *PLOS ONE*, *12*(7), e0181608. <https://doi.org/10.1371/JOURNAL.PONE.0181608>
- Williams, R., & Thornton, M. J. (2020). Isolation of Different Dermal Fibroblast Populations from the Skin and the Hair Follicle. *Methods in Molecular Biology (Clifton, N.J.)*, *2154*, 13–22. [https://doi.org/10.1007/978-1-0716-0648-3\\_2](https://doi.org/10.1007/978-1-0716-0648-3_2)
- Willis, C. M., Stephens, C. J. M., & Wilkinson, J. D. (1991). Selective expression of immune-associated surface antigens by keratinocytes in irritant contact dermatitis. *The Journal of Investigative Dermatology*, *96*(4), 505–511. <https://doi.org/10.1111/1523-1747.EP12470213>
- Wu, H., Niu, C., Qu, Y., Sun, X., & Wang, K. W. (2022). Selective activation of TRPA1 ion channels by nitrobenzene skin sensitizers DNFB and DNCB. *The Journal of Biological Chemistry*, *298*(2), 101555–101556. <https://doi.org/10.1016/J.JBC.2021.101555>
- Wu, J. J., Liu, R. Q., Lu, Y. G., Zhu, T. Y., Cheng, B., & Men, X. (2005). Enzyme digestion to isolate and culture human scalp dermal papilla cells: A more efficient method. *Archives of Dermatological Research*, *297*(2), 60–67. <https://doi.org/10.1007/s00403-005-0554-z>
- Wu, N., Rollin, J., Masse, I., Lamartine, J., & Gidrol, X. (2012). p63 regulates human keratinocyte proliferation via MYC-regulated gene network and differentiation commitment through cell adhesion-related gene network. *Journal of Biological Chemistry*, *287*(8), 5627–5638. <https://doi.org/10.1074/jbc.M111.328120>
- Wufuer, M., Lee, G., Hur, W., Jeon, B., Kim, B. J., Choi, T. H., & Lee, S. (2016). Skin-on-a-chip model simulating inflammation, edema and drug-based treatment. *Scientific Reports*, *6*(1), 37471. <https://doi.org/10.1038/srep37471>
- Xiao, T., Sun, M., Zhao, C., & Kang, J. (2023). TRPV1: A promising therapeutic target for skin aging and inflammatory skin diseases. *Frontiers in Pharmacology*, *14*, 1037925. <https://doi.org/10.3389/FPHAR.2023.1037925/BIBTEX>
- Xie, L., Moroi, Y., Takahara, M., Tsuji, G., Oba, J., Hayashida, S., Takeuchi, S., Shan, B., Uchi, H., & Furue, M. (2011). CD10 expressed by fibroblasts and melanoma cells degrades endothelin-1 secreted by human keratinocytes. *European Journal of Dermatology : EJD*, *21*(4), 505–509. <https://doi.org/10.1684/ejd.2011.1371>
- Xie, L., Takahara, M., Nakahara, T., Oba, J., Uchi, H., Takeuchi, S., Moroi, Y., & Furue, M. (2011). CD10-bearing fibroblasts may inhibit skin inflammation by down-modulating substance P. *Archives of Dermatological Research*, *303*(1), 49–55. <https://doi.org/10.1007/s00403-010-1093-9>
- Xu, A.-N., Liu, D., Dai, Y.-T., Zhang, F., Shen, J., Hu, C.-L., Xu, C.-H., Zhang, Y.-L., Xie, Y.-Y., Huang, Q.-H., Xu, P.-F., Wang, L., Cheng, L., Huang, J., Chen, Z., Chen, S.-J., & Sun, X.-J. (2019). Differential Expression of CD49f Discriminates the Independently Emerged Hematopoietic Stem Cells and Erythroid-Biased Progenitors. *Blood*, *134*(Supplement\_1), 3700–3700. <https://doi.org/10.1182/BLOOD-2019-130429>
- Xuan, N. T., Hoang, N. H., Nhung, V. P., Duong, N. T., Ha, N. H., & Hai, N. Van. (2017). Regulation of dendritic cell function by

- insulin/IGF-1/PI3K/Akt signaling through klotho expression. *Journal of Receptor and Signal Transduction Research*, 37(3), 297–303. <https://doi.org/10.1080/10799893.2016.1247862>
- Yamamoto-Tanaka, M., Makino, T., Motoyama, A., Miyai, M., Tsuboi, R., & Hibino, T. (2014). Multiple pathways are involved in DNA degradation during keratinocyte terminal differentiation. *Cell Death & Disease* 2014 5:4, 5(4), e1181–e1181. <https://doi.org/10.1038/cddis.2014.145>
- Yordanova, D., Schultz, T. W., Kuseva, C., Tankova, K., Ivanova, H., Dermen, I., Pavlov, T., Temelkov, S., Chapkanov, A., Georgiev, M., Gissi, A., Sobanski, T., & Mekenyan, O. G. (2019). Automated and standardized workflows in the OECD QSAR Toolbox. *Computational Toxicology*, 10, 89–104. <https://doi.org/10.1016/J.COMTOX.2019.01.006>
- Young, C. A., Rorke, E. A., Adhikary, G., Xu, W., & Eckert, R. L. (2017). Loss of epidermal AP1 transcription factor function reduces filaggrin level, alters chemokine expression and produces an ichthyosis-related phenotype. *Cell Death & Disease* 2017 8:6, 8(6), e2840–e2840. <https://doi.org/10.1038/cddis.2017.238>
- Young, P., Boussadia, O., Halfter, H., Grose, R., Berger, P., Leone, D. P., Robenek, H., Charnay, P., Kemler, R., & Suter, U. (2003). E-cadherin controls adherens junctions in the epidermis and the renewal of hair follicles. *The EMBO Journal*, 22(21), 5723–5733. <https://doi.org/10.1093/emboj/cdg560>
- Yu, D. W., Yang, T., Sonoda, T., Gong, Y., Cao, Q., Gaffney, K., Jensen, P. J., Freedberg, I. M., Lavker, R. M., & Sun, T. T. (2001). Osteopontin gene is expressed in the dermal papilla of pelage follicles in a hair-cycle-dependent manner. *Journal of Investigative Dermatology*, 117(6), 1554–1558. <https://doi.org/10.1046/j.0022-202x.2001.01568.x>
- Zhan, Y., Carrington, E. M., Zhang, Y., Heinzel, S., & Lew, A. M. (2017). Life and death of activated T cells: How are they different from naïve T Cells? In *Frontiers in Immunology* (Vol. 8, Issue DEC, p. 1809). Frontiers Media S.A. <https://doi.org/10.3389/fimmu.2017.01809>
- Zhang, L., & Zhang, L. (2018). Keratins in Skin Epidermal Development and Diseases. *Keratin*. <https://doi.org/10.5772/INTECHOPEN.79050>
- Zhang, X., Gu, J., Yu, F.-S., Zhou, L., & Mi, Q.-S. (2016). TGF- $\beta$ 1-induced transcription factor networks in Langerhans cell development and maintenance. *Allergy*, 71(6), 758–764. <https://doi.org/10.1111/all.12871>
- Zhao, Q., Li, N., Zhang, H., Lei, X., Cao, Y., Xia, G., Duan, E., & Liu, S. (2019). Chemically induced transformation of human dermal fibroblasts to hair-inducing dermal papilla-like cells. *Cell Proliferation*, 52(5), e12652. <https://doi.org/10.1111/CPR.12652>
- Zhou, L., Yang, K., Wickett, R. R., Andl, T., & Zhang, Y. (2016). Dermal sheath cells contribute to postnatal hair follicle growth and cycling. *Journal of Dermatological Science*, 82(2), 129–131. <https://doi.org/10.1016/j.jdermsci.2016.02.002>
- Zoio, P., & Oliva, A. (2022). Skin-on-a-Chip Technology: Microengineering Physiologically Relevant In Vitro Skin Models. *Pharmaceutics*, 14(3). <https://doi.org/10.3390/pharmaceutics14030682>
- Zoio, P., Ventura, S., Leite, M., & Oliva, A. (2021). Pigmented Full-Thickness Human Skin Model Based on a Fibroblast-Derived Matrix for Long-Term Studies. *Tissue Engineering Part C: Methods*, 27(7), 433–443. <https://doi.org/10.1089/ten.tec.2021.0069>



## APPENDIX AND SUPPLEMENTALS

### APPENDIX 1 List of Figures

<i>Figure</i>	<i>Description</i>
<b>1</b>	The layers and components of the epidermis including the markers and proteins expressed in each layer
<b>2</b>	The collagen structure and provides an example of collagen that exhibits this particular arrangement
<b>3</b>	The reticular dermis and papillary dermis within the dermal layer and the rough indication of the epidermis
<b>4</b>	The immune response to a metal ion in the context of skin sensitization, encompassing both the sensitization and elicitation phases
<b>5</b>	The immune synapse between antigen-presenting cells (APC) and T-lymphocytes during the process of antigen presentation
<b>6</b>	T-lymphocyte subsets based on the expression of CD45RA and CCR7. The upper left quadrant represents naïve T-lymphocytes, while the lower left quadrant depicts terminally differentiated T-lymphocytes re-expressing CD45RA (TEMRA) T-lymphocytes
<b>7</b>	The adverse outcome pathway (AOP) of skin sensitization, as defined by the Organisation for Economic Co-operation and Development (OECD)
<b>8</b>	The differences between each type of model
<b>9</b>	The microanatomy of hair follicles
<b>10</b>	The list of Coplin jars required for the hematoxylin and eosin staining
<b>11</b>	The illustration outlines the sequential creation of the immunocompetent skin models (ImmuSkin)
<b>12</b>	Representative microscopic images and illustrations showing the outgrowth of hair follicles over 21 days
<b>13</b>	Characterization of hair follicle-derived cells versus foreskin-derived cells by Immunofluorescence (IF) staining
<b>14</b>	Characterization of hair follicle-derived cells versus foreskin-derived cells by flow cytometry
<b>15</b>	Assessing the viability and proliferation of hair follicle-derived keratinocyte (HFDK) in various culture media
<b>16</b>	Changes in T-lymphocyte phenotype and mortality over time
<b>17</b>	Changes in T-lymphocyte phenotype and mortality over time in the presence of IL-2 or without IL-2
<b>18</b>	The direct comparison of IL-2 effects on frequency T-lymphocytes over the course of six days
<b>19</b>	Effects of co-culture media and hair follicle-derived keratinocytes (HFDK) on CD4+ T-lymphocyte activation and differentiation
<b>20</b>	Viability and morphology of hair follicle-derived keratinocytes (HFDK) in co-culture media with or without CD4+ T-lymphocytes

<b>21</b>	Comparison of single culture and co-culture of naïve CD4+ T-lymphocytes and hair follicle-derived keratinocytes (HFDK) in KGM-2 without hydrocortisone (KGM-2 wo HC) either alone or with HFDK, for three days
<b>22</b>	Comparison of single culture and co-culture of naïve CD4+ T-lymphocytes and hair follicle-derived keratinocytes (HFDK)
<b>23</b>	Comparison of T-lymphocyte phenotype and hair follicle-derived keratinocytes (HFDK) viability between autologous and allogeneic co-cultures
<b>24</b>	Comparison of T-lymphocyte phenotype and hair follicle-derived keratinocytes (HFDK) viability between autologous and allogeneic co-cultures
<b>25</b>	The effect of 2,4-Dinitrochlorobenzene (DNCB) concentration on the character, mortality, and viability of the cells
<b>26</b>	The effect of treating a 2D co-culture of hair follicle-derived keratinocytes (HFDK) and T-lymphocytes with 0.1µM DNCB
<b>27</b>	The direct comparison between the effect of 24-hour and 48-hour treatment with 2,4-Dinitrochlorobenzene (DNCB) on a co-culture of hair follicle-derived keratinocytes (HFDK) and T-lymphocytes
<b>28</b>	Characterization of T-lymphocytes and monocyte-derived Langerhans cells (MoLC) from a co-culture of hair follicle-derived keratinocytes (HFDK), MoLC, and CD4+ naïve T-lymphocytes
<b>29</b>	The characterization of T-lymphocytes and monocyte-derived Langerhans cells (MoLC) from the autologous versus allogeneic co-culture
<b>30</b>	The characterization of T-lymphocytes and monocyte-derived Langerhans cell (MoLC) from the autologous versus allogeneic co-culture of three cell types
<b>31</b>	The effect of 2,4-Dinitrochlorobenzene (DNCB) on T-lymphocyte and monocyte-derived Langerhans cells (MoLC) from the three cells co-culture
<b>32</b>	The comparison of reconstructed human skin models from foreskin-derived cells (RHS-FD) and hair follicle-derived cells (RHS-HFD)
<b>33</b>	Characterization of monocyte-derived Langerhans cells (MoLC) from co-culture in different media
<b>34</b>	The characterization of T-lymphocytes from the co-culture in different media
<b>35</b>	The characterization of the three-layer constructs from ImmuSkin-MT, ImmuSkin-M, and ImmuSkin-T using Hematoxylin and Eosin (H&E) staining
<b>36</b>	The characterization of the three-layer constructs from ImmuSkin-MT, ImmuSkin-M, and ImmuSkin-T using immunofluorescence (IF) staining
<b>37</b>	The comparison of cells obtained from the lower chamber of transwell of ImmuSkin-MT, ImmuSkin-M, and ImmuSkin-T
<b>38</b>	The characterization of the three-layer construct of the ImmuSkin-MT after treatment with various skin sensitizers
<b>39</b>	Skin sensitizers induce migration, maturation, and T-lymphocyte activation in ImmuSkins. ImmuSkins comprise three variants, which are ImmuSkin-M, ImmuSkin-T, and ImmuSkin-MT
<b>40</b>	Viability of the cells from ImmuSkin-M, ImmuSkin-T and ImmuSkin-MT

## APPENDIX 2 List of Tables

<b>Table</b>	<b>Description</b>
<b>1</b>	The summary of the main types of immunocompetent skin models that involve Langerhans cells or T-lymphocytes, and their relevance for skin immunity research.
<b>2</b>	The amount of sterile filtered ddH <sub>2</sub> O and PureCol EZ Gel required to prepare the collagen solution

## LIST OF CONTRIBUTIONS

### Publication

Dubau, M.\*, **Tripetchr, T.\***, Mahmoud, L., Kral, V., & Kleuser, B (2024). Advancing skin model development: a focus on a self-assembled, induced pluripotent stem cell-derived, xeno-free approach. (*Accepted to be published in the Journal of Tissue Engineering on 01.10.2024*).

\*The authors contributed equally to this work

### Conferences Proceedings

**Tripetchr, T.**, Dubau, M., Hedtrich, S., & Kleuser, B. (2022). Establishment of an *in vitro* immunocompetent skin model system for skin sensitization assay application as an alternative to animal models. *Poster presented at the 12<sup>th</sup> Scientific Symposium: Der wissenschaftliche Nachwuchs stellt sich vor – Young scientists present, Freie Universität Berlin, Berlin, Germany, 08 July 2022.*

**Tripetchr, T.**, Dubau, M., Hedtrich, S., & Kleuser, B. (2022). Establishment of an *in vitro* immunocompetent skin model system for skin sensitization assay application as an alternative to animal models. *Poster presented at the 8<sup>th</sup> The Danish 3R Symposium, Copenhagen, Denmark, November 8 - 9, 2022.*

Dubau, M., **Tripetchr, T.**, & Kleuser, B. (2022). Autologous approach to develop an immunocompetent skin model using iPSC-generated fibroblasts, keratinocytes, and immune cells. *Poster presented at the 8<sup>th</sup> The Danish 3R Symposium, Copenhagen, Denmark, November 8 - 9, 2022.*

**Tripetchr, T.**, Dubau, M., Hedtrich, S., & Kleuser, B. (2023). Establishment of an *in vitro* immunocompetent skin model system for skin sensitization assay as an alternative to animal models. Proceedings of the 2<sup>nd</sup> MPS World Summit (pp. 244). ALTEX Proceedings, 11(1). *Poster presented at the 2<sup>nd</sup> MPS World Summit, Berlin, Germany, June 26 - June 30, 2023.*

Dubau, M., **Tripetchr, T.**, Kral, V., & Kleuser, B. (2023). Autologous approach to develop an immunocompetent skin model using iPSC-generated fibroblasts, keratinocytes, and dendritic cells. Proceedings of the 2<sup>nd</sup> MPS World Summit (pp. 249). ALTEX Proceedings, 11(1). *Poster presented at the 2<sup>nd</sup> MPS World Summit, Berlin, Germany, June 26 - June 30, 2022.*



**DECLARATION OF AUTHORSHIP**

in accordance with the most current valid version  
of the doctoral regulations  
of the Department of Biology, Chemistry, Pharmacy

**Tripetchr**

Last name of doctoral candidate

**Tarada**

First name of doctoral candidate

**Declaration of authorship**

I hereby declare that I alone am responsible for the content of my doctoral dissertation titled

Advancing Skin Sensitization Assessment: The Development of an Immunocompetent Skin Model as a Non-Animal Alternative for Testing Skin Sensitizers

and that I have only used the sources or references cited in said dissertation.

I declare that I have never submitted this dissertation as part of another doctoral procedure.

21.05.2024

Date

Signature of doctoral candidate